Southern African dust sources as identified by multiple space borne sensors

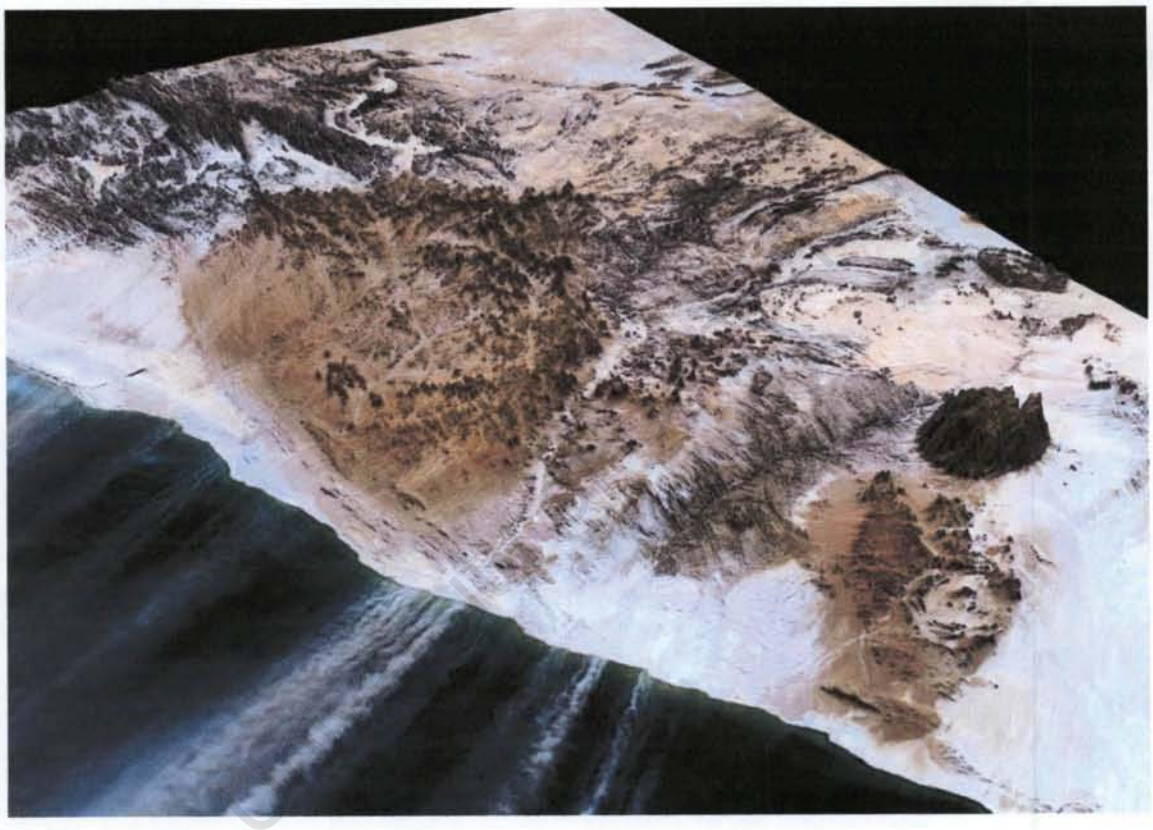

Kathryn J Vickery

Department of Environmental and Geographical Science

UNIVERSITY OF CAPE TOWN
IYUNIVESITHI YASEKAPA • UNIVERSITEIT VAN KAAPSTAD

Southern African dust sources as identified by multiple space borne sensors

Thesis Presented By:
Kathryn Vickery

This dissertation is submitted as an academic requirement for the fulfillment of an MSc in the Department of Environmental and Geographical Science, University of Cape Town

January 2010

This work has not been previously submitted in whole, or in part, for the award of any degree. It is my own work, each significant contribution and quotation in this dissertation from the works of other people have been attributed, cited and referenced.

Signed by candidate

Vast is the kingdom of dust! Unlike terrestrial kingdoms, it knows no limits. No ocean marks it boundaries. No mountains hem it in. No parallels of latitude and longitude define its boundless areas, nor can farthermost stars in the infinitudes of space serve other than as a twinkling outpost of a realm as vast as the universe itself.

J. Gordon Ogden, *The Kingdom of Dust: (1912), 10*

Abstract

Mineral aerosols emitted from arid and semi-arid regions effect global radiation, contribute to regional nutrient dynamics and impact local soil and water quality. Satellite imagery has been central to the identification and determining the distribution of source areas and the trajectories of dust around the globe. This study focuses on the dryland regions of Botswana, Namibia and South Africa. It uses the capabilities of the ultraviolet channels provided by the older Total Ozone Mapping Spectrometer (TOMS), the Ozone Monitoring Instrument (OMI) (a TOMS follow up), the visible bands of Moderate Resolution Imaging Spectroradiometer (MODIS), and the Spinning Enhanced Visible and Infrared Imager (SEVIRI) onboard Meteosat Second Generation (MSG). This study compares various dust detection products but also focuses on the application of thermal infrared bands from MSG through the usage of the new "Pink Dust" visualisation technique using channels 7 (8.7 μm), 9 (10.8 μm), and 10 (12.0 μm). This multisensor approach resulted in a regional maps highlighting the distribution of source points and establishing some of the prevalent transport pathways and likely deposition zones. Southern African dust sources include a few large and many small pans, subtle inland depressions and ephemeral river systems, which are subject to a range of climatic conditions as part of the Kalahari and Namib region. This work in particular examines if source points are productive due to favourable climatic conditions. The debate around transport limit verses supply limit can only be solved at the local scale which requires observation at higher spatial and temporal resolution as provided by the latest dust detection products. MSG and MODIS in particular have shown distinct source point clusters in Etosha and the Makgadikgadi Pans which based on the courser resolution of older TOMS, have so far been treated as homogeneous sources. Data analyses reveal 327 individual dust plumes over the 2005-2008 study period, some of which are more than 300 km in length. These are integrated into existing climate and weather records provided by National Centers for Environmental Prediction (NCEP) data. The results identified a set dust drivers such as the Continental High Pressure, Bergwinds, Tropical Temperate and West Coast Troughs, and Westerly and Easterly Wave Lows. This enhances our ability to predict such events, in particular, if transport acts as the limiting driver. Some of these findings also have the potential to enhance our knowledge of the aerosol generation process elsewhere. The quality of findings are still limited by problems associated with dust plume substrates and clearly require significant surface validation relating to hydrological and climatic controls at the micro-scale. It is furthermore evident that no current instrument fully meets the requirements of the mineral aerosol research community.

Acknowledgements

This project arose out of discussions held in Cape Town (October 2007) between Professors' Dave Thomas and Mike Meadows and Doctors Richard Washington, Giles Wiggs and Frank Eckardt during the initiation of a NERC Proposal. Despite the grant not being awarded through the discussion the idea was developed and the project was proposed. I acknowledge all these and all subsequent contributions and discussions.

Firstly I would like to give thanks to Frank, for his patience and shared passion for this project. His invaluable assistance, dedication, inspiration and wisdom made this project possible.

I would like to acknowledge the technical contribution of Chris Jack who helped me "see pink" through his assistance in editing the script and batch processing the MSG data. I further acknowledge the assistance of Rory Grandin whose technical savvy and willingness to help saved hours of frustration and the life of poor Terrence who would otherwise have suffered many trips to the 'frustrated computer users hospital'.

I would like to thank the elephant, Tyrel Flűgel and Professor Driver for their invaluable contributions to my fieldwork and our adventures on the Pans. Mention too must go to all those who told stories of dust storms when all we saw was water and prayed for our safe journeys.

I would like to thank all those along the way whose contributions, thought provoking discussions and support all added to the project. Here acknowledging the communications with Doctors Rob Bryant, Richard Washington and Sebastian Engelstaedter.

To Prof. Mike Meadows, thank you for all the advice and support that you have provided me throughout my academic career and for allowing me to inspire the young minds – as you did for me.

To Prof. Bruce Hewitson for making it possible for me to pursue my research interests by so generously funding me.

Thanks too must go to my family for their love and support during the years and constant belief in me. To Gran, I got to the 'Pans' and will forever hold onto your passion for geography, and most specifically your love for this continent that you called home. You continue to inspire me.

Lastly but most certainly not least I would like to thank Lynne Quick and Kelly Kirsten for their patience, words of wisdom and continual support. The many cups of coffee drunk, hours of combined laughter and friendship provided during the years made the ominous task of thesis writing and image analysis fun. Special thanks to Kelly for bravely editing where no one else would.

Table of contents

List of figures

List of tables

Abbreviations and Acronyms:

AAI: Aerosol Absorbivity Index

AERONET: AErosol RObotic NETwork

amsl: above mean sea level

AOD: Aerosol Optical Depth

ARL: Air Resources Laboratory

AVHRR: Advanced Very High Resolution Radiometer

BDRF: Biodirectional Reflectivity Distribution Function

BT: Brightness Temperature

BTD: Brightness Temperature Difference

CSAG: Climate Systems Analysis Group

EOS: Earth Observing System

ESRL: Earth Science Research Laboratory

EUMETSAT: European Organisation for the Exploitation of Meteorological Satellites

GESC – DISC – DAAC: Goddard Earth Sciences Data and Information Services Centre Distribution Active Archive Centre

HYSPLIT: HYbrid Single-Particle Lagrangian Integrated Trajectory

IPCC: Intergovernmental Panel on Climate Change

IR: InfraRed

LER: Lambert Equivalent Reflectivity

MODIS: MODerate Resolution Imaging Spectroradiometer

MSG: Meteosat Second Generation

NASA: National Aeronautics and Space Administration

NCEP: National Centres for Environmental Prediction

NOAA: National Oceanic and Atmospheric Administration

OMI: Ozone Monitoring Instrument

PBLH: Planetary Boundary Layer Height

SAFARI: Southern African Fire-Atmospheric Research Initiative

SAHP: South Atlantic High Pressure

SEVIRI: Spinning Enhanced Visible and Infrared Imager

TOMS: Total Ozone Mapping Spectrometer

TTT: Tropical temperate trough

UV: UltraViolet

WMO: World Meteorological Organisation

1. Introduction

Within the earth's atmosphere exists a myriad of airborne particles termed aerosols, including dust, smoke from biomass burning, and anthropogenically produced air pollutants (Prospero, 1999; Piketh et al., 1999; Goudie and Middleton, 2001). Of particular importance in this study are mineral aerosols or dust, which through its origin in arid and semi-arid regions globally, experience a high degree of variability both spatially and temporally.

Aerosols are emitted into the atmosphere through a variety of drivers both climatic and geomorphologic. They have potential to modify the earth's climate (Kaufman et al., 2002; Engelstaedter and Washington, 2007a,b; Bryant et al., 2007) through both the direct and indirect effects of radiation as well as nutrient dynamics and ecosystem functions (Harrison et al., 2001; Piketh et al., 2000; Prospero, 1999). The magnitude and direction of the potential impact is a function of particle morphology and composition, which is determined by the source region among other factors. Thus, knowledge of dust source regions and site characteristics is of utmost importance in increasing our understanding of potential impacts. As Sokolik and Toon (1996) ascertained, regional scale knowledge is of further importance due to the fact that the radiative effects of mineral aerosols potentially exceed those of sulphur and other anthropogenic aerosols and may even be comparable to those of clouds. Therefore the study of dust requires high spatial and temporal resolution to be able to capture source region and emission characteristics of sites. Such strict requirements have meant that globally and regionally dust region and frequency maps fall short of what is needed.

Remote sensing has significantly advanced our understanding, with a range of remote sensing products (e.g. TOMS: Washington et al., 2003; Prospero et al, 2002, AVHRR: Brindley and Ignatov, 2006, Meteosat: Schepanski et al., 2007, MODIS: Huang et al., 2007), each with different benefits and shortcomings, are used globally to identify source areas for individual dust events. TOMS in particular has been used in the development of global dust maps, identifying ephemeral inland depressions globally to be particularly active emission regions. The Etosha and Makgadikgadi Pans in southern Africa have been recognised to be among the top ten dustiest point sources in the world (Washington et al., 2003), with the Bodélé Depression in northern Chad being the 'dustiest place on earth' (Giles, 2005, 816).

Numerous smaller and lower dust plumes which are invisible to TOMS and stand out against the dark Atlantic Ocean have been captured by a multitude of sensors, for example along the Namib coast (Eckardt et al., 2001; Eckardt and Kuring, 2005). Here ephemeral river beds and coastal salt

pans act as significant sources (Eckardt and Kuring, 2005), are particularly active during berg wind conditions (Eckardt et al., 2001) and are analogous of dusty river and sabkha environments elsewhere. In order to further pinpoint target areas, the EUMETSAT Meteosat Second Generation (MSG) – Spinning Enhanced Visible and Infra-Red Imager (SEVIRI) was used to produce a unifying, regional, multi-annual dataset of dust sources for southern Africa which does not have the dust-height bias of TOMS. In TOMS dust below 1000 m is undetected (Herman et al., 1997) and is therefore unable to capture low level dust as well as being limited by its spatial and temporal resolutions.

Therefore, identifying sub-continental scale activity and dust plumes from numerous smaller pans and other low level dust related features, at a high temporal resolution and during both day and night, is increasingly possible through the use of MSG. In summary, this project intends to answer the following key research questions:

- Where are dust sources in southern Africa?
- How have the advances in satellite technology changed and improved how dust sources are detected?
- Can southern African sites be considered analogous of dust sites globally?
- What are the geomorphologic and climatic constraints to emission on a regional scale?

1.1 AIMS

- To develop a regional understanding of southern African dust sources using the capabilities of both MSG and MODIS sensors.
- To use multisensor satellite imagery to detect aerosols sources and determine how advances in satellite technology have improved our understanding of their behaviour.
- To identify the synoptic and climatic controls of circulation on dust emission in southern Africa.

1.2 OBJECTIVES

This study is founded on the basis of the following specific objectives:

- To review the literature on dust detection, focusing on the strengths and weaknesses of products and sensors in the ultravioltet, visible and infrared spectra
- To identify smaller and more intermittent sources undetected by older TOMS system.
- Employ a multi-sensor approach to characterise dust source in southern Africa.
- To produce a regional dust map and
    - Evaluate the potential of a the multisensor dust detection approach
    - Examine if southern African dust sources can be used as analogues for dust sources elsewhere on the globe.
    - Increase our understanding of geomorphological processes associated with active emission regions
    - Contextualise the systems within the synoptic circulation acting over the region.
- To place sources into their geomorphic context and capture their temporal behaviour
- Evaluate the conclusions and interpretations drawn from the above analyses by assessing them against the backdrop of previous and presently studied dust source regions through multi-spectral and multi-sensor studies

1.3 THESIS OUTLINE

Chapter 2 provides a comprehensive summary of aerosols and dust in both historic and contemporary literature before defining dust and outlining the types of terrain favourable for dust deflation. This is followed by a brief discussion on the importance of aerosols on a regional and global scale, before contextualising southern Africa in global aerosol literature. The chapter then provides an extensive review of dust detection methods focussing on three ranges of the electromagnetic spectrum – Ultraviolet, Visible and Infrared, with specific focus on: TOMS and OMI products, true colour imagery and an infrared composite.

This is followed by the methodology chapter (Chapter 3) describing data retrieval to source point identification using GIS software. The chapter provides more detail on the various satellite data sets utilised in this study as per the categories and theories identified and discussed in chapter 2.

Chapter 4 first presents the results of the data sources by sensor, before discussing the setting of contemporary southern African sources as identified in this study. The Chapter concludes with the results by contemporary region, combining the results obtained through both MSG and MODIS.

Chapter 5 provides a definitive discussion of the results in three thematic sections, namely technology, source and circulation. The first is an appraisal of the techniques used in this study, which the second contextualises the sites identified into three broad categories representative of global source regions. The final theme; circulation, attributes plumes to the dominant circulation feature responsible for emission and proposes a revision of existing volume flux transport estimates over southern Africa.

Finally, chapter 6 provides a synthesis of the overall outcomes of the project through the three themes and concludes the thesis through a reflection on the original aims and objectives and the extent to which they have been met.

2. Dust – detection and impacts

The following review commences with a brief discussion on dust in a historical context from dust in early literature through to early observations of dust both at sea and on land. The review then presents a more modern classification of dust before contextualising southern African sources in global and local aerosol literature as well as their impacts on global and regional scales. The introduction of aerosols into southern African circulation and regional circulation literature is then discussed, with the final theme of the review being a comprehensive discussion of dust detection techniques including a four sensor/product comparison.

2.1 DUST RESEARCH – AN HISTORICAL PERSPECTIVE

Scientific observations of dust have been made throughout the last two centuries (Pye, 1987) including accounts by well known English naturalist Charles Darwin (Darwin, 1889). On one occasion, on the 16th of January in 1833 during the voyage of the H.M.S. Beagle (1831-1836), an account is given on the effects of a dust storm ten miles off the north west end of St. Fargo (Cape Verde Islands):

> *...the atmosphere is hazy; and this is caused by the falling of impalpably fine dust, which was found to have slightly injured the astronomical instruments. ... I collected a little packet of this brown coloured fine dust, which appears to have been filtered from the wind by the gauze of the vane at the mast-head.*
>
> (Darwin, 1889:26).

The aforementioned sample and four further samples were sent to Professor Ehrenberg who concluded through analysis of the various infusoria[1] and sileous matter to contain species he knew to be endemic to South America. The account goes on to describe that:

[1] Infusoria is an obsolete collective term for minute aquatic creatures like ciliates, euglenoids, protozoa, and unicellular algae that exist in freshwater ponds. In modern formal classifications the microorganisms previously included in the Infusoria are mostly assigned to the Kingdom Protista (The Concise Oxford Dictionary, 10th Edition, Oxford University Press, 2001).

... I have found no less than fifteen different accounts of dust having fallen on vessels when far out in the Atlantic. From the direction of the wind whenever it has fallen, and from its having always fallen during those months when the harmatten[2] is known to raise the clouds of dust high into the atmosphere, we may feel sure that it all comes from Africa. ... The dust falls in such quantities as to dirty everything on board, and to hurt people's eyes; vessels even have run on shore owing to the obscurity of the atmosphere. It has often fallen on ships ... more than a thousand miles from the coast of Africa, and at points sixteen hundred miles distance in a north and south direction. In some dust which was collected on a vessel three hundred miles from the lands, I was much surprised to find particles of stone above the thousandth of an inch square, mixed with finer matter.

(Darwin, 1889:27)

Darwin's accounts from the voyage of the H.M.S Beagle are but one of the many descriptive reports of dust storms throughout the nineteenth and twentieth centuries. In Australia and New Zealand reports of storms and 'red rain' are observed in literature by Kidson and Gregory (1930) among others, while examples in North America can be found in Malin (1946) and in Europe dust fallout associated with rain and snow are documented by Seignolis and Arago (1846 as cited in Pye, 1987:5). Prior to these more scientific accounts, literal and figurative references to dust were numerous in early literature, including the 800 BC epic of the Trojan War, in *The Iliad* by Homer. Figuratively, the mention of dust in early literature often holds negative connotations; to images of weakness, disease, death and a lack of morality (Amato, 2000). However, dust was also frequently associated with immeasurable wealth in the form of gold dust and in mysticism often associated with magic and the realisation of the impossible. Dust was also often seen as strategic in war, with one of Ancient Rome's greatest victories being attributed to the poor visibility associated with the easterly wind raising great clouds of dust into the enemies eyes (Amato, 2000).

Throughout history, dust and dust movements have been attributed to part of the earth's continual making and unmaking. Desert storms have been recorded to have "filled the skies for thousands of miles and change seasons, vegetation and landscapes" (Amato, 2000: 5). Over centuries, blown dust has accumulated into geological structures like the loess hills of Iowa and the cliffs of north-west China. Nowhere in history is the mention of dust more prolific than in the north-west American Dust Bowl during the 1930s. From 1932 to 1938 large expanses of the 150 000 square mile Dust Bowl

[2] A dry and often dusty west African trade wind forced by the pressure gradient to the south of the Sahara high in winter and south east of the Azores high in summer (Warner, 2004).

recorded dust-darkened skies turning days into night and causing respiratory disease (Amato, 2000); the 'dirty thirties' were acknowledged to be the consequence of unregulated grazing and agriculture in an unsustainable area.

Despite the long history of reporting dramatic dust transport and depositional events such as those by Darwin and further described by Pye (1987), these were largely descriptive and founded on poor understanding of process and source (Goudie and Middleton, 2006). During the past few decades aeolian dust has become a major environmental topic and as a result research on aeolian sources and transport has demanded a more structured, systematic and quantitative approach (McTainsh et al., 1999; Goudie and Middleton, 2006). Consequently, there have been numerous methods employed for the study of aerosols from long term stratigraphic records using ocean and ice cores to archival studies using reports and accounts from varying media (Goudie and Middleton, 2006). Through the rigorous demands necessary to understand and quantify dust, the requirements changed to encompass the need to quantify frequency, distribution and precise location of the sources.

Therefore in order to be able to understand and quantify dust events, an understanding of dust and the classification of materials and processes needs to be considered.

2.2 CLASSIFICATION OF DUST AND DUST STORMS

Pye (1987) defines dust as a suspension of solid particles in a gas, or a deposit of such particles. While dust is frequently referred to as a mineral aerosol, the term aerosol strictly covers both the particle (dust) and the medium in which it is suspended (atmosphere) (Prospero et al., 1983). However, to conform to most existing literature, the use of the term aerosol will be used simply in reference to the particulate matter itself.

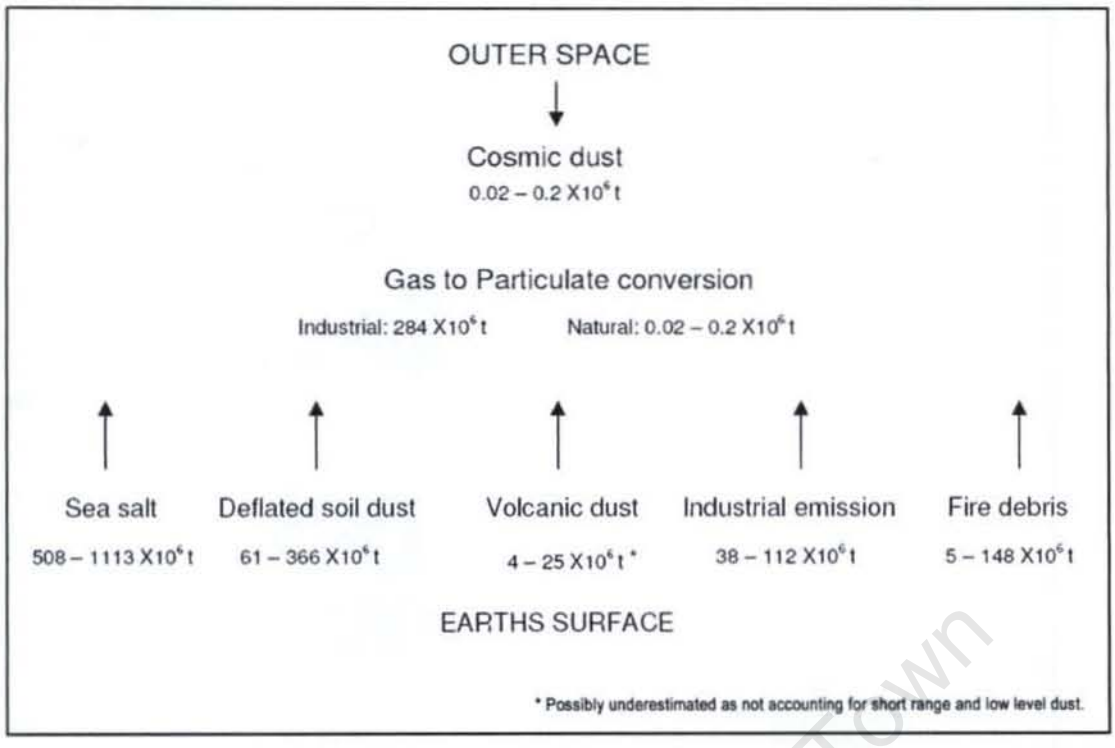

Figure 2. 1 Global sources of airborne particles and approximate annual input into the atmosphere - adapted from Pye (1987).

Classification of aerosols can be conducted through a variety of means including analysis of the grain size, mineralogy and chemical composition. Middleton (1997) and Tyson and Preston-Whyte (2000) provide the following broad classification categories: anthropogenically sourced – e.g. urban pollutants and smoke from biomass burning; and natural sourced – e.g. cosmic dust, volcanic dust, sea salt and soil-derived dust.

While dry and exposed sediments throughout the world have the potential to be classified as soil derived dust once in suspension, the main source of sediment supply sites observed through studies appear to be associated with arid and semi-arid dryland regions. In these regions the prominent role of salt and physical weathering processes act to break down the bedrock and coarse grained products to form dust sized particles (Middleton and Goudie, 2001). Pye (1987) describes atmospheric dust as mostly smaller than 100 µm, while for the particle to be subject to atmospheric transport; grain sizes tend to be in the order of 10 µm to 50 µm, since larger grains settle during decreased turbulence. Middleton (1997) further develops the classification of dust according to particle size with dust particles defined as those smaller than 80 µm or in relation to the silt-sand boundary at less than 62.5 µm (Bagnold, 1941). Prospero (1999) comments that the majority of dust transported over large distances has a median mass diameter of less than 10 µm, while Middleton (1997) elaborates that smaller grain size (2 to 5 µm) results in longer residence time in the atmosphere as well as potential for greater transportation – over hundreds of kilometres.

The precise composition of any dust particle is dependent on the source region and therefore parent material. The most dominant mineral in desert regions is silica, typically in the form of quartz (Goudie, 1978; Middleton, 1997). Other minerals found in deserts include: feldspar, calcite, dolomite, micas, chlorite, kaolinite, illite, smectite, mixed layer clays, palygorskite, heavy oxide and silicate minerals, gypsum, halite, opal, amorphous inorganic material and organic material (Pye, 1987). The dominance of these minerals in the parent material of arid regions allows for the assumption of such minerals dominance in dust (Pye, 1987).

The availability of suitable sediment is not sufficient to result in a dust plume. Aeolian transport will only occur if the multiple forces of interaction are surmounted (Pye, 1987). The sediment once dislodged from the bed, may move by sliding, rolling, saltation or in suspension. Aerosols are then categorized into one of three stages (Pye, 1987:29): (1) entrainment; (2) dispersion; and (3) deposition, with the nature of transport being controlled by both the near ground airflow and the forces of attraction between the sediment and ground surface. The suspended or entrained sediment (dust event) is classified by the World Meteorological Organisation[3] into four categories based on visibility:

1. Dust storms are the result of turbulent winds raising large quantities of dust into the air and reducing visibility to less than 1000 m
2. Blowing dust is raised by winds to moderate heights above the ground reducing visibility at eye level (1.8 m) but not to less than 1000 m
3. Dust haze is produced by dust particles in suspended transport which have been raised from the ground by a dust storm prior to the time of observation
4. Dust whirls (dust devils) are whirling columns of dust moving with the wind and are usually less that 30m high (but may extend to 300 m or more) and of narrow dimension.

Goudie and Middleton (2006) further define the difference between sand and dust storms, concluding that dust storms have the potential to reach higher altitudes, travel longer distances and are mainly composed of silt and clay sized particles. However, despite such finite definitions, due to the dearth of ground based sensors in southern Africa (Prospero, 1999) and with the region further devoid of identified descriptions such as those required for such classification, attributing events to these categories is often not possible. Through the ability of remote satellite sensing to monitor dust events using high spatial and temporal capabilities, we can now remotely detect such storms, although a new set of definitions are required according to the sensors' abilities. While unable to measure the ground based visibility at 1.8 m above the earth's surface, satellites can detect signals

[3] WMO: www.wmo.int – last accessed 10th June 2009

characteristic of dust load according to particle size. The use of multiple sensors introduces a greater chance of detection, although it also introduces multiple definition possibilities. In this study of utmost importance is the differentiation of dust plumes from smoke plumes and background haze. Advances in satellite technology have permitted such differentiation, although there remain many limitations in dust detection.

2.3 GLOBAL DUST SOURCES

Due to the multiple conditions that need to be present and met to result in dust events, there are a set of characteristic terrains that are conducive and most commonly associated with dust deflation. The largest and most persistent dust sources are located in the northern hemisphere (Prospero et al., 2002). These are mainly found in a broad "dust belt" that extends from the west coast of North Africa, over the Middle East, across Central and South Asia, to China. With the exception of a few sites in the southern Hemisphere, there is very little large-scale dust activity outside the "dust belt" (see figure 2.2).

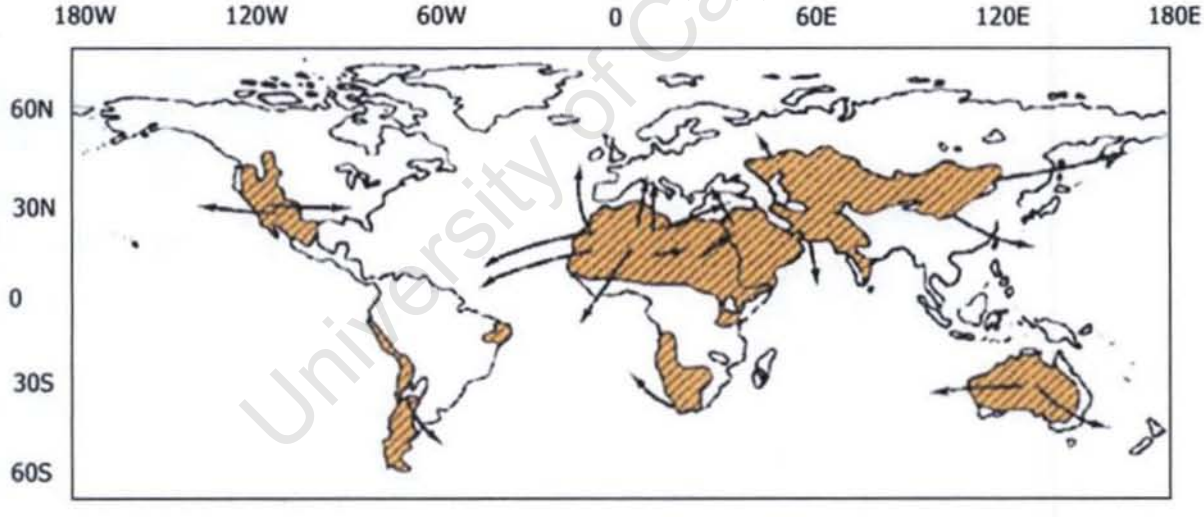

Figure 2. 2 The modern location of dust sources and approximate transport paths reconstructed from observations of dust storms (Livingstone and Warren, 1996).

A study by Engelstaedter and Washington (2007b) has developed a global map of dust hotspots using TOMS, identifying 131 sites globally. Further analysis revealed that 102 (78%) of the 131 hotspots were located in the northern hemisphere dust belt. The approximate location of modern dust sources and their associated transport pathways can be seen in figure 2.2, these dominant regions can be classified into 2 broad categories, as suggested by Pye (1987) to be: 1) sub tropical

desert regions – largely dominated by the dust belt regions, 2) semi-arid and sub-humid regions where dry and ploughed soils are exposed to winds during certain times of the year. These are further classified into more specific terrains with the potential to act as dust sources, with all but the first being associated with arid and semi-arid regions (Pye, 1987); these are: (1) glacial outwash plains and braided fluvioglacial channels; (2) dry wadi beds; (3) dry lake beds; (4) coastal sebkha surfaces; (5) alluvial fans; (6) stony deserts with high weathering rates; (7) exposed argillaceous bedrock areas; (8) areas of loess where the vegetation cover has been reduced by climatic change and/or cultivation; (9) deeply weathered regolith where vegetation cover has been reduced by climate change/human activity; (10) alluvial floodplain sediments, particularly cultivated regions; and (11) areas of formally stabilized dunes which are reactivated through a variety of drivers.

Early research by Goudie (1983) advanced the understanding of source regions, including determining that a threshold mean annual rainfall range of between 100 – 200 mm was optimal for dust production with regions receiving less than 100 mm resulting in markedly fewer dust sources. Globally, Chiapello et al. (1999) suggested that the majority of observed atmospheric dust is derived from susceptible surfaces within dryland environments; regions characterised by desiccated surfaces and reduced vegetation cover allow high velocity winds to deflate and entrain large quantities of dust. An understanding of surface characteristics and correlation of global TOMS studies has led to the development of global dust source maps. Through these studies (Middleton and Goudie, 2001; Prospero et al., 2002; Washington et al., 2003) an understanding of the global distribution of dust sources, regardless of their size or strength, has led to the confirmation of the dominance of arid or semi-arid regions as sources. Using TOMS data, research by Goudie and Middleton (2001) and Washington et al. (2003) developed a world map of annual mean aerosol index (AI) values, identifying numerous sites. Washington et al. (2003) note that it is not merely the AI value of a site which can determine its importance but the areal extent over which emissions occur. However, the two most dominant sources globally, both within North Africa, - namely the Sahara and the Bodélé Depression and the Mauritania-Mali region - contradict the threshold mean annual rainfall range as proposed by Goudie in 1983; this introduces the notion that this region may not be reliant on fluvial input for sediment supply.

The importance of regional and possibly the fluvial constraints on supply result in the dominance of pans, playas and ephemeral systems as sources. Further, these regions are often associated with topographic lows which have the greatest potential for dust deflation. Within arid regions are a network of pans and playas accounting for approximately five percent of modern drylands (Thomas and Shaw, 1991). Despite the small spatial coverage of these systems they are recognised as the dominant source regions (Prospero, 1999; Washington et al., 2003; Bryant et al., 2007). These

hydrological systems are the primary regional sinks for the dust that settles on them or that is transported into them by fluvial processes (either in the past or in the current climate), providing a source of fine grained material that can be readily eroded by the wind (Cooke et al., 1993; Shaw and Thomas, 1997). Ephemeral lake systems with disrupted, wind-erodible surfaces are highly conducive to the work of aeolian processes and the creation of dust (Middleton et al., 1986; Pye, 1987). Evaporite cemented aggregates and cracked, curled edges of bound silt-clay 'skins' protruding into the air on the surface of playas are gradually eroded by the wind and abraded into smaller particles that are deflated from the system.

The natural variability of both aeolian and fluvial processes in dryland environments makes the logistics of monitoring and measuring interactions between them challenging (Bullard and Livingstone, 2002). This highlights the necessity to view them as a coupled system (Bullard and McTainsh, 2003); in addition, at a global scale fluvial activity is not strongly influenced by aeolian systems, while aeolian systems are influenced by fluvial systems. This unequal relationship is in response to the importance of fluvial transport in supplying and sorting sediment (Bullard and McTainsh, 2003). In fluvial systems, the dominant source for aeolian supply is the alluvial material deposited in channels and on floodplains, in some regions these supplies can date back to the Pleistocene providing an extensive supply of deep deposits (Prospero et al., 2002). If fluvial systems fail to provide a consistent supply of fine sorted sediments to source areas, the magnitude and frequency of dust events diminishes (e.g. Clarke and Rendell, 1998). Therefore, where currently active ephemeral streams are a major source of dust, a temporal relationship between the fluvial event and frequency and the dust events can be discerned (McTainsh et al., 1999; Bullard and McTainsh, 2003, Bryant, 2003; Bryant et al., 2007). At the regional scale, interactions between aeolian and fluvial systems take place within dune fields, sand seas and catchments (Bullard and McTainsh, 2003). In particular, perennial or ephemeral rivers act as dust sources through their ability to intercept and create sediment; in some areas even blocking the downwind movement of sand; an example of this is the Kuiseb River which marks the downwind margin of the Namib Sand Sea (Bullard and McTainsh, 2003).

These types of geomorphic features and surfaces are often associated with active landscapes (Pye, 1987) and, while they are frequently located in arid regions with annual rainfall under 200 – 250 mm (Washington et al., 2003), the action of water in the region is often evident from the presence of ephemeral streams, rivers, playas and lakes. Deep alluvial deposits indicative of intermittent flooding are also associated with high deflation potential surfaces (Middleton, 1997; Washington et al., 2003). Additionally, Thomas and Shaw (1997) and Prospero et al. (2002) discuss that such environments are prominent sources of dust due to their nature as receptacles of sediments e.g. the

Bodélé, Taoudenni, Tarim, Eyre, Etosha, Makgadikgadi, Uyuni and the Great Salt Lake (Washington et al., 2003). These sediments are deposited and then exposed through the annual cyclic nature of inundation leading to deposition, followed by deflation through aeolian processes as the waters recede. The periodic renewal of sediments through ephemeral flood inundation events imposes an aspect of supply control on these sources, resulting in a reliance on the flood events to provide the sediment (Shaw and Thomas, 1997). This identifies the importance of large basins of internal drainage as dust sources (Prospero et al., 2002; Washington et al., 2003).

Many sources are associated with areas where human impacts are well documented e.g. the Caspian and Aral Seas, Tigris-Euphrates River Basin, southwestern North America and the loess lands in China (Prospero et al., 2002; Tegen et al., 2004). However, the largest and most active sources are located in truly remote areas where there is little or no human habitation/activity and thus, on a global scale, dust mobilization appears to be dominated by natural sources and processes (Washington et al., 2003). Tegen et al. (2004) confirm the dominance of natural sources, estimating that less than 10% of global dust emissions under present conditions are thought to emanate from agricultural soils – considerably less than previous estimates and therefore further confirming the dominance of natural arid and semi-arid regions globally. Washington et al. (2003) ranked dust sources globally according to a maximum mean aerosol index value as identified by TOMS, with the resultant rankings presented in table 2.1.

Table 2. 1 Maximum mean aerosol index (AI) values (X10) for major global dust sources and their hemispheric location determined from TOMS. (adapted from Washington et al., 2003).

Location	Mean AI Value	Hemisphere
Bodélé Depression of south central Sahara	> 3.0	Northern
West Sahara in Mali and Mauritania	> 2.4	Northern
Arabia (southern Oman/Saudi border)	> 2.1	Northern
Eastern Sahara (Libya)	> 1.5	Northern
Southwest Asia (Makran Coast)	> 1.2	Northern
Taklamakan/Tarim Basin	> 1.1	Northern
Etosha Pan (Namibia)	> 1.1	Southern
Lake Eyre Basin (Australia)	> 1.1	Southern
Makgadikgadi Basin (Botswana)	> 0.8	Southern
Salar de Uyuni (Bolivia)	> 0.7	Northern
Great Basin of the United States	> 0.5	Northern

From an understanding of the chemical and morphological properties of dust, which are indicative of source regions, the resultant broad classification is that globally mineral dusts are dominated by quartz and in the size range commonly referred to as silt/sand and clay. Silt and clay sized particles frequently occur in soils but due to the susceptibility of different surfaces to dust entrainment high silt and clay content does not ensure large scale dust production (Pye, 1987). Compacted, cemented, crusted or armoured surfaces inhibit deflation even during windstorms, while bare, loose and mobile silt and sand sediments are favourable for dust production (Pye, 1987).

The importance of source region characteristics is further discussed in Washington et al. (2003) who emphasise that there are regions globally not identified by TOMS and other satellite products that from surface observations should be active sites. This indicates the need for higher resolution studies and greater characterization of source regions, thus introducing the issues of scale associated with source regions *versus* the spatial resolution of sensors.

2.4 SOUTHERN AFRICAN DUST SOURCES

Southern Africa has unique physical and meteorological characteristics (Ichoku et al., 2003), both of which influence the emission, transport and climate forcing of aerosols. As much of southern Africa is dominated by a savanna type ecosystem (Cowling and Hilton-Taylor, 2003) changing to subtropical and tropical towards the north, while becoming arid and semi-arid to the south west, agricultural practices, vegetation and land cover vary greatly. Since many agricultural practices in savanna type ecosystems are associated with the periodic burning, there is a notable seasonality to aerosol concentration. Based on TOMS data it can be determined that in southern Africa pollution is observed to reach a maximum from September to November as a result of burning in the tropical and subtropical northern reaches of southern Africa (Ichoku et al., 2003). This is confirmed by Torres et al. (2002b) who, when discussing southern Africa and through linking to climatology of rainfall, vegetation distribution and aerosols, assume that the aerosol signals detected in the north-western extent of their study site were entirely a result of biomass burning. Outside of the season typically associated with biomass burning, aerosol concentrations are considerably reduced (Piketh et al., 1999) with dust and industrial pollution then dominating in the aerosol load. Piketh et al. (1999) attempted to quantify an approximate seasonal contribution for each of the four broad categories of aerosols and their relative concentrations to the haze layer. However, limited understanding of aerosol sources and their inclusion in the circulation is vastly oversimplified, thus many sites are not included or the magnitude of their contribution poorly understood.

Regionally, studies on the location and magnitude of terrestrial dust sources have been limited to studies based on TOMS (e.g. Prospero et al., 2002; Washington et al., 2003; Bryant, 2003; Bryant et al., 2007) and a SeaWifs study by Eckardt and Kuring (2005) resulting in the identification of two large pan sources (TOMS) and coastal sources in Namibia (SeaWiFS). This finding is confirmed by Prospero et al. (2002) and Washington et al. (2003), who have shown that global dust sources are often associated with topographic lows in drylands, containing large ephemeral lakes (Table 2.1).

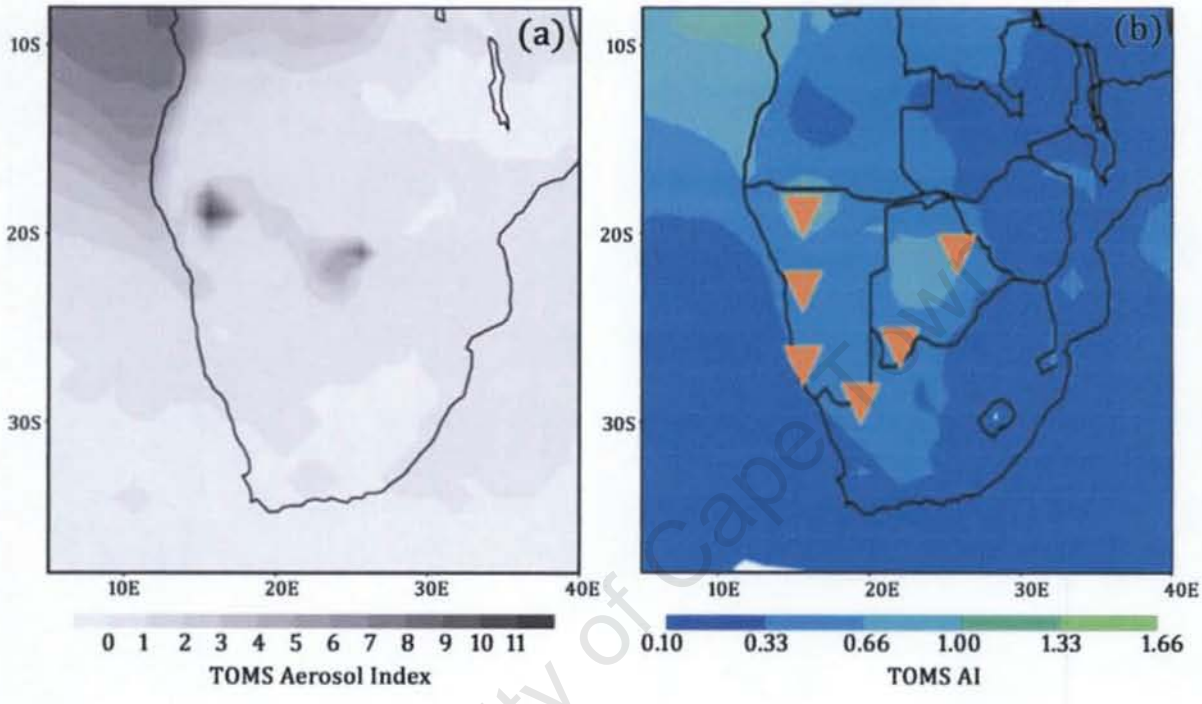

Figure 2. 3 For the domain of southern Africa figure (a) Annual average TOMS aerosol index (AI) values X10 for southern Africa (Washington et al, 2003), (b) Long-term mean TOMS AI averaged over 1984–1990 and location of 6 dust hot spots (modified from Engelstaedter and Washington, 2007a).

Through statistical analysis of TOMS data, Washington et al. (2003) identified the potential of two sources in southern Africa confirming the importance of the Etosha and Makgadikgadi Pans (figure 2.3a). The understanding of southern Africa sources was again advanced in 2007 when Engelstaedter and Washington (2007a) identified 131 dust hot spots. The study identified six regions in southern Africa, using a long term mean TOMS AI to identify regions with an AI mean greater than or equal to 0.5, which was further refined to identify the grid cell with the highest mean AI of the surrounding eight grid cells. This result confirmed the dominance of the Etosha and Makgadikgadi pans and introduced four further regions (figure 2.3b). Figure 2.3b shows the six regions as identified by Enegelstaedter and Washington (2007a); while these regions were not explicitly named or the

sources within these regions identified, the study did provide an increased resolution on which to base subsequent studies.

Dominating the literature are studies based on TOMS which focussed on the two large pan complexes, while studies by Eckardt et al. (2001) and Eckardt and Kuring (2005) using SeaWifs and shuttle photography focus on the Namibian coastline; these have introduced ephemeral river systems as sources. The multisystem interaction between fluvial and aeolian environments has been noted by Bullard et al. (2008) through studies in Australia, highlighting the importance of such interactions at the sub-basin scale. Additionally, Thomas and Shaw (1997) and Prospero et al. (2002) detail that such environments – both pans and rivers – are prominent sources of dust due to their nature as receptacles of sediments. Sediments are deposited and then exposed through the annual cyclic nature of inundation leading to deposition, followed by deflation through aeolian processes as the waters recede. During the inundation, the ephemeral systems function primarily as depositional environments, where fine sediments in suspension in the rivers are transported into the system, and through fluvial processes, sink to the floor of the lake (Engelstaedter et al., 2003).

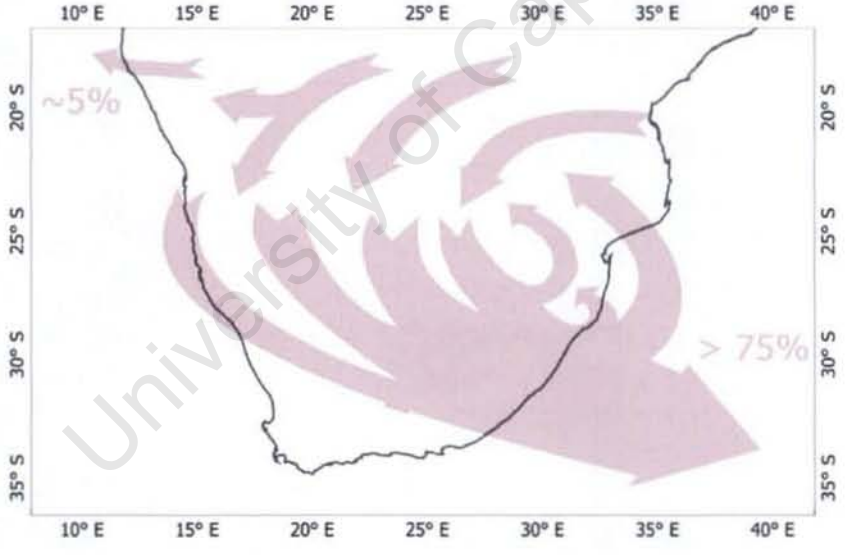

Figure 2. 4 Average Atmospheric transport pathways for aerosols over southern Africa (adapted from Tyson et al., 1996b)

Downscaling current knowledge has evolved through technological developments, from preliminary studies focusing on biomass burning, using approximations of aerosol recirculation and source areas as in figure 2.4. Such studies failed to identify the dominant sources of mineral aerosols due to the focus of the effects of biomass burning.

However, in developing the argument of dust sources from a global/national to more regional scale, Bullard et al. (2008) highlight the importance of inland basins, as per Prospero et al. (2002) and Washington et al. (2003). Importantly it is highlighted by Bullard et al. (2008) that, at this regional resolution (sub-basin scale), surface characteristics are often heterogeneous, frequently containing stone pavements, fluvial systems, aeolian deposits, endorheic depressions and consolidated surfaces. This heterogeneity is of particular importance in the supply-limited system where the dominance of surfaces can determine the supply of sediment through the coupling of the landforms ensuring the sediment source (Bullard et al., 2008).

Global studies on the relationship between geomorphology and dust sources indicate that, while stone pavements may dominate sources in China, stone pavements in the Mojave in the USA resulted in the lowest surface contributor (Bullard et al., 2008). In southern Africa vegetation-free, fine-sedimented ephemeral lakes are thought to be the dominant sources, although the controls on these are poorly understood (Mahowald et al., 2003; Bryant et al., 2007; Bullard et al., 2008).

2.5 GLOBAL AND REGIONAL DUST IMPACTS

Mineral aerosols emitted from sources discussed and many as yet undetected sources globally have the potential to impact the climate system directly by altering the Earth's radiation budget through scattering and absorbing incoming solar radiation, absorbing terrestrial radiation and changing the physical properties of clouds and rainfall (Prospero, 1999; Harrison et al., 2001; Kaufman et al., 2002; Engelstaedter and Washington, 2007; Bryant et al., 2007). The magnitude of the radiative forcing and even the sign (whether the dust forcing will result in a cooling or warming of the Earth's surface) is highly uncertain with estimates ranging from -0.6 Wm^2 to +0.4 Wm^2 (Ramaswamy et al., 2001). Although uncertainties remain with regard to both magnitude and direction of the potential change; the Intergovernmental Panel on Climate Change (IPCC, 2007) has greater confidence in the Fourth Assessment reports than was evident in the Third report regarding their impact. It is now generally agreed that aerosols have a net cooling effect (Ramaswamy et al., 2001). However, there still remains the complication of possible feedback mechanisms which can increase or decrease the radiative forcing effect. Harrison et al. (2001) suggests a net cooling effect, contradicting findings by Brooks and Legrand (2000), which suggests a possible positive feedback mechanism involving rainfall and dust variability.

Other than directly affecting radiation, dust also has an indirect, yet no less important, effect on the nutrient dynamics of both ocean and terrestrial ecosystems at a range of spatial scales (Prospero, 2002; Bryant, 2003; Washington et al., 2003; Reason et al., 2006). As dust particles are in the size

range of a few micrometers and smaller, once in suspension they can remain in the atmosphere without being affected by gravitational settling and thus can exist in suspension for time periods of up to several weeks (Prospero, 1999). Therefore, particles in suspension are subject to distribution by climatic parameters like wind fields and precipitation. Hence they are able to travel thousands of kilometres, with the result that regionalized dust emissions can have a global impact (Middleton and Goudie; 2001).

To illustrate the truly global scale of transport it has been documented that in south Florida north African dust contributed an important part of the ambient aerosol constituent affecting geochemical processes, air quality and therefore human health (Prospero, 1999). Moreover, studies indicate that Saharan dust has an effect on soils in the Canary Islands, the mountains in Cameroon, Barbados, the Bahamas and the Andes (Goudie, 2009) as well as on the ecosystems on the Mediterranean Sea, America coast and Amazon basin, while dust from the Lake Eyre basin (Goudie, 2009; McGowan and Clark, 2006) has been detected in east Antarctica. Another important area of dust research has identified the importance of dust in biogeochemical cycles and soil formation (Yang et al., 2008), with Mahowald et al. (2005) commenting on the role of dust in the delivery of iron and phosphorus to the oceans.

Recent studies in America have concentrated on the effects of aerosols on human health with Prospero (1999) describing that a substantial proportion of wind-borne soil dust is within the classified "respirable" size range, thus having the potential to adversely affect human health. Various studies discuss the possibility of dust outbreaks as disease vectors, with Zender and Talamantes (2006) linking dust outbreaks with coccidiodomycosis[4] and other respiratory and cardiovascular complaints in the United States of America. However, in contrast an asthma incidence study of children living within the depositional range of aerosols from the Aral Sea found no such correlations (Bennion et al., 2007). Therefore while dust storms can result in particulate levels that exceed international standards, not all sources and emissions contain allergens and pathogens including fungi and bacteria (Goudie, 2009) which have the potential to cause disease.

Dust in the atmosphere is indicative of a set of climatic parameters including surface winds and precipitation coupled with surface conditions all of which determine supply (Washington and Todd, 2005). Harrison et al. (2001) note that, according to a model of dust potential, 30% of the total present continental land area, which translates to 5 x 10^6 km² (Sokolik and Toon, 1996), has the potential to be a dust source. Of this determined land area, much is presently not active confirming

[4] A fungal disease caused by infection with *Coccidioides immitis* organisms, causing acute to severe respiratory infections due to inhalation of contaminant spores (Dorlands Illustrated Medical Dictionary, 29th Edition, W.B Saunders Company, 2000 :370)

the unpredictability of both the geomorphology and emissive characteristics of sites and the associated complexity of processes required for emission (Prospero, 1999). This variability coincides with the discovery that the amount of dust reaching polar ice sheets has varied by an order of magnitude on glacial and interglacial time scales (Petit et al., 1981), with increased variability being shown for the most recent decade. Furthermore, supporting evidence for this recent capriciousness of emissions suggests that land use changes are causing a substantial increase in the amount of dust in the atmosphere (Sokolik and Toon, 1996; Neff et al., 2008). Tegen and Fung (1995) estimate that land surface modification by humans or anthropogenically altered mineral dust emissions could be responsible for between 30% and 50% of the total atmospheric dust loadings, with the potential to alter forcing by 1 $W.m^{-1}$, although uncertainty is substantial. Husar et al. (1997) note that aerosol thickness associated with dust aerosol transport from America, Africa and Asia is much greater than those attributed to pollution aerosols. Moreover the dust plumes cover much larger areas and occur more frequently with often greater persistence than those associated with pollutant aerosols.

Considering the important role that dust plays in affecting climate systems and thus the role it may play in future climate change - through its potential to impact the Earth's ecosystems as well as natural and human environments in the future - it is important to determine where the major dust sources are and how dust concentrations vary in space and time. Schepanski et al. (2007) further suggests that much of the discrepancy in terms of the degree to which aerosols affect climate, can be attributed to the chemical, physical and optical properties of the particles, which vary due to different source areas and transport paths. Thus understanding the source characteristics and climatic controls, including transportation from the site, are therefore of great importance.

It is through advances in satellite technology that researchers have developed the potential to better understand where major dust sources are and to a degree detail their variability. Additionally it has provided the ability to track aerosol plumes as they are transported within the atmosphere (Prospero et al., 2002; Washington et al., 2003; Engelstaedter and Washington, 2007). Such advances, have been integral in understanding global and regional aerosols and associated circulation and transportation patterns.

2.6 AEROSOLS IN SOUTHERN AFRICAN CIRCULATION

Acknowledging importance of circulation from the global and synoptic circulation to micro- and meso-scale in both entraining and transporting aerosols and trace gasses in suspension, and understanding circulation is integral to developing both a regional and source specific context to emission. The controls of such circulation are dependant in the vertical scale by the stability of the

column, while the horizontal is primarily driven by surface winds, induced by thermal and topographic gradients as well as synoptic circulation (Tyson and Preston-Whyte, 2000). Due to the lack of topography in regions often dominated by pans (Goudie and Middleton, 2006), induced thermal gradients can be assumed to be the dominant induction method for vertical transport and associated entrainment of mineral aerosols. Over southern Africa it was proposed by Tyson and Preston-Whyte (2000) that despite the multiple synoptic circulation fields that occur in the surface boundary layer and the seasonal migration of pressure fields, the transport of air and entrained aerosols is predominantly towards the east coast and the Indian Ocean. This pattern of circulation results in the "River of Smoke" (figure 2.4) (Tyson et al., 1996; Piketh et al., 1999; Reason et al., 2006) and is estimated to transport 75% of aerosols transported and re-circulated over southern Africa.

This re-circulation is most directly in response to the stable discontinuity at 500 hPa (Tyson and Preston-Whyte, 2000) which traps a pall of aerosols beneath its surface at an altitude of between 4 and 6 km. This stable layer "blankets the whole subcontinent" (Tyson and Preston-Whyte, 2000:288) and occurs throughout the year, most characteristically on rain-free days as are experienced over the subcontinent in the austral spring and summer. These seasons are according to Bryant et al. (2007) typically associated with dust from southern African sources. Despite the claim by Tyson and Preston-Whyte (2000) which identified aeolian dust as the most significant contributor to the regional aerosol load, studies on sources and associated transport are notably absent from quantified studies in southern Africa. Tyson et al. (1996b) comment that many early maps of southern African circulation used "trajectory analyses of one kind or another to determine transport pathways" (Tyson et al., 1996b:266). The majority of analyses are based on individual events or to coincide with field observation periods for example the Southern African Fire-Atmosphere Research Initiatives (SAFARI) of 1992 and 2000, neither of which were initially proposed to measure mineral aerosol load.

Few comprehensive attempts have been made to determine aerosol air transport climatology showing seasonal variations of transport patterns (e.g. Moody et al., 1991; Swap et al., 2003; Abel et al., 2005), although many focus on the effects of biomass burning and associated seasonal signals. Piketh et al. (1999) did attempt to quantify aerosol loadings over southern Africa through the identification of five sites from which they extrapolate a regional scenario – of these, none are associated with regions identified in the literature of the time to be significant source regions e.g. Makgadikgadi and Etosha (identified in amongst others Prospero, 1999).

However, understanding the composition and character of atmospheric transport patterns over southern Africa has advanced over the past five years (Reason et al., 2006). Prior to the SAFARI 1992 much of the research in southern Africa focussed on the concentration of aerosols over the industrialised Highveld. The SAFARI Initiatives in 1992 and 2000 identified that desert dust was a major component of the pall of aerosols to a depth of 500hPa in the atmosphere over southern Africa. This was confirmed in a study by Piketh in 1999 which identified that, in both summer and winter in southern Africa, aerosol loadings are dominated by aeolian dust. This established the importance of including desert dust in the development of a regionalised aerosol map. Reason et al. (2006) outlines that aerosols over southern Africa are from all four broad categories of aerosols: industry, aeolian dust, biomass burning and ocean/sea spray. The distribution and concentration of the observed aerosol gradient was found to reverse between spring and autumn – primarily as a response to biomass burning in the northern parts of southern Africa, with figure 2.5 representing the fire density over the region in September.

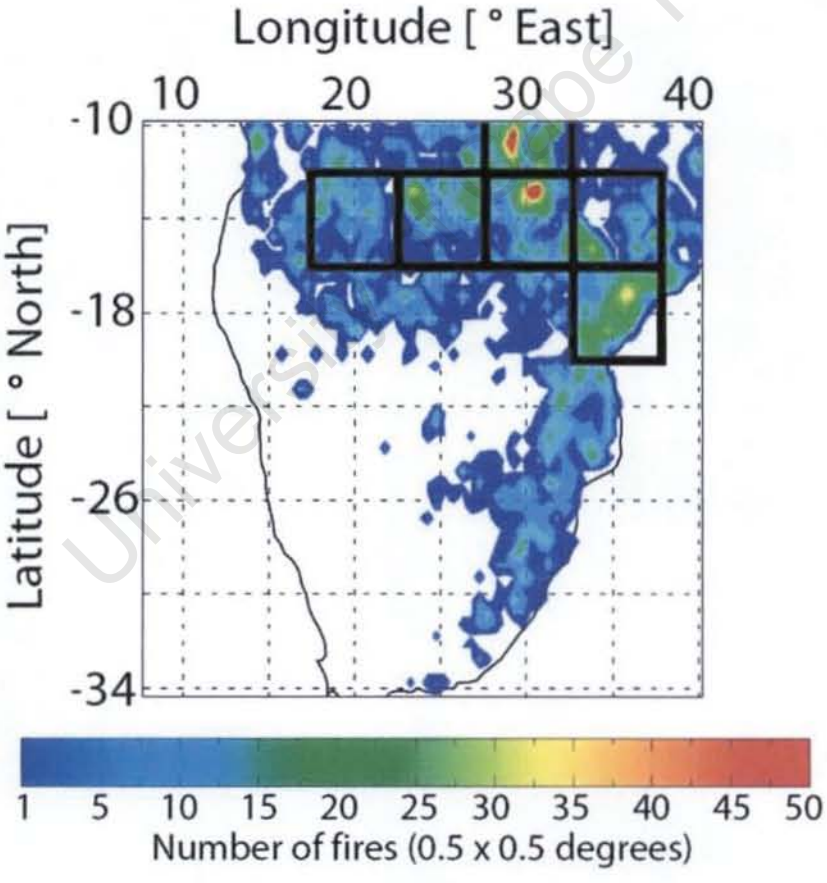

Figure 2. 5 Fire pixels for September (1998–2002 average) over southern Africa as retrieved from the Visible and Infrared Scanner (VIRS) instrument onboard the Tropical Rainfall Measuring Mission (TRMM) satellite. The black squares indicate regions considered in a modelling study in Abel et al. (2005). The figure clearly indicates the extent of biomass burning across the region in September, clearly indicating the prevalence of biomass burning in the north and east – areas typically associated with savanna type ecosystems (Abel et al., 2005).

Biomass burning has been recognized as a significant contributor to the burden of aerosols in continental African and global tropical regions (Abel et al., 2005). The aerosols contain both inorganic compounds and black carbon in addition to many organic substances (Tyson et al., 2002), with the colour and particle size dramatically varying their effects on radiation, further complicating the quantification of their affects on the radiation budget. Tyson et al. (2002) estimate the CO_2 loading, as a result of biomass/biofuel burning over southern Africa, to be 138 $Tg.y^{-1}$ with savanna fires being the largest source of pyrogenic emissions.

The majority of the emitted carbon and other trace gasses contribute to the haze layer that is confined to 500 hPa (4 to 6 km) and is shown to demonstrate seasonal shifting with the frequency and location of burning regions. Figure 2.5, compiled by Abel et al. (2005) shows a four year average for the month of September of fire density over southern Africa. It highlights the importance of the region north of 18°S as a significant contributor to biomass emissions as well as the absence of fires over the west and central interior, thus further confirming that the domain chosen in this study should not be significantly contaminated by biomass burning.

The following section provides a technical literature review of dust detection techniques, looking at three discrete areas in the electromagnetic spectrum, namely the ultraviolet, visible and thermal infra-red. The principles behind aerosol detection as well as the products used for this study based in each range is discussed.

2.7 SPACE BORNE DUST DETECTION TECHNIQUES

The presence of mineral or soil aerosols in the atmosphere has been documented for centuries (Prospero, 1999), extending beyond human history. Torres et al. (2002b) elaborate that the most efficient way to determine aerosol physical properties on the temporal and spatial scales needed to understand and monitor their effects on the earth–atmosphere system is through the use of satellite technology. With the development of this technology, processing capabilities and an increased understanding of the effects of aerosol particles on radiation it has become possible to improve our understanding of the global distribution of aerosols (King et al., 1999). The creation of a global map of aerosols using various methods/products has been seen as a difficult but important challenge (Higurashi and Nakajima, 2002), furthering this challenge, the evolution from exploratory or source detection to a more quantitative based (volume) detection has developed (Kaufmann et al., 2002).

The continuous and repeated mapping of atmospheric dust loadings using remote sensing has been hampered by detection through clouds, the variable spectral response of surfaces, especially bright surfaces, contaminating the signal (Washington et al., 2003) and the inability of products to detect low level plumes (Herman et al., 1997; Hsu et al., 2004; Torres et al., 2002b; Bryant et al., 2007). Figure 2.1 alludes to this underestimate as a caveat when expressing annual input as a function of aerosol type.

The following section discusses detection in the ultraviolet spectrum leading to a TOMS and OMI product discussion, then the visible spectrum using MODIS and finally infrared and MSG; all of these sensors have been successfully used to detect aerosols. The underlying principles behind each technique is presented, showing the evolution in techniques and methods as well as the resolution (temporal and spatial) potential that is now available.

2.7.1. Dust Detection in the Ultra-Violet (UV) spectral range

To interpret the presence of aerosols, more specifically an aerosol index from the radiance measurements made by instruments in the UV spectrum, requires an understanding of how the Earth's atmosphere scatters ultraviolet radiation as a function of solar zenith angle (McPeters et al., 1996). Principally, incoming solar radiation undergoes absorption and scattering in the atmosphere by constituents such as ozone and aerosols and by Rayleigh scattering (McPeters et al., 1996; Herman et al., 1997; Torres et al., 2002a,b). The remaining insolation that penetrates through to the troposphere is scattered by clouds and aerosols and finally, radiation that reaches the ground is scattered by surfaces of widely varying reflectivity/albedo (McPeters et al., 1996). Therefore the requirement for detection involves an understanding of radiation interactions throughout the atmospheric column.

In the near-UV ($\lambda \leq 310$ nm) the incoming radiation is absorbed by ozone, while in the longer wavelengths ($\lambda \geq 310$ nm) the backscattered radiance consists primarily of solar radiation that penetrates the stratosphere and is reflected back by the dense tropospheric air, clouds, aerosols, and the Earth's surface (McPeters et al., 1996), with the intensity of the returned signal being a function of the optical depth above the scattering layer (cloud, aerosol, land surface). Once an understanding of the column ozone and surface albedo has been gained, a further level of complexity is added in that aerosols can be either absorbing of non absorbing in the UV spectrum depending on the characteristics of the aerosol (size, morphology, composition) (Herman et al., 1997; Torres et al., 2002a). With an increased understanding of the nature of absorbing particulates (e.g. smoke from biomass burning, desert dust, and volcanic ash) and particularly their behaviour in response to the longer UV wavelengths (340 nm and 380 nm), many UV products are able to

distinguish between absorbing particulates and non absorbing particulates (e.g. water clouds, haze and H_2SO_4 – volcanic aerosols) (Seftor et al., 1997). An early model, the Lambert Equivalent Reflectivity (LER) model proposed by Dave (1978), detailed the wavelength dependencies of observed radiation. This model utilised an atmosphere bounded by a Lambertian surface of reflectivity *R* estimated from measured radiances. The deviation between the modelled *R* and a pure Rayleigh scattered atmosphere (a function of the biodirectional reflectivity distribution function – BDRF) is as a result of molecular scattering, with a positive residual indicating the presence of UV-absorbing aerosols and a negative residual non absorbing (Herman et al., 1997; Seftor et al., 1997).

In addition, the use of UV reduces many of the limitations associated with the visible wavelengths, permitting a greater degree of type detection, although it also introduces a height bias, further complicated by bright land-surfaces (Herman et al., 1997; Kaufman et al., 1997), that are typically associated with dust sources (Kaufman et al., 1997; Washington et al., 2003; Bryant et al., 2007).

In this study two UV products were used, namely the Total Ozone Mapping Spectrometer (TOMS) and the Ozone Monitoring Instrument (OMI) whose algorithms are comparable.

2.7.1.1. Total Ozone Mapping Spectrometer

The TOMS sensor on board the Nimbus-7 satellite, launched in 1978, made available the first continuous 14.5 year record of global aerosols at an approximate resolution of noon time daily coverage (Herman et al., 1997). The sensor measured solar irradiance and backscattered radiance by the Earth's atmosphere in six wavebands in the range from ultraviolet to visible (McPeters et al., 1996), with the aerosol algorithm based on multispectral measurements in the ultraviolet wavelengths (Prospero, 1999; Washington et al., 2003). This algorithm has been utilised due to its ability to detect aerosols over both land and water due to the low spectral reflectivity from both surface types in this spectral range (Herman et al., 1997; Bryant, 2003).

The measured backscattered UV radiance is confined to six wavebands each 1 nm wide at 313 nm, 318 nm, 331 nm, 340 nm, 360 nm and 380 nm. The longest three utilised in the algorithm due to the low levels of ozone absorption in this range, thus the backscattering is primarily controlled by Rayleigh scattering (molecular), Mie scattering (aerosols and clouds) and surface reflection (Herman et al., 1997; Kaufman et al., 1997). Since the launch in 1978, two further satellites, Earth Probe (EP) and the Aura Space Craft, have provided TOMS and TOMS-like products for long term comparative studies, thus providing an almost 30 year continuous record.

The TOMS aerosol index (AI) developed using the difference between observed spectral contrasts at 340 nm and 380 nm, defined by Herman et al. (1997) using the N-value residual method

$$\Delta N_{340} = -100\left(\log_{10}\left(\frac{I340}{I380}\right)_{obs} - \log_{10}\left(\frac{I340}{I380}\right)_{calc}\right).$$

Where $I_{\lambda meas}$ is the measured backscatter radiance at the given wavelength, and I_{calc} is the calculated radiance corrected using the modified Lambert Equivalent Reflectivity (LER) model attributed to Dave (1978).

The resultant output is a continuous, non-quantitative index with values ranging from 0 (low) to 30 (or 3.0) (high aerosol loading) (see figure 5.1 in Chapter 5). The aerosol product has been corrected using model output data for different aerosol types combined with the ΔN value; and is available online (ftp://jwocky.gsfc.nasa.gov/pub/nimbus7/data) with a 1°X1.25° lat/long grid resolution and daily global coverage. As this modelled component gives a near zero residual in the presence of clouds, positive or negative residuals are indicative of absorption (Herman et al., 1997) with UV absorbing aerosols resulting in positive residuals due to the contrast being smaller than predicted in the LER model, while non-absorbing produce negative residuals. Therefore it is possible to differentiate between absorbing and non-absorbing aerosols, and thus remove a component of cloud contamination (Herman et al., 1997) permitting quantitative calculations of optical depth and single scattering albedo. Further, due to the differing spectral response of various aerosol types, according to dimension, smoke (larger) to soil dust (smaller), are distinguishable as the associated absorptive properties of the aerosols differ in the ultra-violet wavelengths (Herman et al., 1997; Goudie and Middleton, 2001). Also integral to the TOMS aerosol detection technique is the knowledge that the combination of two independent sets of information; namely the I_{340}/I_{380} spectral contrast and the change in backscattered 380 nm radiance which, when combined, allow for the detection of particulates within a Rayleigh scattering atmosphere (Herman et al., 1997).

Limitations associated with TOMS have been attributed to its inability to detect through the presence of cloud (Herman et al., 1997; Goudie and Middleton, 2001), and associated dense atmospheric moisture layers as well as aerosols confined to within 1-2 km of the ground surface – a function of both planetary boundary layer height (PBLH) (Mahowald and Dufresne, 2005) and the relatively small signal received due to the small amount of underlying Rayleigh scattering and the apparent noise from surface reflectance (Herman et al., 1997).

TOMS data was acquired at the 1 X 1.25° spatial and daily temporal resolution from the NASA Goddard Earth Sciences (GES) Data and Information Services Centre (DISC) Distribution Active Archive Centre (DAAC) Giovanni interface.

2.7.1.2. Ozone Monitoring Instrument

The Ozone Monitoring Instrument (OMI) is a Dutch-Finnish ozone monitoring instrument on NASA's Aura Mission, part of the Earth Observation System (EOS), launched in January 2004. OMI has extended the long, continuous daily global record produced by TOMS, using a refined algorithm based on the TOMS original (King et al., 1999; Levelt, 2002; Torres et al., 2002a,b).

The Aura spacecraft is a sun-synchronous polar orbiting satellite with a local afternoon equator crossing time at 13:45, providing daily global coverage. OMI measures the reflected solar radiation in the range between 270 and 500 nm with a spectral resolution of about 0.5 nm. The light, upon entering the instrument, is split into two channels: the UV channel (wavelength range 270 - 380 nm) and the VIS channel (wavelength range 350 - 500 nm) (Torres et al., 2002a). The OMI aerosol algorithm uses the shorter of the two wavelength ranges (ultraviolet), further preferring the longer parts of the UV spectrum (UVA: 320-400 nm) where the surface UV irradiance is mainly determined by clouds, surface elevation, and the presence of aerosol and snow (Stammes, 2002a). In the shorter ultraviolet wavelengths (UVB: 280-320 nm), surface irradiance is increased with stratospheric ozone layer depletion, reducing aerosol detection capability. The result is that the OMI algorithm is based on the interpretation of the reflectance in the range from 331 to 400 nm – where irradiance is mostly controlled by aerosol presence. The algorithm is created using look up tables (LUT's) with a derived radiative transfer model as well as surface albedo data (Stammes, 2002a).

The product extracted for this study, uses the near-UV method which is the best TOMS approximation and experience in the application of this method compared with and to the TOMS data (Torres et al., 2002b) has proven this method to be a robust retrieval approach. The near-UV method utilises two wavelengths in the near ultraviolet range (namely 342.8 and 388 nm) and is able to directly retrieve the optical thickness and single scattering albedo (King et al., 1999; Torres et al., 2002a). Further the near-UV technique is uniquely sensitive to mineral dust and volcanic ash aerosols (Torres et al., 2002a). The other significant advantage of this method over other methods including the multi-wavelength (dominantly over the ocean) approach, is the ability to retrieve aerosol properties over all terrestrial surfaces (free of ice and snow) (Torres et al., 2002a; Krotkov et al., 2002) including arid areas which are highly reflective in the visible and near infrared, but very low reflectivity in the UV.

The algorithm for the OMI aerosol optical thickness product as defined by Torres et al., (2002a) is:

$$a_{\lambda_2} = -100log\left\{\left(\frac{I_{\lambda_1}}{I_{\lambda_2}}\right)_{meas}\right\} + 100log\left\{\left(\left(\frac{I_{\lambda_1}}{A_{LER\lambda_1}}\right) \Big/ \left(\frac{I_{\lambda_2}}{A_{LER\lambda_2}}\right)\right)_{calc}\right\}$$

Where $(I_{\lambda_1}, I_{\lambda_2})_{meas}$ are the measured radiances corresponding to λ_1 and λ_2 ($\lambda_1 < \lambda_2$); and $(I_{\lambda_1}, I_{\lambda_2})_{calc}$ are the corresponding calculated radiances for the same wavelengths as for the measured. A_{LER} is the wavelength dependent surface Lambert equivalent reflectivity (Torres et al., 2002a).

For this study to give the closest TOMS equivalent λ_1 = 342.5 nm and λ_2 = 388.0 nm which results in a UV aerosol index, a_{388}. If 388 nm and 494.5 nm are used the resultant index is at a_{494} and a near visible index which allows the separation of carbonaceous aerosols as they are negative in this wavelength range (Hsu et al., 1996; Torres et al., 2002a). When carbonaceous aerosols exhibit extremely large values (AI<2), smoke and dust are no longer differentiable and therefore the a_{388} index was further deemed the best for this study. Like TOMS, the height bias associated with near surface Rayleigh scattering affects OMI, this is particularly evident for absorbing aerosols (error in optical thickness for strongly absorbing aerosols up to 60%), while non absorbing aerosols are unaffected (error predicted at ±2%). Therefore, depending on the aerosol type, numerous vertical distribution models are used in calculating aerosol profiles to reduce error. For southern Africa an exponential profile is used with a maximum at a 2 km scaled height, while biomass burning uses a single layer Gaussian distribution whose maximum concentration is expected at 3 km (Torres et al., 2002a).

The OMI product has a resolution of 20X20 km^2 which is an improvement of the 50X50 km^2 found in TOMS and the 40 x 320 km^2 available with GOME (for further discussion see Stammes, 2002b). This higher resolution results in more pixels; therefore a greater chance for representing cloud-free scenes and thus a greater potential for aerosol detection (Stammes, 2002a). This improvement in detection and higher pixel resolution can be seen in figure 5.2 representing the OMI product when compared to figure 5.1 representing the TOMS product over the same area.

2.7.2. Detection in the Visible spectral range

Typically the visible spectrum has been reserved for detecting and tracking dust as it is transported over the ocean, where the pale dust contrasts strongly against the dark background (Prospero, 1999; King et al., 1999; Eckardt and Kuring, 2005; Schepanski et al., 2007). Figure 2.6 showing dust plumes over various surfaces highlighting the clear contrast between plumes and the ocean (c and d) as well as different dust sources and perspectives. According to Prospero (1999) dust plumes are one of the most prominent and commonly visible atmospheric constituent features in satellite imagery, due to their potential to cover large areas. The storms seen in figure 2.6a and b are examples where the dust storms covered hundreds of kilometres.

Due to airborne dust having similar reflective properties as the underlying land, Lee (1989) discusses the limitations of using visible images over land concluding that they are generally not suitable alone for detection, and best used in combination with other products. However, developments in algorithms and the knowledge of band combinations have led to algorithms based on visible wavelengths being developed (e.g. Meteosat - Devasthale et al., 2008; Brindley and Ignatov, 2006, MODIS - Hsu et al., 2004, SeaWifs - Miller, 2002, Landsat 5 -Kaufman et al., 2000).

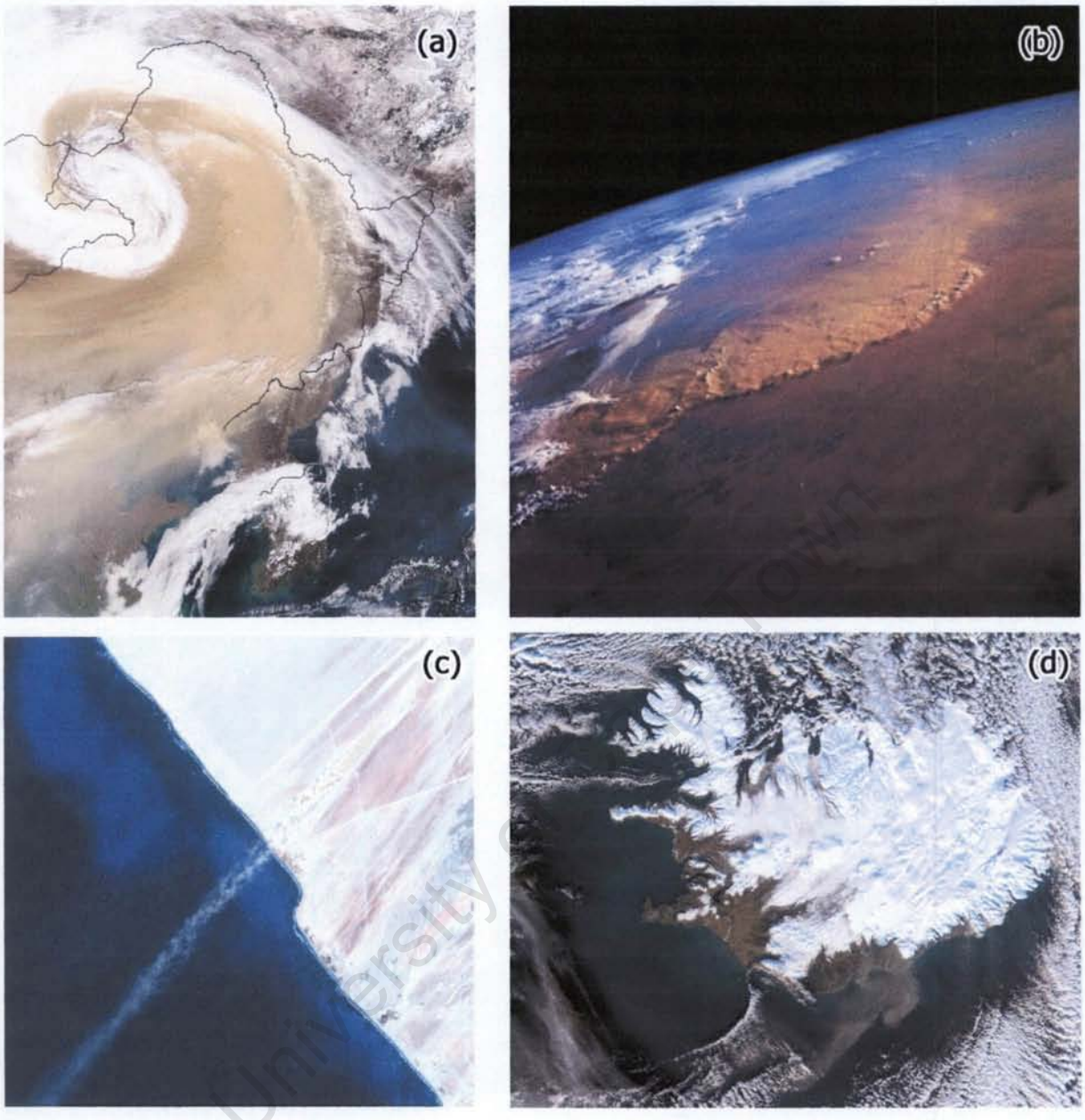

Figure 2. 6 Visible images of dust storms globally by multiple sensors. Figure a) April, 2001: A dust cyclone swirls over north-eastern China. The cyclonic cloud is pushing a wall of dust, which covers the land beneath, and some of the clouds. (MODIS – Terra, Image courtesy NASA/GSFC, MODIS Rapid Response). b)May, 1992. View from the space shuttle Endeavour of a huge dust storm in the Sahara desert, which covered hundreds of miles in Libya and Algeria (Image courtesy NASA online featured imagery). c) July 2000 – Landsat 7 ETM of a dust plume emanating off the Namibian coastline north of Hentiesbaai (image courtesy Dr F Eckardt). d) January 2002 – Terra image capturing glacial outwash dust off Iceland (Image courtesy NASA Earth Observatory Image Gallery)

While the majority of studies of dust in the visible spectrum using true colour images are focussed on detection over the ocean, in this study MODIS images are used to validate coastal and terrestrial plumes identified using primarily the MSG composite (see also Washington and Todd, 2005;

Washington et al., 2006b; Bullard et al., 2008); as well as the primary detector for coastal emissions where the plumes travel over the ocean (Eckardt et al., 2001; Eckardt and Kuring, 2005).

2.7.2.1. Moderate Resolution Imaging Spectroradiometer

The Moderate Resolution Imaging Spectroradiometer (MODIS) flies onboard NASA's Aqua and Terra satellites as part of the NASA-centred international Earth Observing System (Vermote and Vermeulen, 1999). Both satellites orbit the Earth from pole to pole with a near total (95%) daily coverage (Chu et al., 2003). Onboard Terra, the MODIS sensor provides morning coverage while the sensor on Aqua provides afternoon coverage (Vermote and Vermeulen, 1999; Washington et al., 2006b) (equatorial crossing time 10:30 am GMT and 1:30 pm GMT (Chu et al., 2003)) permitting a diurnal analysis. From this diurnal coverage, it is possible to generate a higher temporal resolution, compared to similar products from MISR (Multiangle Imaging Spectroradiometer) also onboard the Terra satellite which provides global coverage in 6-9 days (Chu et al., 2003). MODIS has 36 spectral bands ranging in wavelength from 0.4 μm to 14.4 μm and is designed to remotely sense atmospheric temperature, moisture profile, clouds, aerosols, and surface properties (Huang et al., 2007).

For this study the true colour composite images were analysed for the presence of dust as well as used for validation of signal through correlation with the rapid fire product. The colour composites available online through the Rapid Fire website (http://rapidfire.sci.gsfc.nasa.gov/) at differing resolutions (2 km, 1 km, 500 m and 250 m) provide a time series of images which can be analysed for dust activity. True-colour images were produced from attributing the red (channel 1: 620-670 nm), green (channel 4: 540-570 nm) and blue (channel 3: 460-480 nm) bands to the red, green and blue channels, respectively. This true colour composite which was available for multiple domains over southern Africa were selected for use in this study.

2.7.3. Dust detection in the Thermal Infra-Red (TIR) spectral range

Infrared detection of aerosols has a distinct advantage over visible and to a degree ultraviolet, in that it is able to provide coverage over bright surfaces and during both the day and the night, thus permitting a better understanding of the cyclicity of dust emissions (Ackerman, 1997). Difficulties involved as discussed by Ackerman (1997) revolve around the variability of surface and atmospheric emissivities.

Several techniques have been proposed for detecting mineral dust and volcanic ash using thermal-infrared observations (Ackerman, 1997; Legrand et al., 2001). In this range, detection is based on brightness temperature differences (BTD) in either two or three channels. The former is called the

bispectral split window technique and the latter is the trispectral approach (Darmenov and Sokolik, 2005). Although the split-window techniques have been primarily applied to volcanic aerosols, they have also been used for the detection of dust. With Ackerman (1997) arguing that the trispectral approach is likely to provide a more robust dust detection, as these three channels are associated with weak absorbivity by gases. The largest signal for aerosols in the infrared range is in the spectral variation in the 10-12 μm and 8-10 μm ranges which correspond to a region of high atmospheric transparency and for this reason techniques have been developed using these spectral ranges (Ackerman, 1997).

The fundamentals behind the detection are based on the characteristic depression of brightness temperatures (BT) due to the high absorbivity of aerosols in the three window channels; 8 μm, 10 μm and 12 μm (Ackerman, 1997) and low absorbivity of gases. Further, using a combination or multi-channel approach for detection increases the ability of the product to distinguish between dust and potential contaminants; for example water vapour and ice especially over land, while over oceans a single channel can often be sufficient (Ackerman, 1997). Legrand et al. (2001) summarise the detection principle using the radiance decrease in the thermal infrared bands due to the presence of dust as being the response to (1) a cooled ground surface due to the dust radiative impact on the shortwave outgoing radiation and (2) the fact that measurements by the satellite are made through the cooler attenuating dust layer. With Legrand et al. (2001) estimating that the related drop in temperature, associated with the decrease in downward shortwave irradiance being as much as 10°C for extreme dust events over bare, dry soils, as are characteristic of arid surfaces.

The decreased radiance discussed above can further be used to determine the optical depth of the aerosols if the surface spectral emittance is known (Ackerman, 1997), with increased optical depth increasing $BT_{11} - BT_{12}$ and $BT_8 - BT_{11}$.

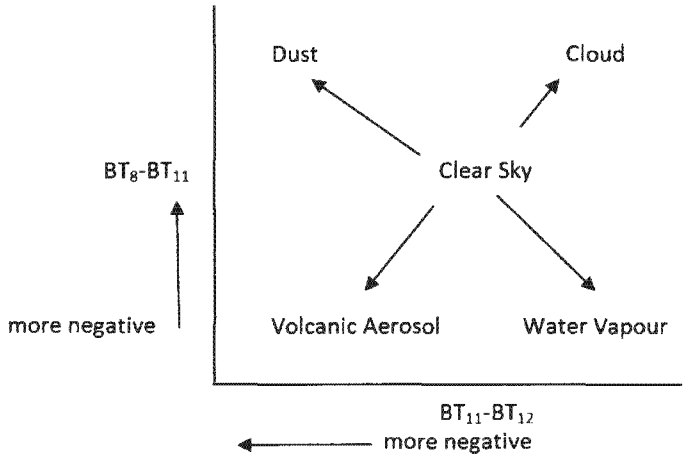

Figure 2. 7 Schematic representation of the effects of different atmospheric constituents on the brightness temperature difference used in infrared detection: 11 – 12 μm and 8 - 11 μm (derived from Ackerman, 1997)

Figure 2.7 shows how the brightness temperature difference between $BT_{11} - BT_{12}$ and $BT_8 - BT_{11}$ can be used to distinguish between the various aerosol types. It is the BT difference between $BT_8 - BT_{11}$ that distinguishes volcanic (sulphur rich) aerosols from soil derived aerosols and $BT_{11} - BT_{12}$ that primarily distinguishes cloud from dust. Li et al. (2007) details that BT_{11} shows a quasi-linear relationship with the aerosols optical thickness, while the BT_{11}-BT_{12} exhibits a quasi-linear relationship with the particle radius and $BT_8 - BT_{11}$ is more dependent on particle size than temperature (Schepanski et al., 2007).

2.7.3.1 Meteosat Second Generation

Due to the high spatial and temporal resolution provided by MSG and the required channels for thermal IR detection being onboard SEVIRI, MSG was chosen as the primary data source for this study. The Spinning Enhance Visible and Infrared Imager (SEVIRI) onboard Meteosat Second Generation (MSG / Meteosat-8), launched in 2002 is part of the new Generation of European meteorological satellites with a nominal position at 0° longitude. The 12 channel imager (Schmetz et al., 2002) provides coverage of the earth's full disk with a 15 minute repeat cycle, with 11 channels providing full coverage at 3 km resolution; while the 12th channel – the high resolution visible (HRV), covers half the full disk in an east west direction and full disk in north south direction at 1.67 km.

The development of the IR algorithm for dust detection discussed above, and more specifically the development of the trispectral brightness temperature difference (BTD) algorithm, for use with the infrared bands from the geostationary Meteosat Second Generation (MSG) satellite, (Schmetz et al., 2002; Legrand et al., 2004; Brindley and Ignatov, 2006; Schepanski et al., 2007) has made high resolution dust detection possible.

A dust index product developed for MSG using a composite picture configuration, (EUMETSAT product guide), uses the three infra-red bands centred at 8.7 μm, 10.8 μm and 12.0 μm (channels 7, 9 and 10 respectively). These are ideally suited to the detection of mineral dust as, at these wavelengths, biomass burning and industrial aerosols are largely undetected due to particles size differences and the associated effects in radiance (Brindley and Russel, 2006). Further mineral dust is well detected in these wavelengths over semi-arid and arid landscapes (Schepanski et al., 2007).

The composite picture configuration discussed by Schepanski et al. (2007) and further detailed on EUMETSAT website (http://www.eumetsat.int) can be summarised as follows:

R : IR12.0 μm – IR10.8 μm

G : IR10.8 μm – IR8.7 μm

B : IR10.8 μm

To this temperature ranges are clipped and gamma enhancements applied; to the red channel, temperatures -4K to 2K with a 1.0 gamma correction; green 0K to +15K with a 2.5 gamma correction and blue 261K to 289K and a 1.0 gamma correction.

This colour composite was designed to monitor the evolution of dust storms, particularly over deserts (Ackerman, 1997) where previous studies were limited. In addition it is capable of tracking dust clouds as they spread over the sea, although the use of the High Resolution Visible (HRV) (1.67 km at nadir) is preferable for the tracking of dust over the ocean. Legrand et al. (2001) discuss the value of this and similar infrared based algorithms on coastal regions, concluding that even in arid regions, the 'edge effects' due to advection of cool humid oceanic air masses have the potential to reduce the feasibility of such method in these regions. For this study the straight composite was used over the full domain (see figures 4.11a,b and c (page 72) for example of the edge effects and 4.15a,b and c (page 77) for pink plume).

2.8 SUMMARY OF DUST DETECTION TECHNIQUES

The previous section has discussed detection in three spectral ranges (ultraviolet, thermal infrared and visible) as well as their application in a selection of products used in this study. While each product has successfully been used to detect aerosols over a variety of surfaces there are

advantages and disadvantages as well as challenges and limitations associated with many of these products as is summarised below.

Table 2. 2 Summary Table of identification of aerosols based in different spectral ranges and the associated challenges/benefits of different products

	Ultra-Violet (TOMS and OMI)	Visible (MODIS)	Thermal Infrared (MSG)
Land	Land surface albedo variability low in near-UV	Pale dust disappears over pale desert surface	Cool dust contrasts well over heated land
Sea	Ocean surface albedo variability low in near-UV	Pale dust contrasts well over dark ocean background	Cool dust disappears over cool ocean background
Cloud	Algorithm to mask out clouds limits the use of the product under cloudy conditions	Thick clouds hide the plume	Clouds have a potential to contaminate the signal
Height	Aerosol height is a limitation for detection in this range	Detection is not affected by the height of the plume	Detection is largely unaffected by the height of the plume
Temporal	Daily coverage limits the use of the product as many plumes are not identifies	Twice daily coverage can detect diurnal variation	Very high temporal resolution can capture sporadic variability of emissions
	Once daily (TOMS) twice daily composite (OMI)	Two images per day – strong diurnal sequence	96 images per day
Spatial	Poor spatial resolution increases possibility of cloud contamination	Very high spatial resolution aids in source identification	High spatial resolution increases possibility of identification

In general, detection and associated challenges can be attributed to the surface over which detection is being made, the spatial and temporal resolution of the sensor and product, the height of the aerosol and the presence/absence of clouds. For the different products one or more of these are relevant, with the presence of clouds being the greatest limitations for space based detection of aerosols, and therefore affecting all sensors/products. The following section will discuss the above tabulated challenges and advantages for each of the relevant products/sensors.

2.8.1. Spectral Resolution

As a result of the different products utilising differing spectral ranges and detection techniques, products have varying sensitivity to both detection and aerosol distinction. Torres et al. (2002b) conclude that the near UV method has a greater accuracy when compared to visible composites due to its smaller sensitivity to aerosol phase function effects – multiple and single scattering properties. However, near UV is unable to separate the different types of absorbing aerosols (Torres et al., 2002b) due to the spectral closeness of the two channels most frequently used with this technique namely 330 nm and 380 nm. Further the associated lack of spectral contrast between different types of absorbing aerosols in this range reduces the sensitivity of this composite. This lack of sensitivity can result in the incorrect identification of smoke and dust aerosols, with an underestimate (smoke identified when dust present) or overestimate (dust identified where smoke present) of the aerosol optical depth and therefore a misrepresentation of conditions (Torres et al., 2002b).

However, for TOMS and OMI under cloud free conditions the accuracy of the retrieved product is assumed to be primarily a response to surface reflectance and aerosol layer height, with issues of misidentification being limited to only a few sites globally where there is both biomass burning and surface deflation of mineral aerosols (Torres et al., 2002b). Another major limitation of many modelled and calibrated aerosol products is the assumption of total particle sphericity, which according to Brindley and Ignatov (2006) is not necessarily representative of a dust particle.

The dependence of dust detection on wavelength, and the optical 'thinness' of dust at certain wavelengths (due to link between particle wavelength interactions and Rayleigh scattering (Torres et al., 2002b)) results in the apparent disappearance of dust in visible and infrared images (Duda et al., 2006). Therefore, MSG and AVHRR images are not optimal for dust detection. In contrast the addition of short wavelengths on MODIS and SeaWifs sensors make these sensors/products more suitable to detection. Despite the identification of the optical 'thinness' of dust in the visible and infrared range, Huang et al. (2007) discuss the sensitivity of the brightness temperature difference approach as being high to dust detection in that it is able to identify weak dust storms. Although like

TOMS and OMI it is unable to discriminate dust from smoke, this major limitation of the composite can be minimized through the correlation with fire products and analysis of individual infrared bands, in which the two signals are less similar (Huang et al., 2007). The independent analysis of selected band widths and their differences can further reduce this limitation of infrared, in that independently the $BT_{11} - BT_{12}$ range can be used to determine aerosol type, to mineralogical resolution (Darmenov and Sokolik, 2005). This sensitivity advantage of IR BTD can aid in the attribution of aerosol plume to source region due to the different sources having different spectral responses in this range.

2.8.2. Challenges of detecting dust over surfaces: a contrast issue

Land surface and, therefore, the domain of a study determines the validity of each product, as TOMS was proven to be useful in detecting over both land and ocean (Torres et al., 2002b) due to the sensitivity of the near UV approach over most surfaces. Swenk and Curran (1974) highlight the applicability of visible wavelengths due to the strong spectral contrast of pale dust over dark ocean surfaces. Thus for oceanic detection, while the visible permits the tracking of plumes for days, in the infrared such contrast is insufficient for optimal detection and so is of limited use. Hsu et al. (2004) expand on this argument for different wavelengths, stating that in shorter wavelengths (blue to ultraviolet) highly reflective surfaces such as those associated with arid landscapes appear relatively darker making detection easier. In this range dust optical properties are more variable. Whereas in the red to infrared range there is little absorption of dust and the land-surface is brighter, therefore reducing the sensitivity in this range.

From table 2.2 and through discussion within this section the many challenges and advantages of different products are highlighted. While TOMS with its poor temporal and spatial resolution is of limited use in a study in which source regions need to be identified, it was the first to produce a long term record of aerosols over both land and the ocean (Torres et al., 2002c) and was used to develop our current understanding of the global distribution of mineral aerosols (Prospero et al., 1999; Washington et al., 2003). The developments in TOMS-like analogues has allowed for a continued time series of data from which seasonal and inter-annual variability of dust can be analysed (Torres et al., 2002b) with developments permitting greater spatial resolutions to these products.

Chu et al. (2003) and Huang et al. (2007) comment on the use of MODIS visible and associated composites to detect dust source regions and mineralogical classification of the aerosol at different optical depths. With Schepanski et al. (2007) utilizing the BTD from MSG to detect dust source regions and associated variation at the high temporal resolution provided by this product.

2.8.3. Cloud cover

Clouds are one of the single largest challenges to detection of aerosols, as both high and low clouds obscure the surface on satellite images (Prospero et al., 1999; Torres et al., 2002b,c). While cloud masking has been used to reduce cloud contamination on signal (particularly in infrared composites), Brindley and Ignatov (2006) conclude that, even through the use of high resolution infrared imagery and algorithms used to separate clear and cloudy conditions, dust continues to be misclassified as cloud and *vice versa*. To reduce this error, the authors suggest visual analysis as the best alternative (Brindley and Ignatov, 2006).

Even though cloud masks are becoming more widely utilised (Brindley and Ignatov, 2006) they are heavily reliant on calibrabration, owing to the OMI sensor not having thermal channels (King et al., 1999). However for OMI this error is partially reduced as the relatively small pixel size permits a greater chance of a cloud free pixel. The height of the cloud greatly affects the detection and masking capabilities due to the temperature associated with different clouds, for example high level cirrus clouds which are often associated with frontal systems have very similar temperature responses to those associated with aerosols (Huang et al., 2007). This is further complicated as in many regions dust transport is associated with frontal systems, as discussed by Huang et al. (2007) in the context of Asian dust storms. Huang et al. (2007) states that the BTD algorithms and many associated infrared products are unable to detect under cirrus clouds or differentiate the signal. This leads the authors to conclude that, due to the visible-infrared radiance and associated sensitivity to thick high level cirrus clouds layers, the approach is nearly useless when event detection is associated with frontal cirrus conditions.

2.8.4. Bias in dust height for detection

Torres et al. (2002b) attribute the height bias as one of the main limitations associated with UV products like TOMS (and to a lesser degree OMI). This height bias is of great importance in detection when considering the synoptic drivers behind dust emissions, and associated particle size – as well as the radiative impact of the aerosol layer. The height bias of TOMS when compared to OMI can be clearly seen in figures 5.1 and 5.2 of TOMS and OMI respectively, indicating the clear offset between source for emission and height of detection assuming significant vertical transport. While the effects of the height bias is limit source attribution, the known offset has meant that in a study by Bryant et al. (2007) and Vickery (2007) TOMS grid cells to the south west of the pan complex were selected to best represent the TOMS aerosol signal for the Makgadikgadi Pans and linked to hydrological controls in Bryant et al. (2007) and regional synoptic settings in Vickery (2007).

While visible and associated techniques cannot differentiate the height of the aerosol within the atmospheric column (Krotkov et al., 2002), for the UV algorithm, the height is of utmost importance. For if the aerosol layer occurs high in the atmosphere, nearly all light that reaches the detector has to pass twice through the absorbing layer (Torres et al., 2002b); if, on the other hand, the aerosol layer is located near the surface, only a fraction of the light that reaches the detector has to pass through this layer. For non-absorbing aerosols, the altitude of the aerosol layer is much less important because scattering by aerosols does not significantly reduce the amount of multiple Rayleigh scattering (Torres et al., 2002b). Krotkov et al. (2002) highlight the importance of the near UV method over land (OMI and TOMS) despite the many errors primarily attributed to uncertainties in the aerosols size distribution, refractive index and aerosol layer height, as well as uncertainties in the surface reflectivity and cloud masking. Nevertheless, according to Torres et al. (2002b) the height bias for TOMS is far less obvious for 'coloured' aerosols (mineral dust) than for 'grey' aerosols (soot) due to the spectral dependence of the differing optical properties.

While height may be a disadvantage for the UV technique, Kaufman et al. (2000) confirms the advantage of using visible over the IR or UV techniques in that it is equally sensitive to dust in the entire vertical column. Even so, from visible imagery it is not possible to determine the altitude of the dust and therefore other then determining presence/absence (Torres et al., 2002b), it is not possible to construct a dust height climatology. The MSG composite is reliant on height as height effects the temperature of the plume and it is the signature temperature depressions which determines successful detection.

2.8.5. Temporal resolution

Satellite aerosol products dominate the detection literature; this is despite the limitations associated with temporal coverage (e.g. D'Almieda et al., 1991). The superior spatial coverage now provided when contrasted with the previous surface based identification and associated advances in satellite technology have dramatically revised the literature. In discussing limitations associated with aerosol detection issues using satellites, Remer et al. (2008) attribute the infrequent and sporadic nature of emission, with dust often appearing and disappearing in a matter of hours, as being one of the major challenges to detection. In a paper by Kaufman and colleagues (2005) the use of TOMS is discussed with primary focus on its ability and use in seasonal and inter-annual scales. It is at these scales that TOMS has proved most useful as it is able to, through the use of averages (Cakmur et al., 2001), reduce the limitations of resolution.

However, advances and the use of sun-synchronous satellites which provide often near global coverage (MODIS 95%) at nearly constant local solar times, enabling the study of diurnal aerosol

variation on a global scale (Torres et al., 2002c). While this has increased the possibility of detection of plumes which have a sporadic and sometimes short lived residence time over source area (Prospero et al., 2002), Schepanski et al. (2007) comment on the benefits of using measurements from geostationary satellites. These are primarily the improved detection of atmospheric dust close to its source due to the higher temporal resolution of the retrievals compared to daily retrievals from polar-orbiting instruments like OMI. Hsu et al. (2004) confirms the importance of high temporal resolution over both the source and sink regions to be able to better understand their climatic drivers, emission and depositional behaviour. This is owing to the nature of aerosols as being subject to transport through atmospheric drivers (Washington and Todd, 2005) and thus they may travel many kilometres from their sources within hours of emission. Further limitations in temporal detection can be attributed to the dominance of day time coverage due to the use of temperature differences in the spectral signatures limiting dust detection during the night.

Li et al. (2007) also comment on the high temporal resolution of geostationary satellites in particular MSG and its ability to permit a greater understanding of the temporal variability of dust events. Additionally, Li et al. (2007) argues that it can detail the dust cyclicity at a daily scale, permitting the identification and evolution at high resolution, providing the potential to map emission close to source. Further, the MSG composite used in this study provides the possibility to detect dust storms as they are transported/emitted during the night, thus allowing for a greater understanding of the plume evolution (Li et al., 2007), although Schepanski et al. (2007) conclude that the dust signature at night is often weak or fails to depict the full contrast/magnitude of the event.

So while daily global images from polar-orbiting satellites (Husar et al., 1997; Herman et al., 1997; Torres et al., 2002a) and more frequent imagery from geostationary satellites (Schepanski et al., 2007; Li et al., 2007) have the potential to resolve the temporal patterns resulting from the short lifetimes of aerosols, which are on the order of a few days to a week (Remer et al., 2008), there remain many other challenges to aerosol detection.

2.8.6. Spatial Resolution

The spatial extent of a dust storm is often as sporadic and difficult to define as its temporal variability, with source detection hampered by resolution of the product and the ability to locate the source due to plume transport (Prospero et al., 1999; Torres et al., 2002c). The resolution of TOMS (1 x 1.25°) has been discussed by Chu et al. (2003) and Torres et al. (2002c) who state that while the resolution is poor, before TOMS aerosols optical retrievals over land were not possible due to the large visible reflectance of land surface in both the visible and infra-red. King et al. (1999) build on this argument stating that the coarse resolution, while useful in providing the first land retrievals, is

now a major limiting factor. Although, technological advances using the principles of TOMS have now allowed for products like OMI with a higher resolution (0.25° x 0.25°). A further significant advantage of the continual record provided by the TOMS and subsequent 'TOMS like' products highlights the importance of the product as well as its continual use in global background aerosol climatologies and basis for fundamental aerosol research.

2.9 CONCLUSION

Despite the importance of dust on global and regional scales and the continual interest and documentation throughout history, there remains a vast disparity between observational records and scientific knowledge. The emission potential of surfaces, source characteristics, entrainment principles, transportation and deposition of aerosols, have been discussed to varying degrees in the contemporary literature. Through developments in satellite technology and the potential to model air parcel trajectories, interest in aeolian geomorphology, particularly studies on aerosol and aeolian processes, has shown resurgence.

As there is no single sensor that has been used to develop a global dust source map at a significantly high spatial and temporal resolution, a combination of sensors provides the best solution. Equally, the varied dynamics specific to each region mean there is no single theory that can be applied to understand dust sources, their processes and system interactions. Global dust literature is further dominated by inconsistencies in naming dust events, as names are often a function of their detection method, with events either quantitative for indexed products or qualitative in nature from observational records. Therefore, for this research, the term dust event is used to refer to an event that is visible in true colour imagery at a resolution of 250 m and sufficiently depresses the brightness temperatures of the 8.7 μm, 10.8 μm and 12.0 μm wavelengths to those which are considered to represent dust activity as per Ackerman (1997) and such that the characteristic hue associated with dust is present.

In the southern African context, a disproportionate amount of aerosol research has examined the effects of biomass burning and anthropogenically produced aerosols. This is despite a study by Piketh et al. (1999) which demonstrated that, in both summer and winter, aerosol loadings over southern Africa are dominated primarily by crustal derived aeolian dust. Therefore, through the use of imagery with high temporal and spatial resolution, studies should increase the potential to locate the source of the dust as well as detect smaller and more variable sources over shorter time scales. The need to re-assess and increase the knowledge of southern African sources has been presented

and through the use of MSG and MODIS imagery a high resolution understanding of the region can be obtained as was observed by Schepanski et al. (2007) in a north African study.

3. Dust detection method

3.1 DATA RETRIEVAL – TOMS, OMI, MODIS, MSG

In order to develop a dust source map of southern Africa, an integrated multi-sensor technique was applied. The products used were selected for their ability to take full advantage of the potential of modern satellite and associated products in detecting atmospheric loadings and their sources to a significant temporal and spatial resolution. Thus a synergy of data sets, namely TOMS AI, OMI, MODIS and MSG-BTD are utilised for differing time periods and at different spatial and temporal resolution.

Table 3.1 summarises the four sensors and, where applicable, the associated products used in this study as well as the spatial and spectral resolutions provided by the sensors.

Table 3. 1 Summary of sensors used in this study, including the launch date, spatial and spectral resolutions and selected channels used for this study. A selection of other studies using each product has been included.

Platform	Launch date	Spatial Resolution	Temporal Resolution	Spectral channels used in this study
TOMS AAI onboard Nimbus-7	1978 – 1993	0.25° X 0.25° (50 km at Nadir)	Product produced at daily resolution	Two ultraviolet channels centered at 340 nm and 380nm
		e.g. Herman et al., 1997; Torres et al., 2002c; Washington et al., 2003; Bryant et al., 2007;		
OMI onboard Aura	2004 to present	0.25° X 0.25°	Product produced at daily resolution	Two ultraviolet channels centred at 342.5 nm and 388 nm
		e.g. King, 1999; Huang et al., 2007; Kaufman et al., 2002		
MODIS True colour onboard Terra and Aqua	2000 to present	250 m (channels 1,2) 500 m (channels 3 – 7)	Twice daily imagery – Terra (am); Aqua (pm)	Three visible channels centered at (1) 670 nm, (4) 565 nm and (3) 479 nm
		e.g. Vermote and Vermeulen, 1999; Kaufman et al., 2005		
MSG BTD onboard Meteosat-8	2002 to present	3 km X 3 km	Images available every 15 minutes – for this study, three images 09:00, 12:00 and 15:00 daily	Three infrared channels centred at (7) 8.7 µm, (9) 10.8 µm and (10) 12 µm
		e.g. Schmetz et al., 2002; Udehemka, 2007; Schepanski et al., 2007		

From the above table, and through the technical review in chapter 2, the importance of a multisensor analysis is evident. The section below details the multiple levels of data sourcing required for the identification of dust sources in southern Africa – as well as the method utilised in the creation of the source map and frequency surfaces.

3.1.1 TOMS

In order to correlate with existing studies and highlight advancements in detection, data from the TOMS sensor onboard Nimbus-7 satellite was utilised. TOMS has been utilised extensively in aerosol studies due to its long time series of data from which background climatology could be created and discussed (TOMS discussed in Chapter 2 or for further technical information see Torres at al., 2002b and for application see Washington et al., 2003). The re-projected aerosol optical depth data has a resolution of 1° x 1.25° latitude/longitude (Herman et al., 1997) and is available for the time period 1978 – 1993 in daily or monthly averaged format from the National Aeronautics and Space Administration (NASA) FTP site[5]. The data was divided into subsets to enclose the region specified for this study and a combination of monthly averages was used to create the 15 year climatology of southern Africa (as used in Washington et al., 2003; Engelstaedter et al., 2003; Bryant et al., 2007). To conform to existing studies the aerosol index product was multiplied by ten, to produce AI values in the range from 0 to 30.

3.1.2 OMI

Correlation was performed with the aerosol product derived from the Ozone Monitoring Instrument, primarily to utilise the increased resolution provided by this product. It was further chosen due to the product coverage of the 2005 – 2008 time period, thus making it an ideal source to compare both with MSG and MODIS identified signals. Through its similarity with TOMS (Baddock et al., 2009), in terms of spectral range and principles of detection, correlation with OMI shows the developments in terms of spatial and to an extent temporal resolution now possible (Schepanski et al., 2007). OMI data available through the NASA GIOVANNI interface[6] was extracted for the years 2005 to 2008 inclusive, to correspond with the MSG data. The OMI data product is a daily level 3 global gridded product, generated from level 2 data products with a 13X14 km spatial resolution into a 0.25° x 0.25° latitude/longitude resolution (Levelt et al., 2006), and was extracted at both monthly and daily resolution for the time period and domain discussed above.

[5] ftp://toms.gsfc.nasa.gov/pub/nimbus7/data/aerosol/
[6] http://gdata1.sci.gsfc.nasa.gov/daac-bin/G3/gui.cgi?instance_id=omi

3.1.3 MODIS

To validate and introduce a secondary data product to refine the results of MSG, true colour MODIS imagery available from MODIS Rapidfire online[7] was utilised. As a result of the known limitation of MODIS aerosol products especially under heavy dust loads (Darmenova et al., 2005; Darmenov and Sokolik, 2005), identification of plumes was performed through the manual classification of retrieved visible composite imagery. MODIS Terra (morning) and Aqua (afternoon) images with approximate equatorial crossing times of ≈10:30 and ≈13:30 respectively provided good spatial resolution (Bullard et al., 2008), with each image representing a true colour composite of a single Level-1B daytime five minute granule of MODIS data. Figure 3.1 shows the domain of the MODIS tiles selected for this study, due to online release and data coverage, the tiles selected have differing coverage dates and availability. Tiles were selected to both represent the domain of study and also those areas identified to be synonymous with both known and potential sources. For each of the tiles all available images were analysed at 250 m resolution.

[7] http://rapidfire.sci.gsfc.nasa.gov/

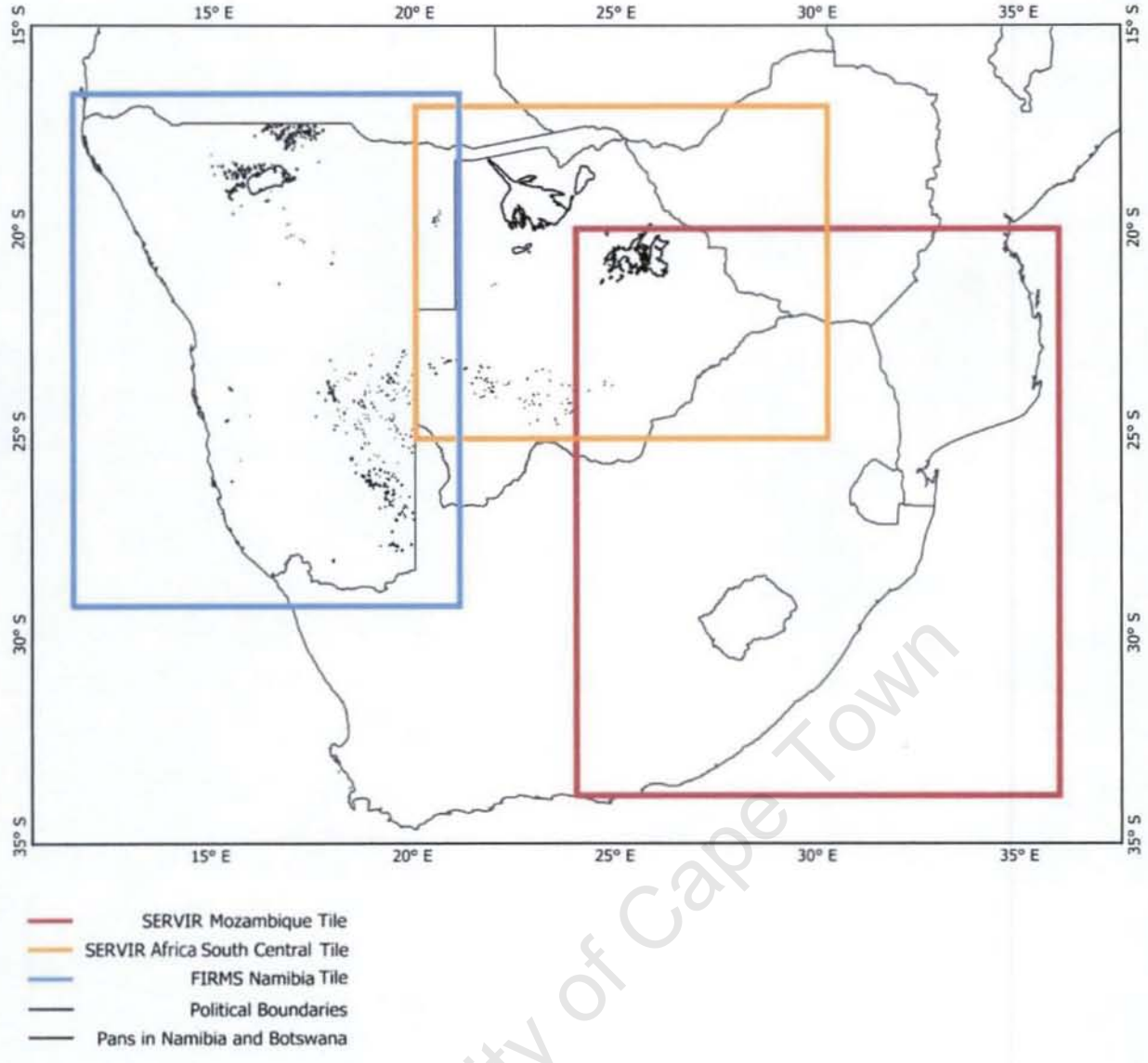

Figure 3.1 Map showing the domain of the study region with the subsetted domains of the three MODIS tiles utilised in this study from left to right, FIRMS Namibia, SERVIR Africa South Central Tile and SERVIR Mozambique.

3.1.4 MSG

To achieve the high temporal and spatial resolution required for this study MSG data was chosen as the primary data source to which correlation with MODIS and later with existing indexed products was performed. Correlation with TOMS/OMI was performed to further inform the feasibility of MSG as a product in southern Africa. The Meteosat-8 (MSG) satellite is located at 3.5°W above the equator, and is a geostationary satellite with a nominal coverage including the whole of Africa, all of Europe and locations at which the elevation to the satellite is greater than or equal to 10° (figure 3.2).

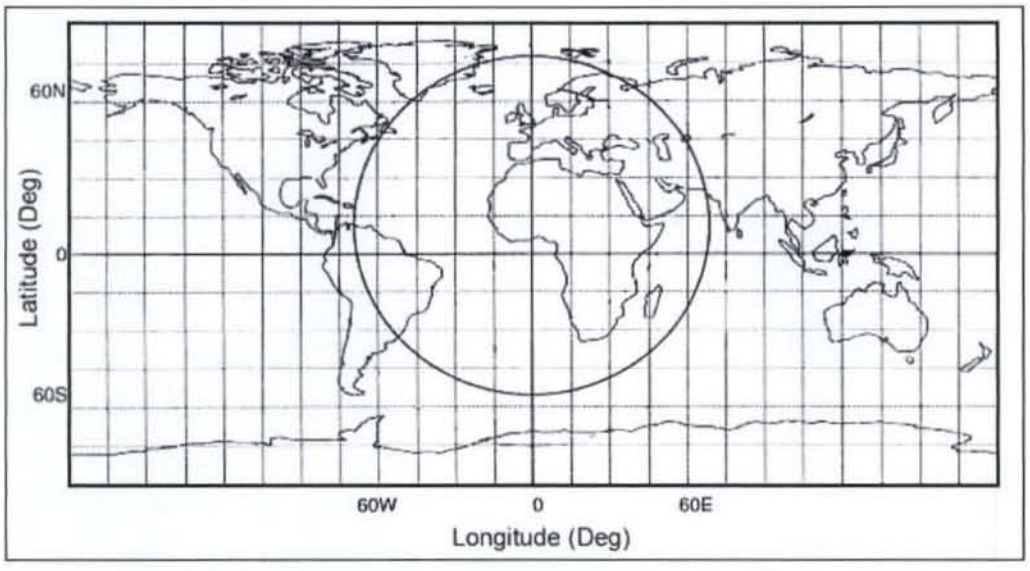

Figure 3. 2 MSG coverage – showing the region of nominal coverage (http://www.eumetsat.int).

Raw MSG data (level 1) is received by EUMETSAT and processed in real time before being released as Level 1.5 data, the released data has been corrected for all unwanted radiometric and geometric effects, as well as being geolocated using a standardised projection, the output is further calibrated and radiance-linerarised (EUM/MSG/ICD/105, 2007).

For this study MSG Level 1.5 data, available from the University of Cape Town's Climate Systems Analysis Group (CSAG) were collected. The MSG-BTD algorithm available from EUMETSAT[8] offered a high resolution dust index product based on the brightness temperature difference between three window channels, as discussed in chapter 2 and based on the theory of dust detection in the infrared discussed extensively by Ackerman (1997). A subset of the available archived data was made; namely the selection of channels 7, 9, 10 centred at (8.7 μm, 10.8 μm and 12.0 μm respectively) (Schmetz et al., 2002) and further, due to the regional focus of this study, the domain was limited to the area enclosed by 15°S to 35°S and 10°E to 35°E – representing southern Africa.

3.2 SATELLITE IMAGERY TO SOURCE POINT IDENTIFICATION

Through correlation of the four sensors/products introduced above, a new dust source map of southern Africa was created using the MSG-BTD algorithm and MODIS true colour composite. This new map could be correlated with the TOMS and OMI products to highlight the increased resolution now possible. The following sections identify the methodologies used in this study from image

[8] http://oiswww.eumetsat.org/IPPS/html/MSG/RGB/DUST/index.htm

acquisition, manual processing through to the GIS processing of imagery to source identification and classification.

3.2.1 Image acquisition and processing

From the application of the BTD algorithm (see chapter 2 for extensive technical discussion) to the MSG-L1.5 data a colour composite was created in which dust is identified as pink/magenta while dry land looks pale blue during day time – transforming to a pale green at night, with thick, high level clouds appearing red to red-brown and thin high level clouds appearing almost black. The three image times selected were specifically chosen in an attempt to determine the temporal patterns and characteristic of emissions and to maximise detection of plume transport.

MODIS imagery was batch downloaded for all relevant tiles for the full time period of online availability from the MODIS Rapidfire website. For OMI, monthly data extracted from the GIOVANNI Interface which was combined to form a four year average over the domain. TOMS monthly data, available from the NASA ftp site, was extracted and monthly averages were combined to form the 15 year climatology used for correlation in this study.

3.2.2 Image analysis and sub setting

Plumes and sources were identified through visual analysis of three daily images, timed at 09:00, 12:00 and 15:00 for the time period 2005-2008 inclusive. Knowledge of the colour responses of various surfaces and characteristic features to the BTD algorithm was integral to detection of plumes. Due to the varying response of land surfaces and associated temperatures to the BTD algorithm (Legrand et al., 2001), analysis was limited to day time imagery to limit the potential contamination associated with these variations. Additionally, the three images were chosen to best represent morning, noon and afternoon conditions associated with the region (supporting technical information can be found in chapter 2 and for the processing script of the BTD algorithm see appendix 2).

Sequential viewing of MODIS imagery was performed to optimize detection, as often dust plumes appeared visually very similar to the surfaces over which they travelled. Therefore sequential viewing was determined to be the best method as distortions or total masking/blocking of surface features as the plume traversed the region aided the detection of the plume.

Through visual analysis of both MSG and MODIS imagery, a subset was derived containing only images classified with an unambiguous presence of dust plumes. To reduce the possible contamination of non-dust plumes, images available on the MODIS Rapid Fire website were analysed

to ensure that smoke plumes from fires were not misidentified as dust plumes over shorter time periods, and further correlated with visual mapping of burn scars. To confirm the direction of the plumes that were only visible on a single image, cross-referencing with meteorological data was performed to identify the dominant surface and upper level air circulations which were assumed to control plume transport.

3.2.3 GIS analysis and source classification

These images were then imported into *Manifold System 6.50* GIS software wherein both the source and track of the plume were marked indicating direction and plume length. The length of the plume was determined from the point of its first appearance through to the end of the last definable point; for some plumes which persisted for more than one image, the plume length was determined through the use of the multiple images on which it occurred. For each source, the time and date were identified and entered into the corresponding attribute table (see appendix 3 and 4). The latitude and longitude co-ordinates of the upwind edge of each plume was recorded (*sensu* Bullard et al., 2008), as this is assumed to be the best method of source identification (Lee et al., 2008).

TOMS and OMI monthly averages for the domain of interest were combined to form a dust climatology of the region, these were used to compare the resolution capabilities and performance of the various products utilised in this study.

Once all plumes had been identified, the source type and name were determined through correlation with Landsat data which provided high resolution imagery of the area to confirm and correlate sources. Source names were primarily determined through the use of 1: 250 000 topographical maps of South Africa and Namibia obtained from the relevant departments of surveys and mapping, as well as correlation with geological maps and existing studies on the pans; e.g. Eckardt et al. (2001) and Jacobsen et al. (1995) for the Namibian coast. Correlations with existing regional and non-aerosol studies were further performed to ensure consistency of naming.

3.2.4 MSG and MODIS source and plume frequency map

Once all images had been analysed for sources and plumes, and marked and identified in *Manifold 6.50*, a 0.10° x 0.10° grid was placed over the entire domain, the central point of which was marked and the number of sources or plumes in the grid cell annotated and information added to attribute table. The 0.10° cell dimension was chosen as it was assumed to be the error associated with identification with the MSG product further, it could be representative of transport due to sampling time bias. This grid corresponded to four MSG pixels and, while it does reduce the high resolution

potential of the product, the outcome has the potential to detail a greater accuracy. From these data, surfaces were created which could be used to look at frequency by year or by source.

These surfaces were the correlated with OMI data for the same time period to compare the resolution and ability to detect sources as well as with the TOMS climatology.

3.2.5 Synoptic and circulation analysis

For all days on which plumes were detected, gridded climate data representing the 500 hPa, 850 hPa and 1000 hPa surfaces were created using NCEP reanalysis data available online from the NOAA ESRL (National Oceanic and Atmospheric Administration, Earth Science Research Laboratory) website[9]. Monthly mean circulation and annual monthly means were also downloaded against which event days were compared. In accordance with studies by Tyson et al. (1996b) archetypal conditions were linked to all events to summarise findings into existing literature.

The Hybrid Single-Particle Lagrangian Integrated Trajectory (HYSPLIT) was the final product used in this study and is available online through NOAA ARL[10] (Air Research Laboratory). Two HYSPLIT products available from NOAA ARL were used – the first was the HYSPLIT Trajectory modelling output, the second the Dispersion/Concentration modelling output. For the trajectories NCEP Reanalysis data were used on which to model the emissions to ensure consistency with the geopotential surfaces. These were determined for all plumes and run for 24 hours to ascertain the dominant transport pathways of aerosols emitted from all sources. The secondary HYSPLIT product was through the use of the dispersion model again using NCEP Reanalysis data. The product, which models a potential depositional footprint for a source or emission, was calculated for all plumes emitted from the Makgadikgadi Pans for the 2004 to 2008 period. Zero wet deposition was assumed from any single source emitting one single emission and calculated for a six hour period, deposition was calculated once every hour.

[9] http://www.esrl.noaa.gov/psd/data/gridded/
[10] http://www.ready.noaa.gov/ready/open/hysplit4.html

3.3 CONCLUSION

Following the comprehensive review of advances in satellite technology and a selection of sensors and products presented in the previous chapter, and through the methodologies introduced in this chapter. The possibility of a multisensor high resolution dust map of southern Africa is now possible. Further, through data products many of which are now available online, it is possibly not only to determine source regions to a higher resolution but determine and contextualise these regions within the circulation associated with emission and transportation over the domain. The results of the above methodologies will be presented in the following chapter.

4. Dust in southern Africa - Results

4.1 RESULTS INTRODUCTION

Having discussed the importance of dust in the climate system and described the principles of detection, and in particular the principles and methods utilised in this study, the results of the analyses are presented in this chapter. Due to the observed and discussed limitations associated with both TOMS and OMI, this chapter primarily considers the results obtained from MSG and MODIS which have permitted the creation of a 'best possible' dust source map utilizing available technology. Owing to the multiple definitions existing in the literature surrounding this research, the following definitions hold for this study (for more clarification see appendix 1 – glossary of terminology). *Plumes* are defined as the unambiguous presence of mineral aerosols identified in suspension, while *sources* are the geographical setting for the best approximation of the origin of the plume. An *event* is defined to be the occurrence of a plume or activation of a source.

The first section will discuss the data and technical results initially from MSG and then from MODIS. The second will begin with a synthesis of the contemporary setting of southern African sources, before presenting the results by region.

4.2 DATA COVERAGE AND DATA RESULTS FROM PRIMARY SOURCE: MSG

The primary data source for this analysis was retrieved from MSG; however gaps do occur in the data due to receiver malfunctions during the data collection process and transmission. Figure 4.1 details the coverage of the MSG data for the time period over the study region. Full (100%) coverage occurred when all three images (09:00, 12:00 and 15:00 local time) were present over the entire domain for all days within the month.

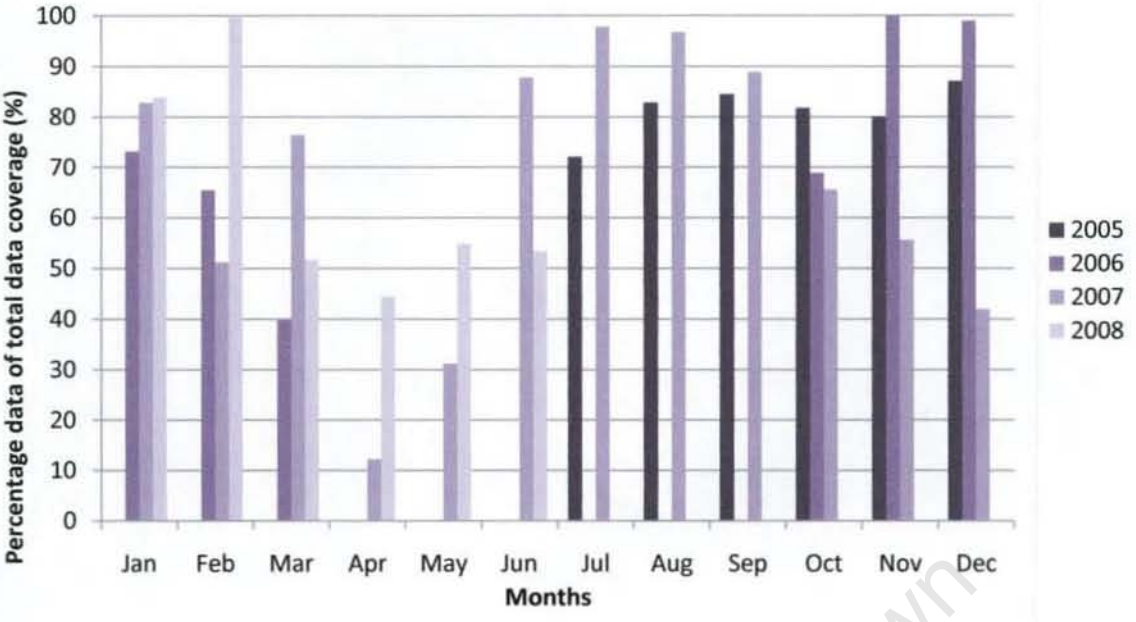

Figure 4. 1 Plot of percentage of total potential coverage of MSG data by month for the time period 2005 – 2008.

The most consistent year of coverage was 2007 with near total coverage over the second half of the year, which is typically associated with dust activation in the region (Bryant et al., 2007). While 2007 has an average data coverage of 68% over the 12 month period, the percentage of total identified events was almost 44%. Conversely, 2005 saw an average data coverage of only 40% yet included almost half of the observed events (48.48%). This could confirm the findings of Bryant et al. (2007) on the importance of the latter half of the year for significant dust entrainment or indicate the importance of other mechanisms for deflation.

Table 4. 1 Events and percentage of total observed events and the average percentage of data coverage for the year as observed by MSG.

	Events	% of total events	Ave. data coverage (%)
2005	32	48.48	40.68
2006	3	4.55	37.18
2007	29	43.94	65.68
2008	2	3.03	32.34

To determine how the inconsistencies in the data coverage affect the detection of plumes, figure 4.2 details the percentage coverage by month and by year, and includes the associated emission event frequency. This figure clearly accentuates the dependence on the image frequency for the detection

of plumes, but also further confirms the importance of the latter half of the year for dust activation. The disrupted coverage from the Meteosat sensor resulted in an intermittent coverage in the archived data, limiting the potential to discuss emission frequency and seasonal/inter-seasonal variations. Although it remains possible to observe that the greatest number of events occurs during the latter half of the year. This figure therefore further introduces the complexity and importance of the argument of climatic drivers on plume frequency as well as supply limitation on the source for deflation.

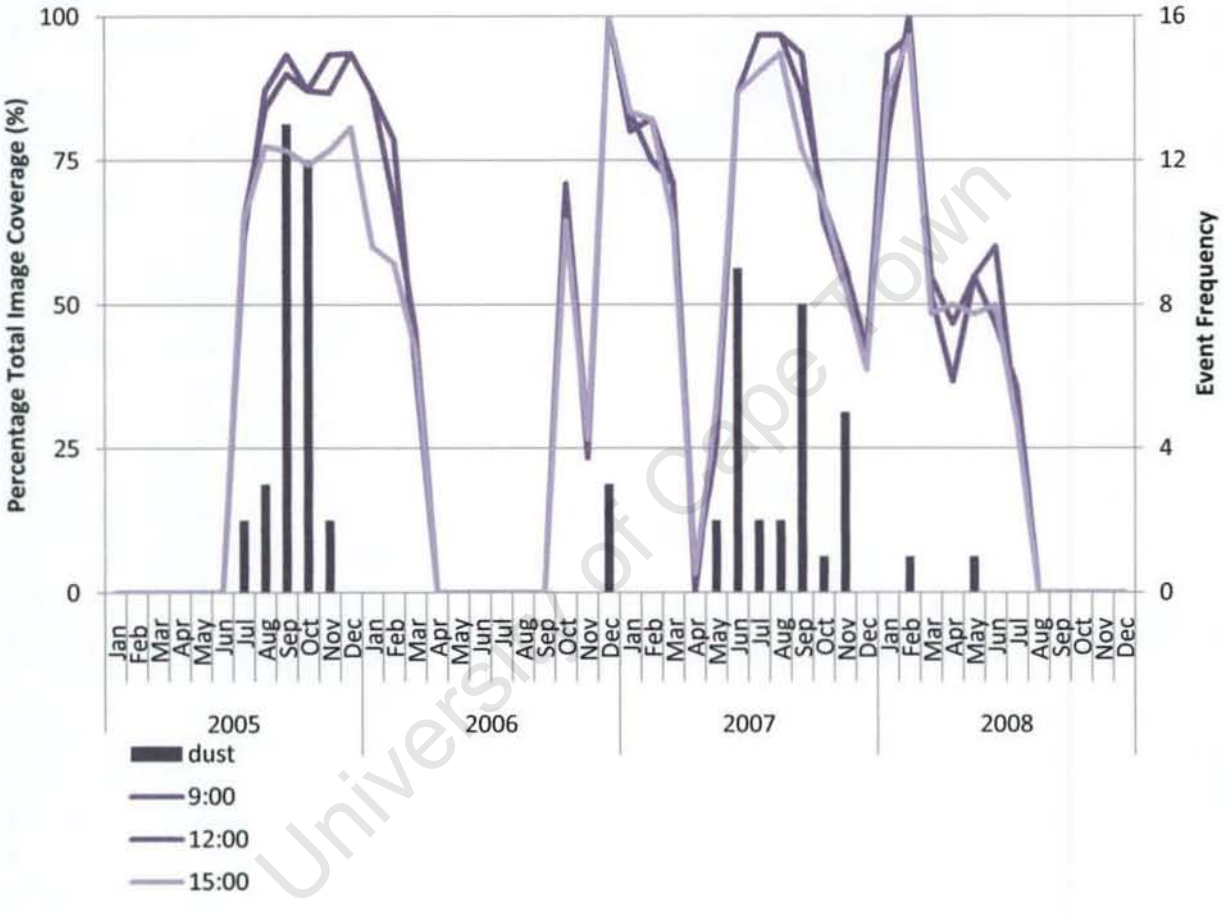

Figure 4. 2 Plot showing the occurrence of dust events by year and month (event frequency) plotted against the percentage of total data coverage for the MSG composite algorithm for each of the three image times.

Further validation of the use of the MSG data set was conducted through correlation with the MODIS Rapidfire data set which provided near total coverage for the entire time period of the study. Correlation confirmed the existence of all plumes identified using MSG and expanded the data set through the identification of coastal plumes, invisible to the MSG composite due to edge effects as discussed by Legrand et al. (2001). This correlation provided further evidence that sources emitting during the 2005 – 2008 time period should all be identified, therefore while it is not possible to

perform time series analysis of emission frequency, identification of plumes to specific sources is possible.

4.3 DATA COVERAGE AND DATA RESULTS FROM SECONDARY SOURCE: MODIS

The secondary data source was MODIS true colour images from three tiles that were chosen to best represent dust source regions in southern Africa, as identified by the MSG pink composite and by existing studies. The domains of the tiles are presented in figure 4.3 below:

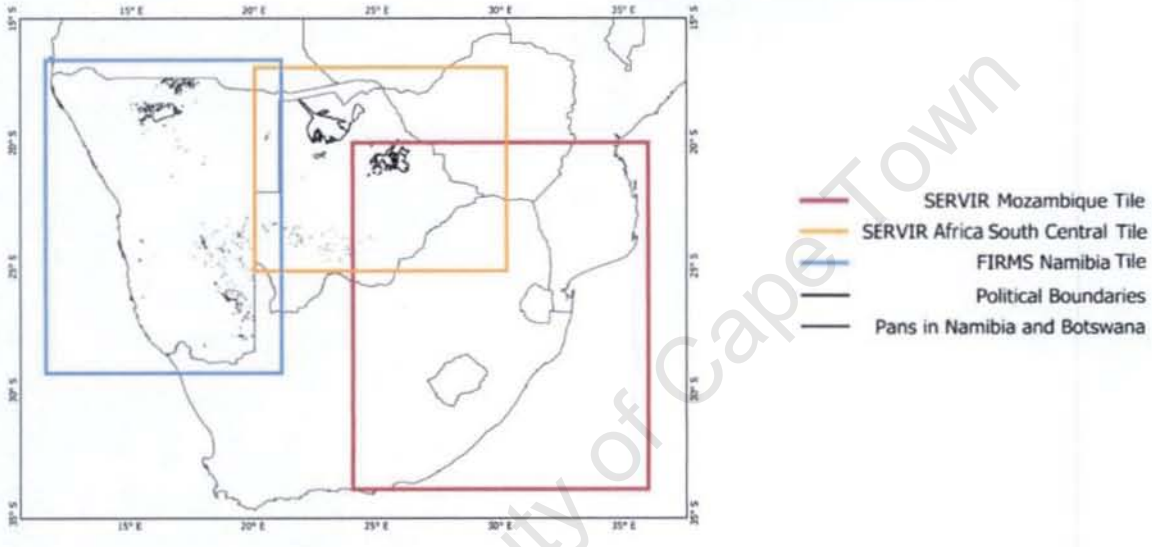

Figure 4. 3 Outlines of domains of the three MODIS tiles used in this study to augment and validate the MSG data set.

Full coverage for the study period was not possible due to satellite malfunction and calibration errors, as well as the availability of data release for the tiles chosen for this study. Figure 4.4 indicates the coverage for each of the three tiles for the studied time period. Full (100%) coverage occurred when both the Terra and the Aqua images were present for the entire tile for all days within the month.

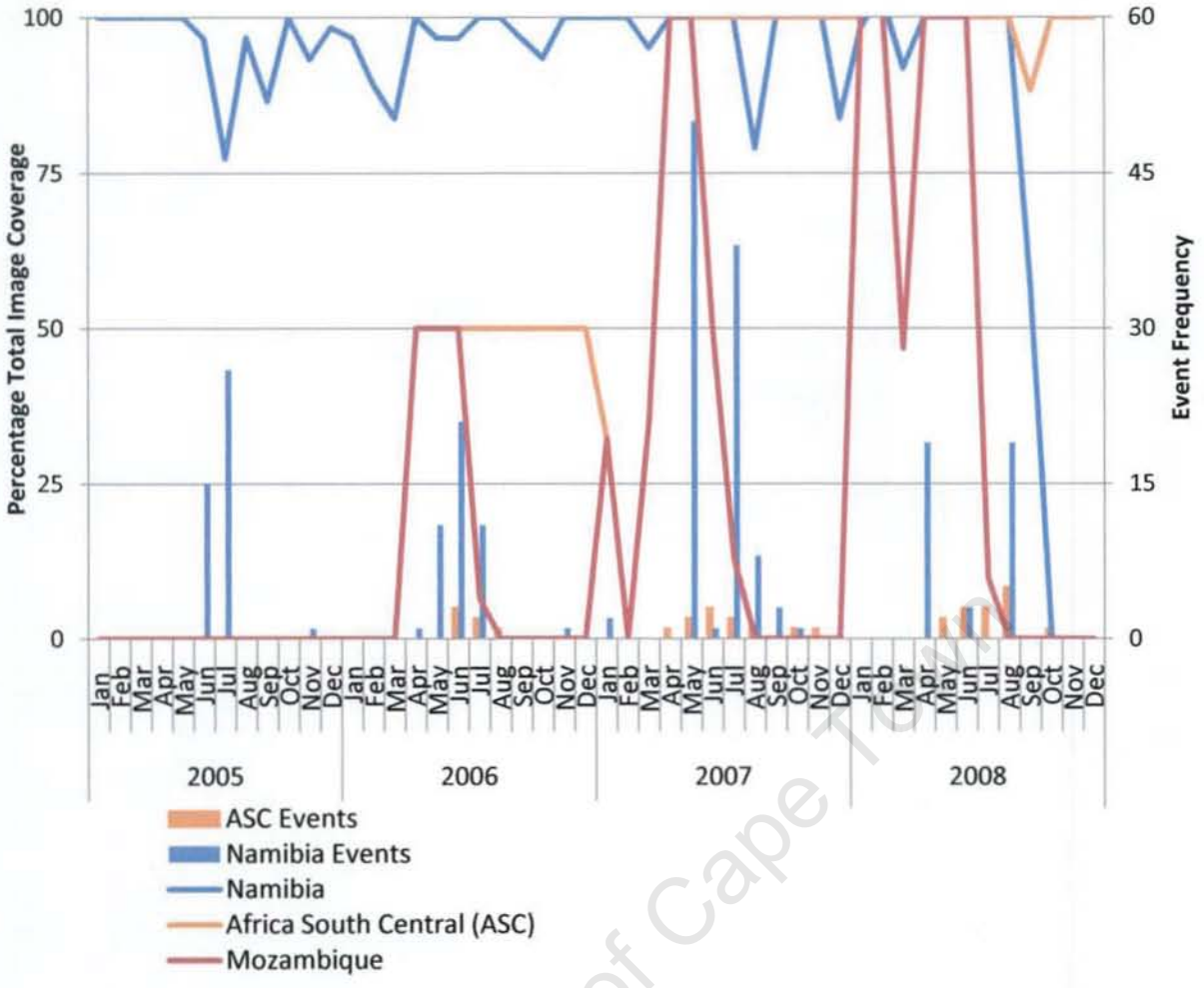

Figure 4. 4 Plot of percentage of total potential coverage of MODIS data by month for the time period 2005 – 2008 (Africa South Central and Mozambique tiles begin online coverage on the 1st of April 2006; images before this date are not available online). The associated dust emissions by year and month for the two dominant images are plotted the latter half of the year is again identified as being significant for dust emission over the entire domain.

The most consistent year for coverage was 2007 with near total coverage for two of the three tiles. The Namibian tile was the most consistent, averaging 89.89% coverage over the four year study period. Due to the overlap between the Africa South Central and Mozambique tiles over the Makgadikgadi Pan (the only source identified within these tiles); these tiles are grouped together for this study and the resultant coverage is assumed synonymous with the combination of their extent.

Table 4.2 details the percentage coverage as well as the percentage of events identified by year. For Africa South Central (ASC) there appears to be a greater dependence on the image coverage for the detection with increased data coverage resulting in a greater number of identified events. For Namibia this does not appear to be as important; for example: in 2007 44% of the events were

identified (almost double the two preceding years) on similar data coverage statistics. This could be in response to multiple plumes being detected on any single image.

Table 4. 2 Events and percentage of total observed events and the average percentage of data coverage for the year as observed by MODIS for Africa South Central and Namibia.

Year	Tile	Events	% of total events	Ave. data coverage (%)
2005	ASC	0	0.00	0.00
2006	ASC	12	19.35	25.19
2007	ASC	11	35.48	54.10
2008	ASC	14	45.16	70.23

Year	Tile	Events	% of total events	Ave. data coverage (%)
2005	Namibia	42	18.18	95.77
2006	Namibia	45	19.48	96.13
2007	Namibia	103	44.59	96.78
2008	Namibia	41	17.75	70.88

The addition of true colour MODIS imagery improved the coverage of the three selected domains, which through MSG analysis were determined to be the significant dust producing regions in southern Africa. These regions were also selected as, through literature and preliminary studies on surface geomorphology, they were considered the most likely domains of source regions. The combination of which provided high spatial resolution data with which to identify plumes, as well as identify regions which could be potential sites. Despite the limitations discussed in this and previous sections, the identification of both plume and sources was possible using both MSG and MODIS. The following sections present the plume results followed by the contemporary setting of sources and then the results of the multisensor analysis by region.

4.4 PLUME IDENTIFICATION

Plumes were identified using a combination of MSG and MODIS imagery. For MSG, 1889 images were analysed, resulting in 65 identified plume events on 40 days; while 4489 MODIS images were analysed identifying 262 plumes occurring on 56 days.

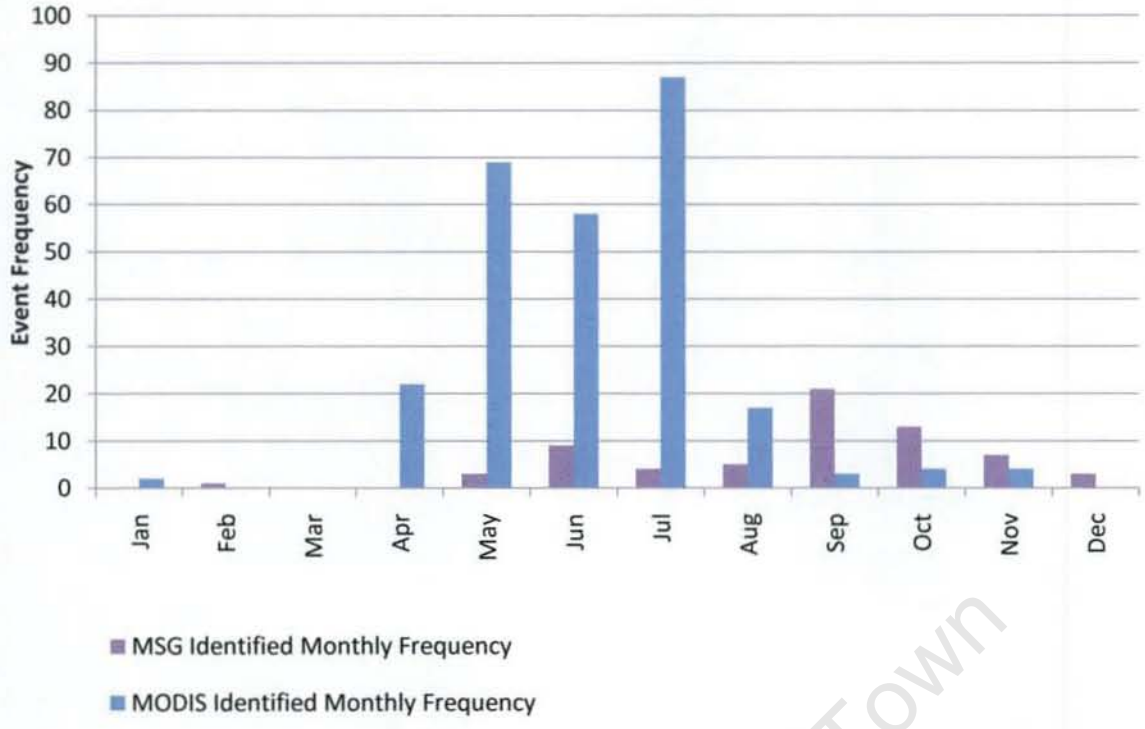

Figure 4. 5 Plot of dust source activation averaged by month for the 2005 – 2008 time period for southern Africa as identified by either MODIS or MSG. The MODIS identified sources primarily correspond to the Namibian coastline with the addition of eastern Botswana, Limpopo and North West provinces in South Africa on a separate tile (figure 4.3) while MSG encompasses the entire southern African domain.

Figure 4.5 shows evidence of an offset between the peak for MODIS and the peak for the MSG composite. The offset could be ascribed to the difference in the locations as identified by each sensor; while MODIS identifications are dominated by the Namibian Coast, the majority of MSG identified sources are inland pans. Therefore the offset could be attributed to the difference in seasonality between the regions or possibly as a result of the data coverage for each region.

All anthropogenic sources have been marked and their location and frequency recorded, as per methodology, however due to the focus of this study on mineral aerosols from natural sources, these sources are not included in the discussion.

4.4.1 MSG Identified plumes

The 65 identified plumes occurring on 40 days could be assigned to 23 sources in southern Africa. The Makgadikgadi Pans in Botswana had the greatest recorded frequency of emission (22 plumes, 34%) with the Etosha Pan in Namibia being the second most frequently identified plume source (19

plumes, 29%). The remaining 21 sources were identified by either single or multiple emissions (see appendix 3 for more detailed information on emission characteristics of sites).

Of the sites identified by MSG, pans dominated the detection, accounting for 12 of the 23 sources and 52 of the 65 events, while there were seven rivers identified each emitting only once. Two marshes and vleis were identified resulting in three plume events. The final two sources were identified to originate from a lake margin and a dam, indeterminate pan or form of agricultural activity near Bloemfontein, both only emitting once.

For the 65 identified plumes, 50.8% (33 events) were identified on the 12:00 images while the 09:00 images showed 31% of the events (20 events), the remaining 18.5% (12 events) occurred on the 15:00 images. The two dominant sources namely Makgadikgadi and Etosha, showed 72.7% at 12:00 and 63.2% at 09:00 respectively; therefore indicating noon time dominance for emission on the Makgadikgadi Pans and morning emission dominance for the Etosha Pan.

To further refine the results, the sources and associated trajectories were grouped according to their geographical location, the resultant regions for MSG are: Etosha, Makgadikgadi, Northern Cape, Namibian Coastline and Free State. The sources included in each of these groupings are defined in Table 4.3:

Table 4. 3 Source names grouped by geographical location into emission regions as identified by MSG. The location, type, frequency and time of emission detailed in APPENDIX 3 with figure 4.7 detailing the location of the sources.

Region	Source Names
Etosha	Etosha Pan
Makgadikgadi	Makgadikgadi Pan, Lake Ngoni, Linyandi Marshlands
Northern Cape	Duwisib River, Helmering River, Koichab, Swartput se Pan, Hakskeenpan, Kiriis Ost Pan, Grundorner, Noenieput, Konkiep River, Koemkoep Pan, Skemerhoek Pan, Marcel Pan, Samahaling Pan, Salztal Pan
Free State	Bloemfontein, Gannapan / Bloemhofdam
Namibian Coast	Orawab River, Gui Uin

Regionalised bearing analysis revealed that the mean bearing for plumes from the Makgadikgadi Pans is 243°; this corresponds to south westerly transport off the pans and is similar to the Etosha Pan which had a mean bearing of 232°. The Northern Cape Pan belt showed significant variation when compared with Etosha and Makgadikgadi, with plumes ranging from 130° to 230° that is a south easterly to south westerly direction. Plumes identified in the Free State region, while fewer in count, experienced the greatest variation ranging from 100° to 256°. Due to the relative location of

these regions within the mean synoptic circulation of southern Africa it can be provisionally proposed that the plumes are primarily a response to the high pressure system that dominates the region during the latter half of the year.

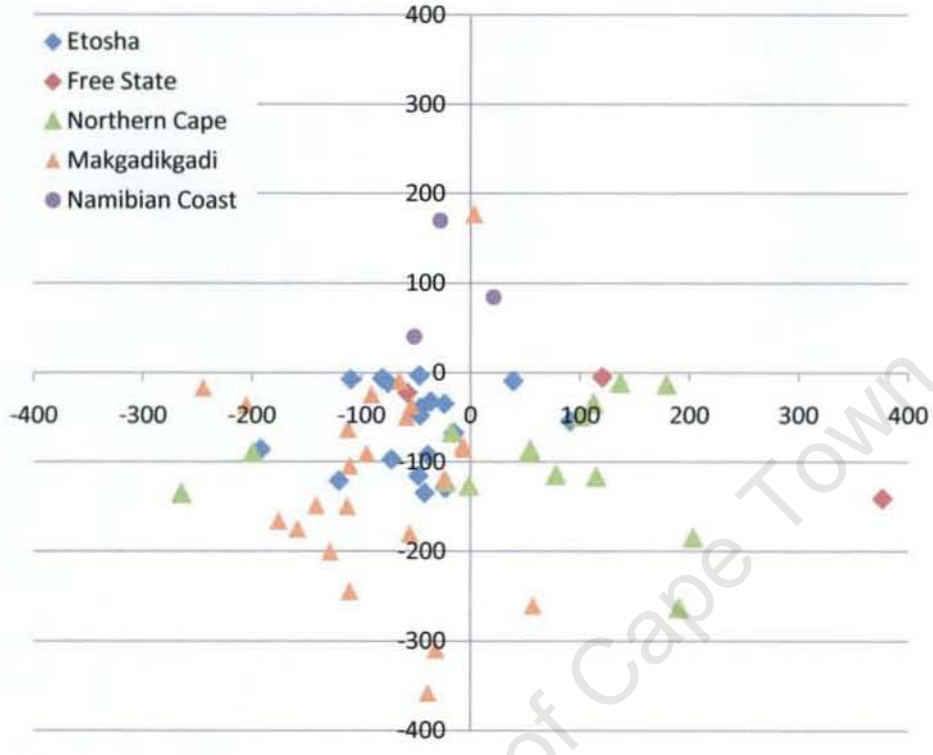

Figure 4. 6 Plumes as a function of distance (km) and from source (0;0) in x and y plains - grouped by major region. Negative y-direction indicates southward transport from source, while negative x indicates westward transport.

Plume lengths were marked according to the maximum extent of the plume on the last image on which it could be identified, therefore plumes that were visible for multiple images on average showed greatest length. The mean length of plumes emanating from the Makgadikgadi Pans was 179.9 km, while from Etosha Pan the average plume lengths were only 95.7 km. The Northern Cape pan belt averaged 165.9 km. Only three events were detected in the Free State Pan one of which resulted in the identification of a 402.0 km plume, the other two were 120.6 km and 61.8 km; hence the average showed strong bias and therefore was not representative of the observed conditions. Three plumes from two sources on the Namibian coast resulted in anomalous trajectories as all identified plumes travelled north from source region.

All but one of the 23 identified plumes was associated with sources on the escarpment with a minimum altitude of 600 m above mean sea level (amsl), one such source the Gui Uin Marsh was identified at 208 m amsl. For sources recognised by MSG, the Etosha and Makgadikgadi Pans

dominated source identification, both are large inland depressions which experience annual inundation periods followed by drying; resulting in these sources being active sediment receptacles. The remaining sources are all associated with ephemeral rivers or pans, all of which are thought to behave in a similar manner; accumulating sediment through fluvial controls, which are deposited and then dried, exposed and deflated (Engelstaedter et al., 2003).

The results of the plume location and trajectories as identified through the MSG composite are summarised in Figure 4.7.

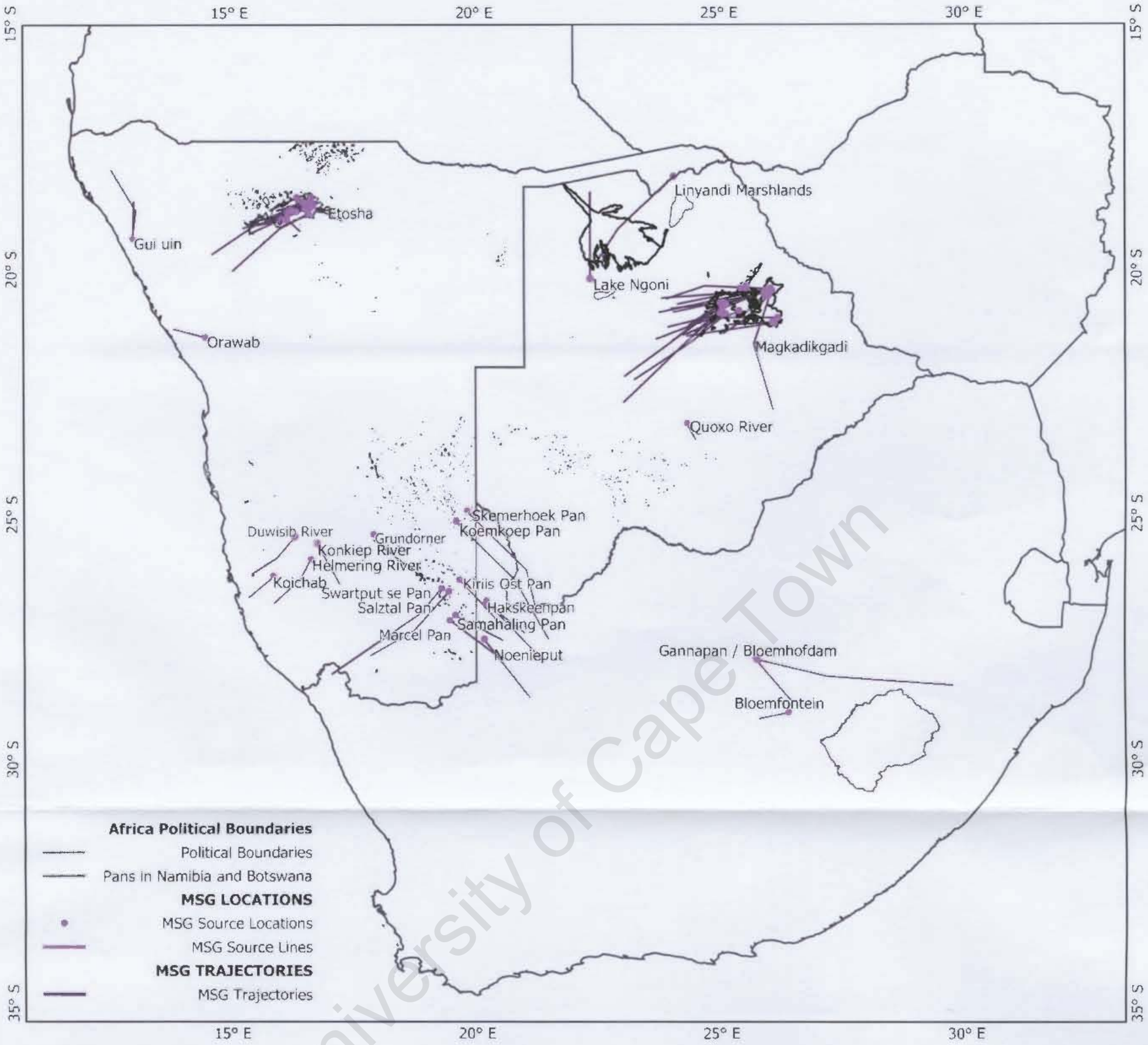

Figure 4. 1 Map of MSG sources and trajectories as identified for the period 2005 – 2008. Trajectories were mapped from source as identified, to the maximum extent of the plume. Source names have been attributed to plumes and included, this map includes the entire domain of study. Pans in Namibia and Botswana as well as political boundaries have been included for spatial reference.

4.4.2 MODIS Identified Plumes

This study identified 262 plumes on 56 days which were attributed to 93 sources in southern Africa. The Namibian coastal sources dominated, averaging five emissions per day with a maximum of 23 on a single day. The Makgadikgadi Pan in Botswana had the greatest recorded frequency with 31 plumes occurring on 20 days, the Kuiseb River and Delta had the second greatest recorded frequency of emission with Omaruru River and the Etosha Pan being the third most frequently observed source with 12 emissions each occurring on 12 separate days. Ten further sources: Torra Bay Pan, Ugab Pan 1, Ugab River, Hoanib Pan, Hunkab Pan, Meob Bay Pan, Conception Bay Pan, Huab River, Kuiseb River, Uniab River all emitted more than 5 times, with the remaining 75 sources being identified by fewer than five emissions.

Of the 93 identified sources 50% (46 sources) were pans, while 33.69% (31 sources) could be attributed to rivers, 5.4% (5 sources) were perennial marshes, 4.3% (4 sources) were associated with gravel plains and evaporation points; while 3.2% (3 sources) could be linked to human activity and mine tailings, the remaining 4% (4 sources) could not be defined and either were associated with perennial rivers or smaller unidentified pans.

MODIS had a definite bias towards detection in Terra (morning) than in Aqua (afternoon) with 236 of the 262 (90.1%) identified plumes being detected on this sensor. Aqua (afternoon) accounted for the remaining 9.9% of identified plumes with 15.1% of plumes identified on Terra remaining visible in the Aqua image.

To further refine the results, the sources and associated trajectories were grouped according to their geographical location, the resulting regions for MODIS are Etosha, Makgadikgadi the Northern Cape Pans and the Namibian coastline. The sources included in each of these groupings are defined in table 4.4.

Table 4. 4 Source names grouped by geographical location into emission regions as identified by MODIS. The location, type, frequency and time of emission detailed in APPENDIX 4 with figure 4.9 and 4.10 detailing the location of the sources.

Region	Source Names
Etosha	Etosha Pan, Onanzi Pan
Makgadikgadi Pan	Makgadikgadi Pan
Northern Cape Pan Belt	Donavan se Pan, Fish River, Gamanas Pan, Gemsbokbrak, Gemsbokhoorn, Grasheuwel Pan, Groot - Witpan, , Grundorner, Hakskeenpan, Haseweb River, Kanibes River, Klein - Aarpan, Koeipan, Kongapan, Konkiep, Koppieskraalpan, Kuubmaansvlie, Morgenzon Pan, Salt Pan, Samahaling Pan, Saulstraatpan, Swaartput se Pan, Vrysoutpan
Namibian Coast	18 Latitude Pan, Cape Cross Pan, Cape Fria Pan, Conception Bay Pan, False Cape Fria, Gui uin, Hoanib, Hoanib Pan, Hoarusib, Huab Pan, Huab Pan 2, Huab Pan 3, Huab Pan 4, Huab River, Hunkab Pan, Hunkab River, Ilhea Point, Isirub River, Khan River, Khumib, Koigab Pan 1, Kuiseb River, Kuiseb River Delta, Langer Werner, Meob Bay Pan, Omaruru River, Ombonde, Orange River, Oranjemund, Panther Pan, Rock Bay, Rocky Point, Rottrout Pan, Sechomib, Swakop River, Terrace Bay 2, Torra Bay Pan, Toscanini Pan, Tsauchab River / Sossusvlei, Tsondab River/Pan, Tumas River, Ugab Pan 1, Ugab Pan 3, Ugab Pan 4, Ugab Pan 5, Ugab River, Uniab River, Unknown 1, Unknown 2, Unknown 3, Unknown 4, Unknown 5, Unknown 6, Unknown 7, Unknown 8, Unknown 9, Unknown 10, Unknown River, White Lady Salt Pan,

Plume lengths were marked according to the maximum extent of the plume on the last image on which it could be identified as this was only relevant for 15% of the images, the average plume length is markedly shorter than those identified using MSG. The mean length of plumes emanating from the Etosha Pans were 113.3 km while the Makgadikgadi Pans averaged 153.6 km significantly longer then the Namibian Coast with an average plume length of 72.6 km, despite the marked contrast between the pale plume and dark ocean. The Northern Cape pan belt averaged 56.2 km, and showed the greatest variation in bearing.

The mean bearings for each of the regions revealed that the Etosha and Makgadikgadi Pans and Namibian Coastal sources were dominated by plumes travelling off the source in a south westerly direction at 246.45°, 244.56° and 231.97° respectively. While for the Northern Cape the average was 158.67° although there were two definite trajectory groupings, one averaging at 187.9° (South-South-East) and the second at 149.8° (South-West) and as a result are activated by a greater variety of climatic conditions.

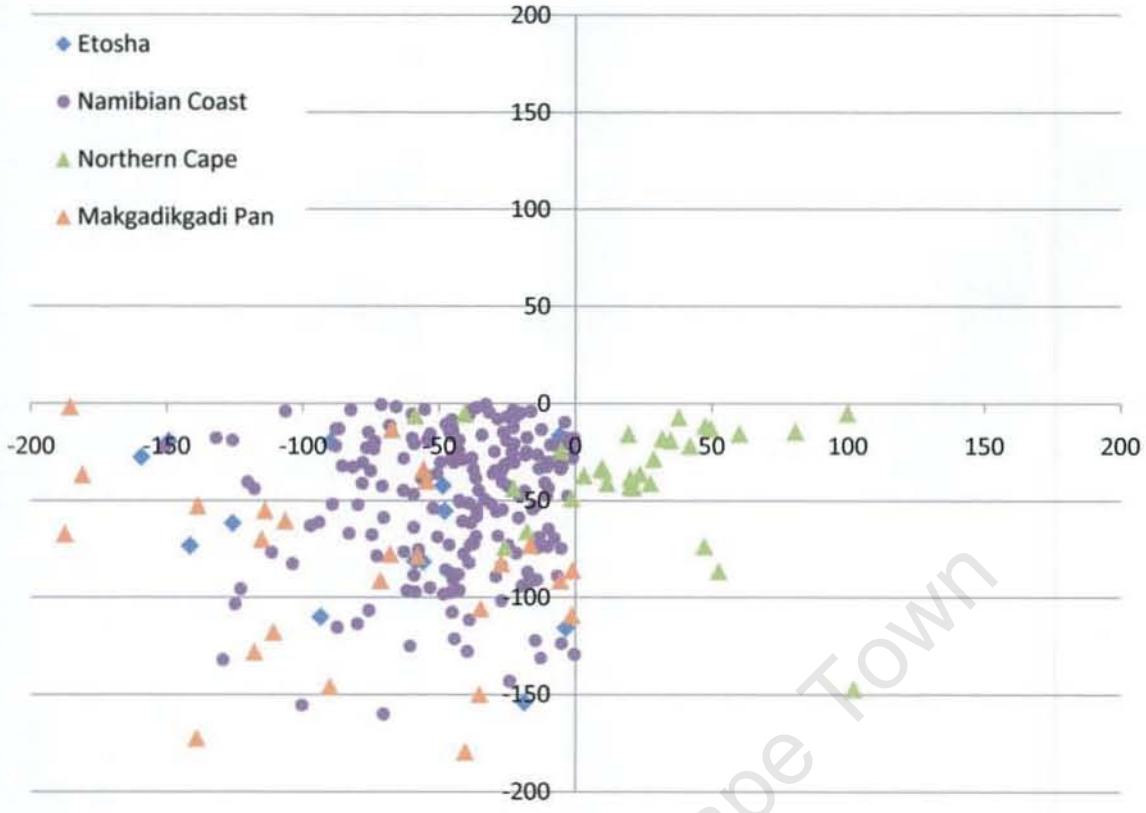

Figure 4. 8 Plumes as a function of distance (km) and from source (0;0) in x and y plains - grouped by major region. Negative y-direction indicates southward transport from source, while negative x indicates westward transport. For these regions no plumes were transported in a northerly direction.

The results of the plume location and trajectories as determined through the MODIS images are summarised in Figure 4.9 and 4.10. Figure 4.9 represents the plumes detected through the use of the Namibian tile, while figure 4.10 shows the only other source identified using MODIS. Four clear regions can be surmised in figure 4.9: the Etosha Pan, the Namibian coastline which has two emission regions: those located at the coast and those lying further inland, with all these regions resulting in plumes travelling in a general south westerly direction. While the final region; the Northern Cape pan belt results in south westerly transport from source.

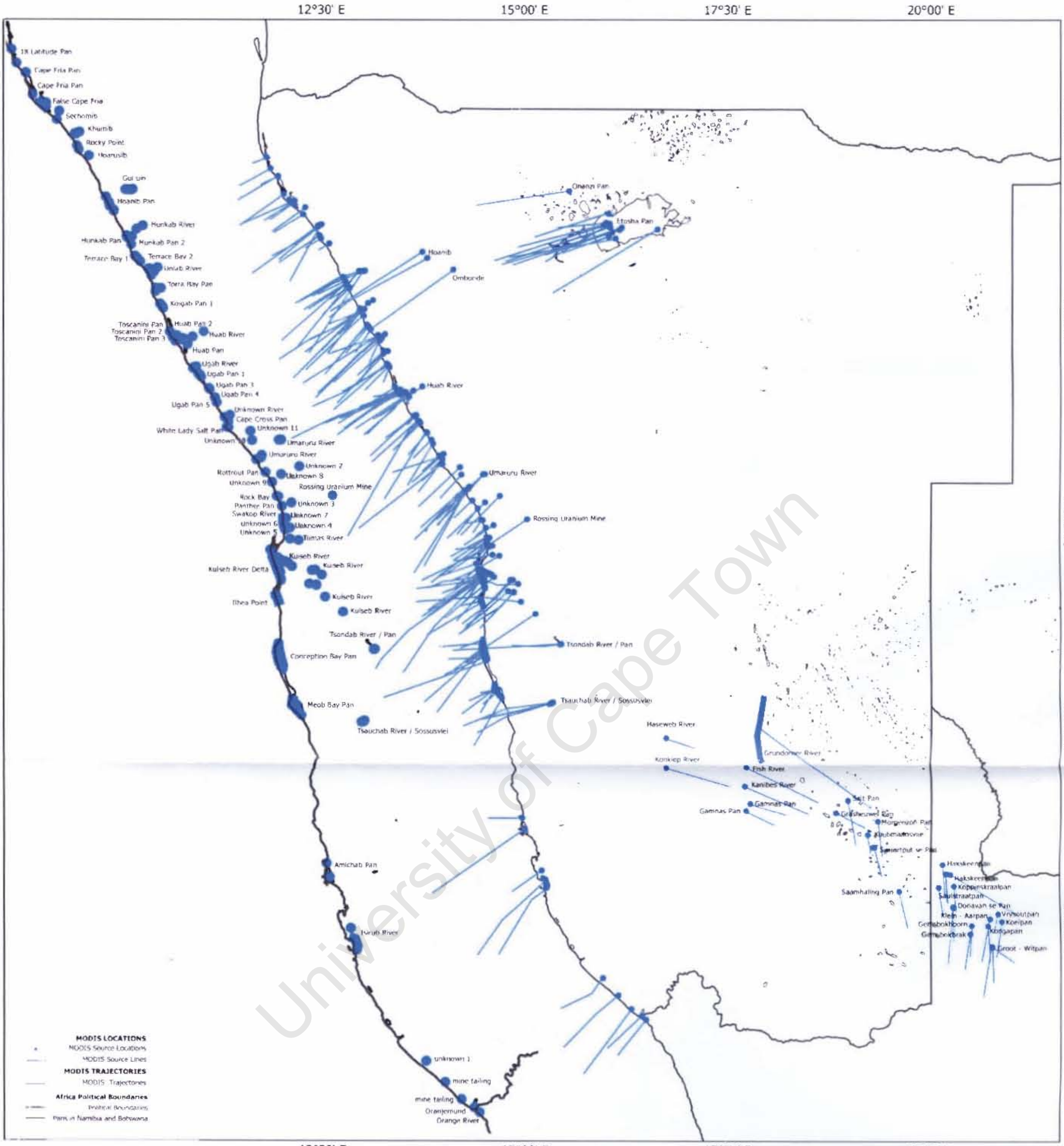

Figure 4. 2 Map of MODIS sources and trajectories as identified for the period 2005 – 2008 using the Namibian Tile. Trajectories are mapped from source as identified to the maximum extent of the plume. Source names have been included for all identified sources.

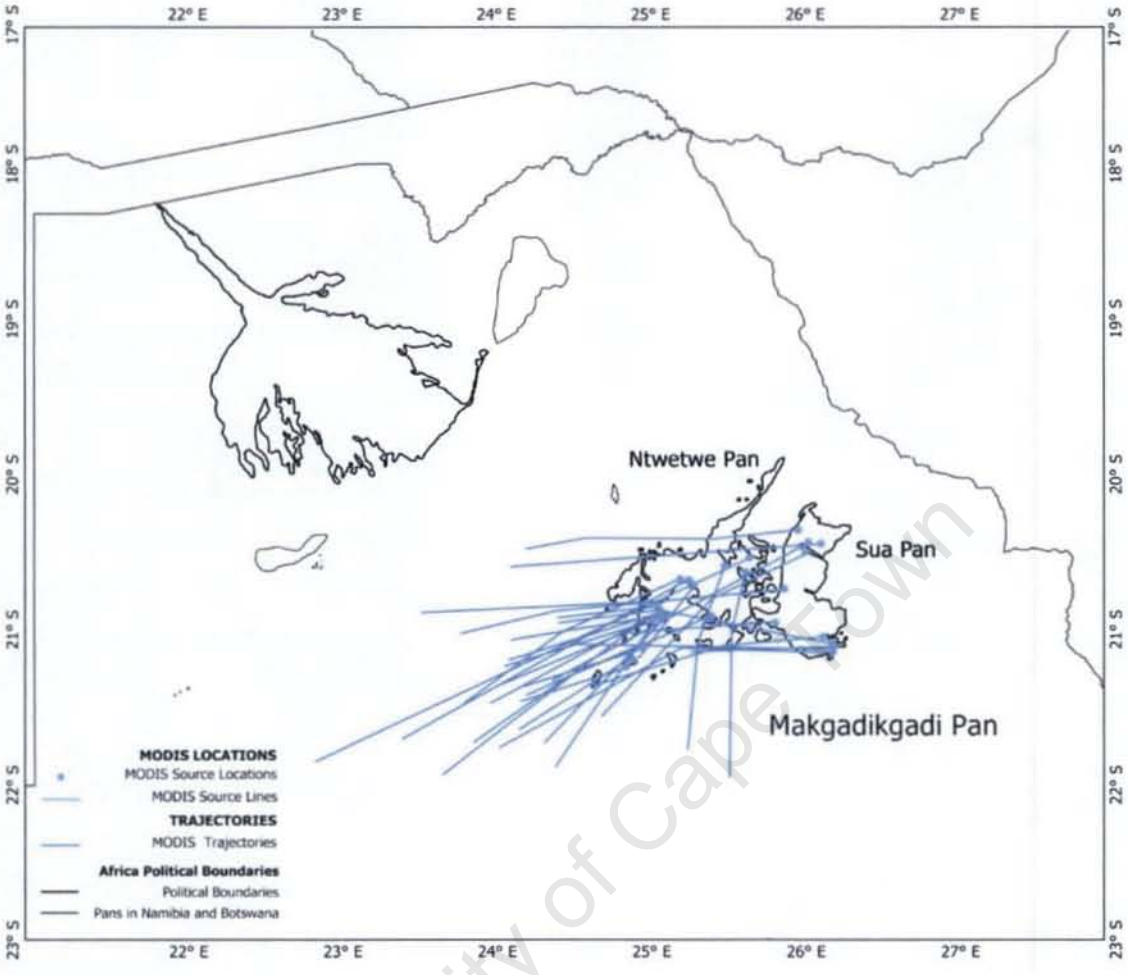

Figure 4. 10 Map of MODIS sources and trajectories as identified for the period 2005 – 2008 using the Africa South Central Tile. Trajectories are mapped from source as identified to the maximum extent of the plume. Source names have been included.

The following section discusses the contemporary setting of the dominant regions identified in this study and is followed by the results utilising the synthesis of both MSG and MODIS imagery detailing the results of both plume identification and the sensors ability to detect dust in each region.

4.5 CONTEMPORARY SETTING OF SOUTHERN AFRICAN SOURCES

From the above results as identified by both MODIS and MSG, six major regions have been defined, namely: the Namibian coastline, Namibian interior, the Northern Cape Pan Belt, the Free State and the Makgadikgadi and Etosha Pans. The following section discusses the contemporary setting of southern African sources before presenting the regional source results

4.5.1. Namibian Coastline

The Namibian coastline is dominated by the arid Namib Desert, with a north south extent of 1 500 km. Harsh and variable climate, steep topography and a series of pans and ephemeral rivers characterise the region (Jacobson et al., 1995). The location of the Namibian coastline on the western margin of the continent affords for very little moisture retention in the air masses that reach the region; as most of the moisture from the warm Indian Ocean is precipitated out over the eastern and central continent (Tyson, 1996a). This, combined with the effects of the cool Benguela current running along the coast, result in the region experiencing less than 200 mm of annual rainfall along the full 1 500 km extent (Tyson, 1996a). More than 12 major catchments span the coastline, ranging from 2000 km^2 to 30 000 km^2 in area, with the associated rivers draining towards the west. Along the length of the river systems the rainfall gradient is marked with the coastal plains receiving nearly no rainfall, while 250 km inland in the upper catchments rainfall exceeds 300 mm per year. Jacobson et al. (1995) propose that all these rivers respond in a similar manner to flood events, and as such can be assumed a single unit. Covering the present surface are largely recent sands and calcrete, while on the western margins harsh climates have limited soil development leaving ancient surfaces exposed. The northern Namib coastline is underlain largely by Damaran sequence granites formed between 500 Ma and 850 Ma and have been significantly folded and subsequently covered in sedimentary deposits (Jacobson et al., 1995), while the southern coastline sub-surface geology is covered by the extensive Namib Sand Sea (Shaw and Thomas, 1997).

4.5.2. Makgadikgadi Pans

The Makgadikgadi pans covering approximately 6000 km^2 are found within the Makgadikgadi Basin, are situated in semi-arid central Botswana (Thomas and Shaw, 1991). The 37 00 km^2 basin represents a range of fluvial, lacustrine and aeolian surface morphologies as defined by Bryant et al. (2007). Covering the present surface of this region are two large ephemeral pans, the Sua Pan to the east with an area of ~3000 km^2 and the slightly larger Ntwetwe Pan to the west (Thomas and Shaw, 1991). The pans are underlain by ancient Precambrian rocks forming the base geology of the region (Thomas and Shaw, 1991) with Carboniferous to Triassic Karoo Supergroup dispersed throughout the region. These two groups outcrop through Kalahari sediments throughout the region.

The Makgadikgadi Basin and most notably the two major pans have consistently been identified to be the primary source of dust in Botswana and the second greatest in southern Africa (Washinton et al., 2003). The mean annual precipitation is approximately 500 mm with 80% of the rainfall for the region falling in high magnitude events during the summer months of October to April (Tyson, 1987). The majority of the rainfall for this region is derived from convective processes such as instability showers and thunderstorms and therefore the incidence of rainfall is highly irregular (Thomas and Shaw, 1991). To add to the variability of rainfall the major rivers that drain into the basin have catchments in the wetter northwest regions, for example the Nata River whose catchment extends into Zimbabwe (Bryant et al., 2007).

4.5.3. Etosha Pan

The Etosha Pan covers an area of approximately 5000 – 6000 km^2 and is the centre of an endorheic, ephemeral basin; draining the inland interior of northern Namibia and southern Angola above the Great Escarpment (Bryant, 2003). The Pan is located in the southern part of the Basin on the western margins of the Kalahari Desert and is underlain by Kalahari sediments (Thomas and Shaw, 1991). Covering the present surface of the pan at an elevation of 1080 m amsl are saline silts, clays and sands. Mean annual rainfall across the basin ranges from 450 mm to 500 mm principally falling in the summer months from October to April although the region experiences high inter-annual variability (Bryant, 2003) with peak potential evaporation between October and December. The catchment within the Etosha basin and more specifically in the Etosha Pan is derived from an extensive network of ephemeral channels to the north of the Pan, which during the wet season results in

sufficient flow to create a shallow inundation on the Pan (Thomas and Shaw, 1991). During the dry season, these networks of channels are visible as large tracts of sparsely vegetated, fine grained, fluvial sediments (Bryant, 2003).

4.5.4. Northern Cape Pan Belt

Pans occur throughout the south western Kalahari/Northern Cape region within inter-dune corridors (Lancaster, 1986). In this area, which extends from Koës in Namibia to Upington in the Northern Cape exists a high concentration of pans, particularly in the vicinity of the lower Molopo valley (Lancaster 1986). Bedrock, mostly Dwyka and Ecca Shales and sandstones of the Karoo system, dominate below a thin cover of Kalahari sands (Lancaster, 1986). Calcretes occur between the pans and locally on pan margins (Lancaster, 1986). The region on the southern margins of the Kalahari-Highveld is arid (Cowling and Hilton-Taylor, 2003) experiencing approximately 250 mm of rainfall annually, falling in the interior summer rainfall zone (Tyson, 1996). Within this region are two major groupings of pans as identified by Lancaster (1986) which is divided by the Molopo River. Pans in both regions have a dominant north south orientation and tend to be in the range of 10 km^2 to 15 km^2 (Lancaster, 1986). Dunes on the pan margins to the west of the Molopo River have typically three major ridges, with the prominent ridge on the pan margins comprised mainly of sand, with 10 – 15% clay silt content being calcareous in nature. Pan margin dunes are poorly developed in the southern extent of this region (Lancaster 1986). While there appears to be no apparent drainage features into the pans, groundwater controls are presumed to be significant (Lancaster, 1986), with springs on pan margins forming in periods of high ground water levels. The low but fluctuating groundwater levels are proposed to result in the deflation of sand and clays effect the formation of the lunette dunes on the south eastern margins of the pans (Lancaster, 1986).

4.5.5. Free State

The Free State on the interior plateau of South Africa has a mean altitude of 1500 m amsl and falls within the catchments of the westward-draining Vaal and Orange (Gariep) Rivers that form the northern and southern borders of the region. Maximum rainfall occurs in summer with monsoonal influence resulting in the highest rainfall during February and March (Tyson, 1996). The region has a mean annual rainfall of between 500 mm and 600 mm per annum experiencing a strong west east gradient associated with the Drakensberg Mountains to the west. Northerly winds ranging from north-west to north-east dominate,

with maximum wind speeds experienced in October (Holmes et al., 2008). The underlying geology for the region is the Karoo Supergroup, with shales dominating the western regions and fluvially derived Beaufort Group sediments dominating the east (Holmes et al., 2008). While dolerite capped mesas increase the relief of the central and eastern Free State, the northern and western regions are flat to gently undulating landscapes. The north and western Free State are widely covered in Pleistocene deposits, comprising primarily of calcretes and unconsolidated sands, with Kruger (1983 cited in Holmes et al., 2008:1195) describing the northwestern Free State as 'plains and pans'. These pans can be found in their highest density to the west of the province, with Holmes et al. (2008) stating that the province exhibits the greatest concentration of pans in South Africa.

The importance of source region characteristics is further discussed by Washington et al. (2003) who states that there are regions globally not identified in TOMS maps and other satellite products that from surface observations should be active sites. Thereby, indicating the need for higher resolution studies and a greater characterisation of source regions to develop a truly global classification of dust source regions.

4.6 REGIONAL SOURCE DISCUSSION

The Namibian coastline has a north south (N/S) extent of approximately 1 500 km and for this study has been defined to extend 300 km inland from the coast, accounts for 180 identified plumes for both MSG and MODIS. The Namibian inland sources are those located at a distance further than 300 km from the coast for the full N/S extent; this includes 14 plumes associated with inland rivers and pans. Detection for the coastal region was dominated by MODIS with MSG providing only 4 source regions along the Namibian coastline all of which were greater than 300 km from the coast; this is possibly explained by edge effects as proposed by Legrand et al. (2001) which was one of the greatest shortcomings of MSG detection. Figure 4.11 shows both the MSG and MODIS imagery from one identified event. It is evident that while plumes are clearly visible on the MODIS image, the MSG composite does not show clear signals for the presence of dust. The event chosen was visible in both Terra and Aqua and should therefore be visible on MSG as no time sampling bias could be attributed to the lack of detection. This figure therefore highlights the importance of the use of MODIS imagery for detection of plumes along the Namibian coastline and further emphasises the limitations of the MSG composite. Figure 4.11f which represents the OMI composite for the day indicates areas of significant load; however these

do not match the plumes visible on the MODIS imagery. Further, it is evident through visual comparison of all of the available imagery shown in figure 4.11 that source attribution and detection for this region is highly variable by sensor.

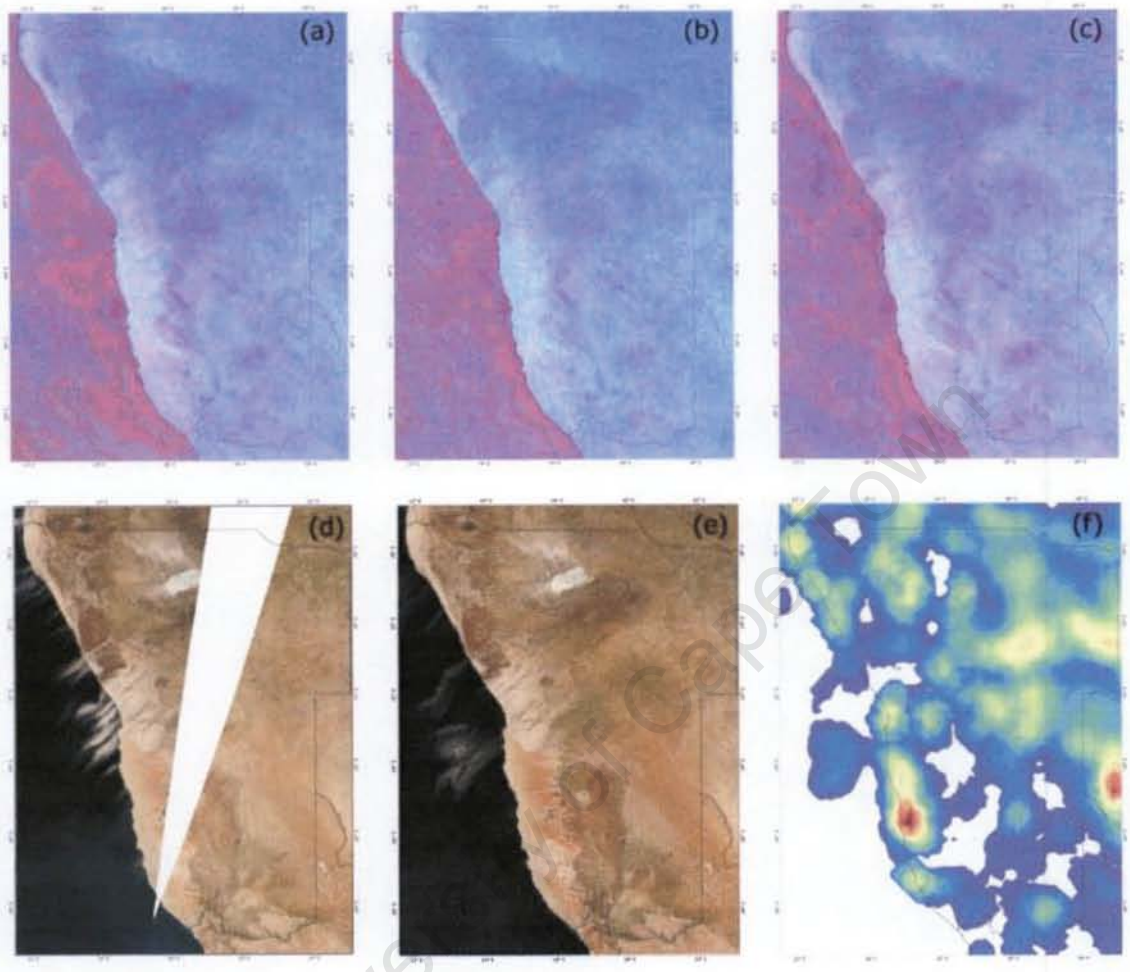

Figure 4. 11 Namibian coastline: the MODIS and MSG images for an event on the 10th of July 2005 (Julian day 191). a) MSG 09:00, b) MSG 12:00 and c) MSG 15:00, d) MODIS Terra 250 m composite of 5 minute passes at 08:15 and 09:55am, e) MODIS Aqua 250 m 12:35 and f) OMI shaded daily product, with purple/blue indicating low aerosol values to orange/red indicating higher loadings. This figure clearly shows the plumes in the true colour images (images (d) and (e)) while no clear signal is present in the MSG composites (images (a) to (c)), with some signal is evident in the OMI (f), although not finitely attributable to the signal in the MODIS imagery.

Geomorphologically, the sites identified on the Namibian coast show the greatest interaction between pan and river systems as dust sources along the length of the coastline. Further inland, numerous rivers, gravel plains and pans add complexity to the multiple systems interacting to produce dust in this region highlighting the importance of fluvial and aeolian interaction for both system recharge and sediment accumulation at sub catchment scale. The pans along the Namibian coastline are recharged through groundwater and have

very little surface flow input. Interspersed amongst the pans are networks of river systems producing plumes at either the mouth or beside the meanders further inland as well as at numerous evaporation points scattered on gravel plains throughout the length of the coastline.

The sources are not equally distributed along the coast and appear to respond quasi-independently to drivers along the length of the coastline. A 200 km stretch between the Hoanib and the Ugab rivers produce the highest density of plumes, with 69 plumes occurring on 14 days. The highest plume frequency happened in 2007 when seven non-consecutive days resulted in 32 plumes; within this area are 5 rivers and 10 coastal pans. The Kuiseb River was the most significant single contributor for the Namibian coastline, with plumes emanating from the river mouth as well as along its meanders further inland. From the Kuiseb River, river mouth and adjacent gravel plains, 19 plumes were detected, second only to the Makgadikgadi Pan in frequency using the MODIS images.

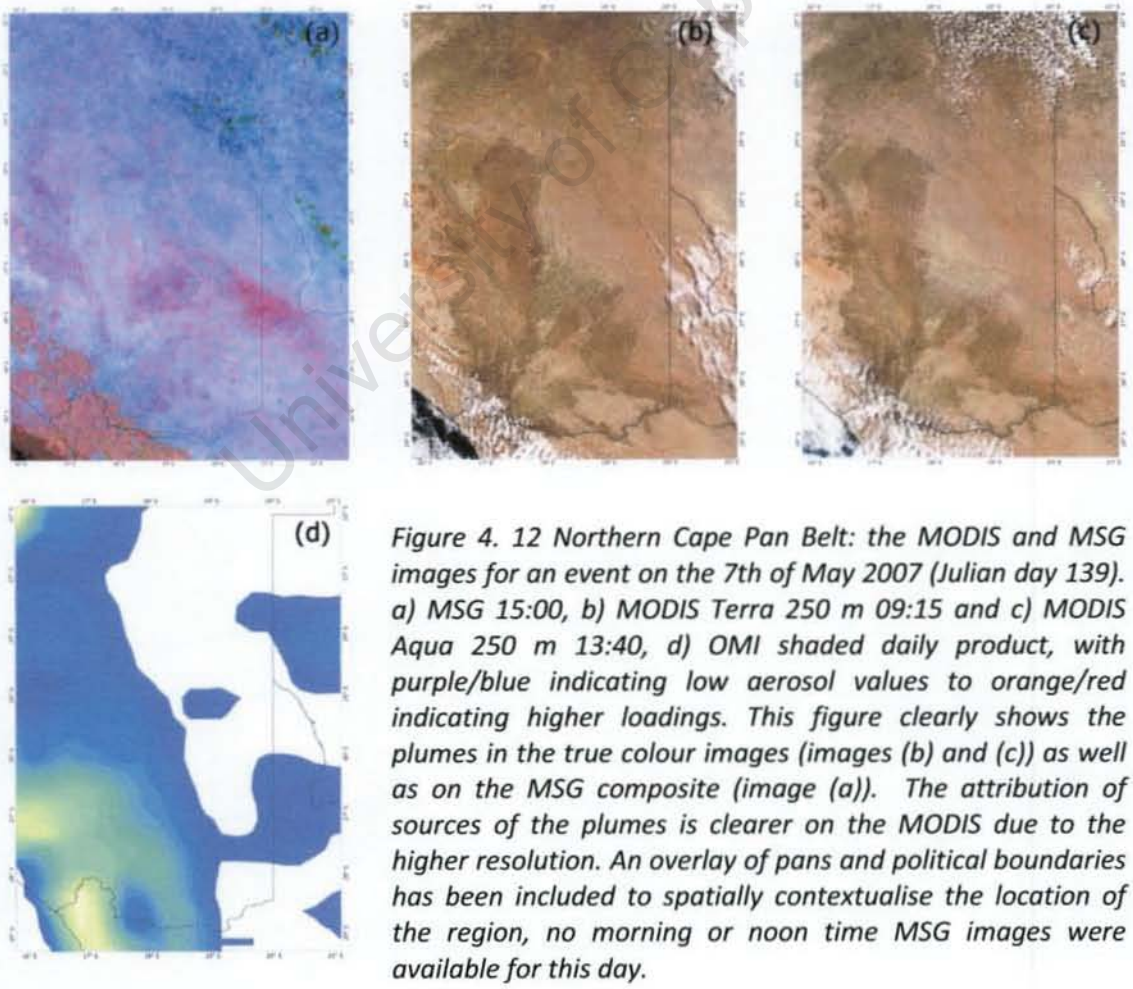

Figure 4. 12 Northern Cape Pan Belt: the MODIS and MSG images for an event on the 7th of May 2007 (Julian day 139). a) MSG 15:00, b) MODIS Terra 250 m 09:15 and c) MODIS Aqua 250 m 13:40, d) OMI shaded daily product, with purple/blue indicating low aerosol values to orange/red indicating higher loadings. This figure clearly shows the plumes in the true colour images (images (b) and (c)) as well as on the MSG composite (image (a)). The attribution of sources of the plumes is clearer on the MODIS due to the higher resolution. An overlay of pans and political boundaries has been included to spatially contextualise the location of the region, no morning or noon time MSG images were available for this day.

The second region, the Northern Cape Pan belt extends in a north-west/south-east direction for 500 km terminating near Upington in South Africa. Forty point source and one area source were identified in this belt, with 90% (37 sources) attributable to pans and rivers or perennial sources accounting for the remaining 10%.

Figure 4.12 above clearly illustrated the ability of both sensors to detect plumes in this region and further highlights the ability of the MODIS imagery to pin point source location to a higher accuracy than the MSG composite. The image also highlights the inability of the OMI product to detect the source and the significant number of missing values (in white) indicates cloud presence or missing data.

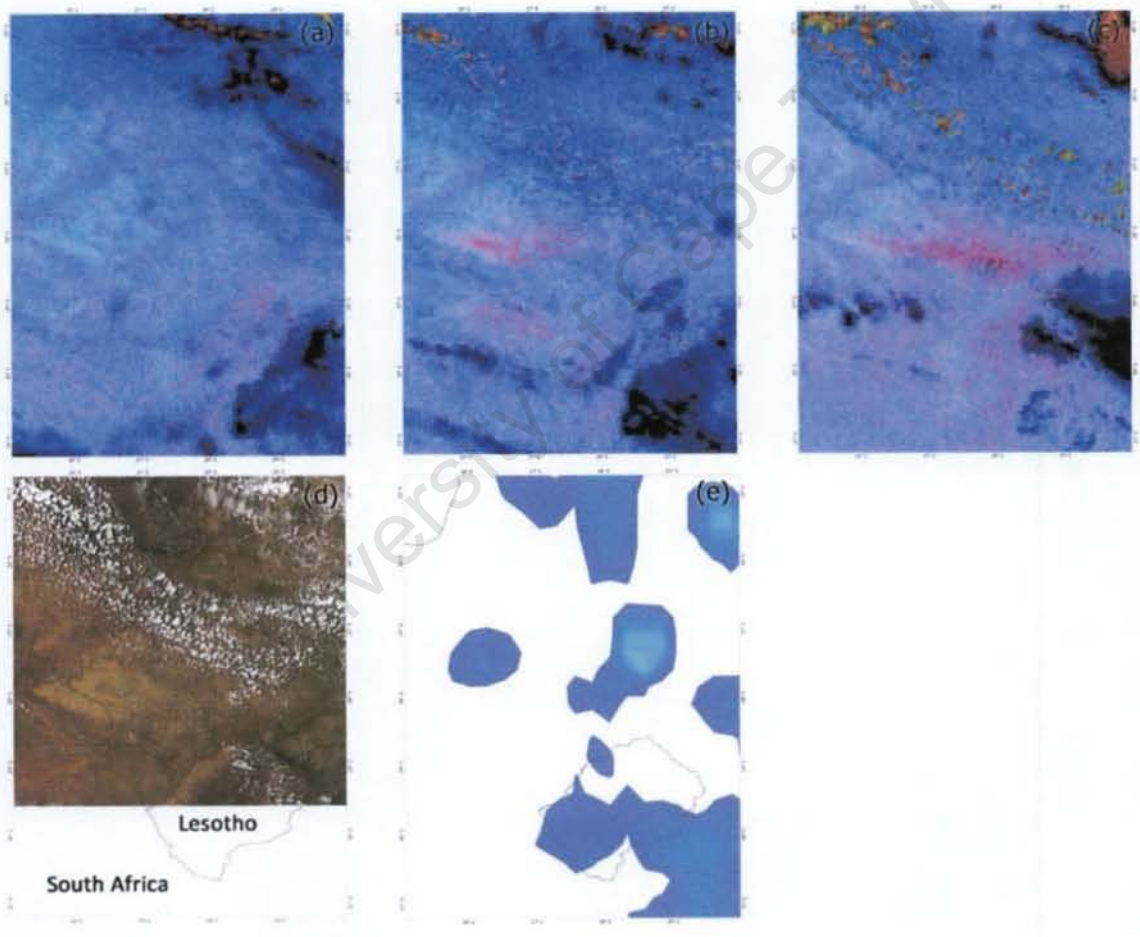

Figure 4. 13 Free State: the MSG images for an event on the 3rd of December 2006 (Julian day 337). a) MSG 09:00, b) MSG 12:00, c) MSG 15:00, d) MODIS Aqua 250 m 11:55am, e) OMI shaded daily product, with purple/blue indicating low aerosol values to orange/red indicating higher loadings. This figure clearly shows the characteristic pink plume in images (b) and (c) indicative of dust plumes. The MODIS Terra image was not available and no dust signal was evident in image (d). Image (e), fails to identify anything of significance due to the presence of clouded pixels in cloud. An overlay of political boundaries has been included on all images to spatially contextualise the location of the region.

The third region, the Free State, was less frequent in emissions and all plumes in this region were identified through MSG. Thus the source location has less confidence than other regions due to the coarser resolution of MSG. All sources within this region have been attributed to either indeterminate pans/dam margins or agricultural/anthropogenic activity due to the dominance of these practices or features in the region of identification. Figure 4.13 clearly shows the characteristic pink plume associated with dust using the MSG algorithm, however for this source MODIS imagery failed to confirm the presence of dust, stressing the discrepancy between the two sensors in detecting plumes in this region. For this event, there appeared to be no signal in the OMI product to suggest the presence of dust; additionally the composite had a significant number of pixels which had no AI value further limiting the value of such products on event based time scales.

The final two regions identified are the Etosha and Makgadikgadi Pans in northern Namibia and Botswana respectively. These two large inland pan sources were the most prominent sources in the study with 31 and 53 plumes emanating from the Etosha and Makgadikgadi (pan areas of 5000 km^2 and 6000 km^2) respectively. These large ephemeral systems showed strong seasonality, with the majority of the emission occurring between May and September. A significant finding was that the location of sources within these large systems showed marked variation. For the Etosha Pan a strong bias was evident towards the east of the pan while with MSG a dominance of points to the west was identified through MODIS (figure 4.14 a.).

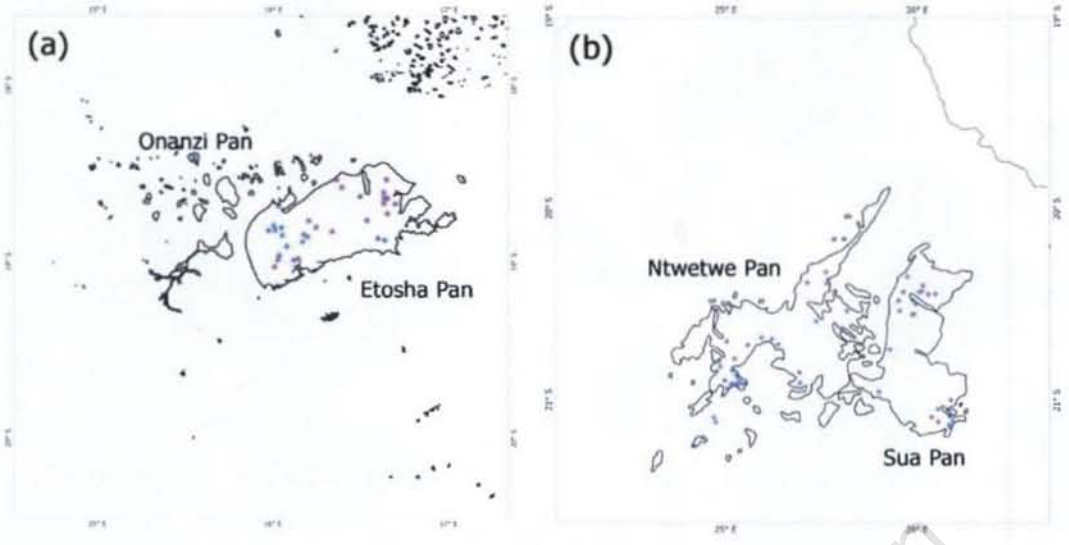

Figure 4. 14 Maps of (a) the Etosha pan and (b) the Makgadikgadi Pans showing the source of the plumes as identified by MODIS (blue) and MSG (purple). From figure a there appears to be no dominant regions instead emissions appear to result from the entire pan surface. Figure (b) however shows clear groupings across the two pan surfaces showing the dominant regions within the pan complex suggesting a north and south dominance on both the Ntwetwe and Sua Pans.

This could indicate a bias due to pixel size and differing resolution, although the aforementioned trend was not evident on the Makgadikgadi Pans. For Makgadikgadi, there were four dominant regions on the north and south margins of both the Ntwetwe and Sua pans (figure 4.14 b.); although these appear to be consistent in both sensors. Therefore the possibility of an influence of sampling time bias could be an alternative explanation for the Etosha Pan.

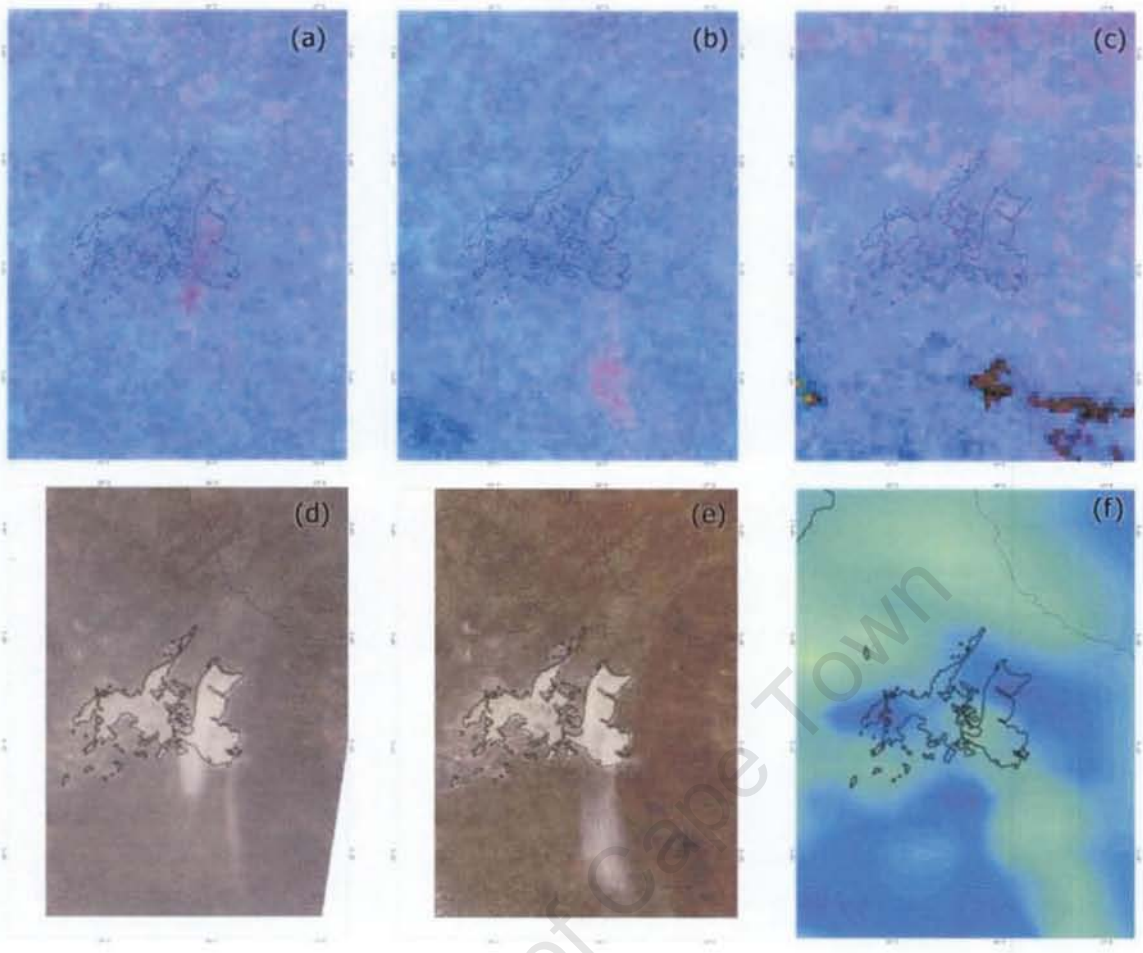

Figure 4. 15 Makgadikgadi Pan: the MSG images for an event on the 26th of August 2005 (Julian day 238). a) MSG 09:00, b) MSG 12:00, c) MSG 15:00, d) MODIS Terra 250 m composite of 5 minute passes at 07:35 and 09:10am, e) MODIS Aqua 250 m composite of 5 minute passes at 11:50 and 11:55am, f). OMI shaded daily product, with purple/blue indicating low aerosol values to orange/red indicating higher loadings. This figure clearly shows the characteristic pink plume in images (a) and (b) indicative of dust plumes, the plume has travelled and dissipated as is no longer visible in the 15:00 image. This event is confirmed in both the Terra and Aqua images from MODIS, the OMI index fails to capture the event. An overlay of political and pan boundaries has been included on all images to spatially contextualise the location of the region.

Figure 4.15 shows a plume travelling southward off the Sua Pan, such a plume accounted for only 10% of the total plumes identified using both MODIS and MSG the remaining 90% resulted in plumes travelling in a westerly direction.

The persistent presence of pink pixels over the Etosha pan; which, when correlated with true colour imagery could not be indicative of dust, is potentially a greater misidentification for this region, such a trend was not evident on the Makgadikgadi Pan (see images a,b,c in figures 4.15 and 4.16).

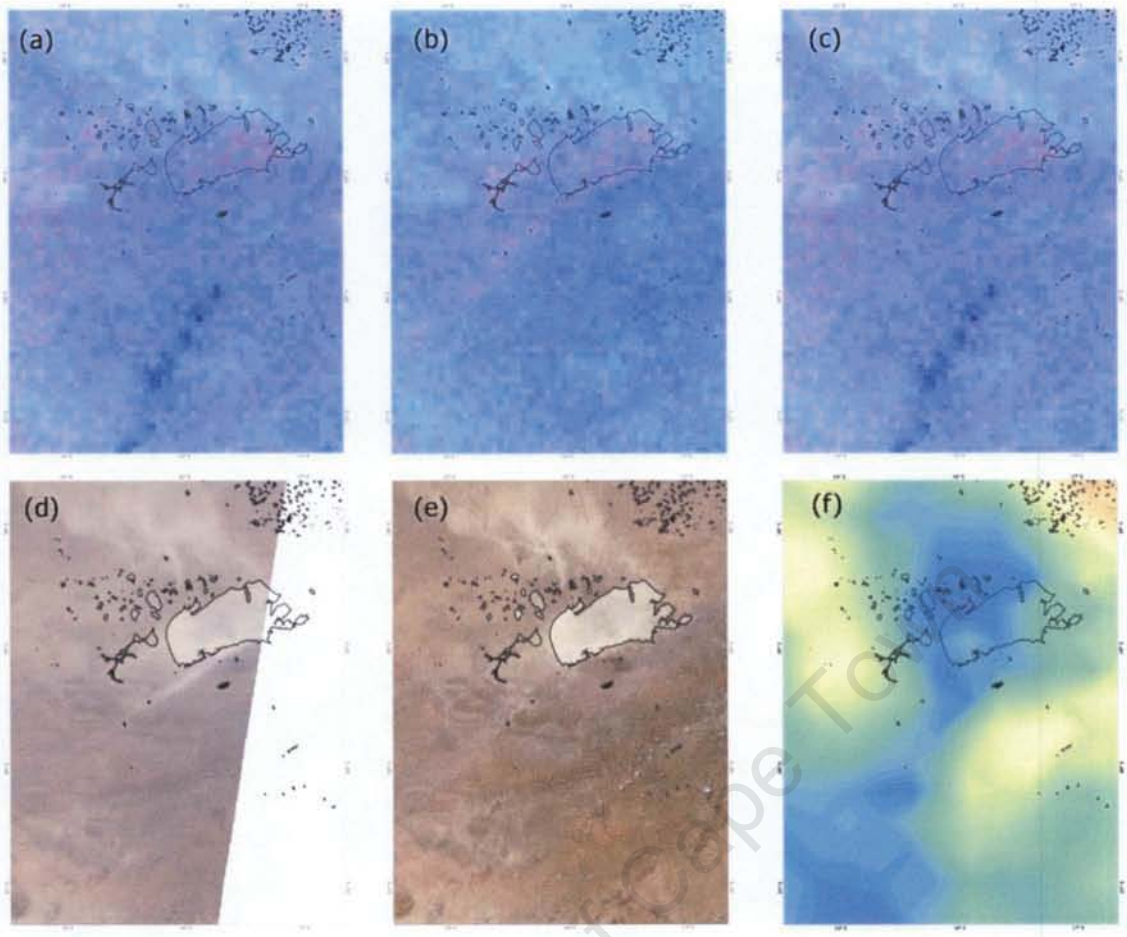

Figure 4. 16 Etosha Pan: the MSG images for an event on the 18th of September 2007 (Julian day 261). a) MSG 09:00, b) MSG 12:00, c) MSG 15:00, d) MODIS Terra 250 m composite of 5 minute passes at 08:15, 08:20 and 09:55am, e) MODIS Aqua 250 m composite of 5 minute passes at 12:35 and 12:40am, f) OMI shaded daily product, with purple/blue indicating low aerosol values to orange/red indicating higher loadings. This figure clearly shows the characteristic pink plume in image (b) indicative of dust a plume, from the true colour image, most notably in Terra (d). It is possible to see the haze that covers this region during the latter half of the year as a result of biomass burning (Abel et al., 2005). The OMI image for this event does not significantly detect the plume, further this product in fact details lower values over the pan surface and detects an aerosol signal to the north east of the Etosha Pan which is not seen in figures (a) through to (e). An overlay of pan boundaries has been included on all images for spatial contextualisation.

4.7 CONCLUSION

This chapter has presented the data coverage, plume and source results derived from MSG and MODIS. The results confirm the Makgadikgadi and Etosha pans in southern Africa as the dominant dust producing regions (Prospero, 1999; Washington et al., 2003) and further introduce the Kuiseb River on the central Namibian coastline into this category. However, the limitations associated with data coverage does not allow for the opportunity discuss the seasonal or inter-annual event frequency associated with any of the sources, although it remains possible to determine areas which during the 2005 to 2008 time period were active source regions.

This study provided a four year analysis of both true colour (MODIS) and composite algorithm derived imagery (MSG) to determine dust source regions in southern Africa and confirmed the dominance of six regions. Firstly, the Namibian coastline with a combination of pans, rivers and gravel plain evaporation points resulting in plumes. Inland of the Namibian coast was a second region whose sources were primarily associated with rivers with the possible influence of anthropogenic practices. The third region, extends from southern Namibia into north western South Africa, namely the Northern Cape Pan belt; comprises of pans (90%) and (10%) ephemeral rivers was a significant addition to the understanding of sources in southern Africa and resulted in 44 events. Two sources in the Free State resulting in three plumes was the fourth region identified, with the fifth and sixth regions being the Etosha and Makgadikgadi Pans.

Due to the availability of multiple images per day, events could be analysed for persistence and temporal dominance of emissions, MODIS Terra was the dominant sensor for detection which is associated with morning coverage while MSG detection primarily occurred on the 12:00 image. Analysis of plume length and trajectory by region revealed that plumes were grouped by direction in their respective region which could suggest a synoptic condition contributing to the control on emission.

Analysis of the two sensors in terms of their ability to detect plumes has illustrated that while MSG performs over the interior, it is unable to detect sources along the coastline. This would further promote the use of a multi-sensor approach to source region determination. For all regions, OMI failed to significantly detect plumes on an event based time scale and thus further reduces its use.

The results presented in this chapter highlight the importance of pans and rivers as a source of dust in southern Africa as well as illustrating the ability to produce a high resolution dust source map of the region using a multi-sensor approach. The following chapter will contextualise the above results in the three themes as identified and discussed in chapter 2.

5. Discussion

The following discussion follows the three main themes identified to be significant in this study, namely: technical, source and circulation. The discussion commences with detection through an appraisal of the products/images and their ability to detect sources in southern Africa – particularly focussing on the strengths and limitations associated with detection over various surfaces, through cloud, biases with height and resolution issues both temporal and spatial. The second theme surrounding source characteristics and typologies is then discussed and promotes the ability to use southern African sources as global analogues; the final theme discusses the regional synoptic circulations influence on emission.

5.1 SPACE BORNE DETECTION OVER SOUTHERN AFRICA

Preliminary observation of the data set has confirmed the results of previous studies which identified two large pan complexes in southern Africa as key dust producing regions. The analysis of MSG using MODIS and TOMS/OMI data presented the opportunity to investigate the use of the MSG-BTD algorithm as proposed by Ackerman (1997) utilising the infrared wavelengths to detect dust. With many known limitations of dust detection in the visible (Lee, 1989), infrared (Ackerman, 1997) and ultraviolet (McPeters et al., 1996) spectra; a multisensor approach was determined to be the best means of obtaining a dust map with the highest possible spatial and temporal resolution as well as limiting the potential contamination inherent in each technique.

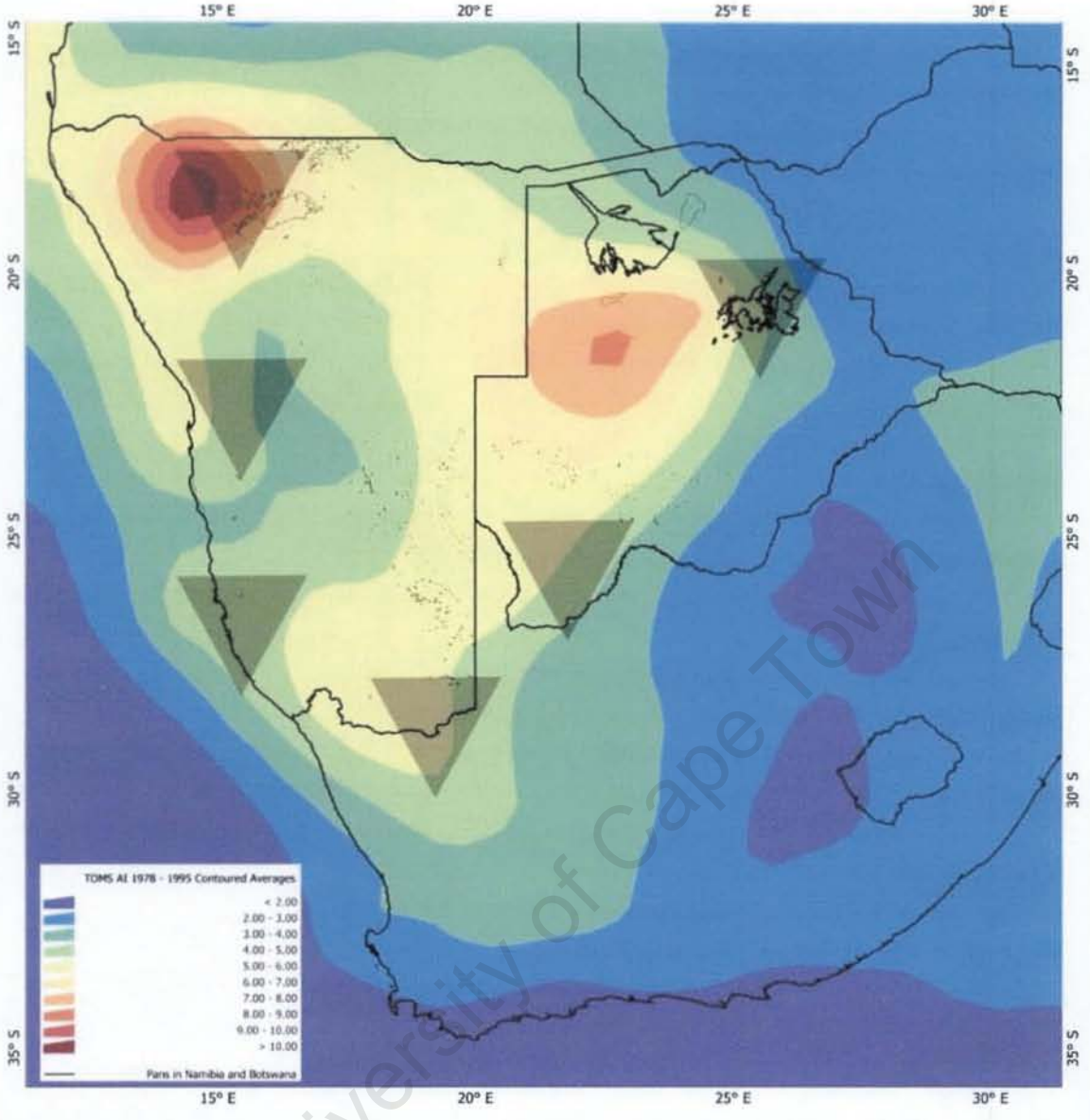

Figure 5. 1 Plot showing monthly averaged TOMS AAI data for the time period 1978 to 1993, X10. (TOMS AAI data resolution 1.0 X 1.25° with political boundaries as well as pans in Namibia and Botswana included for spatial reference). The six regions identified in Engelstaedter and Washington (2007a) have been included (semi-transparent grey triangles) to spatially contextualise the statistical advantages offered by indexed products.

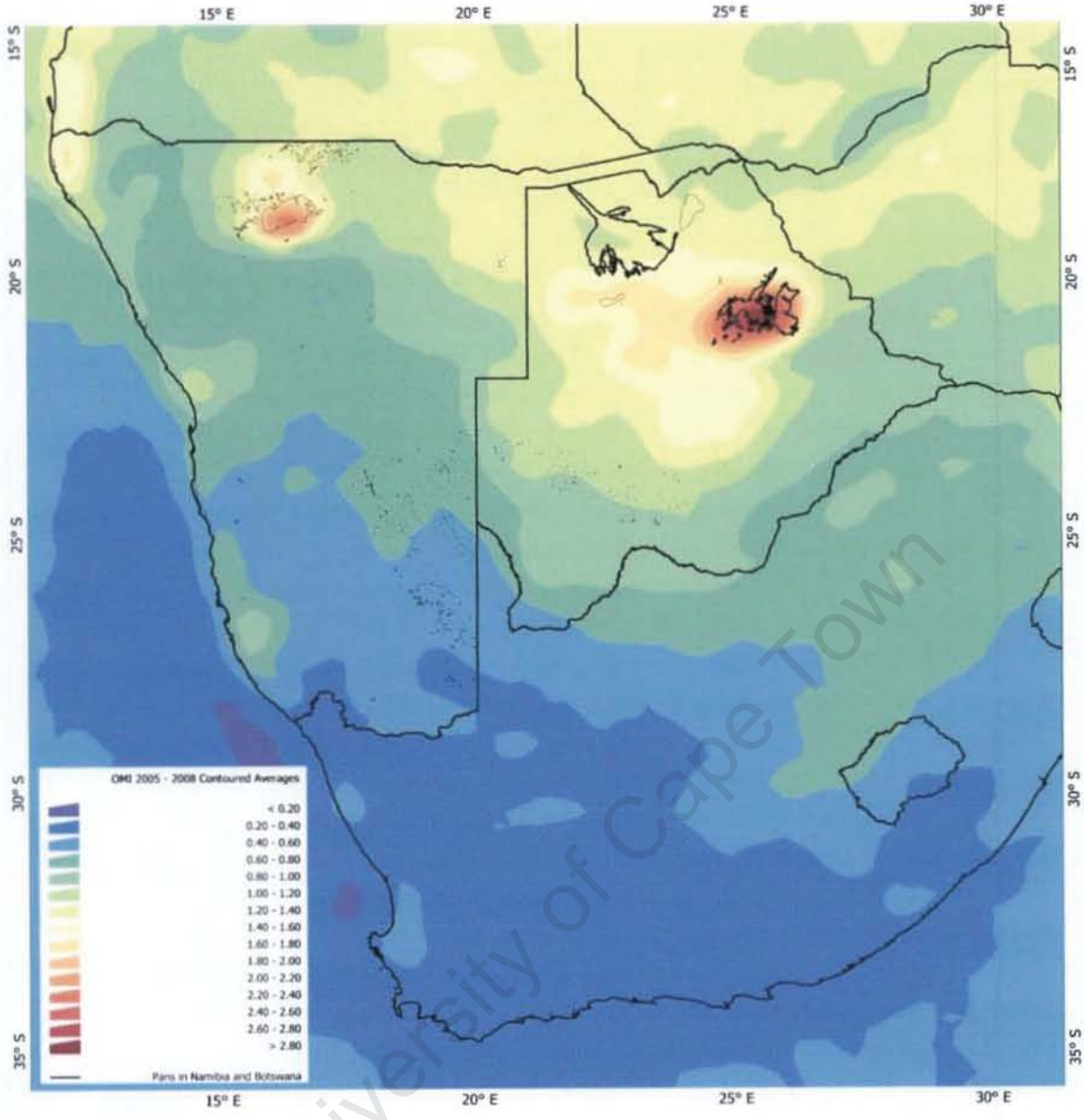

Figure 5. 2 Plot showing monthly averaged OMI AI data for the time period 2005 to 2008 correlating with the time period of MSG and MODIS imagery used in this study. (OMI AI data resolution 0.25 X 0.25° with political boundaries as well as pans in Namibia and Botswana included for spatial reference)

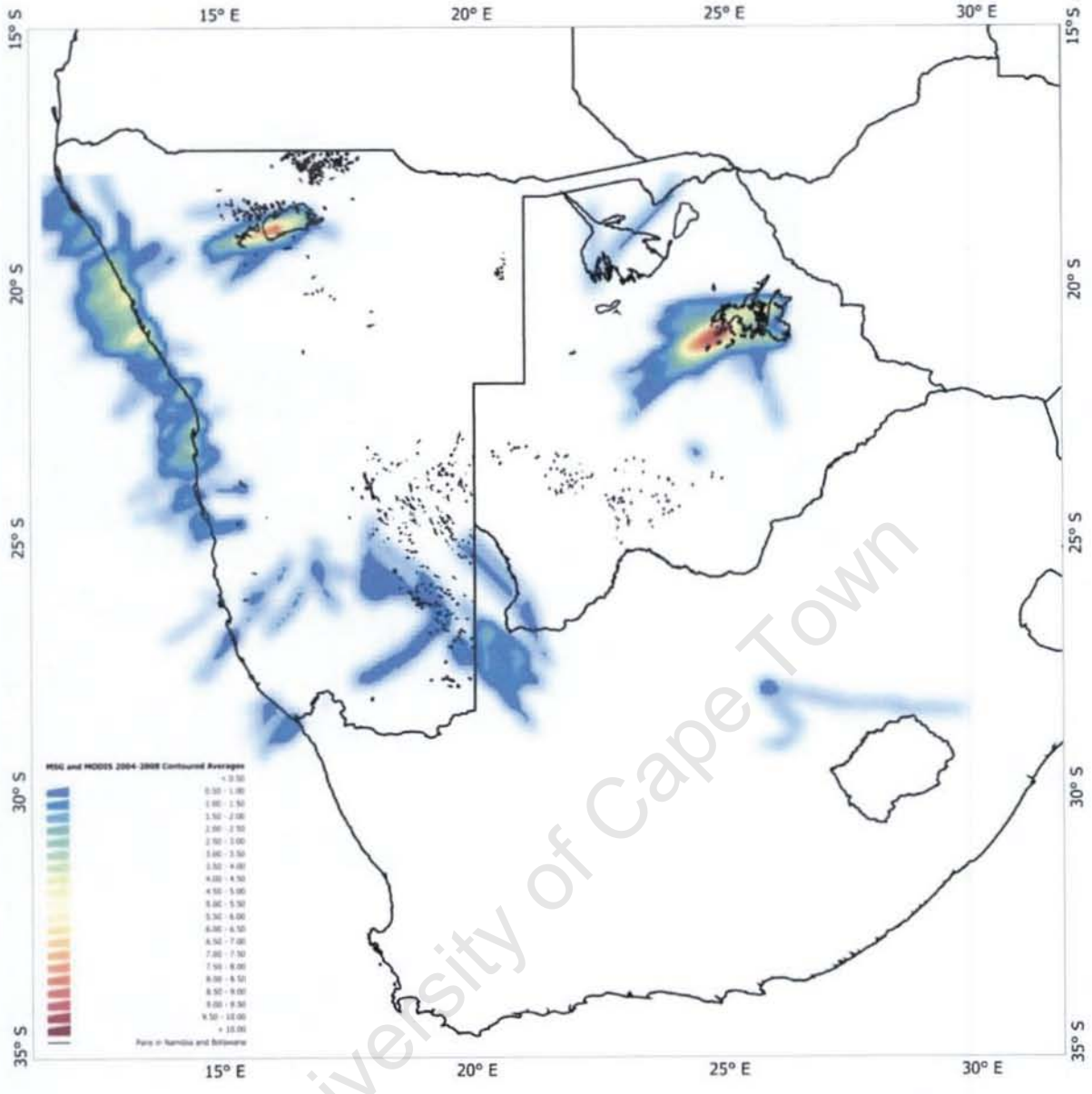

Figure 5. 3 MSG and MODIS contoured and shaded plot showing the frequency of dust activity over a 0.10X0.10° grid over the entire domain for all plumes identified from 2004 to 2008. (Political boundaries and pans in Namibia and Botswana have been included for spatial reference)

Primary correlation of the MSG and MODIS data sets permits the high resolution detection of source regions which, despite the inconsistency in data coverage, and has resulted in the identification of 23 sources using MSG and 93 using MODIS. This can be seen as a significant advancement on the TOMS based studies by Washington et al. (2003) and Prospero et al. (2002) which identified two sources. More recently statistical analysis in a study by Engelstaedter and Washington (2007b), again on TOMS data, increased this from two to six in southern Africa, although the Engelstaedter and Washington (2007b) study failed to identify any more than a non-attributable surface region from which dust could originate and remains significantly less than the number of sites identified in this study and as highlighted along the Namibian coast in a study by Eckardt et al. (2005).

Through correlating the visible, infrared and ultraviolet products or imagery, the various limitations and advantages can be identified. Through preliminary observations of the TOMS (1978-1993) average product, the OMI (2004 to 2008) averaged product and the frequency product derived from MSG and MODIS, the incremental increase in resolution can be seen together with a greater potential for source attribution. However, as discussed below, there remain limitations.

5.1.1 Detecting over surfaces - contrast:

The lack of contrast between the desert surface and the dust plume was highlighted by Bullard et al. (2008) to be a significant challenge to visible terrestrial detection. The method applied in this study utilising the sequential viewing of images which permitted the identification of the plume through the distortion of surface features as the plume traversed the region, proved to be the best method for dust detection in the visible spectrum. While, for visible imagery manual analysis was determined to be the best method of detection, the MSG composite did successfully identify terrestrial sources. Confirming findings by Legrand et al. (2001) who proposed that the infrared method is most appropriate over land surfaces particularly around midday, confirmed by 51% of all plumes being identified on the noon time image. In contrast to a study by Schepanski et al. (2007) in north Africa where the vast Saharan expanse results in relatively homogeneous surface coverage, the land surface of southern Africa with variable geology, topography and vegetation appears to have a non-uniform response to the pink composite. In southern Africa the regions surrounding the Cape Fold Belt, The Great Karoo, Strydpoortberge, Richtersveld, Grootkarasberge, Tsarisberge and Mariental consistently appear pink in the MSG composite as a result of non-uniform surface heating. Thus visual masking was necessary to remove the false

identification of these features. Despite the potential for false identification from the aforementioned features, MSG successfully identified continental plumes. Along the coastal regions, MSG identified only two sites, both located markedly inland, a possible explanation is offered by Legrand et al. (2001) who attributes the effects of water vapour contamination in the use of infrared channels for detecting aerosols, particularly in coastal regions and thus termed "edge effects".

Legrand et al. (2001) propose that, in both continental northern and southern Africa the columnar water vapour is below the threshold of 2.5 $g.cm^{-3}$. This is considered to be a significant threshold for affecting radiation and contaminating signals, therefore detection should not be compromised. However a potential source of contamination over the Namibian coastal region is the presence of fog and low level cloud cover, both of which result in values greater than 2.5 $g.cm^{-3}$ atmospheric columnar water vapour threshold (Shanyengana et al., 2002). This finding could result in the lack of observations from the Namibian coastal regions as identified in the pink composite, as fog is known to occur between 60 and 200 days per year and extends for some distance inland (Shanyengana et al., 2002:1). Therefore, despite the classification of much of the domain to be arid and semi-arid (Shanyengana et al., 2002; Warner, 2004; Eckardt and Kuring, 2005), the advection inland of cool moist air provides a significant moisture loading, reducing the applicability of the MSG composite over coastal southern Africa. Nevertheless, the clear contrast between the pale dust and dark ocean in MODIS imagery resulted in multiple clear plume detections in the region.

5.1.2 Cloud and height:

While, historically, clouds are proposed to be the greatest contaminant in detection (Prospero et al., 1999; Torres et al. 2002b,c) it was not observed to be a significant limitation for this study, due to the seasonality of emissions in southern Africa being associated with winter. Typically the conditions over the interior and coastal regions are clear and cloudless in response to the dominance of the continental high pressure system (Tyson et al., 1987). Through the linking of events with synoptic circulation it was further observed that the intensification of the continental high pressure system for interior sources, and the intensification of the west coast trough for coastal sources, were the most common circulation systems resulting in plumes. Both of these circulations are not typically associated with cloudy conditions over the domain, thus the potential for cloud contamination appears to be negligible. Summer downdrafts with strong convective systems

are associated with localised dust fronts although are often smaller than available pixel size and as a result many of these features are largely undetected while their presence, formation and associated sediment transport is well documented.

Attributable to the limited coverage provided by the daily TOMS and OMI products through missing data pixels (figures 4.12d and 4.13e) and cloud masking, correlation was performed over long periods to compare the climatology provided by the various products and assess their detection ability over an extended period. This further aid the separation of dominant source signals from background aerosol noise. The height bias which is associated with the UV method (Torres et al., 2002b) is not evident in the IR and visible techniques where aerosol height does not affect detection (Kaufman et al., 2000; Krotkov et al., 2002). It is this fundamental limitation of TOMS that resulted in the greatest differentiation between the TOMS and the MSG/MODIS composite annual averages (Figures 5.1 and 5.3). While for TOMS the dominance of the Makgadikgadi and Etosha can be observed (from figure 5.1), the offset between the source and the maximum index value is notably west of the source region. While for the MSG/MODIS composite the Pans are the source of the highest frequency of plumes. Further, the use of TOMS requires the correlation of the maximum AI value to a source feature that is assumed to be the contribution regions. This would introduces a level of assumption in source attribution as discussed in Eckardt et al. (2005).

The use of MODIS and MSG negate this, as for all detected plumes in this study the upwind edge of each plume was marked, as this is considered the best method of detection at this scale confirmed in Lee et al. (2008). The method successfully indentified the proposed significant source regions and confirmed the dominance of pans as dust sources (Prospero et al., 2002). As shown in figure 5.1, six source regions were identified as per Engelstaedter and Washington (2007a) which is based on statistical analysis and correlation with the TOMS composite. The horizontal offset in response to the height bias highlights the assumptive nature of this product in the identification of source regions, as for the Makgadikgadi Pans, the maximum AI value is south and west of the pan complex, while the region identified in the study correlates perfectly with the domain of the pans. Therefore a significant offset can be assumed to be inherent in the site selection in response to both the transport and height of first detection as associated with the TOMS product (Prospero et al, 1999; Torres et al., 2002c). Thus the non-attributable surface regions as identified in the Washington and Engelstaedter (2007a) study are further limited in their use for increasing the understanding of surface sources.

5.1.3 Resolution (Spatial and Temporal):

For the detection of dust, which has a dynamic lifespan and variable manifestation in the atmosphere (Schepanski et al., 2007), high temporal and spatial resolution is required. TOMS, which was the first product to produce a global aerosol distribution map (Kaufman et al., 2002), is further suitable for use due to the long data time period it provides and has resulted in the indexed product being used for much of the foundational research in global dust source regions (e.g. Prospero, 1999; Prospero et al., 2002; Washington et al., 2003; Engelstaedter and Washington, 2007). Figure 5.1 utilises the TOMS aerosol indexed product for a 15 year average (1978 – 1993), identifying the climatology of aerosols over southern Africa. The daily temporal resolution of the TOMS product and 1.0 X 1.25° spatial resolution has further limited its application. Continuing the use of the principles of ultraviolet detection the OMI product has significantly increased the resolution to 0.25 X 0.25°, although the temporal resolution remains limited to daily coverage (Levelt, 2002). Figure 5.2 shows the greater attribution of significant aerosol loading to the Makgadikgadi and Etosha Pans, thereby highlighting the increase in potential for studying aerosols regionally. This figure also shows a greater index load present over the Makgadikgadi Pans which could confirm the dominance of this pan complex over the Etosha Pan in terms of southern African sources as is identified through the use of MODIS and MSG.

While in this study on an event based resolution, TOMS and OMI failed to detect the nuance of dust events due to either the poor spatial or temporal resolution (figures 4.11f, 4.12d, 4.13e, 4.15f and 4.16f). This is typically in response to the inability of the products to detect low level sources or the potential of cloud contamination. Despite this, the TOMS and OMI products have proved valuable in their ability to detail and ascertain the mean aerosol loadings and climatologies of the region and global overviews.

For the coastal domain of this study, detection was possible despite the inability of MSG to detect coastal plumes. This was achievable due to the marked contrast between the dark ocean surface and the pale dust plumes in the visible spectrum (Swenk and Curran, 1974). Therefore, for coastal southern Africa, particularly the western coast where fog affected MSG detection, detection using true colour imagery proved the most appropriate technique. With the true colour imagery multiple coastal sources were identified confirming the results of studies by Eckardt and Kuring (2005) and Eckardt et al. (2001). In the study by Eckardt and Kuring (2005) using SeaWifs imagery, a high resolution map of the Namibian coastline was

developed, identifying 43 point sources accounting for both pans and rivers which resulted in dust plumes between 1998 and 2001. As no clear signal had been identified from the TOMS and UV products (as can be determined from figure 5.1 and 5.2 along the Namibian coastline), this highlights the inability of TOMS to detect significant contributors in this region. Despite the two possible sources as indicated by Engelstaedter and Washington's (2007a) study which indicates two possible Namibian coastal sources, there appears to be limited correlation between the proposed sources and significant regions in either OMI or the MSG/MODIS plots. Thus, as both the TOMS and OMI product are based on similar detection methods and both fail to detect coastal plumes and dust below 1000 m (Prospero, 2002) for this study these products were not found to significantly advance current knowledge on southern African sources.

5.2 TECHNICAL CONCLUSION

While confirming the dominance of the Makgadikgadi Pans and the Etosha Pan which were ranked globally 9th and 7th respectively by Washington et al. (2003), this study identified the Makgadikgadi Pan to be the most frequently identified source, with the Kuiseb River catchment being the second and the Etosha Pan the third most active sources. This both confirms and challenges the existing literature of southern African sources, in particular the inclusion of the Kuiseb River in this group. In confirmation, a study by Eckardt and Kuring (2005) highlight the dominance of the Kuiseb River, although Eckardt et al. (2001) in a similar study over a different time period did not observe this dominance. This indicates both the complexity of fluvial systems as sediment sources and the variability of these systems over time. Such variability could be an indicator for the argument of source versus supply limitations at site level.

The rankings defined by Washington et al. (2003) were not mirrored in this study. This could be attributed to the differences between the TOMS AAI product and the presence/absence approach which resulted from identification using MSG and MODIS. The main difference is that the TOMS product, which is an aerosol indexed product, includes an element of the concentration of aerosols, on a linear scale with high values being associated with greater dust loading then lower values (Torres et al., 2002b), although both products utilised in this study provide a presence/absence understanding of aerosols rather than the quantitative response provided by TOMS and OMI. It can therefore be argued that, while in this study the Etosha Pan was not identified to be the most significant contributor in terms of emission

frequency. It is possible that in fact by deflated volume it may indeed remain the most significant contributor. Thus, while correlation with TOMS and OMI products can confirm southern African sites, it must be understood that quantitatively correlation has its limitations.

While MODIS was initially only proposed to be the secondary data set with which to correlate and confirm findings by MSG, the superior ability of the true colour imagery to detect plumes was evident. Thus, despite the limitation associated with this method, in terms of manual detection of plumes, analysis of true colour imagery has for this study provided the greatest potential for dust source detection. Despite the high resolution provided by MSG, this product was unable to detect coastal sources which were confirmed to be significant following studies by Eckardt and Kuring (2005) and Eckardt et al. (2001). Further, due to signal from geology and standing water being falsely identified as dust in the MSG composite, masking would be required should the automation of this product be performed.

From the above discussion it is evident that through the use of MSG and MODIS there has been a significant advance in the understanding of southern African sources. This can be most significantly observed in the identification of multiple previously unidentified sources, and for large sources with significant areas within these sources. This then introduces the complexity of scale. On a global scale we have advanced from area points to source specific locations, while on a regional scale the multiple system interactions within the sources become dominant as drivers or inhibitors. On the site scale, surface chemistry and roughness as well as wind shear dominate the literature – however such resolution did not fall within the scope of this research nor was it provided by the sensors or products utilised. It does however provide a base on which surface analysis can be performed. For this study the key aim was to identify source regions and locate these within their regional context and therefore, while the resolution has increased to the site scale, discussion remains on the regional scale.

Some techniques which could be used to increase our understanding of regions are presented in the following section, with relevance to specific sites where alternative data were available or the significance of the region necessitated its inclusion in the discussion. Further, the following section discusses the applicability of using southern African sources as analogues of global sources according to a set of previously identified site typologies.

5.3 SOURCE DISCUSSION

The regional context as outlined in chapter 2 and discussed in chapter 4 confirm that there are a wide range of geomorphologic surfaces and settings in southern Africa that have the potential to be dust sources. Through the results seven geomorpholological surfaces were identified to be significant over the domain, these dominant source-types can be recognised as pans, rivers, marshes/vleis, dam margins, gravel plains, dunes and evaporation points. Furthermore, these can be grouped into four broad categories which occur recurrently within the world's drylands as identified by Prospero et al. (2002) Washington et al. (2003) and Goudie and Middleton (2006). The following are the resultant classifications: A) large, dry active or former lake beds and pans B) seasonally dry river valleys and sabkhas C) small, closed ephemerally flooded depressions and pans and D) sand dune systems.

However, the degree of wind-driven sediment movement and the generation of dust vary, not only between source areas but by region and event at individual sources. Such variability within sources can be seen in figure 4.14 and between sources, such as in the inconsistency of emission along the length of the Namibian coastline or through the sources in the Northern Cape Pan belt. A possible explanation for this is discussed in section 5.5, which assesses the regions of emission against the synoptic circulation and thus determines synoptic controls on emission.

Within the domain, three of the four site typologies were identified (A,B and C) which highlight the potential to use southern African sources as global analogues and, through this, increase our understanding of basin scale processes and constraints on emission. The importance of southern African sites is founded on the fact that much of the region is currently emitting dust (Bryant et al., 2007) and also shows evidence of active sand transport (Wiggs et al., 1995). Analysis of palaeo-dunes and marine cores (Thomas, 1997) indicate periods of strong aeolian activity in presently dormant areas, many such areas are modelled to be active in the near-future (Thomas et al., 2005) and are therefore potentially important for global system feedbacks.

The following section discusses the three site typologies identified in this study in the context of the five identified regions. Each type is contextualised through an introduction to the global setting and set typology before discussing the regional analogue as identified in this study. For the whole domain, 61% of all identified sources were type A, with type B receiving 27% and the remaining 12% being attributed to type C. Further, the identification of type A sources can be linked to the Etosha and Makgadikgadi Pans, while type B

encompasses much of the Namibian coast. Type C accounts for the remainder of the Namibian Coastal sources, the Northern Cape and the Free State region with this source type showing the greatest variation in surface geomorphologies, geographical and climatological settings. These results demonstrate that dust sources are associated with a range of geomorphologies at both basin and sub-basin scale, again confirming the ability to use southern African sources as global analogues. A similar outcome was obtained by Bullard et al. (2008) on a study of the sub-basin scale geomorphology of the Lake Eyre Basin in Australia.

Where multiple sources of data are available, a greater level of detail can be added to the discussion to highlight the importance of the complexities and possibilities for increasing our understanding of sources both regionally and through analogues and assumptions raising the prospect of a global scale picture. Thus there is no uniform approach to discussing the following regions and typologies, this does not reflect on the level of importance attributed to any source type or region.

A. Large, dry active or former lake beds and inland pans:

In terms of source type, the initial findings by Prospero (1999) and Washington et al (2003), who identified pans to be the dominant source of dust emission, are confirmed in this study. In both MSG and MODIS, over half of all emission sources were attributed to pans with these pans accounting for almost 80% of all detected plumes in MSG and 56% in MODIS. Of all pans identified between 2005 to 2008, 29% of the total identified MSG plumes could be attributed to the Etosha pan, while the Makgadikgadi resulted in 34% of the identified emission, thereby possibly indicating that either the dominance of the Etosha pan as detailed in existing literature may require revision or that, due to the discontinuous nature of the data, the Etosha pan was under identified.

In Shaw and Thomas (1997) the complexity of pan environments and their dependence on local conditions is highlighted, making generalisations about these landforms and therefore their response to processes difficult. A major source of variability among pans is the presence and seasonality of standing water (Shaw and Thomas, 1997) with the extent, frequency and duration dependant on climatological and hydrological regimes. It is important to understand the climatological controls on these systems (see section 5.5 for further discussion), viewing them in the context of both their hydrological and circulatory regimes is therefore important. Shaw and Thomas (1997) further elaborate that micro-scale

variations on the pan surface can serve both to inhibit and promote dust deflation, arguing that the development of evaporite and clay crusts can protect surfaces from deflation. The lack of protective vegetation cover, high sodium concentrations, the development of wind-susceptible clay desiccation curls and pellets as well as the presence of fine sediments all favour the operation of deflation from playa and pan floors when they are not inundated by water (Shaw and Thomas, 1997). As the surface morphology of pans is the product of periodic flooding and desiccation, including the effects of rainfall onto the pan surface, crystal growth and dissolution and aeolian deflation, multiple micro-scale processes need to be understood to better comprehend the complexities. Such systems were described by Shaw and Thomas (1997) to be "... among the most ephemeral of geomorphological phenomena...lasting no longer than the interval between one rainfall event and the next."(Shaw and Thomas, 1997:309). Nowhere is this complexity and lack of homogeneity of coverage more obvious than on the Makgadikgadi Pans, where discreet areas of the pan proved to be consistent sources, while others that in theory should be, did not result in detectable plumes.

A.1 Makgadikgadi

Due to the high resolution potential obtained in this study it was possibly to derive a sub-basin scale emission signature for the region. Within the basin four regions were identified to be dominant occurring on both the northern and southern margins of the Ntwetwe and Sua Pans. This could suggest that the sub-basin scale geomorphology is not as homogeneous as was initially proposed and that the entire system may not be an active sediment source as was initially thought. Middleton (1997) ranks surfaces based on the variable nature of the surfaces to deflation and susceptibility for entrainment or inhibition from most erodible to least erodible in order: disturbed soils, sand dunes, alluvial and aeolian sand deposits, disturbed playa soils, skirts of playas, playa centres and desert pavements. This variability could explain the observed distribution of source regions across the pans, since no sources are associated with the centres of the large pans and confirms the dominance of the pan margins'. As can be seen from figure 5.4, the pan surface does not have homogeneous surface coverage in response to differential wetting across the pan complex and links to the micro-scale variations as discussed by Shaw and Thomas (1997). Reheis (2006) has demonstrated that changes in surface hydrology of ephemeral lakes can lead to extreme changes in regional dust emission, characteristics that Bryant et al. (2007) assume to be relevant to the Makgadikgadi Pans. This study has confirmed the role of surface hydrology in

both supply and inhibition of dust deflation, further establishing the pans as a supply limited system. Recent work by Bryant (*pers. comm.*, 2009) using MODIS imagery to identify surface water on the pans, has revealed that there is a wetting trend towards the eastern margins of both pans, although due to the similarity in the spectral signature of the highly reflective pan surface, wet surface clays and standing water, the possibility of both underestimation and overestimation remains. Through the knowledge that the pans are a supply limited system, it may be assumed that the wetting trend would result in a greater supply of sediment on the eastern margin. However there does not appear to be an easterly bias in sites, therefore it is possible that, during the dry season, there remains sufficient water to inhibit deflation.

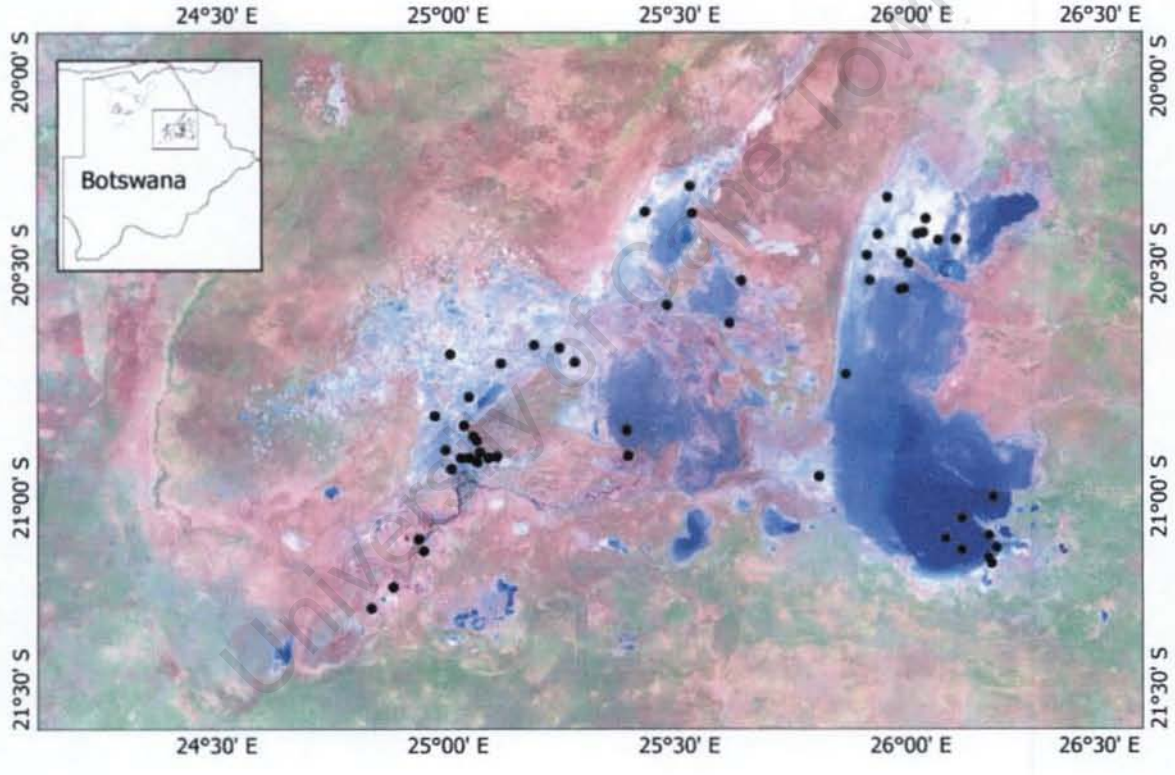

Figure 5. 4 Landsat image of the Makgadikgadi Pans. Source regions identified using both MODIS and MSG (black circles) have been included to show the discreet source regions within the pan complex where dust emanates. The Inset shows the location of the pan complex within Botswana.

This research has increased the resolution of dust emission from the Makgadikgadi Pans, highlighting the spatial variability of emission from a large pan complex. The lack of surface homogeneity across the pans highlights the necessity for a systematic analysis of the pan

surface correlating hydrological controls to surface wetness versus standing water in an attempt to refine our spatial understanding of the pan hydrology.

A.2 Etosha

The above discussion on the Makgadikgadi Pans demonstrates that dust sources are associated with a range of geomorphologies, while Bryant et al. (2007) and Bryant (*pers. comm.*) have shown that remote sensing products increase the potential to map surface water coverage. However this alone cannot determine the presence/absence of dust for the region. The response to wind velocities and thresholds and dust appears to show no clear relationship (Bryant, 2003). This may be because different environments respond in varying ways to seasonal precipitation or drought according to the balance between sediment supply and physical sediment availability which is affected by other aspects, including surface roughness and vegetation cover. Prospero et al. (2002) determine that a further complication to understanding emission characteristics for this region is the introduction of human induced impacts. In the north part of the area covered by figure 5.5 the effects of land clearing, agriculture and land degradation can be seen; this region supports the highest population density in Namibia and this intensive land use has an effect on the regional hydrology and vegetation which could affect the dust emission over the region.

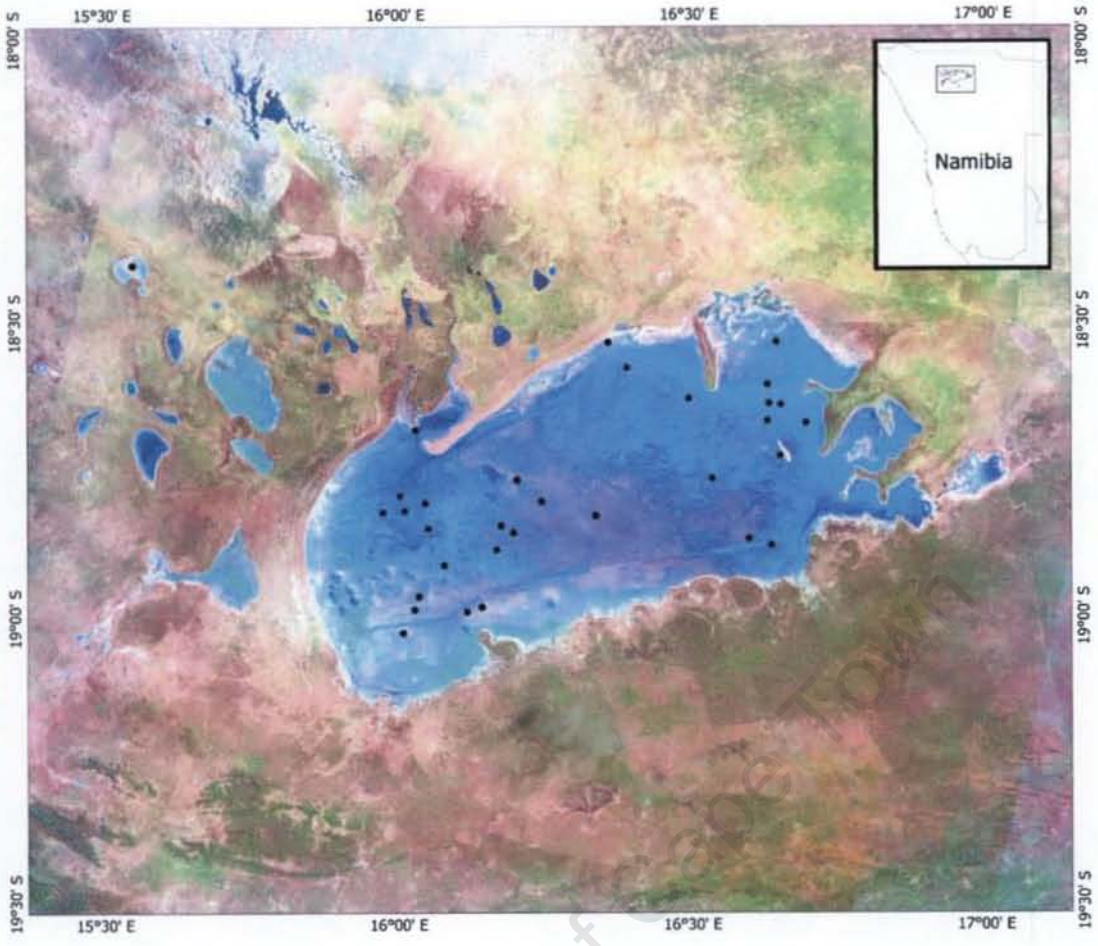

Figure 5. 5 Landsat image of the Etosha Pan. Source regions identified using both MODIS and MSG (black circles) have been included to show the source regions within the pan where dust emanates, a single source to the north west of the figure can be attributed to the Onanzi Pan. The Inset shows the location of the pan complex within Namibia.

The Etosha pan provides a similar variability in emission characteristics as was identified on the Makgadikgadi Pan. However, here near the total seasonal coverage of water (Bryant, 2003) provides a uniform sediment supply from which dust is deflated. Thus, unlike the Makgadikgadi pans, there appears to be no spatial bias in emission from this region. Nevertheless, multiples sources from which emission results on a pan surface is by no means unique to type A sources, with Prospero et al. (2002) commenting that Etosha is not unusual in having multiple sources within its bounds. In a hydrology and dust study by Bryant (2003) on the Etosha Pan, it is proposed that the pan is not the sole dust source in this region, although other than a single event from Onanzi Pan no other sources were identified in the region. Regardless of the extensive network of ephemeral channels (*oshanas*) (Bryant, 2003; Goudie and Middleton, 2006) to the north west of the Etosha Pan and the relatively large ephemeral lakes and swamps to the west (Prospero et al., 2002) it appears that, as identified

in this study, the Etosha Pan and the Onanzi Pan are the most important sources of dust in the region.

The area to the north of the Etosha Pan is presently supporting almost 25% of the national population (Mendelsohn et al., 2002) and is, as a result, experiencing extensive land degradation (Prospero et al., 2002). Despite this, the strain imposed on the system does not appear to be a mechanism of dust activation or promote the availability of surface sediment in the region. As a result, this region experiences less emission then its sediment potential would prescribe, as the region is occupied by several potential sediment sinks with much of the sink area further stressed due to extensive land pressures as a result of anthropogenic activity.

Thus as these type A sources have been identified to be characterised by variability and a range of geomorphologic surfaces, a greater coupled understanding of the hydrology of these large, dry inland former lake beds and pans is needed. Together with more detailed and high resolution climatic observations and an understanding of their surface thresholds for deflation is necessary to truly get closer to understanding these large dynamic systems.

B. Seasonally dry river valleys and coastal pans

Reid and Frostick (1997) identify the importance of ephemeral streams for transporting vast quantities of sediments during flood events, in both bed and suspended load. They further emphasise the importance of ephemeral rivers stating that when they flow, they are more efficient erosional agents than their perennial counterparts. Along the Namibian coastline this is apparent in the frequency of emissions from ephemeral rivers along the length of the coastline on an annual basis. Further, the coincident emissions for both pans and rivers highlight the interconnected nature of these systems along this expanse.

B.1 Namibian Coastline

The Kuiseb River has been identified as one of the most active sources on the Namibian coastline by Eckardt and Kuring (2005). Confirming these results, this study has identified the site to not only be the most significant contributor in terms of emission days along the coastline, but has identified it as the second most frequently identified source using the MODIS true colour composites for the southern African domain as a whole, second only to the Makgadikgadi Pans. Therefore, as this river system was not identified in TOMS based literature and is representative of the importance of river systems as a dust source, this

region will serve as representative of ephemeral river systems along the Namibian coastline in this chapter. Further, this serves to emphasise highlight the inability of both TOMS and OMI to detect aerosols along the coastline and therefore underestimates the region's significance as an aerosol source. The importance of rivers as dust sources in southern Africa is also highlighted.

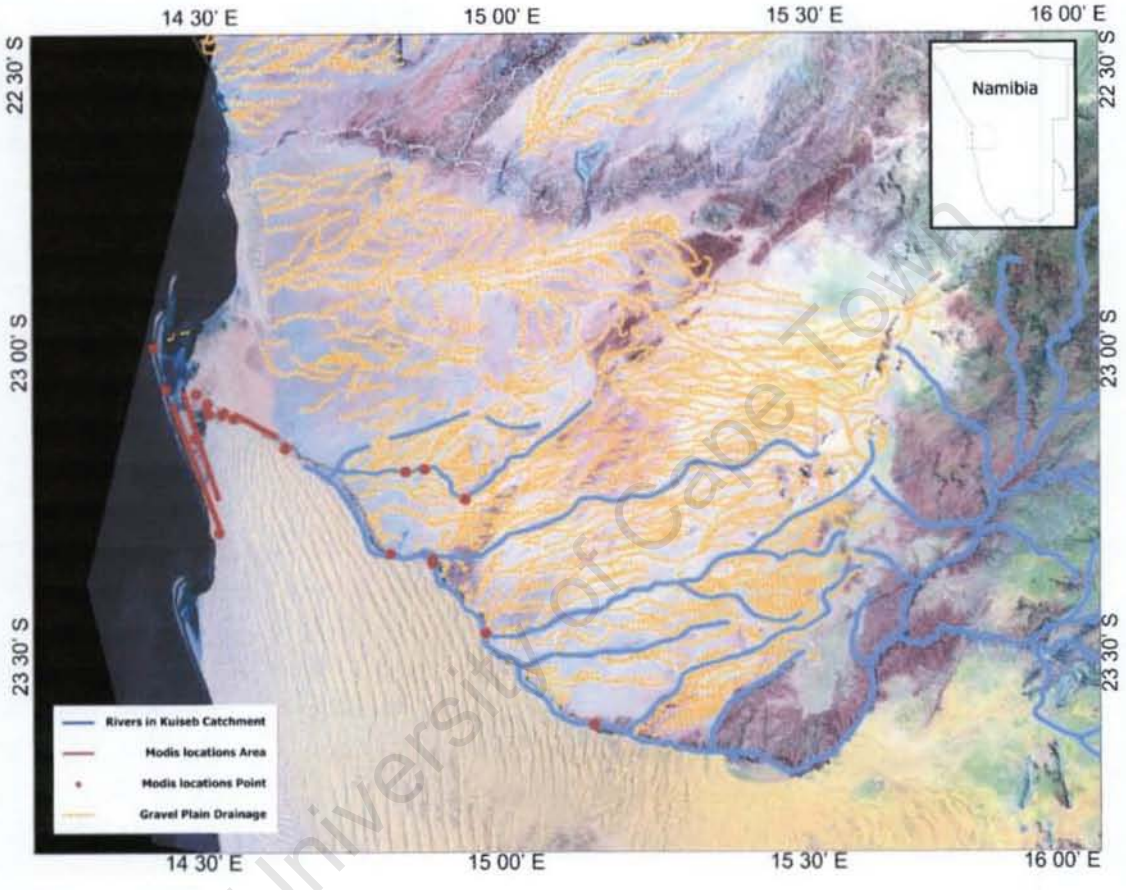

Figure 5. 6 Landsat image of the Kuiseb River delta, with the river, tributaries and gravel plain overlain. Inset shows the location of the Kuiseb River along the Namibian coastline. MODIS identified point and line sources for this region have been included.

Located in the central Namib coastline, the Kuiseb River has a catchment area which extends over 250 km inland encompassing 15 500 km^2 (Jacobson et al., 1995). From coastal headlands to its watershed on the escarpment, a 2 000 m increase in altitude is experienced. Along this gradient, rainfall increases from near zero at the coast to over 300 mm, although only half (52%) of the catchment experiences rainfall in excess of 100 mm annually (Jacobson et al., 1995). Within the catchment, four major geomorphological features were identified; these include the river channel and associated flood plains, the Namib sand sea,

the gravel plains and the river delta (Figure 5.6). While the sand sea is not detected as a significant dust source within the Kuiseb system, the presence of this feature and the transport of dust across it result in its inclusion. Further, the Kuiseb importantly marks the northern limits of the Namib sand sea (Jacobson et al., 1995). The remaining three features have all been identified to be dust contributors with varying significance (Figure 5.7).

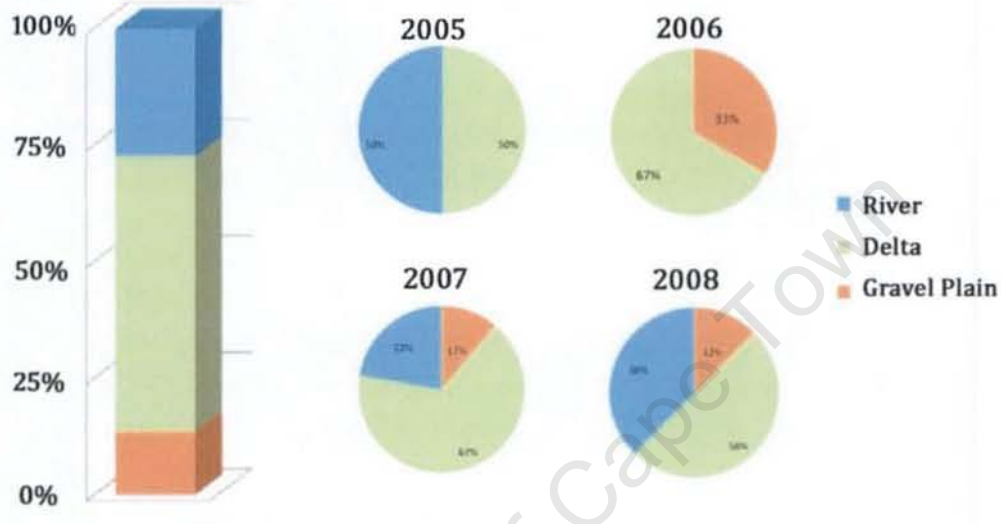

Figure 5. 7 Annual contribution of all surfaces for the Kuiseb River Basin for 2005 to 2008 showing the variability of each surface during the time period.

The variable emission frequency from the surfaces as identified from the Kuiseb, highlights the multiple aspects of the fluvial/aeolian coupled system and the associated controls on the sediment storage and removal cycles within this system. It is possible that in a system such as the Kuiseb River, where seasonal flow transports sediment along its profile, that aeolian sediment may be stored in the ephemeral channels as a result of low magnitude, high-frequency events and transported by a single high-magnitude, low frequency flood event during the wet season. The combination of transport and storage within systems enables the sediment to move across the rainfall gradient from higher rainfall regions to the drier source regions, where high magnitude low frequency wind events then entrain the sediment. This trend of source and supply regions existing on opposing ends of the rainfall gradient further supports supply as a dominant limiting factor. Over longer time scales, Bullard et al. (2003) discuss the modelled potential of storage–removal cycles and their relation to the

interaction of sediment production, availability and transport capacity through the arid and wet cycles and sediment budgets.

C. Small, closed ephemerally flooded depressions and inland pans

The terms 'pan' and 'playa' have been used loosely in the literature, driven by as much by regional variations in usage of the terms as well as by the local origins and scales of these features globally. Therefore, differentiation between those larger systems discussed above and these smaller systems is required. The importance of pans as palaeoenvironmental archives – and therefore indicators of climate change – has seen the larger systems being more extensively studied than their smaller counterparts (Telfer et al., 2009). One reason for this, and an important factor to further examine these systems, is due to the possibility that sediments in smaller systems are more likely to show evidence of interruptions in their depositional characteristics. These result from often more localised and dynamic surface deflation of the sediments. Bowler (1986) argues that the surface water on these smaller pans is typically a response to their proximity to the groundwater table and thus often only experienced on a seasonal time scale or following periods of heavy rain. The following two regions, both dominated by small pans highlight the importance of these features for global emissions while introducing the final issue of scale. Smaller pan systems often fall below the scale of satellite detection and characterise the possible underestimate, as highlighted in figure 2.1.

C.1 Northern Cape

The region has over 500 pans of varying sizes and, while not all pans were actively emitting during the study period, this region has shown how smaller pan sources with intermittent emission are now detected through the use of higher spatial and temporal resolution data. Of the forty point sources detected in this region, 90% can be attributed to type C sources, thus this region is highly representative of this final site typology. The largest pan in the region, Hakskeenpan, covering approximately 140 km^2 was identified by both MODIS and MSG and was a significant source in 2005, 2006 and 2007. Subsequent ground based analysis of the region introduced the complexity of regionally confined dust devils. Dust devils are defined by Pye (1987) to be small-scale convective vortices, commonly a response to surface heating and typically in the size range of less than 10 m in diameter and up to a 100 m high, they are active on the pan surface and are one of the WMO's defined meteorologically entrained dust typologies. Such dimensions result in these features occupying less than the

spatial resolution provided by the satellite products used in this study, but do not diminish the feature's potential to transport dust. Dust devils have the ability to transport fine grained sediment across surfaces even providing greater sediment sinks by exposing new sediments through saltation of particles as they move over the surface (Pye, 1987).

Figure 5. 8 Initiating (top) and developed (bottom) dust devils on Haskskeen pan (photographs by K. Vickery, 22/09/2009).

The thermally induced events seen in figures 5.8 indicate the potential of this surface as a sediment source through the induced thermal gradient in response to surface heating, and dust devils entraining sediment off the pan surface. Thus there is a supply of sediment which has the potential to result in large scale transport, provided a significantly high magnitude wind event occurs, can be detected in the MODIS and Meteosat imagery. The events identified from this region resulted in multiple plume directions and lengths, thus this region appears to be highly dynamic. As multiple sources were shown to have emitted on the same day, it would confirm the proposed groundwater fluctuations as identified by Lancaster (1986) are applicable to much of this region; these fluctuations serve to promote sediment supply in the region.

Therefore, due to the density of pans in this region and the annual emissions resulting from the many sources, the Northern Cape has potential to increase our understanding of small

pans in a systematic manner through determining the importance of ground water recharge for sediment supply and local scale thresholds for both small and large dust emission.

C.2 Free State

The Free State has the highest pan densities in southern Africa (Holmes et al., 2008) (figure 5.9). However, no significant sources for this region could be definitively determined from this study. Thus, despite work conducted by Holmes et al. (2008) on the lunette dunes to the south and south east of the pans, which proposes that transport of sediments off the pans, has accumulated to from these landforms. Shaw and Thomas (1997) indicate that the presence of down-wind dunes cannot be definitely indicative of sediment transport and thus cannot be the sole determinant of volume flux transport. It was proposed (Shaw and Thomas, 1997) and has since been reinforced that particles may travel beyond the depression and that down-wind dunes often have differing composition to the pan surface; thus the presence of dunes is not sufficient to assume source activation.

However correlating dune alignment, while not prescriptive of transport, with plumes identified in this study would serve to confirm two of the three plumes. These plumes were recorded to travel off the region in a south easterly direction (ID 612021200 – Appendix 3). Despite the clear pink plume as identified in the Meteosat pink algorithm there was no definite plume seen in the MODIS imagery. Therefore even with the two plumes from one source and a single plume from a secondary source, there is the possibility that cloud contamination or a false signal was identified on two separate days. Alternatively, time sampling bias could provide an explanation, thus further highlighting the importance of high temporal resolution data.

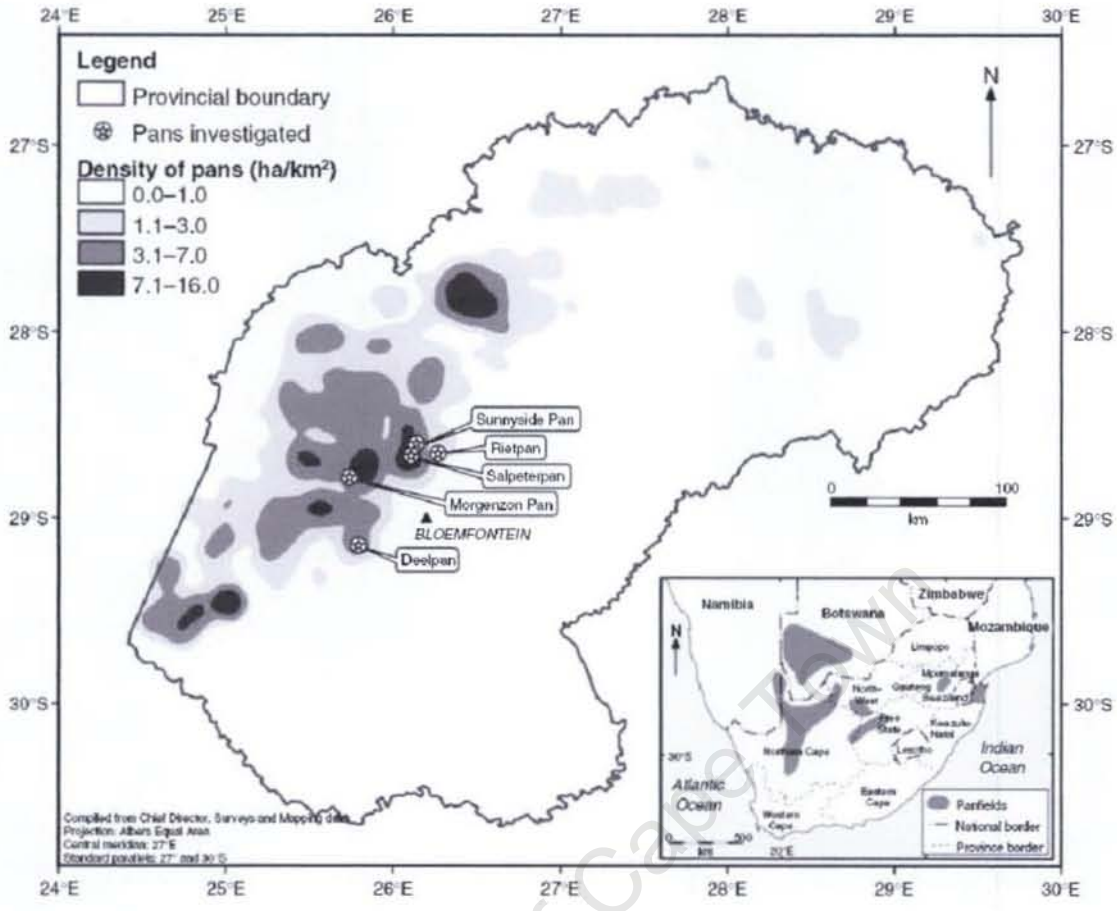

Figure 5. 9 Pan densities in the western Free State and the location of the pans investigated in a study by Holmes et al. (2008). The inset highlights the extensive network of pans within the study domain and the relative location of the Free State in southern Africa (Holmes et al., 2008).

The apparent lack of detection does not however reduce the significance of this region as an aerosol source, as Holmes et al. (2008) further proposes that activation of these lunette dunes could result in significant fine sediment deflation. Through sedimentological analysis of these dunes it was shown that beneath the coarser particles is a supply of fine grained particulates. There is also the possibility that, due to issues of scale with dust devils identified in the Northern Cape, this region could be producing smaller scale low level plumes that remain undetected. Tegen et al. (2004) estimated that less than 10% of dust sources are associated with agricultural soils, therefore despite the aeolian research focus on this area by Holmes et al. (2008); in this study as few significant emissions were detected. Despite the apparent lack of activity identified in this study, the region continues to be the focus of numerous ground based studies by amongst others Holmes et al. (2008).

5.5 REGIONAL SYNOPTIC DISCUSSION

Due to the importance of surface winds, and therefore circulation, for entrainment of sediments, the following section discusses the circulation features significant for entrainment per region. Through this study, it is now possible to analyse the synoptic circulation to daily event resolution. This advances our understanding of where aerosols will be transported once entrained, increases our ability to predict dust storms and attribute aerosol load to a set of synoptic drivers. Further, as early aerosol research in southern Africa either failed to include mineral dust in volume flux estimates or had a poor understanding of specific source regions, this study has the potential to revise much existing research in this field.

Much of the earlier research proposing substantial recirculation, so analysis of trajectories from dominant sites in the domain did not detail any significant recirculation. It can be argued that this could be a result of the seasonality of emissions being associated with spring and to an extent summer; coinciding with the partial break down of the stability layer (Tyson et al. 1996b). However, HYSPLIT[11] Trajectory modelling (Draxler and Rolph, 2003; Rolph, 2003) further identified no significant increase in altitude which would be expected of the stability breakdown. Nor did the plots identify any form of recirculation and thus questions the applicability of the recirculation component; therefore much of the early literature is of limited use in this study (figure 5.10a and 5.10c), as earlier studies focussed on assumed recirculation which was identified in this study not to be a regular process concerning aerosols.

As it can be assumed from understanding the stability layers and associated transport mechanisms for dust over southern Africa, trajectories were computed for air parcels leaving the source at near surface level (10 m). These air parcels, modelled through the use of NCEP Reanalysis data, were mapped for 96 hours.

Figure 5.10 depicts three versions of aerosol trajectories over the domain. Figure 5.10a schematically represents early research by Piketh et al. (1999) on aerosol circulation although there is minimal inclusion of source regions in the schematic. Thus this model merely represents mean dominant air circulation patterns over southern Africa rather than aerosols trajectories *per se* which are proposed to result from the intensification of features

[11] HYSPLIT (HYbrid Single-Particle Lagrangian Integrated Trajectory) Model access via NOAA ARL READY Website (http://www.arl.noaa.gov/ready/hysplit4.html). NOAA Air Resources Laboratory, Silver Spring, MD. For this study, NCEP Reanalysis data provided through the online interface was used for all plots

While this region is only identified on three occasions in this study, it can be acknowledged as a significant source and has the potential to, through climate change, contribute on both a seasonal and inter-annual scale possibly even becoming a significant source. This is especially important if the identified pan density and known significance of small ephemeral pans as sediment sources is an indicator of potential emissions.

5.4 SOURCE CONCLUSION

While early research did not identify many southern African sources due to the dearth of ground based observations (Middleton, 1997), regionally based studies have increased our understanding of sources and source typologies. Despite the inclusion of sand dunes and sand seas in the list of surfaces that could result in dust deflation, during the time period 2005 to 2008 and for the southern African domain, mobile dunes were not considered to be important dust sources. This is confirmed by Middleton (1997) who argued that it is the saltating grains liberated from dunes that are important initiators of dust entrainment from non-dune sediments through ballistic impacts on smaller particles. In confirmation of the literature, pans have dominated the source regions in southern Africa (Prospero, 1999; Washington et al., 2003). More specifically the two large pan complexes in southern Africa have been consistently identified to be active during the 2005 to 2008 time period, with both showing strong signals of inter-annual variability. The precise composition of source regions and analysis of both upwind and downwind samples have the potential to further increase our understanding of these dynamic systems through the development of deposition footprints and therefore can determine the local impact of such sites. To further understand the large scale climatological and radiation impacts of desert dust and associated derived aerosols, the systematic modelling of these systems with a high resolution understanding of their emission characteristics and frequency is required.

The following section deals with circulation and considers both the southern African and regional circulation in relation to regional aerosol transport.

rather than the mean. Figure 5.10b, identifies dominant transport routes through the grouping of plume trajectories, length and extent as identified in this study, but represents a very short time slice of the aerosols lifespan in the circulation feature.

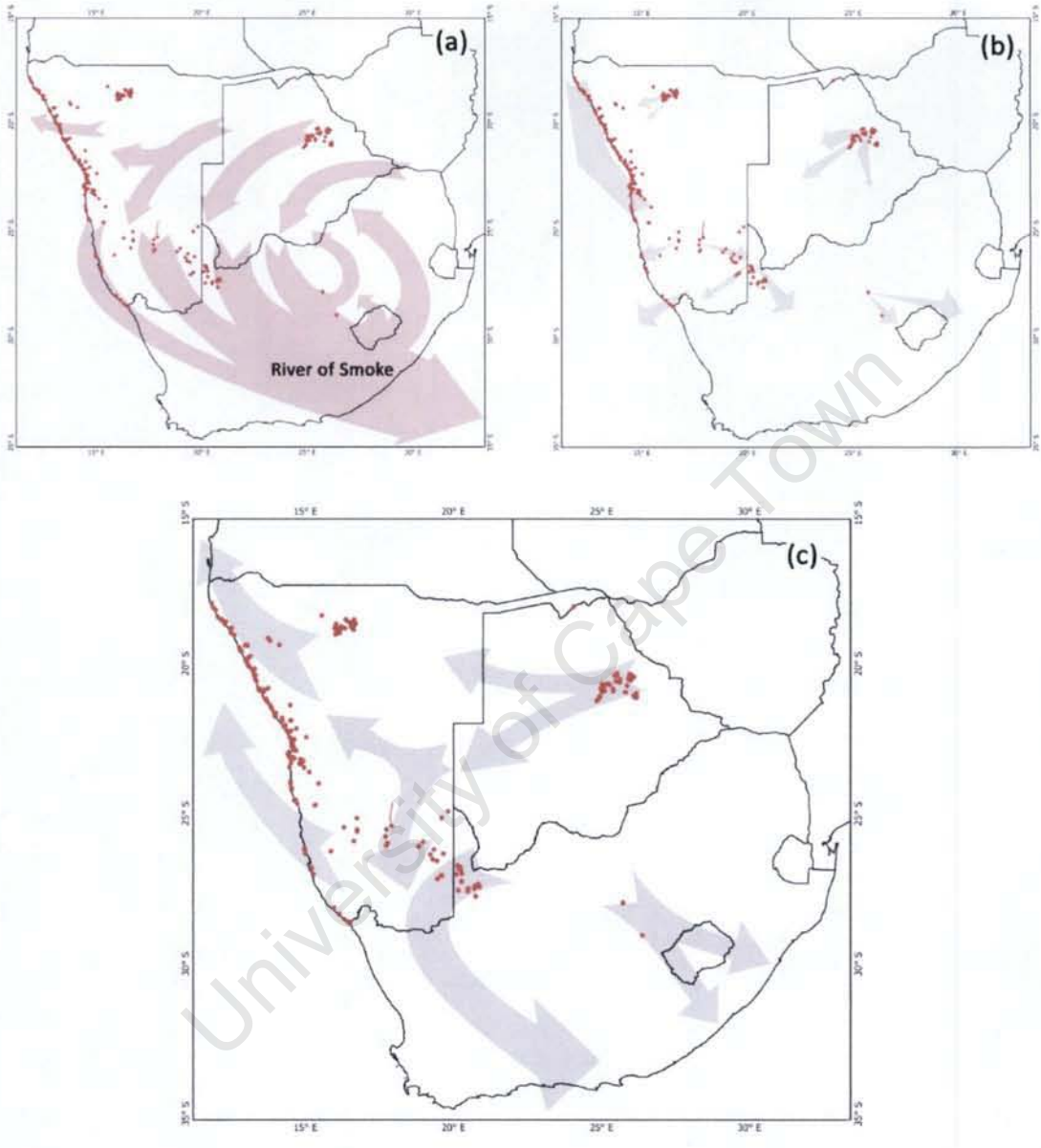

Figure 5. 10 a) Schematic representation of the major transport pathways and recirculating aerosols trapped beneath the ~500 hPa layer over southern Africa as identified in Piketh et al. 1999-source regions identified in this study included for depiction of contemporary source regions. b) Schematic representation of aerosol transport trajectories as identified using the MODIS and MSG imagery Trajectories mapped to cover the full extent of all mapped plumes in the study. c) Schematic representation of plumes from known sources as determined through the use of multiple HYSPLIT trajectory plots run for 96 hours from approximate time of emission.

Through the use of HYSPLIT Trajectory modelling, trajectories based on all individual source plumes identified in this study were combined to produce a mean aerosol circulation schematic for the years 2005 to 2008 (figure 5.10c). The trajectories proposed by HYSPLIT were further confirmed through the analysis of both surface and 850 hPa pressure fields to determine the validity of the plots, this resulted in the confirmation that once entrained aerosols can be assumed to be transported via the dominating synoptic circulation and in a similar pattern to that proposed by Piketh et al. (1999). The dominance of two major pathways, namely a south easterly plume termed the 'River of Smoke' and the Angolan plume to the west as identified in Tyson et al. (1996b) appear to hold for this study.

Figure 5.10c clearly illustrates the greater potential for aerosol transport and trajectory analysis that is now possible through the application of HYSPLIT or similar products. It is worth noting that like the Piketh et al. (1999) figure (figure 5.10a), similar studies presented the quasi-seasonal approximation of circulation and failed to attribute the synoptic circulations associated with emissions. In a study by Tyson et al. (1996b) a greater proportion of aerosol transport is proposed to travel in accordance with the Indian ocean plume, while in this study, there is a greater possibility of trajectories following the proposed Angolan plume to the west as a result of the importance of the easterly wave in the circulation patterns experienced over the North of the domain. However, dust is most frequently initially entrained by the anticyclonic circulation (upper level westerly transport), despite the frequency of easterly waves as proposed by Tyson et al., (1996a) in table 5.1.

The transport of plumes as seen in figures 5.10b and 5.10c confirm the findings of existing studies (figure 5.10a), with departures particularly to the north of the domain, and over the interior where this study was devoid of significant sources. Therefore volume flux of aerosols over southern Africa and thus quantitative understanding of the transport structures remains poorly understood. Due to the coarse resolution attributed to determining volume fluxes over southern Africa as based on a study by Tyson et al. (1996b) which extrapolated daily data through the use of percentage frequency of synoptic circulations to assume an annual mass flux, a great potential for both underestimation and overestimation is possible. This is in part attributed to the spatial variability of sources as well as the sporadic nature and frequency of emissions as has been identified in this study.

To further understand the importance and magnitude of the transport and volume of aerosols that is transported, Piketh et al. (2000) used a case study of the 20th and 21st of May 1998 to approximate the volume flux of iron loaded aerosols reaching the Indian Ocean. The

Table 5.1 represents the four dominant circulation features of southern Africa and is shown schematically (figure 5.11). It is evident that different sets of circulations would be expected to be significant for each region. The following discussion focuses on the Makgadikgadi Pans, Northern Cape pan belt and the Kuiseb River with the aim of setting each region within the circulation features responsible for deflation and the relative frequency of each feature.

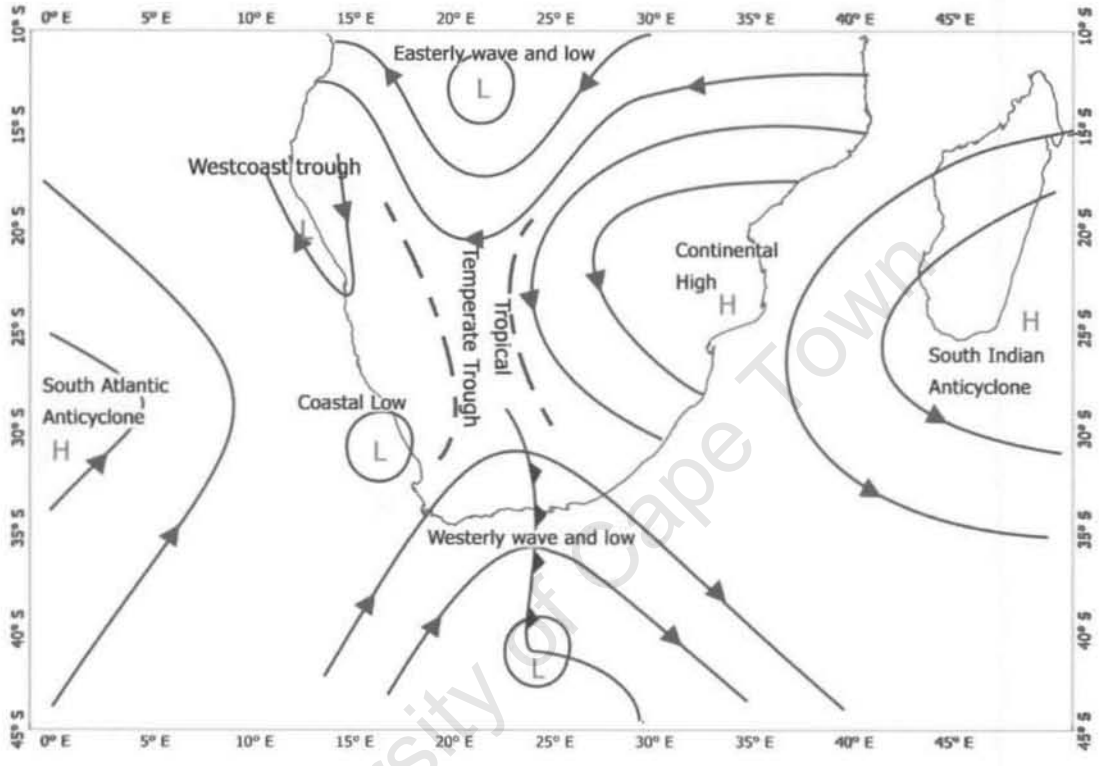

Figure 5. 11 Important features of the surface (1000 hPa) atmospheric circulation over southern Africa identifying the circulation features and composite features associated with dust emission in the domain. Schematic isobars representative of surface pressures, names and approximate circulation typologies modified from Tyson and Preston-Whyte (2000), with the dominant features selected from Tyson et al. (1996b).

While not all five regions are discussed, additional sources of analysis have been included to highlight the potential to increase our understanding. Different data sources were used for each of the three regions to highlight the potential of alternative sources of information. The Kusieb was chosen as additional information was available, while the Northern Cape pan belt is a previously unidentified aerosol source in southern Africa, finally the Makgadikgadi Pans were chosen due to their dominance in both detection and in existing literature.

5.5.1 Makgadikgadi Pans:

iron was, through analysis of both size and specific chemistry, determined to be from industrial emissions in the Highveld. A deposition volume of 0.89 $\mu m.m^{-3}$ was detected between 60°E and 85°E which corresponds to eight times the level shown to produce significant phytoplankton blooms in the equatorial Pacific (Piketh et al., 2000). Such a peak is expected to occur 33 days per year, showing the importance of southern African aerosols on Indian Ocean nutrient dynamics. On a smaller scale, a study by Soderberg and Compton (2006) looked at the importance of dust for fynbos ecosystems using a Cederberg case study. The aerosols were deemed, through chemical analysis, to be sourced from the interior although a precise source site was not determined in the study nor could be definitively identified by Compton (2010 *pers. comm.*). The schematic representation of the mean aerosol transport pathways over southern Africa (figure 5.10c) shows the transport route of nutrients contained within aerosols is evident and the link to Indian Ocean iron fertilization as identified by Piketh et al. (2000) is further apparent. Further, due to atmospheric recirculation, aerosols transported off surfaces in this region have the potential to impact on both nutrient dynamics and the haze layer across much of southern Africa. Therefore in order to be able to estimate the volume flux more appropriately attributing events to synoptic circulations is required.

The following discussion presents an analysis of the circulation features on all days on which plumes were identified in an attempt to better understand the circulation features associated with emission. To conform to existing literature on dominant circulation patterns, 850 hPa and 1000 hPa geopotential height surfaces were analysed for all days resulting in plumes and compared with the monthly mean in which the event fell. The synoptic settings for each event is discussed in accordance with Tyson and Preston-Whyte's (2000) classifications of important features of atmospheric circulation (figure 5.11), and categorized where possible in accordance to Tyson et al. (1996a) four dominant circulations features associated with southern Africa (Table 5.1).

Table 5. 1 Monthly percentage frequencies of circulation types over subtropical southern Africa, 1986 – 1992 (Tyson et al., 1996b)

	Jan	Feb	Mar	Apr	May	Jun	Jul	Aug	Sep	Oct	Nov	Dec
Continental highs	15	21	42	55	62	56	60	48	41	21	25	18
Ridging highs	7	10	14	12	10	14	10	15	18	20	17	14
Westerly waves	21	18	25	22	24	27	22	33	38	41	29	27
Easterly waves	55	45	15	9	4	3	1	1	4	16	26	36

From the Makgadikgadi Pans plumes were emitted on 4 dominant circulation patterns with the intensification of the continental anticyclone centred between 27°S and 31°S resulting in westerly transport off the pans. This accounted for 26 plumes on 18 days (figure 7.3). Tropical temperate troughs (TTT) to the east and approaching the pan complex when formed were the second most dominant circulation type with two clear trajectories associated with this circulation both in a west to south westerly direction. With this circulation pattern a greater southerly component can be expected when the TTT was fully formed and the dominant surface flow over the region was affected by the cyclonic low pressure circulation.

Regional circulation patterns associated with westerly wave lows were also found to affect the transport of plumes off the Makgadikgadi pans. This had been observed at case study level by Resane et al. (2004) who determined that the synoptic circulation associated with a particular event referred to as 'The day of the white rain' which saw an unusually strong westerly wave low extending over the interior. The resultant transport was in a strongly southerly direction and through wet deposition of sediment, determined to be sourced from the Makgadikgadi Pans (Resane et al., 2004), rained out over Johannesburg. A similar event, although the influence of the westerly wave low was not experienced as far north, was observed on the 26th of October 2006, with the centre of the systems low pressure being located at approximately 18°S (significantly further north then all other events identified from this source in this study which averaged at approximately 25°S), and the resultant plume was in a south easterly direction.

The final noteworthy circulation system associated within this region is the presence of a coastal low to the west of the Pan complex. The effect of the coastal low, while indirect to the Pan system, influences of the location of the main continental pressure systems. Further, the west-east location of this system resulted in the greatest influence over plume bearing, with a greater southerly component of the trajectory expected with a greater westward migration of the low. In confirmation, a study by Bryant et al. (2007) confirmed westerly transport off the pan to be the most common trajectory, an observation supported by a mean bearing of 243° identified in this study.

Circulation Type	Comment	plume direction	Events	Days
Continental Anticyclone	27S *	←	16	11
	31S *	←	10	7
Tropical Temperate Trough	forming to the west	←	8	5
	formed	↙	6	2
Westerly wave low	25S *	←	8	4
	18S *	↘	2	2
Costal low	18E 30S X	←	2	2
	21E 30S X	↘	1	1
	mean plume: 243°	←	53	32

* denotes centre of Continental HP system
X denotes centre of Low pressure system

Figure 5. 12 Summary of circulation types resulting in plumes off the Makgadikgadi Pans. The associated plume directions and frequency of days (Days) resulting in this circulation and number of plumes (Events) are also included. The comments either indicate the stage of the circulation system or the central location of minimum^{X} or maximum* pressure. As the Makgadikgadi Pans are located in the north west of the domain and features the westerly wave lows and coastal lows do not directly affect this region but instead affect the location of the continental high pressure system, thus the northerly extent of the lows are marked by their central location. The further north the systems extends the more northerly the high pressure system is forced.

This is further confirmed by the dominance of the maximum AI value as evident in particular in the TOMS product to the south west of the Makgadikgadi Pans (e.g. Washington et al., 2003) (and see figure 5.1). Bryant et al. (2007) and White and Eckardt (2006) establish the dominance of westerly transport off the pans, substantiated through synoptic discussion in Tyson et al. (1996a) who attribute the transport of the region to the high pressure systems which lie between the easterly waves to the north and the westerly waves to the south. This would confirm that once entrained aerosols from this region are transported in the dominant circulation features to an altitude at which they are detected by the TOMS product. Through the correlation of events to the synoptic circulations dominant on the day and days preceding the event, it can be determined that for the Makgadikgadi Pans a set of synoptic controls can be considered to be conducive to events. Despite this, it is not sufficient merely to determine the frequency of the circulation feature and assume dust entrainment, as correlating the proposed frequency of circulation features as per Tyson et al. (1996a) which were deemed significant in this study, would show that the region was not satisfactorily active. Therefore a complex set of surface hydrological conditions must be met at the pan surface to result in sediment supply (Bryant et al., 2007).

5.5.2 Northern Cape:

For the Northern Cape four circulation patterns were determined to be significant resulting in the 35 plumes on 9 days. This region showed the greatest variation in plume bearing, possibly due to the response of this region to low pressure systems from both the easterly wave belt or the westerly wave belt. Therefore the location of the region and the northerly or southerly approach of the low pressure systems strongly affect the bearing of the plumes.

In general, and from figure 5.13, it can be observed that there are two dominant directional groupings, one in a south westerly direction with this bearing being associated with five events on three days and the other in a south easterly direction was related to 30 events on six days. The south westerly plumes are both associated with low pressure systems approaching from the north and directly linked to the location of the region to the south of the low pressure system and therefore in response to cyclonic circulation.

The south easterly dominance could confirm early work by Lancaster (1986) who, in a preliminary report of pans in the southern Kalahari, identified a strong south easterly pattern to linear dunes in the region, which he proposed were the result of accumulation of materials deflated off the pans. Soutpan (Salt Pan) which was identified in this study as a source of a single emission was described by Lancaster (1986) to have "...seven to ten linear dunes which enter the pan depression from the west, [...] extending to the southeast..." (Lancaster, 1986:65). These dunes would confirm the results of plume bearing highlighted in this study.

Thomas et al. (1993) investigate the lunette sediment cycling with particular focus on Witpan, although not identified in this study is subject to the same groundwater activity which influences pan floor sediment availability throughout the region and thus proposed sediment transport. This is confirmed through the high number of events occurring on any single day from multiple pans, which further substantiates the uniform response across this region to synoptic circulations, provided a sufficient sediment supply is present. The proposed dominance of various circulation features verifies that, for this region, it is the intensification of a system rather than its presence which is important for deflation. Westerly waves are proposed to occur between 7 to 11 days per month between May and September which is when this circulation feature resulted in dust, yet dust occurred on only four discreet days during the four year period. Therefore the associated intensification of the system or the interaction between the wind speed and the available sediment can be

proposed to be the greatest limiting factor for this region. Further, for the Northern Cape, emissions were identified to occur in all four years, with 2005 accounting for 23 plumes, ten in 2007 with a single event in 2005 and 2008, respectively. As there was near consistent data coverage over this region during the study a possible inter-annual control could be responsible for the amount of sediment that was available for deflation.

Circulation Type	Comment	plume direction	Events	Days
Costal low	15E 26S [x]	↙	4	2
West Coast trough		↓	17	2
Westerly wave low	supressed by Continental HP	→	8	3
	extended to affect southern coastline	↓	5	1
Easterly wave low		↙	1	1
	mean plume: 159°	↓	35	9

[*] denotes centre of Continental HP system
[x] denotes centre of Low pressure system

Figure 5. 13 Summary of circulation types resulting in plumes off the Northern Cape Pan Belt. The associated plume directions and frequency of days (Days) resulting in this circulation and number of plumes (Events) are also included. The comments either indicate the stage of the circulation system or the central location of minimum[x] or maximum[*] pressure.

5.5.3 Namibia: The Kuiseb River

Due to the large north south extent of this region and the identified variable emission characteristics along its length, the Kuiseb River which was identified as the single dustiest source in the region and second dustiest in the domain will be analysed as representative of ephemeral rivers along the Namibian coastline.

The location of the river on the west coast results in the most likely influences on this region being the south Atlantic anticyclone, the west coast trough and a coastal low. For the Kuiseb it was identified that the west coast trough was the most important circulation feature especially when the continental high pressure system to the east intensified. This circulation, which is typical of the region, is often found to be intensified by the subsidence of air off the escarpment and associated warming. Goudie and Middleton (2000) and Tyson and Preston-Whyte (2000) identify this circulation feature as being associated with dust transport off the Namibian coastline, with Eckardt et al. (2001) adding that a ridging anticyclone (SAHP) further promotes coastal emission. This study has confirmed the existing literature

identifying the dominance of the west coast trough and associated berg wind conditions as dominant, with only a single event attributable to the alternative circulation feature as noted by Eckardt et al. (2001). Towards the end of the dust season for the Namibian coastline, which peaked between April and August, a ridging SAHP behind a tropical easterly disturbance resulted in two plumes with strong westerly components in response to their location of the northern edge of the SAHP. The mean transport from this source region is in a south westerly direction (233°) in response to dominance of the west coast trough.

For the entire Namibian coastline a similar pattern was evident although due to the associated complexity introduced through supply limitations there was no uniform control to dust emission for this region. Although on average there were five events per day, suggesting that circulation features like the west coast trough which can extend the full north-south length of the coastline (Tyson and Preston-Whyte, 2000) has the potential to result in multiple plumes along the coastline. Soderberg and Compton (2007) confirm the importance of Berg Wind events, which can occur up to several times a year during the winter months for offshore transport from the coastal regions. They further emphasise the importance of this circulation in terms of aerosol transport from the interior to the coastal regions where they provide an important component to nutrient cycling. Soderberg and Compton (2007) discussed one event in particular, which resulted in dust values which were significantly higher than usual for the region and persisted for the duration of the passing of a low pressure cell along the west coast confirming the importance of the circulation feature as recognised in this study.

Circulation Type	Comment	plume direction	Events	Days
West coast trough		←	1	1
	- with ridging SAHP	←	2	1
	- with intensified CHP	↙	18	13
Tropical Easterly disturbance	SAHP ridging in behind flattened easterly wave disturbance resulting in stronger westerly component then expected	←	1	1
	mean plume: 233°	↙	22	16

Figure 5. 14 Summary of circulation types resulting in plumes off the Kuiseb River and flood plains. The associated plume directions and frequency of days (Days) resulting in this circulation and number of plumes (Events) are also included. The comments indicate the additional features associated with the circulation over the region and notes on specific features.

To gain a truly local understanding of such sources viewing the system at the scales at which dust is entrained is required. For the Kuiseb River, figures 5.15 and 5.16 of station data from Gobabeb Research and Training centre permitted the analysis of wind speed and direction data as well as high resolution flood records for the Kuiseb River. Figure 5.15 identifies the low magnitude (2 $m.s^{-1}$) high frequency dominance of easterly winds while identifying the highest magnitude (12 - 14 $m.s^{-1}$) winds occurring less frequently and in a north to north-north-easterly direction which corresponds to the proposed wind direction associated with dust deflation. Further, from figure 5.15 it is possible to see south-south-westerly winds which have sufficient velocity to entrain sediment although no plumes were detected to travel with these winds. Therefore either these plumes were invisible due to a lack of contrast or the north-north-easterly winds are sufficiently accelerated by the localised offshore winds to be the dominant activation winds. This would serve to confirm the requirements of high velocity winds necessary to entrain sediments and transport them from source region (Pye, 1987). Assessing the days on which these high magnitude winds occurred against synoptic circulations showed the dominance of the west coast trough and an intensified continental high pressure system to the east.

This north-north-easterly wind dominance confirms the synoptic analyses performed in this study and as shown in figure 5.14 and the south-south-westerly transport. Analysis of wind speed revealed that both mean and peak wind speeds for the region occur between 09:00 and 13:00 which confirm the identified dominance of MODIS Terra (90.1%). The observed

peak wind speeds could be the response to the land breeze further intensified by air descending off the escarpment (Tyson and Preston-Whyte, 2000; Warner, 2004).

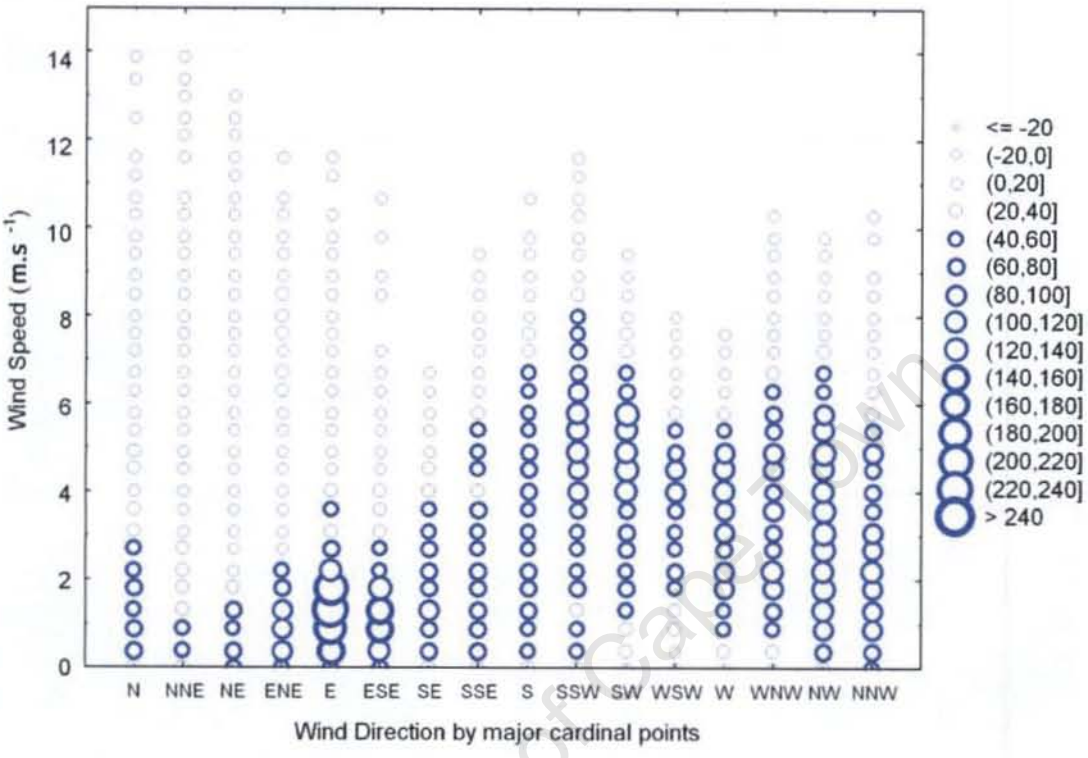

Figure 5. 15 Plot of 30 minute wind speed by direction at Gobabeb for the years 2004 to 2008. The size of the circle indicates the relative frequency of the wind direction at the given magnitude. For this region the low frequency, high magnitude north and north-north-easterly winds are primarily responsible for dust deflation from the Kuiseb region. (Data provided by Gobabeb Research and Training Centre)

Figure 5.16 represents May 2007 during which three events were identified highlights the correlation between wind speeds which exceeded 10 $m.s^{-1}$ and dust emission from the region. This figure clearly identifies peaks in wind speeds to be associated with dust emission, although there are two peaks, one on the 5th of May at 11:00am and the second on the 22nd of May at 10:30am, both of which have wind speeds in excess of those proposed to be sufficient to entrain sediment (Pye, 1987) and both from a north easterly direction yet neither result in plumes. Despite these two events not resulting in plumes, within days (7th and 23rd of May) wind speeds from similar directions and of equal magnitude resulted in plumes.

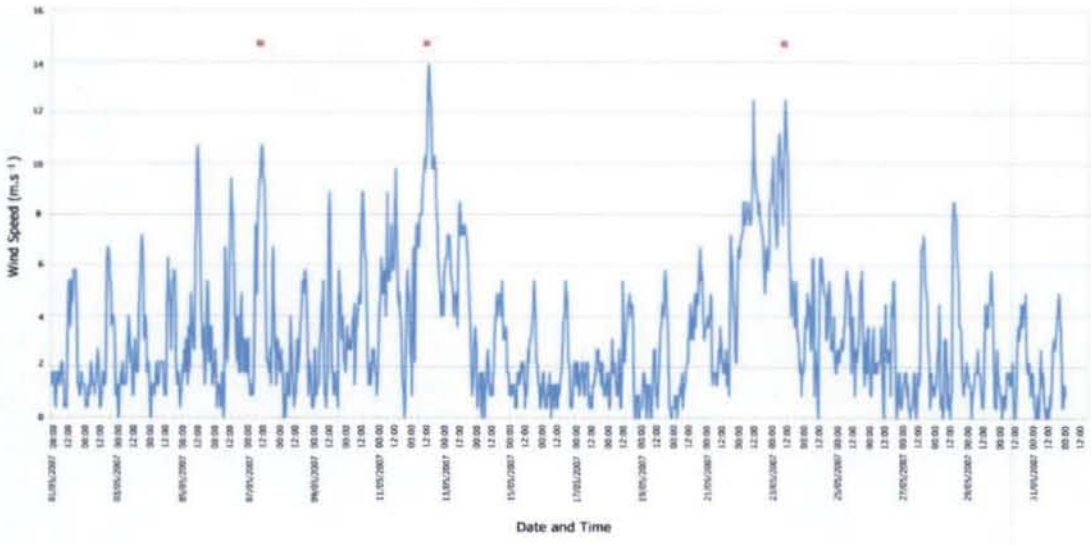

Figure 5. 16 Thirty minute wind speed data from Gobabeb for May 2007. Red markers identify events, and can be seen to be associated with maximum wind speeds at the station. (Data provided by Gobabeb Research and Training Centre)

Therefore, wind speed alone cannot determine the presence/absence of dust for the region, thus the argument of supply limitation can be proposed for this region and stresses the importance in understanding fluvial and aeolian interactions (Bullard and McTainsh, 2003). Flood data can assist in the prediction of dust; figure 5.17 graphically represents the number of days in which the Kuiseb River flowed per month for the four year period as well as indicating when dust events were observed. This shows the strong inter-annual variability experienced at this site, in 2005 twelve flow days and six events were recorded whereas 2008 saw 31 flow days and eight events, there was no flow data available for 2007. Despite flowing for 28 days in 2006 only three events were identified, this again highlights the complexity of interactions at the local scale for dust emission.

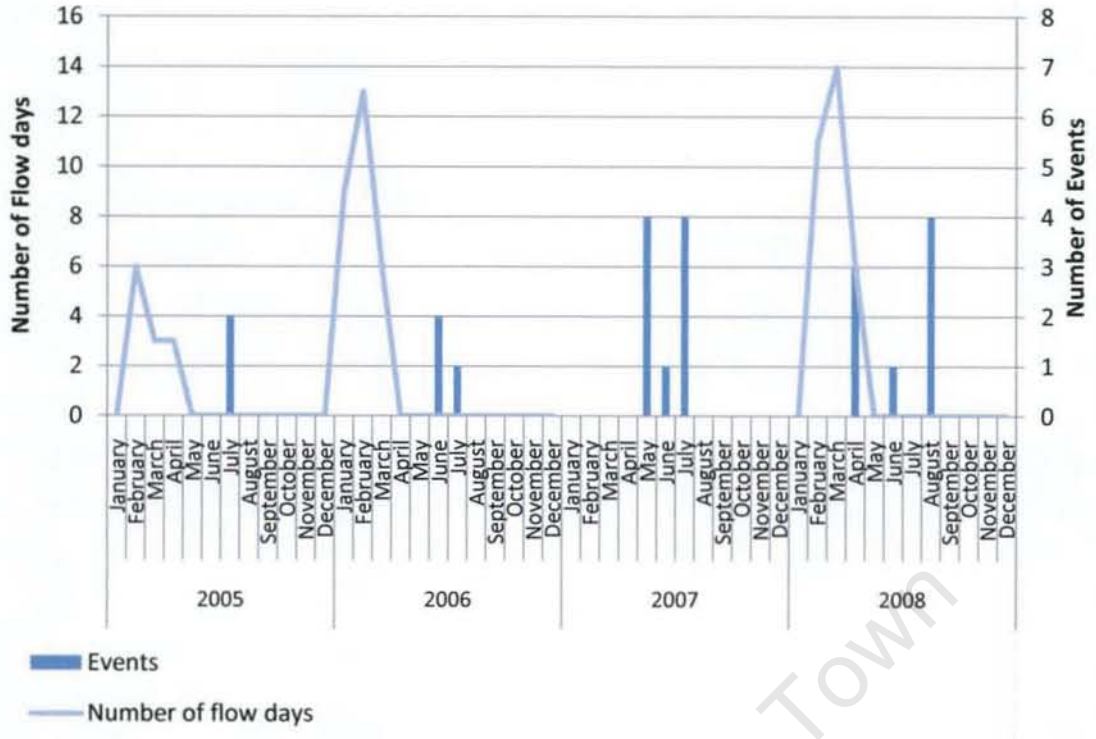

Figure 5. 17 Plot of the number of flow days versus number of events by month, highlighting the importance of seasonal flow to provide sediment to the system. (Data provided by Gobabeb Research and Training Centre)

5.6 REGIONAL TRANSPORT AND VOLUME FLUX

Figure 5.10 confirms the existing research on the dominance of two major pathways; a south easterly plume, i.e. the Natal plume (Tyson et al., 1996b), termed the 'river of smoke' and the Angolan plume to the west. The transport pathways identified in this study conform to existing literature, while not quantitative in nature, they challenge the proposed volume fluxes associated with the two dominant pathways. Existing volume fluxes are based primarily on the work of Tyson et al. (1996b) which extrapolate scenarios through the use of volumetric weighting associated with certain synoptic circulations. From the above discussion it is evident that there is now a greater understanding of source location and emission characteristics. An increased potential now exists to re-evaluate volume transport along the major routes, through a greater understanding of surface geomorphology and the potential to include sites in regional aerosol models. This will further permit developing a new scenario of the associated impacts on nutrient cycle through deposition during transportation.

The intensification of the HP feature is associated with dust emission over the Makgadikgadi pans, which is the most active source during the time period 2005 to 2008. As this system is proposed to occur on average 42% of the days from July to October which has been identified to be significant emission months for this region, the load associated with this circulation feature is most likely to have been underestimated in early research due to the lack of source region inclusion in calculations.

Figure 5. 18 Plume identified on both MSG pink composite (left) and MODIS Aqua image – a plume can be clearly seen crossing the Okavango delta, provided an element of dry deposition occurs during transport this would confirm the importance of regional aerosols in nutrient cycling in the Okavango as suggested in Tyson and Gatebe (2001).

Without a greater understanding of deposition and entrainment of particulate matter from large pan and river systems in southern Africa dust flux volumes remain estimates based loosely on background volumes and transport pathways based on near seasonally resolution extrapolated data. Piketh et al. (2000) acknowledged this caveat in research proposing that without further observations it is impossible to quantify the volume flux of iron transport and the link to south Indian Ocean productivity.

It was proposed by Tyson and D'Abreton (1998) that transport into the Indian Ocean is 60% greater than transport into the Atlantic, however from Figure 5.10c, this study determined that there is more circulation exiting the west coast than was proposed by Piketh et al. (1999). Further associated with transport is aerosol volume, as sources were not considered and with a significant contribution found to be originating along the Namibian coast (Eckardt et al., 2001; Eckardt and Kuring, 2005), an increase in volume flux would be assumed to be transported into the Atlantic Ocean. Tyson and Gatebe (2001) further note that upon consideration of the importance of mineral aerosols from southern Africa in nutrient cycles

in both marine and terrestrial ecosystems, a greater understanding of the nutrient cycle in the Benguela upwelling system is required. Piketh et al. (2000) discuss the importance of iron from southern Africa in the nutrient cycle in the south Indian Ocean, with the course fraction iron being sourced from aeolian dust lifted from the continental surface. As this is considered to be in the order of 450 tonnes per day during events (approximately 100 days per year), and is linked to iron enrichment levels comparable to those used in phytoplankton bloom studies the possibly flux from the Namibian coastline could be considerable. The significant contribution identified from the Namibian coast in this study in both frequency and spatial coverage of plumes combined with the proposed underestimate of westerly transport in the Angolan plume, in conjunction with findings by Eckardt and Kuring (2005) and Weeks et al. (2002) highlight that there is great potential for further study within this system.

Due to the analysis from this study focusing on known sites associated with mineral aerosols, the distribution is biased towards these aerosols and possibly does not consider industrial aerosols sourced from the interior. Despite this potential underestimate, figure 5.19 shows the proportional contribution of source types to course and fine fractioned aerosols sampled at Ben MacDhui. This figure accentuates the dominance of course fraction soil dust, while in the fine fraction industrial sulphur is more prevalent. The fine fraction dominance could be argued to be a response to the proximity of the site to the industrial Highveld, as Tyson and D'Abreton (1998) and Tyson and Preston-Whyte (2000) identified industrial and biomass burning derived aerosols appeared to be a far less significant source except in the immediate vicinity of fires or industry. This would suggest that a high degree of site selection bias is intrinsic in such studies limiting their value in regional up-scaling of aerosol conditions.

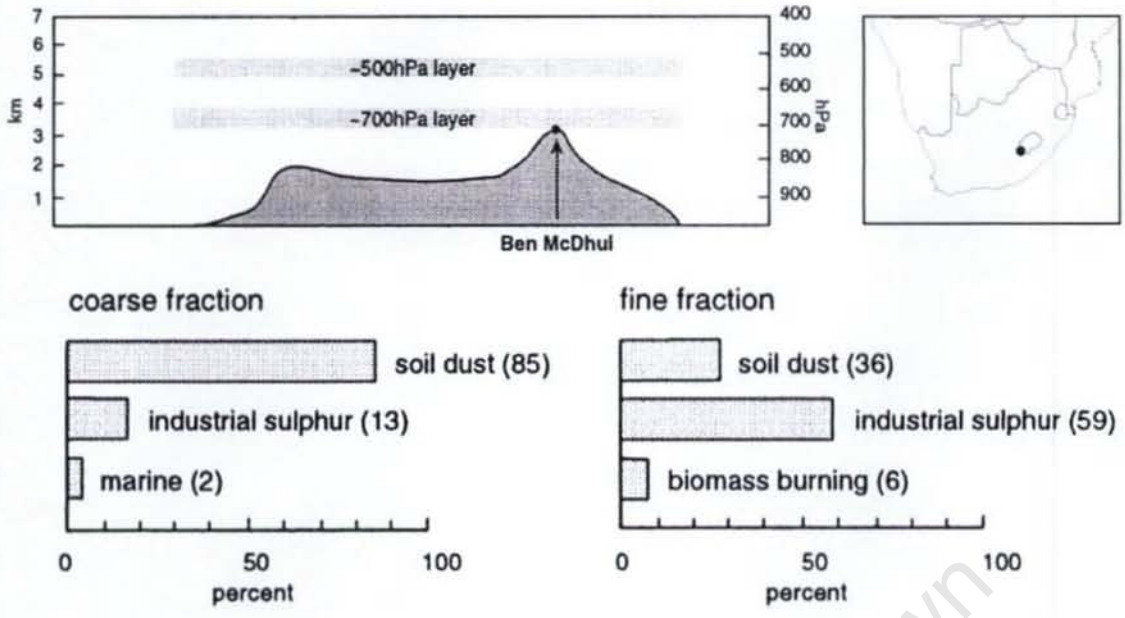

Figure 5. 19 A cross sectional profile from west to east with the location of the high-altitude, Ben MacDhui site in relation to the ~700 and ~500 hPa absolutely stable layers over South Africa(top left).The location of Ben MacDhui marked in relation to the domain used in this study (top right). Bottom from left to right, the annual source apportionment of coarse and fine-fraction of aerosols sampled at Ben MacDhui (adapted from Tyson and Gatebe, 2001)

Tyson and D'Abreton (1998) further argue that it is the dominance of the semi-permanent continental high and the transient ridging highs that result in the greatest aerosol load transport – partially in response to these systems being associated with the austral spring (Tyson et al., 1996) which is typically related to increased biomass burning in the northern limits of the domain (as confirmed by Abel et al. (2005)). In both Tyson et al. (1996b) and Tyson and D'Abreton (1998) the introduction of the west coast low, typically associated with Namibian coastal dust emission, is not included in the discussion as it is assumed that the continental high pressure system is principally connected to the aerosol load over southern Africa. This further serves to highlight the underestimate in the volume mass flux into the Atlantic Ocean. Tyson and D'Abreton (1998) approximate a transport trajectory off the Namibian coast although through seasonal bias the transport is linked to the circulation associated with a continental high pressure system. While this transport may be applicable for the high pressure system, events along the Namibian coast are not related to the high pressure extending across the sub-continent and are more typically associated with either the southward displacement of the tropical easterly disturbance or the intensification of the west coast trough both of whose cyclonic circulation result in the direct off shore transport.

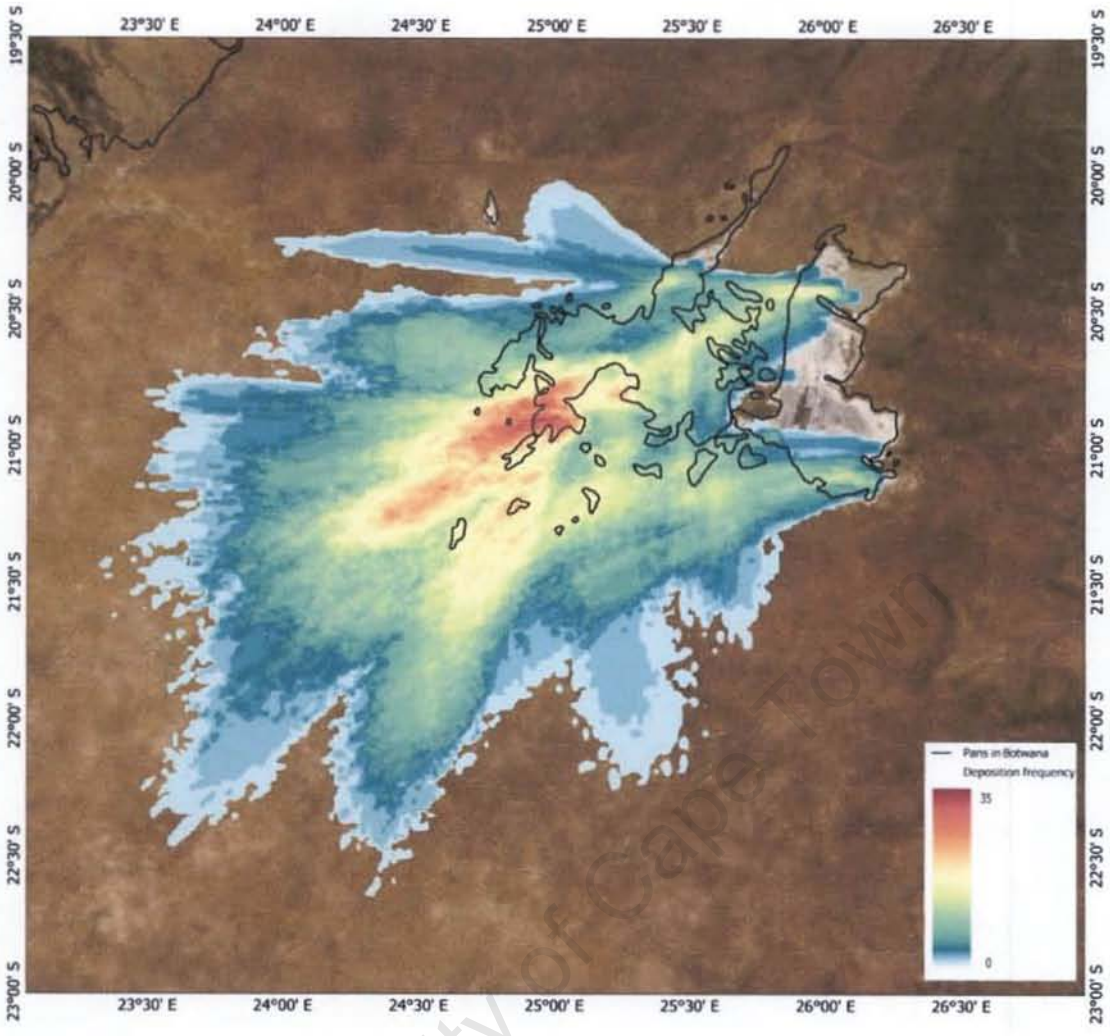

Figure 5. 20 Hysplit depositional footprint over the Makgadikgadi Pans for all events identified in this study. The Deposition frequency is the count of times an exponentially decreasing emission with an initial output of a single unit for one time period is over a unit area. The plot is run for six hours from time the emission was identified, depositional areas calculated every hour. The greatest depositional footprint is identified over the south-western edge of the Ntwetwe Pan in response to this region being both an emitting source and in the pathway of the dominant transport off the pan.

Furthermore, Tyson et al. (1996b) assume no deposition of particulate matter during transportation, figure 5.20 clearly identifies the footprint of deposition assumed to result from the Makgadikgadi Pans and through chemical analysis of surface samples taken both upwind and downwind of the pan source (Eckardt *pers. comm.*), zero deposition cannot be assumed to be a valid representation of aerosol transport over southern Africa. This is not to be confirmed as an all encompassing representation as Tyson and Gatebe (2001) note the contribution of atmospheric particulates in the biogeochemical cycling of nutrients specifically regional aerosols to the Okavango Delta Region (figure 5.18). This would serve to

confirm that there must be an element of wet or dry deposition which was not considered in early aerosol research (e.g. Tyson et al., 1996b).

Therefore despite the lack of quantitative understanding derived from the products used in this study, through following methodologies provided in existing literature, volume flux and transport of aerosols could now be calculated at higher resolution. By integrating a greater understanding of their source location, relative emission frequency and associated synoptic circulations to existing aerosol studies, it is possible to dramatically increase our understanding of both background haze and significant load transport.

This research highlights the necessity to re-quantify oceanic and terrestrial nutrient cycling associated with both wet and dry deposition, using similar concentration and deposition HYSPLIT modelling as can be seen in figures 5.10c and 5.20.

5.7 CIRCULATION CONCLUSION

From the above discussion there appears to be a set of synoptic drivers which are conducive to dust entrainment and associated transport over southern Africa at both regional and more local scales, as well as hydrological controls as seen at a local scale (Kuiseb). Through analysis of individual events and the correlation with the proposed frequency as determined by Tyson et al. (1996a) (Table 5.1), it was found that viewing synoptic controls in isolation could not determine the potential for significant events. This conclusion of supply limitations for southern Africa is confirmed by Washington et al. (2003). They further generalises that southern African dust sources, including the Etosha Pan and the Makgadikgadi Basin are not located in regions where significant topographic channelling of winds could result in sufficiently accelerated speeds to transport sufficient dust to the region on an annual basis. Thus hydrological transport of sediment is the only possible source of significant dust for the region.

Products such as HYSPLIT have furthered the understanding of aerosol transport and depositional footprints. These products and the attribution of aerosol load to specific circulation features have been introduced in this study, and through this the potential to revise aerosol loads in the southern African haze layer. Despite early literature focusing on recirculation there was no evidence of recirculation mapped on any plumes when using HYSLIT during this study. Regardless of not confirming recirculation, HYSPLIT has provided a significant advancement through our ability to understand where aerosols are transported

once entrained, as well as increase our ability to predict dust storms and attribute aerosol load to a set of synoptic drivers.

6. Synthesis and Conclusions

The use of multiple space borne sensors utilising different spatial and spectral resolutions, has resulted in this study producing a dust source map of southern Africa. Furthermore, through correlating the sites identified with both the circulation and preliminary geomorphology of the dominant regions it can be seen that a complex set of drivers control these systems. This chapter begins with a synthesis of the key outcomes following the three themes identified in the study. This is followed by a review of the original aims and objectives and concludes with a brief outline of future and potential research directions.

6.1 TECHNICAL SYNTHESIS

Through advances in satellite technology and the evolution from exploratory to more quantitative detection, many smaller previously unidentified sites failed to attract the interest of aeolian researchers. This was particularly evident in southern Africa where a disproportionate amount of focus was aimed at the Makgadikgadi and Etosha Pans as they were identified to be significant in early studies by researchers, among others Prospero (1999) and Washington et al. (2003) and to an extent sources along the Namibian coastline by Eckardt and Kuring (2005).

Despite many of the limitations and advantages of the products discussed in this study and in King (1999), satellites are continuing to increase our understanding of aerosols on a global and regional scale. Qualitative analyses from various products have confirmed the existence of a number of sites, which are the greatest contributors to mineral aerosol loadings in the atmosphere (Prospero et al., 1999; Washington et al., 2003), quantitative analyses have proved more contentious (Remer et al., 2008). Resolving the often significant differences in mean aerosol optical depth between satellite derived products is according to Remer et al. (2008) an "...ongoing challenge for the research community."(Remer et al., 2008:4). Therefore, while this study did not attempt to quantify aerosol optical depth; source attribution and preliminary temporal characteristics were determined.

The temporal resolution of both MSG and MODIS has provided a greater possibility of detecting source regions through the reduction in time sampling bias. Both TOMS and OMI provided daily coverage and therefore averaged daily aerosol load or represented a single time slice. Therefore, unless an overpass coincided with an event, identification was markedly downwind of the source points. From the twice daily coverage from MODIS and

for this study the three daily images from MSG, it was possible to detect emissions where the plume was still emanating from the source region.

Further due to multiple daily images it was possible to identify the temporal emission signature for each region and develop an understanding of the duration of events. Through the study it was possibly to determine that sources were most active on the noon time imagery for MSG with 50% of all plumes detected on this image, while the morning (Terra) images captured 90% of MODIS dust plumes. While the high spatial resolution provided by most notably the MODIS imagery, allowed for the identification of sub-basin scale source areas. In the case of the Makgadikgadi pans, this increased the resolution of emissions from being assumed to occur from the entire Pan complex to the present resolution of four dominant regions located on the north and south of both the Ntwetwe and Sua Pans. This would serve to further confirm the use of both the MSG and MODIS products for detection and further highlight their ability to increase both the spatial and temporal understanding of sources.

While it was initially proposed that the high resolution capabilities of MSG would provide the best means of identification of southern African sources, this did not eventuate. The theoretical ideals of MSG had many domain specific limitations that were not experienced in a similar study over the Bodélé by Schepanski et al. (2007). These included the lack of surface homogeneity over southern Africa and the significant inclusion of water vapour to the west of the domain masking or complicating detection. However, it was found that, despite the proposed lack of observed contrast between land surfaces and the dust plumes in the true colour imagery, the use of the visible imagery provided the most significant advancement of current knowledge.

6.2 SOURCE SYNTHESIS

Through this study the understanding of both source region and aerosol transportation have been significantly advanced in southern Africa. From a regional source perspective the study identified six dominant areas in southern Africa that during the time period of 2005 to 2008 inclusive were active dust sources. This advancement saw the addition of the Northern Cape Pan Belt as a dust source; challenged the inclusion of the Free State and highlighted the importance of the Kuiseb River. In addition, these sites and regions were further determined to include a set of surface geomorphologies, namely: pans, rivers, gravel plains and

evaporation points. Despite many limitations associated with both products, 23 sources were identified using the MSG composite product, while 93 were identified using MODIS.

Due to the varied geomorphology of dust producing regions it is proposed that southern Africa can serve as an analogue of global sites with three out of the four global categories being represented within southern Africa. Large active or former lake beds and pans accounted for 61% of identified emissions with the Etosha and Makgadikgadi Pans dominating this category – these could be representative of the Bodélé Depression and Lake Eyre although supply and source controls differ greatly by region. Seasonally dry rivers and coastal pans accounted for 27% of sites, with these source types further introducing the role of fluvial systems as sediment sinks and introduced the Kuiseb River which was the second most frequently identified source. This inclusion further highlights the importance of fluvial controls on sediment supply. The final site typology which includes small inland active or former lake beds and pans was the greatest finding over the domain, as this site typology identified the Northern Cape Pan Belt, a region which has previously not been identified. This region was further associated with the greatest variability both on an inter-annual time scale and through the plume trajectories and associated climatic drivers.

Through the increased understanding developed on source scale, the complexity of scales for both detection and systems was introduced. The complexities of scales from global source regions to site specific regions coincides with advances in satellite technology with increased resolution potential comes increased detection ability. Despite this, through a more finite knowledge of source regions, the complexity of sub-pixel sized dust activation and surface variability further necessitate more localized ground based studies.

6.3 CIRCULATION SYNTHESIS

Within southern Africa a myriad of surfaces that are conducive to dust emission were identified. Of these sources many were proposed to respond to supply limitations for emissions. Through linking synoptic drivers to emission events and analysing the proposed frequency of these events against the circulations frequency, the proposition of supply limitations held. It was found that, for each region within the domain, a set of circulation features could be identified to be significant, although could not be viewed in isolation of surface conditions and supply controls. It was, in most cases, an intensification of a system or an anomalous location of the pressure system that resulted in plumes. Further, as plumes

followed similar pathways on more than one occasion it is proposed these features are recurrent in nature.

Additional information provided for discreet systems within the domain revealed that supply limitation is further restricted by wind thresholds and associated localised variability. Through station data provided for the Kuiseb River, the complexities of scale were further highlighted through the inability to link station data to large scale synoptic circulations. Furthermore, at site specific scale and at the high resolution provided by the station data, attributing the visual plume to the initiating wind feature is not possible. Therefore, while higher resolution – both spatial and temporal, have the ability to increase our understanding of these systems, correlating the multiple levels and resolutions of the data provides a secondary challenge.

Of significance in southern African circulation, is the ability to introduce sources into the regional circulation systems through the use of the HYSPLIT product methodology. While existing studies used volume flux estimates with minimal source knowledge, through the use of HYSPLIT and similar technologies it was possible to model trajectories of all identified plumes for the duration of the study. This not only revised the proposed recirculation over the sub-continent but places a greater load to the Angolan plume than the Natal plume in terms of mineral aerosol volume. Consequently, while the Natal plume is termed the "River of Smoke", it is the Angolan plume during April to September that is a significant "River of Dust" transporting large swathes of aerosols off the sub-continent.

6.4 REVIEW OF AIM AND OBJECTIVES

The primary aim of this research was to use MSG imagery to investigate dust source regions and associated aerosol dynamics in southern Africa over the period 2005 to 2008.

To address this aim, a thorough examination of the MSG-BTD algorithm took place (for technical discussion see chapter 2) and a review of the existing aerosol literature, detection techniques and dust impacts was undertaken. This revealed that while the MSG composite successfully detected source regions, the secondary data source, MODIS, outperformed the MSG composite over much of the domain, resulting in the inclusion of MODIS and the ensuing study utilised a multi-sensor analysis over the full domain. The three themes as identified to be significant highlighted the dearth of information available on southern African dust sources and further highlighted the bias in site selections.

The potential to use a multisensor approach was firmly established in chapter 4 which laid forth the results of both MODIS and MSG, and is further confirmed in chapter 5 indicating the advance in knowledge provided by this study. The identification of multiple previously undetected sites, most notably the Northern Cape Pan belt and the identified importance of the Kuiseb River in southern Africa, has significantly increased our understanding of both site typologies and resulted in the inclusion of ephemeral rivers as significant sources in southern Africa.

6.5 FUTURE RESEARCH DIRECTIONS

As a result of the discontinuous nature of the data set it was not possible to determine any temporal behaviour or finite emission characteristics for any source. Therefore, to better understand the temporal behaviour of systems as well as the site dynamics on annual and inter-annual scales, analysis of a continuous data set would be required. It is again proposed that a synthesis of data products be utilised; as throughout this study it was confirmed that this reduces the inherent biases associated with each sensor. This could further be aided by a greater grasp of surface inundation in sediment supply, the frequency of flood waters and associated ground water levels. While automated detection would be a significant advancement in such a study, the lack of significant contrast in visible imagery is not sufficient for automation, and considerable biases in the MSG-BTD limit its automation potential.

As has been identified, issues of scale are pertinent to aerosol research. In order to understand systems at the resolution of emissions, sub-basin scale analysis is required. Further such analysis would increase the present understanding of system chemistry which could assist in determining the radiative impacts and nutrient cycling associated with aerosol transport and deposition. To be able to better model southern African sources in literature, a greater understanding of localised constraints to emissions would also be needed.

Anthropogenic sources, including agricultural and industrial emissions were detected through the methodology utilised in this study. They were however not included in discussion as the study aimed to determine the characteristics and sources of mineral dust. It was however observed that within the domain a number of sites – dominated by industrial smoke stacks, were detected to be persistent sources throughout the time period. Therefore the study of anthropogenic aerosols could follow a similar methodology as highlighted in this

study and would better attribute source regions in background and anthropogenic aerosol contributions over southern Africa.

The preliminary nature of this study and the previously untested response of MSG over the domain, reveals that the product did not provide the ideal detection as the literature proposed. While the MSG-BTD algorithm has advanced the knowledge, further refinements to the algorithm or an alternative product utilising the resolution capabilities of MSG are proposed. Through the inclusion of station data for the Kuiseb and the HYSPLIT modelling of the Makgadikgadi Pans depositional footprint, the potential to increase our understanding of dust dynamics is evident. Therefore refining the study area and using multiple scaled products should result in the better identification, classification and contextualising of source regions.

6.6 CONCLUSION

The impact and use of remote sensing in aeolian research has developed significantly from its early contributions to deciphering the nature of the world's dust sources and the links between sources, wind regimes and hydrological controls. With increased focus on climate change and atmospheric composition, aerosol research has become more important. Despite this, and the identified importance of aerosols, there remains no dedicated instrument for their detection. Therefore a multi-sensor comparison of derived products, and the use of difference spectral ranges; together with a comprehensive network of ground-based sensors and surface calibration are required to advance our quantitative understanding of global aerosols, their sources, emissions and characteristics. The study has therefore provided a significant base upon and within which regionalised dust source studies can be performed.

The three central themes to this discussion: technology (satellites), sources (geomorphology) and circulation (synoptic controls) have all provided greater detail at various scales to the existing literature. The study further highlighted the overarching limitation to aerosol research through the multiple issues of scale that have been introduced. On a global scale detection has advanced from source areas to source points, while on a regional scale discreet areas have been identified. Despite the high resolution now possible there remains a disparity in scales; it is in linking the different resolutions that will truly increase our understanding of these systems. These issues of scale, global to regional to sub-basin and

surface process complicate and necessitate the need for a multisensor approach to aeolian research, and further introduce the need to couple remotely sensed studies with foundational ground based observation.

Geomorphologically the study confirmed the importance of large pan complexes as dust sources and added the Kuiseb River as an important fluvial-aeolian coupled system. The inclusion of smaller pans was confirmed in this study, although many smaller pans which are found throughout the domain (Goudie and Wells, 1995) were not detected. Many of these systems were found to respond to circulation controls although the circulation should not be viewed in isolation as supply limitations are proposed to be significant to all southern African sources. Further, confirming existing work by Vickery (2007) the identified set of synoptic drivers responsible for regional emissions are intensifications of more frequently occurring systems.

An identified trend amongst all sources was their existence over a west-east gradient. Most sources having their sediment supplied from the west with the resulting transported sediment being entrained and further transported eastwards. This particular trend in aerosols over the sub-continent highlights the dominance of the Angolan plume as a "River of Dust" while the Natal plume to the south east is dominated by regional haze and is as such confirmed to be the "River of Smoke".

Therefore, due to the many limitations discussed in the study and by King et al. (1999), no single sensor/product is capable of providing totally unambiguous information. Despite such limitations, satellites have significantly advanced in the development of global maps. Through the advantages offered by multiple images daily it was possibly to detect atmospheric dust close to the source, furthermore as a result of near cloud free conditions being associated with the climatic features identified to be significant for dust emission, the presence of cloud was not identified to be a significant limiting factor.

Accordingly, the establishment of a new southern African dust source map, linked to the source typology and circulation controls responsible for emission, not only provides greater insight into the nature of aerosols over southern Africa, but provides an improved understanding of global aerosol source regions and circulation.

7. References

Abel, S.J., Highwood, E.J., Haywood, J.M. and M.A. Stringer, (2005) The direct radiative effect of biomass burning aerosols over southern Africa. *Atmospheric Chemistry and Physics*, Volume 5, Pages 1999–2018

Ackerman, S.A., (1997) Remote sensing aerosols using satellite infrared observations. *Journal of Geophysical Research*, Volume 120, Number D14, Pages 17069 - 17079

Ahmad, S. P., Torres, O., Bhartia, P. K., Leptoukh, G. G., & Kempler, S. J. (2006). Aerosol index from TOMS and OMI measurements. *Proc. Amer. Meteorological Soc. 14th Joint Conf. on the Applications of Air Pollution Meteorology with the Air and Waste Management Assoc, Atlanta, Georgia, Jan 28 - Feb 3*

Alpert, P., Kaufman, Y.J., Shay-El, Y., Tanre, D., da Silva, A., Schubert, S., and J.H. Joseph, (1998) Quantification of dust forced heating of the lower troposphere. *Nature*, 24 September 1998, Volume 398, Pages 367-370

Amato, J.A. (2000) Dust: a history of the small and invisible, Berkeley, California, University of California Press

Baddock, M. C., Bullard, J.E., and R.G. Bryant, (2009) Dust source identification using MODIS: A comparison of techniques applied to the Lake Eyre Basin, Australia. *Remote Sensing of Environment*, Volume 113, Issue 7, Pages 1511-1528

Bagnold, R.A., (1941), The Physics of wind blown sand and desert dunes. Methuen, London

Bardaji, T. and A. Harvey, (2008) Dryland Geomorphology and Interacting Processes. *Geomorphology*, Volume 102, Pages 205–206

Barett, E.C. and L.F. Curtis, (1995) Introduction to Environmental Remote Sensing 3rd Ed., Chapman and Hall, London

Bauer, B. O., (2009) Contemporary research in aeolian geomorphology. *Geomorphology*. Volume 105, Issues 1-2, Pages 1-5

Bennion, P., Hubbard, R., O'Hara, S., Wiggs, G., Wegerdt, J., Lewis, S., Small, I., van der Meer, J., and R. Upshur, (2007) The impact of airborne dust on respiratory health in children living in the Aral Sea region. *International Journal of Epidemiology*, Volume 36, Issue 5, Pages 1103-1110

Bowler, J.M., (1986) Spatial variability and hydrologic evolution of Australian lake basins: analogue for Pleistocene hydrologic change and evaporite formation. P*alaeogeography, Palaeoclimatology, Palaeoecology*. Volume 54, Issues 1-4, Pages 21-41

Brindley, H.E., and A. Ignatov (2006) Retrieval of mineral aerosol optical depth and size information from Meteosat Second Generation SEVIRI solar reflectance bands. *Remote Sensing of Environment*, Volume 102, Issues 3-4, Pages 344-363

Brindley, H.E., and J.E. Russell (2006) Improving GERB scene identification using SEVIRI: Infrared dust detection strategy. *Remote Sensing of Environment*, Volume 104, Issue 4, Pages 426-446

Brooks, N., and M. Legrand, (2000) Dust variability and rainfall in the Sahel. In Linking climate change to land-surface change, ed. S. McLaren and D. Kniveton, 1–25. Dordrecht: Kluwer Academic Publishers

Bryant, R.G., (2003) Monitoring Hydrological Controls on dust emissions: Preliminary observations from Etosha Pan, Namibia. *The Geographical Journal*, Volume 169, Number 2, Pages 131–141

Bryant, R.G., Bigg, G.R., Mahowald, N.M., Eckardt, F.D. and S.G., Ross, (2007) Dust emission response to climate in southern Africa. *Journal of Geophysical Research* – Atmosphere, Volume 112, Issue D09

Bullard, J., M. Baddock, G. McTainsh, and J. Leys, (2008), Sub-basin scale dust source geomorphology detected using MODIS. *Geophysical Research Letters*, Volume 35, L15404

Bullard, J.E. and G.H. McTainsh, (2003) Aeolian–fluvial interactions in dryland environments: examples, concepts and Australia case study. *Progress in Physical Geography*, Volume 27 Issue 4, Pages 471-501.

Bullard, J.E. and I. Livingstone, (2002) Interactions between aeolian and fluvial environments in dryland environments. *Area*, Volume 34, Issue 1, Pages 8–16

Cakmur, R. V., R. L. Miller and I. Tegen, (2001) A comparison of seasonal and interannual variability of soil dust aerosols over the Atlantic Ocean as inferred by the TOMS AI and AVHRR AOT retrievals. *Journal of Geophysical Research*, Volume 106 Issue D16, Pages 18287–18303.

Castillo, S., Moreno, T., Querol, X., Alastuey, A., Cuevas, E., Herrmann, L., Mounkaila, M. and W. Gibbons, (2008) Trace element variation in size-fractionated African desert dusts. *Journal of Arid Environments,* Volume 72, Issue 6, Pages 1034-1045

Chiapello, I., Prospero, J.M., Herman, J.R. and N.C. Hsu, (1999) Detection of mineral dust over the North Atlantic Ocean and Africa with Nimbus 7 TOMS, *Journal of Geophysical Research*, Volume 104, Issue D8, Pages 9277-9291

Chu, D. A., Y. J. Kaufman, G. Zibordi, J. D. Chern, J. Mao, C. Li, and B. N. Holben, (2003) Global monitoring of air pollution over land from the Earth Observing System-Terra Moderate Resolution Imaging Spectroradiometer (MODIS). *Journal of Geophysical Research*, Volume 108, Issue D21

Clarke, M.L. and H.M. Rendell, (1998) Climate change impacts on sand supply and the formation of desert sand dunes in the southwest USA. *Journal of Arid Environments*, Volume 39, Pages 517–531

Cooke, R.U., Warren, A., and A.S., Goudie, (1993) Desert Geomorphology, UCL Press, London

Cowling, R.M. and C. Hilton-Taylor, (2003) Phytogeography, flora and endemism. In Cowling, R.M., Richardson, D.M. and Pierce, S.M., Eds, Vegetation of Southern Africa, Cambridge University Press c1997, Chapter 3, Pages 43 - 61

Crutzen, P.J. and M.O. Andreae, (1990) Biomass burning in the tropics: impact on atmospheric chemistry and biogeochemical cycles. *Science*, Issue 250, Pages 1669 -1678

D'Almeida, G.A., P. Koepke and E.P. Shettle, 1991: Atmospheric aerosols. Global climatology and radiative characteristics. Deepak Publishing.

Darmenov, A., and I. N., Sokolik (2005), Identifying the regional thermal-IR radiative signature of mineral dust with MODIS. *Geophysical Research Letters*, Volume 32, L16803

Darmenova, K., Sokolik, I.N. and A. Darmenov (2005), Characterization of east Asian dust outbreaks in the spring of 2001 using ground-based and satellite data. *Journal of Geophysical Research*, Volume 110, D02204

Darwin, C. (1889) Journal of Researches into the Natural History and Geology of the Countries Visited During the Voyage of the H.M.S. Beagle Round the World, second edition; London et al: Ward, Lock and Co., Limited.

Darwin, C. (1945) Charles Darwin and the voyage of the Beagle, London Pilot Press Ltd. Great Russell Street London.

Dave, J.V., (1978) Effect of aerosols on the estimation of total ozone in an atmospheric column from the measurement of its ultraviolet radiance. *Journal of Atmospheric Science*, Issue 35, Pages 899 - 911

De Paepe, B., Ignatov, A., Dewitte, S, and A. Ipe, (2008) Aerosol retrieval over ocean from SEVIRI for the use in GERB Earth's radiation budget analyses. *Remote Sensing of the Environment*, Volume 112, Issue 5, Pages 2455-2468

Devasthale, A., Thomas, M.A., Singh, R.P., Krueger, O., Grassl, H., (2008) Monitoring dust outbreaks over the ocean using METEOSAT visible images, *Geophysical Research Abstracts*, Vol 10, 2008

Draxler, R.R. and Rolph, G.D., (2003) HYSPLIT (HYbrid Single-Particle Lagrangian Integrated Trajectory) Model access via NOAA ARL READY Website (http://www.arl.noaa.gov/ready/hysplit4.html). NOAA Air Resources Laboratory, Silver Spring, MD.

Duda, D.P., Minnis. P., Trepte, Q., Sun-Mack, S., (2006) The Continuous Monitoring of Desert Dust using an Infrared-based Dust Detection and Retrieval Method, 12th AMS Conference on Atmospheric Radiation (Remote Sensing of Clouds and Aerosols: Aerosols) 10-14 July 2006 Madison, Wisconsin

Eckardt, F.D., and N. Kuring, (2005) SeaWiFS identifies dust sources in the Namib Desert. *International Journal of Remote Sensing*, Volume 26, Number 19, Pages 4159–4167

Eckardt, F.D., Washington, R. and J. Wilkinson, (2001) The origin of dust on the West Coast of Southern Africa. *Palaeoecology of Africa*, Volume 27, Pages 207-219

Eitel, B., Blumel, W.D., Huser, K. and B. Mauz, (2001) Dust and loessic alluvial deposits in Northwestern Namibia (Damaraland, Kaokoveld): sedimentology and palaeoclimatic evidence based on luminescence data, *Quaternary International*, Volumes 76-77, Pages 57-65

El-Askary, H., Gautam, R. and M Kafatos, (2004) Remote Sensing of dust storms over the Indo-Gangetic Basin. *Journal of the Indian Society of Remote Sensing*, Volume 32, Number 2, Pages 121 - 124

Engelstaedter, S., and R. Washington, (2007a) Temporal controls on global dust emissions: The role of surface gustiness. *Geophysical Research Letters*, Volume 34, L15805,

Engelstaedter, S., and R. Washington, (2007b) Atmospheric controls on the annual cycle of North African dust. *Journal of Geophysical Research*, Volume 112, D03103

Engelstaedter, S., K. E. Kohfeld, I. Tegen, and S. P. Harrison, (2003) Controls of dust emissions by vegetation and topographic depressions: An evaluation using dust storm frequency data. *Geophysical Research Letters,* Volume 30(6), 1294,

Engelstaedter, S., Tegen, I., and R. Washington, (2006) North African dust emissions and transport. *Earth Science Reviews*, Issue 79, Pages 73 - 100

EUM/MSG/ICD/105, issue: V5A, date: 22 August 2007, available online and accessed on the 19th of March 2008 at: http://www.eumetsat.int

EUM/MSG/ICD/105: MSG Level 1.5 Image Data Format Description, document code:

EUMETSAT Product guide: http://www.eumetsat.int - accessed 19th March 2008

Giles, J., (2005) The dustiest place on Earth, *Nature*, 434, Pages 816– 819.

Gordon Ogden, J., (1912) The Kingdom of Dust, Chicago: Popular Mechanics Company, 1912: 10

Goudie, A.S. and G.L. Wells, (1995) The nature, distribution and formation of pans in arid zones, *Earth Science Reviews*, Issue 38, Pages 1 - 69

Goudie, A.S. and N.J. Middleton, (2001). Saharan dust storms: nature and consequences. *Earth-Science Reviews,* Volume 56, Issues 1–4, Pages 179–204

Goudie, A.S. and N.J. Middleton, (2006) Desert Dust in the Global System, Berlin, Springer

Goudie, A.S., (1978) Dust Storms and their geomorphological implications. *Journal of Arid Environments*, 1, Pages 291 - 310

Goudie, A.S., (1983) Dust storms in space and time. *Progress in Physical Geography*, 7, Pages 502- 530

Goudie, A.S., (2009) Dust storms: Recent developments, *Journal of Environmental Management,* Volume 90, Pages 89–94

Gu, Y., Rose, W.I., and G.J.S. Bluth, (unpublished) Retrieval of Mass and Sizes of Particles in Sandstorms Using Two MODIS IR Bands: A Case Study of April 7 2001 Sandstorm in China, available online: http://www.modis.gsfc.nasa.gov/ accessed 21 March 2008.

Hansell, R. A., S. C. Ou, K. N. Liou, J. K. Roskovensky,S. C. Tsay, C. Hsu, and Q. Ji, (2007) Simultaneous detection/separation of mineral dust and cirrus clouds using MODIS thermal infrared window data, *Geophysical Research Letters*, Volume 34, L11808

Harrison, S.P., Kohfeld, K.E., Roelandt, C. and T. Claquin, (2001) The role of dust in climate changes today, at the last glacial maximum and in the future. *Earth-Science Reviews,* Volume 54, Issues 1–3, Pages 43–80.

Herman, J. R., Bhartia, P. K., Torres, O., Hsu, N.C., Seftor, C and E. Celarier, (1997) Global distribution of UV-absorbing aerosols from Nimbus 7/TOMS data. *Journal of Geophysical Research,* Voume 102 (D14), Pages 16,911 –16,922

Hess, M., Koepke, P., and I. Schult, (1998) Optical Properties of Aerosols and Clouds: The Software Package OPAC. *Bulletin of the American Meteorological Society*, Volume 79, Number 5, Pages 831-844

Higurashi, A., and T. Nakajima, (2002) Detection of aerosol types over the East China Sea near Japan from four-channel satellite data, *Geophysical Research Letters*, Volume 29, Issue 17,

Holben, B.N., Tanre, D., Smirnov, A., Eck, T.F.,Slutsker, I., Abuhassan, N., Newcomb, W.W., Schafer, J., Chatenet, B., Lavenue, F., Kaufman, Y.J., Vande Castle, J., Setzer, A., Markham, B., Clark, D., Frouin, R., Halthore, R., Karnieli, A., O'Neill, N.T., Pietras, C., Pinker, R.T. Voss K., and G. Zibordi, (2001) An emerging ground-based aerosol climatology: Aerosol Optical Depth from AERONET. *Journal of Geophysical Research,* Volume 106, Pages 12 067-12 097

Holmes, P.J., Bateman, M.D., Thomas, D.S.G., Telfer, M.W., Barker, C.H. and M.P. Lawson, (2008) A Holocene-late Pleistocene aeolian record from lunette dunes of the western Free State panfield, South Africa. *The Holocene*, Volume 18, Pages 1193-1205

Hsu, N.C., (2007) Global retrieval of aerosol properties from sources to sinks by MODIS. *Developments in Earth Surface Processes*, Volume 10, Page 23

Hsu, N.C., Tsay, S.C., and M.D. King, (2004) Aerosol Properties Over Bright-Reflecting Source Regions. *IEEE Transactions on Geoscience and Remote Sensing*, Volume 42, Number 3

Huang, J., Ge, J. and F. Weng, (2007) Detection of Asia dust storms using multisensor satellite measurements. *Remote Sensing of the Environment*, Volume 110, Pages 186 - 191

Husar, R. B., Prospero, J.M. and L.L. Stowe, (1997) Characterization of tropospheric aerosols over the oceans with the NOAA advanced very high resolution radiometer optical thickness operational product. *Journal of Geophysical Research*, Volume 102, Issue D14, Pages 16889-16910

Ichoku, C., L. A. Remer, Y. J. Kaufman, R. Levy, D. A. Chu, D. Tanre´, and B. N. Holben, (2003) MODIS observation of aerosols and estimation of aerosol radiative forcing over southern Africa during SAFARI 2000. *Journal of Geophysical Research*, Volume 108, Issue D13, Page 8499

IPCC, (2007): Climate Change 2007: The Physical Science Basis. Contribution of Working Group I to the Fourth Assessment Report of the Intergovernmental Panel on Climate Change. Editors, Solomon, S., Qin,D., Manning, M., Chen, Z., Marquis, M., Averyt, K.B., Tignor M., and H.L. Miller. Cambridge University Press, Cambridge, United Kingdom and New York, NY, USA

Jacobsen, P.J., Jacobsen, K.M. and M.K. Seely, (1995) Ephemeral Rivers and their Catchment, Windhoek, Namibia: Desert Research Foundation of Namibia

Jacobson, P.J., Jacobson, A., Angermeier, K.M., Cherry, P.L. and D. S. Cherry, (2000) Hydrologic influences on soil properties along ephemeral rivers in the Namib Desert, *Journal of Arid Environments*, Volume 45, Pages 21–34

Jickells, T.D., An, Z.S., Andersen, K.K., Baker, A.R., Bergametti, G., Brooks, N., Cao, J.J., Boyd, P.W., Duce, R.A., Hunter, K.A., Kawahata, H., Kubilay, N., laRoche, J., Liss, P.S., Mahowald, N., Prospero, J.M., Ridgwell, A.J., Tegen, I. and R. Torres, (2005) Global Iron Connections Between Desert Dust, Ocean Biogeochemistry, and Climate. *Science*, Volume 308, (5718), Page 67

Kalu, A.E., (1979) The African dust plume: its characteristics and propagation across West Africa in winter. In: C. Morales, Editor, Saharan Dust: Mobilization, Transport, Deposition, John Wiley & Sons, New York, Pages 95–118.

Kaufman, Y. J., Koren, I., Remer, L. A., Tanré, D., Ginoux, P. and S. Fan (2005), Dust transport and deposition observed from the Terra-Moderate Resolution Imaging Spectroradiometer (MODIS) spacecraft over the Atlantic Ocean, *Journal of Geophysical Research*, Volume 110, D10S12

Kaufman, Y. J., Tanre, D. and O. Boucher, (2002) A satellite view of aerosols in the climate system, *Nature*, Volume 419, Pages 215–223

Kaufman, Y.J., Karnieli, A. and D. Tanré, (2000) Detection of Dust Over Deserts Using Satellite Data in the Solar Wavelengths. *IEEE Transactions on Geoscience and Remote Sensing*, Volume 38, Number 1,

Kaufman, Y.J., Tanre, D., Gordon, H.R., Nakajima, R., Lenoble, J., Frouin, R., Grassl, H., Herman, B.M., King, M.D. and P.M. Teillet, (1997) Passive remote sensing of tropospheric aerosol and atmospheric correction for the aerosol effect. *Journal and Geophysical Research*, Volume 102, Number D14, Pages 168150 - 16830

King, M., Kaufman, Y., Tanré, D. and T. Nakajima, (1999) Remote sensing of tropospheric aerosols from space: past, present, and future. *Bulletin of the American Meteorological Society*, Volume 80, Pages 2 229–2 259.

Krotkov, N.A., Herman, J., Seftor, C.J., Arola, A., Kaurola, J., Taalas, P. and A. Vasilkov, (2002) OMI Surface UV Irradiance Algorithm, in in Stammes, P (ed) OMI Theoretical Algorithm Basis Document: Clouds, Aerosols and Surface UV Irradiance, Version 3. NASA Reference Publication, ATBD (Algorithm Theoretical Basis Document - Version 2, August 2002) ATBD-3-OMI, Pages 72 - 110

Kruger, G.P., (1983) Terrain morphological map of southern Africa. Soil and Irrigation Research Institute, Department of Agriculture.

Lancaster, N., (1986) Pans in the southwestern Kalahari: A preliminary report, *Palaeoecology of Africa*, Issue 17, Pages 59 - 67

Lee, T.F., (1989) Dust tracking using composite Visible/IR images: A Case Study, Notes and Correspondence in Weather and Forecasting, Volume 4, Pages 258 - 263, June 1989

Legrand, M., Plana-Fattori, A. and C. N'Doume, (2001) Satellite detection of dust using the IR imagery of Meteosat 1. Infared difference dust index. *Journal of Geophysical Research*, Volume 106, Issue D16, Pages 18251 - 18275

Legrand, M., Verge-Depre, G. and O. Pancrati, (2004) Remote Sensing of Dust in Africa using MSG/SEVIRI: Towards and Multichannel Dust Index, Proc Second MSG RAO Workshop, Salzberg, Austria 9-10 September 2004 (ESP SP-582, November 2004)

Levelt, P.F., (2002) Introduction, in Levelt, P.F. (ed) OMI Instrument, Level 0-1b processor, Callibration and Opertions, Version 1. NASA Reference Publication, ATBD (Algorithm Theoretical Basis Document) ATBD-1-OMI, pp 7 - 8

Levelt, P.F., van den Oord, G.H.J., Dobber, M.R., Malkki, A., Visser, H., de Vries, J., Stammes, P., Lundell, J.O.V., Saari, H., (2006) The ozone monitoring instrument. *IEEE Transactions on Geoscience and Remote Sensing*, Volume 44, Number 5, Pages 1093-1101,

Li, J., Zhang, T.J., Schmit, T.J., Schmetz, J. and W.P. Menzel, (2007) Quantitative monitoring of Saharan dust event with SEVIRI on Meteosat-8. *International Journal of Remote Sensing*, Volume 28, Number 10, Pages 2181 - 2186

Lim, J.Y. and Y. Chun, (2006) The characteristics of Asian dust events in Northeast Asia during the springtime from 1993 to 2004. *Global and Planetary Change,* Volume 52, Pages 231–247

Livingstone, I. and A. Warren, (1996) Aeolian Geomorphology: An Introduction. Longman, London, p. 211.

Mahowald, N. M., Bryant, R.G., del Corral, J. and L. Steinberger, (2003) Ephemeral lakes and desert dust sources. *Geophysical Research Letters*, Volume 30, (2),1074

Mahowald, N., and J.L. Dufresne, (2004) Sensitivity of TOMS AI to PBLH: Implications for detection of mineral aerosol sources. *Geophysical Research Letters,* Volume 31, (3)

Mahowald, N.M., Ballantine, J.A., Feddema, J. and N. Ramankutty, (2005) Global trends in visibility: implications for dust sources. *Atmospheric Chemistry and Physics*, Issue 7, Pages 3309–3339,

Malin, J.C., (1946) Dust Storms, Part 1, May 1946, *Kansas Historical Quarterly*, Volume 14, Number 2, Pages 129 - 133

McGowan, H. and A. Clark, (2008) Identification of dust transport pathways from Lake Eyre, Australia using Hysplit. *Atmospheric Environment* Issue 42, Pages 6915–6925

McPeters, R.D., Bhartia, P.K., Krueger, A.J., Herman, J.R., Schlesinger, B.M., Wellenmayer, C.G., Seftor, C.J., Jaross, G., Taylor, S.L., Swissler, T., Torres, O., Labow, G., Byerly, W. and R.P. Cebula, (1996) Nimbus-7 Total Ozone Mapping Spectrometer (TOMS) Data Products User's Guide, NASA Reference Publication 1384, April 1996

Mctainsh, G. and C. Strong, (2007) The role of aeolian dust in ecosystems, *Geomorphology* Issue 89 , Pages 39–54

McTainsh, G., Chan, Y., McGowan, H., Leys, J. and K. Tews, (2005) The 23rd October 2002 dust storm in eastern Australia: characteristics and meteorological Conditions. *Atmospheric Environment*, Volume 39, Issue 7, Pages 1227-1236

McTainsh, G.H., Leys, J.F. and W.G. Nickling, (1999) Wind erodibility of arid lands in the Channel Country of western Queensland,Australia. *Zeitschrift für Geomorphologie,* Volume 116, Pages 113 – 130.

McTainsh, G.H., Lynch, A.W. and E.K. Tews, (1998) Climatic controls upon dust storm occurrence in eastern Australia. *Journal of Arid Environments,* Volume 39, Pages 457–466

Mendelsohn, J., Jarvis, A., Roberts, C. and T. Robertson, (2002) Atlas of Namibia: A Portrait of the Land and its People, David Philip Publishers, Cape Town, South Africa

Middleton, N.J. (1997) Desert Dust. In D.S.G. Thomas, Arid Zone Geomorphology: Processes, Form and Change in Drylands, 2nd Edition. John Wiley and Sons, Chichester. Chapter 18 Pages 413 - 436

Middleton, N.J. and A.S. Goudie, (2001) Saharan dust: sources and trajectories. *Transactions of the Institute of British Geographers*, NS 26, Pages 265 – 181

Miller, S. D., (2002) SeaWiFS True Color, Vegetation, and Dust Enhancement Processing at NRL Monterey, NRL Formal Report, NRL/FR/7540-02-2, 22 pp., Naval Research Laboratory, Washington DC.

Moody, J.L., Pszenny, A.A.P., Grandry, A., Keene, W.C., Galloway, N.J. and G Polian, (1991) Precipitation composition and its variabililty in the southern Indian Ocean: Amsterdam Island, 1980 - 1987. *Journal of Geophysical Research*, Volume 96, Pages 20769 - 20786

Mucina, L., and M.C. Rutherford, (2006) The Vegetation of South Africa, Lesotho and Swaziland. South African National Biodiversity Institute, Pretoria.

Nash, D.J., Bullard, J.E. and C.P. North, (2007) Drylands: Linking landscape processes to sedimentary environments. *Sedimentary Geology, Volume* 195, Issues 1-2, Pages 1–3

Natsagdorj, L., Jugder, D. and Y.S. Chung, (2003) Analysis of dust storms observed in Mongolia during 1937 – 1999. *Atmospheric Environment,* Issue 37, Pages 1401–1411

Neff, J.C., Ballantyne, A.P., Farmer, G.L., Mahowald, N.M., Conroy, J.L., Landry, C.C., Overpeck, J.T., Painter, T.H., Lawrence, C.R. and R.L. Reynolds, (2008) Increasing eolian dust deposition in the western United States linked to human activity. *Nature Geoscience*, Advanced online publication, DOI10.1038

Nobileau, D. and D. Antoine, (2005) Detection of blue-absorbing aerosols using near infrared and visible (ocean color) remote sensing observations. *Remote Sensing of Environment*, Volume 95, Issue 3, Pages 368-387

Nyanganyura, D., Maenhaut, W., Mathuthu, M., Makarau, A. and F.X. Meixner, (2007) The chemical composition of tropospheric aerosols and their contributing sources to a continental background site in northern Zimbabwe from 1994 to 2000. *Atmospheric Environment*, Volume 41, Issue 12, Pages 2644-2659.

O'Hara, S.L., Clarke, M.L., Elatrash, M.S., (2006) Field measurements of desert dust deposition in Libya. *Atmospheric Environment, Issue* 40, Pages 3881 - 3897

Partridge, T.C. (2003) Evolution of Lanscapes. In Cowling, R.M., Richardson, D.M. and Pierce, S.M., Eds, Vegetation of Southern Africa, Cambridge University Press c1997. Chapter 1, Pages 3 - 27

Petit, J.R., Briat, M. and A. Royer, (1981) Ice age aerosol content from East Antarctic ice core samples and past wind strength. *Nature,* Volume 293, Number 5831, Pages 391–394.

Piketh, S.J., Annegarn, H.J. and P.D. Tyson, (1999) Lower Tropospheric aerosol dust loadings over South Africa: The relative contribution of aeolian dust, industrial emissions, and biomass burning. *Journal of Geophysical Research*, Issue 104, Pages 1597 - 1607

Piketh, S.J., Tyson, P.D. and W. Steffen, (2000) Aeolian Transport from southern Africa and iron fertilisation of marine biota in South Indian Ocean. *South African Journal of Science*, Volume 96, Pages 244 - 246

Power, H.C., (2008) The Geography and climatology of aerosols, *Progress in Physical Geography,* Volume 27, Issue 4, Pages 502–547

Prospero, J.M., (1999) Long-range transport of mineral dust in the global atmosphere: Impact of African dust on the environment of the south eastern United States. *Proc. National Academy of Science* USA, Volume 96, Pages 3396-3403 Colloquium Paper

Prospero, J.M., Charlson, R.J., Mohnen, V., Jaenicke, R., Delany, A.C., Moyers, J., Zoller, W. and K. Rahn, (1983) The atmospheric aerosol system: an overview. *Review of Geophysical Space Physics*, Volume 21, Pages 1607 - 1629

Prospero, J.M., Ginoux, P., Torres, O., Nicholson S.E. and T.E. Gill, (2002), Environmental characterization of global sources of atmospheric soil dust identified with the Nimbus 7 total ozone mapping spectrometer (TOMS) absorbing aerosol product. *Review of Geophysics,* Volume 40(1), 1002

Pye, K., (1987) Aeolian dust and dust deposited. Academic Press Inc. London

Ramaswamy, V., Boucher, O., Haigh, J., Hauglustaine, D., Haywood, J., Myhre, G., Nakajima, T., Shi, G.Y. and S. Solomon, (2001) Radiative forcing of climate change, in Climate Change 2001: The Scientific Basis, edited by J.T. Houghton et al., pp. 349–416, Cambridge Univ. Press, New York.

Reason, C.J.C. and A. Keibel, (2004) Tropical Cyclone Eline and Its unusual penetration and imapacts over the southern African mainland. *Weather and Forecasting*, Volume 19, Number 5, Pages 789 -805

Reason, C.J.C., Engelbrecht, F., Landman, W.A. Lutjeharms, J.R.E., Piketh, S., de W.Rautenbach C.J. and B.C. Hewitson, (2006) A review of South African research in atmospheric science and physical oceanography during 2000–2005. *South African Journal of Science,* Volume 102, Pages 35 - 45

Reheis, M.C., (2006) A 16-year record of eolian dust in Southern Nevada and California, USA: Controls on dust generation and accumulation. *Journal of Arid Environments, Volume* 67, Pages 487–520

Reid, I. and L.E. Frostick, (1997). Channel form, flow and sediments in deserts. In D.S.G. Thomas, Arid Zone Geomorphology: Processes, Form and Change in Drylands, 2nd Edition. John Wiley and Sons, Chichester. Chapter 11, Pages 205 - 229

Remer, L., Kaufman, Y., Tanré, D., Mattoo, S., Chu, D., Martins, J., Li, R.R., Ichoku, C., R. C. Levy, R. G. Kleidman, T. F. Eck, E. Vermote, and B. N. Holben, (2005).The MODIS aerosol algorithm, products, and validation. *Journal of the Atmospheric Sciences,* Volume 62, Pages 947–973.

Remer, L.A., Kleidman, R.G., Levy, R.C., Kaufman, Y.J., Tanre, D., Mattoo, S., Vanderlie Martins, J., Ichoku, C., Koren, I., Yu, H. and B.N. Holben, (2008) Global Aerosol climateology from the MODIS satellite sensors. *Journal of Geophysical Research Atmospheres*, Issue 113, D14S07

Rolph, G.D., (2003) Real-time Environmental Applications and Display sYstem (READY) Website (http://www.arl.noaa.gov/ready/hysplit4.html). NOAA Air Resources Laboratory, Silver Spring, MD.

Roskovensky, J. K. and K. N. Liou, (2003) Detection of thin cirrus from 1.38 mm/0.65 mm reflectance ratio combined with 8.6–11 mm brightness temperature difference. *Geophysical Research Letters*, Volume 30, Number 19

Roskovensky, J. K. and K. N. Liou, (2005) Differentiating airborne dust from cirrus clouds using MODIS data. *Geophysical Research Letters*, Volume 32, L12809

Schepanski, K., I. Tegen, B. Laurent, B. Heinold, and A. Macke, (2007) A new Saharan dust source activation frequency map derived from MSG-SEVIRI IR channels. *Geophysical Research Letters,* Volume 34, L18803

Schmetz, J., Pili, P., Tjemkes, S., Just, D., Kerkmann, J., Rota, S. and A. Ratier, (2002) An Introduction to Meteosat Second Generation (MSG), *American Meteorological Society,* BAMS, Pages 977-992

Seftor, C.J., Hsu, N.C., Herman, J.R., Bhartia, P.K., Torres, O., Rose, W.I., Schneider, D.J. and N. Krotkov, (1997) Detection of volcanic ash clouds from Nimbus 7/Total Ozone Mapping Spectrometer. *Journal of Geophysical Research,* Volume 102, D14, Pages 16794 - 16759

Seignolis, C. and F. Arago, (1846) Pluie coloree en rouge dans le departement de departement de l'Ardeche. C.R Acad. Sci. Paris, 23, 832

Shanyengana, E.S., Henschel, J.R., Seely, M.K. and R.D. Sanderson, (2002) Exploring fog as a supplementary water source in Namibia. *Atmospheric Research,* Volume 64, Issues 1-4, Pages 251 - 259

Shaw, P.A. and D.S.G Thomas, (1997) Pans, playas and salt lakes. In D.S.G. Thomas Ed, Arid Zone Geomorphology: Process, Form and Change in Drylands, 2nd Edition. John Wiley & Sons, Chichester. Chapter 14, Pages 293 - 318

Soderberg, K. and J.S. Compton, (2006) Dust as a Nutrient Source for Fynbos Ecosystems, South Africa. *Ecosystems,* Volume 10, Number 4, Pages 550–561

Sokolik, I. N., (2002) The spectral radiative signature of wind-blown mineral dust:Implications for remote sensing in the thermal IR region. *Geophysical Research Letters,* Volume 29, Number 24, Page 2154

Sokolik, I.N. and O.B. Toon, (1996) Direct radiative forcing by anthropogenic airborn mineral aerosols. *Nature,* Volume 381, Issue 6584, Pages 681–683.

Stammes, P., (2002) Introduction and Algorithm Overview, in Stammes, P (ed) OMI Theoretical Algorithm Basis Document: Clouds, Aerosols and Surface UV Irradiance, Version 3. NASA Reference Publication, ATBD (Algorithm Theoretical Basis Document - Version 2, August 2002) ATBD-3-OMI, Pages 8 - 16

Stammes, P., (2002b) Summary and Conclusions, in Stammes, P (ed) OMI Theoretical Algorithm Basis Document: Clouds, Aerosols and Surface UV Irradiance, Version 3. NASA Reference Publication, ATBD (Algorithm Theoretical Basis Document - Version 2, August 2002) ATBD-3-OMI, Pages 111-114

Stein, D.C., Swap, R.J., Macko, S.A., Piketh, S.J., Doddridge, B. and R. Bruintjes, (2003) Preliminary Results of dry-season trace gas and aerosol measurements over the Kalahari region during SAFARI 2000. *Journal of Arid Environments,* Volume 54, Issue 2, Pages 371–379

Swap, R.J., Szuba, T.A., Garstang, M., Annegarn, H.J., Marufu, L. and S.J. Piketh, (2003) Spatial and temporal assessment of sources contributing to the annual austral spring mid-tropospheric ozone maxima over the tropical South Atlantic. *Global Change Biology,* Volume 9, Pages 336-345

Swenk, W.E. and R.J., Curran, (1974) The Detection of Dust Storms Over Land and Water With Satellite Visible and Infrared Measurements, *Monthly Weather Review,* Volume 102, Pages 830 - 838

Tanskanen, A., Krotkov, N.A., Herman, J.R. and A. Arola, (2006) Surface ultraviolet irradiance from OMI. *IEEE Transactions on Geoscience and Remote Sensing,* Volume 44, Number 5, Pages 1267-1271

Tegen, I., and I. Fung (1995), Contribution to the atmospheric mineral aerosol load from land surface modification, *Journal of Geophysical Research*, Volume 100, Issue D9, Pages 18707–18726.

Tegen, I., Werner, M., Harrison, S.P. and K. E. Kohfeld, (2004) Relative importance of climate and land use in determining present and future global soil dust emission. *Geophysical Research Letters*, Volume 31, L05105,

Telfer, M.W., Thomas, D.S.G., Parker, A.G., Walkington, H. and A.A Finch, (2009) Optically Stimulated Luminescence (OSL) dating and palaeoenvironmental studies of pan (playa) sediments from Witpan, South Africa. *Palaeogeography, Palaeoclimatology, Palaeoecolog,y* Volume 273, Pages 50–60

Thieuleux, F., Moulin, C., Breon, F.M., Maignan, F., Poitou J. and D. Tanre, (2005) Remote sensing of aerosols over the oceans using SG/SEVIRI imagery, *Annales Geophysicae*, Volume 23, Number 12, Pages 3561–3568,

Thomas, D.S.G and P. Shaw, (1991) The Kalahari Environment, Cambridge University Press, Cambridge

Thomas, D.S.G. and G.F.S. Wiggs, (2008) Aeolian systems response to global change: challenges of scale, process and temporal integration. *Earth Surface Processes and Landforms*, Volume 33, Issue 9, Pages 1396-1418

Thomas, D.S.G., (1997) Reconstructing ancient arid environments. In D.S.G. Thomas, Arid Zone Geomorphology: Processes, Form and Change in Drylands, 2nd Edition. John Wiley and Sons, Chichester. Chapter 26, Pages 577 - 605

Thomas, D.S.G., Knight, M. and G.F.S. Wiggs, (2005) Remobilization of southern African desert dune systems by twenty-first century global warming. *Nature*, Volume 435, Pages 1218-1221.

Thomas, D.S.G., Nash, D.J., Shaw, P.A. and C. Van der Post, (1993) Present day lunette sediment cycling at Witpan in the arid southwestern Kalahari Desert. *CATENA*, Volume 20, Issue 5, Pages 515-527

Todd, M. C., Washington, R., Martins, J.V., Dubovik, O., Lizcano, G., M'Bainayel, S. and S. Engelstaedter (2007), Mineral dust emission from the Bodélé Depression, northern Chad, during BoDEx 2005. *Journal of Geophysical Research,* Volume 112, D06207

Tooth, S., (2000) Process, form and change in dryland rivers: a review of recent research. *Earth-Science Reviews,* Volume 51, Pages 67–107

Tooth, S., (2008) Arid geomorphology: recent progress from an Earth System Science perspective. *Progress in Physical Geography,* Volume 32, Number 1, Pages 81–101

Torres, O., Bhartia, P.K., Herman, J.R., Sinyuk, A., Ginoux, P., and B. Holben, (2002a). A long-term record of aerosol optical depth from TOMS observations and comparison to AERONET measurements. .*Journal of the Atmospheric Sciences,* Volume 59, Number 3, Pages 398–413

Torres, O., Decae, R., Veefkind, P. and G. de Leeuw, (2002b) OMI Aerosol Retrieval Algorithm, in Stammes, P (ed) OMI Theoretical Algorithm Basis Document: Clouds, Aerosols and Surface UV Irradiance, Version 3. NASA Reference Publication, ATBD (Algorithm Theoretical Basis Document - Version 2, August 2002) ATBD-3-OMI, pp 47 - 71

Torres, O., Herman, J.R., Bhartia, P.K. and A. Sinyuk, A., (2002c) Aerosol properties from EP-TOMS near UV observations. *Advanced Space Research*, Volume 29, Number 11, Pages 1771-1780

Tyson, P.D and P.C. D'Abreton, (1998) Transport and recirculation of aerosols off southern Africa - macroscale plume structure, *Atmospheric Environments*, Volume 32, Number 9, Pages 1511 - 1524

Tyson, P.D. (1987) Climate Change and Variability in southern Africa, Oxford University Press, Cape Town, 1987

Tyson, P.D. and C.K. Gatebe, (2001) The atmosphere, aerosols, trace gases and biogeochemical change in southern Africa: a regional integration. *South Africa Journal of Science,* Volume 97, Pages 106 - 118

Tyson, P.D. and R.A. Preston-Whyte, (2000) The Weather and Climate of Southern Africa, Second Edition, Oxford University Press Southern Africa, Cape Town, South Africa.

Tyson, P.D., Garstang, M. and R. Swap, (1996a) Large-Scale Recirculation of Air over Southern Africa. *Journal of Applied Meteorology*, Volume 35, Pages 2218-2236

Tyson, P.D., Garstang, M., Swap, R.J., Edwards, S. and P. Kallberg, (1996b) An air transport climatology for subtropical southern Africa. *International Journal of Climatology*, Volume 16, Pages 265 - 291

Tyson, P.D., Odada, E., Schulze, R. and C. Vogel. (2002) Regional-Global Climate Change Linkages: Southern Africa In Global-Regional Linkages in the Earths System, Tyson, P.D., Fuchs, R., Fu, C., Lebel, L., Mitra, A.P., Odada, E., Perry, J., Steffen, W. and H. Virji, (Eds.) Springer, Chapter 2, Pages 3 - 73

Udahemuka, G., van den Bergh, F., van Wyk, B.J. and M.A. van Wyk., (2007) Robust fitting of diurnal brightness temperature cycle. 18th Annual Symposium of the Pattern Recognition Association of South Africa (PRASA), Pietermaritzburg, Kwazulu-Natal, South Africa, 28-30 November 2007, pp 6

Veefkind, J.P., de Leeuw, G., Stammes, P and R.B.A. Koelemeijer, (2000) Regional Distribution of Aerosol over Land Derived from ATSR-2 and GOME. *Remote Sensing of the Environment* Volume 74, Pages 377 - 386

Vermote, E.F. and A. Vermeulen, (1999) MODIS Algorithm Technical Background Document, Atmospheric Correction Algorithm: Spectral Reflectances - MOD09, NASA contract document, NAS5-96062, version 4, April 1999

Vickery, K.J, (2007) Atmospheric controls on mineral dust emissions in southern Africa and the potential response to climate change. Unpublished Honours thesis (BSc), University of Cape Town, South Africa.

Wang, S., Wang, J., Zhou, Z. and K. Shang, (2005) Regional characteristics of three kinds of dust storm events in China. *Atmospheric Environment,* Volume 39, Issue 3, Pages 509–520

Warner, T.T, (2004) Desert Meteorology, Cambridge University Press, United Kingdom, 2004

Washington, R., and M.C. Todd, (2005) Atmospheric controls on mineral dust emission from the Bodélé Depression, Chad : The role of the low level jet. *Geophysical Research Letters*, Volume 32, Issue L17701

Washington, R., Todd, M., Middleton, N.J. and A.S. Goudie, (2003) Dust-Storm source areas determined by the Total Ozone Monitoring Spectrometer and Surface Observations, *Annals of the Association of American Geographers*, Volume 93, Issue 2, Pages 297 – 313

Washington, R., Todd, M.C., Engelstaedter, S., Mbainayel, S. and F. Mitchell, (2006), Dust and the low-level circulation over the Bodélé Depression, Chad: Observations from BoDEx 2005. *Journal of Geophysical Research*, Volume 111, Issue D03201

Washington, R., Todd, M.C., Lizcano, G., Tegen, I., Flamant, C., Koren, I., Gineaux, P., Engelstaedter, S., Bristow, C.S., Zender, C.S., Goudie, A.S., Warren, A. and J.M. Prospero, (2006), Links between topography, wind, deflation, lakes and dust: The case of the Bodélé Depression, Chad. *Geophysical Research Letters,* Volume 33 L09401

Weeks, S.J., Currie, B. and A. Bakun, (2002) Massive emissions of toxic gas in the Atlantic. *Nature*, Volume 415, Pages 493 - 494

White, K. and F.E. Eckardt, (2006) Geochemical mapping of carbonate sediments in the Makgadikgadi basin, Botswana, using moderate resolution remote sensing data. *Earth Surface Processes and Landforms*, Volume 31, Issue 6, Pages 665-681.

Wiggs, G.F.S., Livingstone, I., Thomas, D.S.G. and J.E. Bullard, (1995) Dune mobility and vegetation cover in the southwest Kalahari desert. *Earth Surface Processes and Landforms*, Volume 20, Issue 6, Pages 515-529.

Yang, Y.Q., Q. Hou, C. H. Zhou, H. L. Liu, Y. Q. Wang, and T. Niu, (2008) Sand/dust storm processes in Northeast Asia and associated large-scale circulations. *Atmospheric Chemistry and Physics*, Volume 8, Number 1, Pages 25-33

Zender, C.S. and E.Y. Kwon, (2005) Regional Contrasts in Dust Emission Responses to Climate. *Journal of Geophysical Research*, Volume 110, D13201

Zender, C.S. and J. Talamantes, (2006) Climate controls on valley fever incidence in Kern Country, California. *International Journal Biometeorology,* Volume 50, Number 3, Pages 174 - 182

Zhang, P., Lu, N., Hu, X. and C. Dong, (2006) Identification and physical retrieval of dust storm using three MODIS thermal IR channels. *Global and Planetary Change,* Volume 52, Pages 197–206

8. Website References

WMO website: www.wmo.int – last accessed 10th June 2009

GIOVANNI website: http://gdata1.sci.gsfc.nasa.gov/daac-bin/G3/gui.cgi?instance_id=omi - last accessed March 2009

HYSPLIT website: http://www.ready.noaa.gov/ready/open/hysplit4.html - last accessed December 2009

NASA ftp site: ftp://toms.gsfc.nasa.gov/pub/nimbus7/data/aerosol/ - last accessed March 2009

NOAA ESLR website: http://www.esrl.noaa.gov/psd/data/gridded/ - last accessed November 2009

MODIS Rapidfire: http://rapidfire.sci.gsfc.nasa.gov/ - last accessed December 2009

EUMETSAT PINK: http://oiswww.eumetsat.org/IPPS/html/MSG/RGB/DUST/index.htm - last accessed December 2009

Appendix 1: Glossary

dust event will be used to refer to an event that is visible in true colour imagery at a resolution of 250 m and sufficiently depresses the brightness temperatures of the 8.7 μm, 10.8 μm and 12.0 μm wavelengths to those which are considered to represent dust activity as per Ackerman (1997) and such that the characteristic hue associated with dust is present. Further a dust event is defined to be the occurrence of a plume or the activation of a source

plumes are defined as the unambiguous presence of mineral aerosols identified in suspension.

sources are the geographical setting for the best approximation of the origin of the plume.

event is defined to be the occurrence of a plume or activation of a source.

aerosol a particulate matter – most commonly in this study, a particulate of soil derived origin and of significantly small radius such as to be prone to wind deflation.

Appendix 2: MSG-BTD script

```
# CREATE DUST IMAGES FROM EUMETSAT IR087, IR108 AND IR120 IMAGES
# CHRIS JACK, 2008

IMPORT SYS
IMPORT OS
IMPORT IMAGE
IMPORT IMAGEMATH
#IMPORT IMAGEOPS
IMPORT IMAGESTAT
IMPORT DATETIME

# METEOSAT IMAGE FILE PREFIX
PREFIX = "HMSG2_"
GAMMA = 1/2.5
# SET DATE RANGE TO PROCESS
STARTDATE = DATETIME.DATE(2007,8,14)
ENDDATE = DATETIME.DATE(2008,11,25)
DATE = STARTDATE

# STEP THROUGH ALL THE DATES IN THE RANGE
WHILE (DATE <= ENDDATE):

  # CREATE THE DATE STRING FOR THE FILENAME
  DATESTRING = DATE.STRFTIME("%Y%M%D")
  PRINT DATESTRING

  # PROCESS 9, 12 AND 15 HOURS
  FOR HOUR IN [9,12,15]:
    IR087FILENAME  =  "%SIR_087_%S_%02D00.PNM-SA.DAT"  %  (PREFIX,  DATESTRING,
HOUR)
    IR108FILENAME  =  "%SIR_108_%S_%02D00.PNM-SA.DAT"  %  (PREFIX,  DATESTRING,
HOUR)
    IR120FILENAME  =  "%SIR_120_%S_%02D00.PNM-SA.DAT"  %  (PREFIX,  DATESTRING,
HOUR)

    # JUST TO KEEP TABS ON PROGRESS
    PRINT IR087FILENAME

    # TRY AND OPEN THE REQUIRED FILES, SKIP THE HOUR IF ANY FILE FAILS
    TRY:
      IR087FILE = OPEN(IR087FILENAME)
    EXCEPT:
      PRINT "PROBLEM OPENING DATAFILE", IR087FILENAME
      CONTINUE

    TRY:
      IR108FILE = OPEN(IR108FILENAME)
    EXCEPT:
      PRINT "PROBLEM OPENING DATAFILE", IR108FILENAME
      CONTINUE
    TRY:
      IR120FILE = OPEN(IR120FILENAME)
    EXCEPT:
      PRINT "PROBLEM OPENING DATAFILE", IR120FILENAME
      CONTINUE

    # WE HAVE THE FILES WE NEED
    PRINT "FOUND DATA FOR %S" % (DATESTRING)

    # CREATE THE OUTPUT FILENAME
    OUTFILENAME = "DUST_%S_%02D00.TIFF" % (DATESTRING, HOUR)

    # CHECK WE HAVEN'T ALREADY CREATED THIS FILE, SKIP IF WE HAVE
    IF OS.ACCESS(OUTFILENAME, OS.F_OK):
      PRINT "OUTPUT FILE %S ALREADY EXISTS, SKIPPING THIS DATE" % (OUTFILENAME)
      CONTINUE
    # NOW ACTUALLY READ THE FILE DATA
    IR087DATA = IR087FILE.READ()
    IR108DATA = IR108FILE.READ()
    IR120DATA = IR120FILE.READ()
```

```
# CLOSE THE IMAGE FILES, WE DON'T NEED THEM ANYMORE
IR087FILE.CLOSE()
IR108FILE.CLOSE()
IR120FILE.CLOSE()

# CONVERT RAW DATA TO  IMAGE DATA
IR087 = IMAGE.FROMSTRING("F",(1000,900),IR087DATA,"RAW","F;32NF",0,1)
IR108 = IMAGE.FROMSTRING("F",(1000,900),IR108DATA,"RAW","F;32NF",0,1)
IR120 = IMAGE.FROMSTRING("F",(1000,900),IR120DATA,"RAW","F;32NF",0,1)
# GET SIZE FROM IR087 IMAGE FILE
XSIZE = IR087.SIZE[0]
YSIZE = IR087.SIZE[1]

# PRINT SAMPLE PIXEL AS A DIAGNOSTIC
PRINT IR087.GETPIXEL((500,500))
PRINT IR108.GETPIXEL((500,500))
PRINT IR120.GETPIXEL((500,500))

# DO THE MATHS STUFF...
RPRE = IMAGEMATH.EVAL("((A-B)+4)*(255.0/6.0)",A=IR120,B=IR108)
GPRE = IMAGEMATH.EVAL("(A-B)*(255.0/15.0)",A=IR108,B=IR087)
BPRE = IMAGEMATH.EVAL("(A-261)*(255.0/29.0)",A=IR120)
# GET RAW VALUES BACK FROM THE IMAGE
RVALS = RPRE.LOAD()
GVALS = GPRE.LOAD()
BVALS = BPRE.LOAD()

# NOW WE CREATE THE FINAL OUTPUT DATA
FOR X IN RANGE(0,XSIZE):
  FOR Y IN RANGE(0,YSIZE):
    IF GVALS[X,Y] >= 0:
      GVALS[X,Y] = ((GVALS[X,Y]/255)**GAMMA)*255
    ELSE:
      GVALS[X,Y] = 0.0
        IF RVALS[X,Y] < 0:
      RVALS[X,Y] = 0
    IF GVALS[X,Y] < 0:
      GVALS[X,Y] = 0
    IF BVALS[X,Y] < 0:
      BVALS[X,Y] = 0

    IF RVALS[X,Y] > 255:
      RVALS[X,Y] = 255
    IF GVALS[X,Y] > 255:
      GVALS[X,Y] = 255
    IF BVALS[X,Y] > 255:
      BVALS[X,Y] = 255

# MORE PARANOID DIAGNOSTICS
PRINT RPRE.GETPIXEL((700,500))
PRINT GPRE.GETPIXEL((700,500))
PRINT BPRE.GETPIXEL((700,500))

# AND SOME MORE...
PRINT IMAGESTAT.STAT(RPRE.CONVERT("L")).MEDIAN
PRINT IMAGESTAT.STAT(GPRE.CONVERT("L")).MEDIAN
PRINT IMAGESTAT.STAT(BPRE.CONVERT("L")).MEDIAN

# CONVERT TO GREYSCALE CHANNELS
R = RPRE.CONVERT("L")
G = GPRE.CONVERT("L")
B = BPRE.CONVERT("L")

# COMPOSITE TO RGB IMAGE
OUTIMAGE = IMAGE.MERGE("RGB",(R,G,B))

#R.SAVE("RED.TIFF")
#G.SAVE("GREEN.TIFF")
#B.SAVE("BLUE.TIFF")

# WRITE OUT THE FILE
OUTIMAGE.SAVE(OUTFILENAME)
PRINT "WROTE OUT %S" % (OUTFILENAME)
```

Appendix 3: MSG Sources

ID	Source Name	Source Type (PRU)	Longitude	Latitude	Length (km)	Bearing (°)	Year	Month	Day	Time
507060900	Etosha	Pan	16.535	-18.765	42.0	245.6	2005	7	6	9:00
507091200	Magkadikgadi	Pan	26.061	-20.448	235.8	264.1	2005	7	9	12:00
508040900	Magkadikgadi	Pan	24.995	-20.899	81.0	220.8	2005	8	4	9:00
508260900	Magkadikgadi	Pan	25.988	-20.551	266.4	178.2	2005	8	26	9:00
508261500	Etosha	Pan	16.630	-18.606	76.2	252.8	2005	8	26	15:00
509131200	Duwisib River	River	16.299	-25.460	124.2	226.4	2005	9	13	12:00
509131200	Helmering River	River	16.635	-25.917	126.7	216.8	2005	9	13	12:00
509131200	Koichab	River	15.859	-26.253	68.8	226.4	2005	9	13	12:00
509140900	Etosha	Pan	16.029	-18.987	99.7	244.6	2005	9	14	9:00
509140900	Etosha	Pan	16.653	-18.640	204.6	259.3	2005	9	14	9:00
509140900	Magkadikgadi	Pan	25.907	-20.480	76.1	243.6	2005	9	14	9:00
509140900	Magkadikgadi	Pan	26.076	-21.089	94.0	266.7	2005	9	14	9:00
509151200	Etosha	Pan	16.009	-19.027	170.4	242.7	2005	9	15	12:00
509191200	Orawab	River	14.481	-21.387	65.2	285.9	2005	9	19	12:00
509270900	Lake Ngoni	Lake Margin	22.348	-20.196	197.0	0.4	2005	9	27	9:00
509271500	Gui uin	Marshes / Vlei	13.008	-19.377	87.0	1.8	2005	9	27	15:00
509290900	Magkadikgadi	Pan	26.034	-20.401	244.8	256.9	2005	9	29	9:00
509300900	Swartput se Pan	Pan	19.295	-26.517	296.8	228.2	2005	9	30	9:00
510031200	Quoxo River	River	24.326	-23.147	41.4	153.2	2005	10	3	12:00
510060900	Magkadikgadi	Pan	25.981	-20.477	208.2	256.8	2005	10	6	9:00
510060900	Magkadikgadi	Pan	25.115	-20.712	310.8	224.1	2005	10	6	9:00
510070900	Linyandi Marshlands	Marshes / Vlei	24.056	-18.110	261.8	220.1	2005	10	7	9:00
510070900	Magkadikgadi	Pan	25.427	-20.387	188.4	230.6	2005	10	7	9:00
510070900	Magkadikgadi	Pan	25.978	-20.553	128.4	228.2	2005	10	7	9:00
510100900	Magkadikgadi	Pan	25.524	-20.332	65.6	225.4	2005	10	10	9:00
510100900	Magkadikgadi	Pan	25.912	-20.534	65.5	245.0	2005	10	10	9:00
510150900	Etosha	Pan	16.633	-18.638	141.0	251.6	2005	10	15	9:00
510150900	Etosha	Pan	16.359	-18.535	66.3	242.7	2005	10	15	9:00
510150900	Etosha	Pan	16.651	-18.727	80.6	246.5	2005	10	15	9:00
511121500	Etosha	Pan	16.496	-18.630	69.1	239.0	2005	11	12	15:00
511131500	Etosha	Pan	16.203	-18.768	59.9	241.0	2005	11	13	15:00
612021200	Bloemfontein	Dam Margin / Agricultural	26.376	-29.045	61.8	256.4	2006	12	2	12:00
612031200	Gannapan / Bloemhofdam	Pan	25.720	-27.943	402.0	99.3	2006	12	3	12:00
612160900	Gannapan / Bloemhofdam	Pan	25.732	-27.970	120.7	143.0	2006	12	16	9:00
705191500	Hakskeenpan	Pan	20.199	-26.823	138.6	140.8	2007	5	19	15:00
705191500	Kiriis Ost Pan	Pan	19.658	-26.336	104.4	131.4	2007	5	19	15:00
706050900	Etosha	Pan	16.143	-18.982	40.2	133.3	2007	6	5	9:00
706050900	Etosha	Pan	16.391	-18.578	106.0	117.3	2007	6	5	9:00
706101200	Etosha	Pan	16.630	-18.668	109.6	246.5	2007	6	10	12:00
706230900	Etosha	Pan	16.696	-18.671	124.8	247.8	2007	6	23	9:00
706251200	Grundorner	River	17.907	-25.413	137.5	130.3	2007	6	25	12:00
706251200	Hakskeenpan	Pan	20.213	-26.766	179.7	139.7	2007	6	25	12:00
706251200	Konkiep River	River	16.747	-25.594	163.3	145.3	2007	6	25	12:00
706251200	Noenieput	Pan	20.165	-27.551	102.1	153.4	2007	6	25	12:00
706271200	Etosha	Pan	16.337	-18.828	120.9	252.0	2007	6	27	12:00
707020900	Magkadikgadi	Pan	26.028	-20.431	237.9	265.4	2007	7	2	9:00
707020900	Magkadikgadi	Pan	26.179	-20.999	268.2	259.0	2007	7	2	9:00
708080900	Magkadikgadi	Pan	26.112	-21.113	187.2	261.0	2007	8	8	9:00
708250900	Etosha	Pan	16.245	-18.804	48.7	241.1	2007	8	25	9:00
709110900	Magkadikgadi	Pan	25.931	-20.435	359.9	236.7	2007	9	11	9:00
709111200	Koemkoep Pan	Pan	19.600	-25.145	324.5	145.1	2007	9	11	12:00
709111200	Skemerhoek Pan	Pan	19.820	-24.926	274.7	148.5	2007	9	11	12:00
709180900	Etosha	Pan	16.598	-18.867	210.1	231.3	2007	9	18	9:00
709180900	Etosha	Pan	16.176	-18.845	46.7	246.7	2007	9	18	9:00
709211500	Magkadikgadi	Pan	25.528	-20.390	152.1	257.7	2007	9	21	15:00
709211500	Magkadikgadi	Pan	25.046	-20.784	76.5	228.0	2007	9	21	15:00
709250900	Magkadikgadi	Pan	25.046	-20.916	121.3	255.2	2007	9	25	9:00
710081500	Gui uin	Marshes / Vlei	13.011	-19.376	172.2	343.5	2007	10	8	15:00
711131200	Magkadikgadi	Pan	25.006	-20.693	241.4	232.6	2007	11	13	12:00
711131200	Magkadikgadi	Pan	25.106	-20.913	85.4	233.3	2007	11	13	12:00
711141500	Magkadikgadi	Pan	25.387	-20.856	131.3	245.2	2007	11	14	15:00
711291500	Marcel Pan	Pan	19.463	-27.166	111.6	120.5	2007	11	29	15:00
711291500	Samahaling Pan	Pan	19.580	-27.057	117.3	130.7	2007	11	29	15:00
802120900	Salztal Pan	Pan	19.441	-26.575	218.0	227.3	2008	2	12	9:00
805121200	Etosha	Pan	16.646	-18.534	131.1	245.2	2008	5	12	12:00

Appendix 4: MODIS Sources

ID	Source Name	Source Type (PRU)	Longitude	Latitude	Length (km)	Bearing (°)	Year	Month	Day	Platform	Julian Day
5062301	Gemsbokbrak	Pan	20.485	-27.582	49.1	188.0	2005	6	23	Terra	2005174
5062301	Gemsbokhoorn	Pan	20.504	-27.480	40.9	183.7	2005	6	23	Terra	2005174
5062301	Klein - Aarpan	Pan	20.728	-27.398	59.1	190.2	2005	6	23	Terra	2005174
5062301	Koeipan	Pan	20.874	-27.430	48.7	188.5	2005	6	23	Terra	2005174
5062301	Kuubmaansvlie	Pan	19.218	-26.362	43.1	167.0	2005	6	23	Terra	2005174
5062301	Morgenzon Pan	Pan	19.341	-26.195	24.8	170.5	2005	6	23	Terra	2005174
5062301	Salt Pan	Pan	18.975	-25.939	62.0	171.0	2005	6	23	Terra	2005174
5062301	Samahaling Pan	Pan	19.610	-27.060	51.2	167.8	2005	6	23	Terra	2005174
5062301	Saulstraatpan	Pan	20.100	-27.013	40.2	176.7	2005	6	23	Terra	2005174
5062301	Swaartput se Pan	Pan	19.291	-26.514	49.0	173.4	2005	6	23	Terra	2005174
5062301	Vrysoutpan	Pan	20.829	-27.338	24.8	191.4	2005	6	23	Terra	2005174
5062301	Donavan se Pan	Pan	20.277	-27.250	78.3	185.0	2005	6	23	Terra	2005174
5062301	Groot - Witpan	Pan	20.750	-27.743	68.0	188.2	2005	6	23	Terra	2005174
5062301	Hakskeenpan	Pan	20.144	-26.728	36.4	171.7	2005	6	23	Terra	2005174
5062301	Hakskeenpan	Pan	20.185	-26.842	43.1	176.5	2005	6	23	Terra	2005174
5070701	Huab River	River	13.521	-20.883	138.9	229.9	2005	7	7	Terra	2005188
5070701	Conception Bay Pan	Pan	14.531	-24.199	138.9	248.6	2005	7	7	Terra	2005188
5070701	White Lady Salt Pan	Pan	13.987	-21.777	90.9	245.5	2005	7	7	Terra	2005188
5070901	Unknown 1	unknown	13.028	-19.865	77.4	234.2	2005	7	9	Terra	2005190
5070901	Unknown 2	River	14.204	-21.814	65.3	238.9	2005	7	9	Terra	2005190
5070901	Unknown 9	unknown (river)	14.547	-22.782	37.9	228.7	2005	7	9	Terra	2005190
5070901	Huab Pan 2	Pan	13.427	-20.858	86.2	231.9	2005	7	9	Terra	2005190
5070901	Langer Werner	River	14.222	-21.906	42.5	220.6	2005	7	9	Terra	2005190
5070901	Toscanini Pan	Pan	13.403	-20.819	88.8	235.5	2005	7	9	Terra	2005190
5070901	Ugab Pan 5	Pan	13.871	-21.524	88.3	233.6	2005	7	9	Terra	2005190
5070901	Rocky Point	Pan	12.478	-18.955	44.9	236.3	2005	7	9	Terra	2005190
5070901	Sechomib	River	12.302	-18.607	65.2	235.0	2005	7	9	Terra	2005190
5070901	False Cape Fria	Pan	12.136	-18.547	48.6	223.4	2005	7	9	Terra	2005190
5070901	Hoanib	River	12.766	-19.466	24.6	237.5	2005	7	9	Terra	2005190
5070901	Torra Bay Pan	Pan	13.267	-20.382	48.2	226.0	2005	7	9	Terra	2005190
5070901	Khumib	River	12.455	-18.836	73.7	235.2	2005	7	9	Terra	2005190
5070901	Terrace Bay 2	Pan	13.070	-20.071	23.1	225.8	2005	7	9	Terra	2005190
5070901	Hoanib Pan	Pan	12.804	-19.559	59.5	235.0	2005	7	9	Terra	2005190
5070901	Hoanib Pan	Pan	12.846	-19.599	30.4	237.9	2005	7	9	Terra	2005190
5070901	Huab River	River	13.740	-20.816	32.3	228.7	2005	7	9	Terra	2005190
5070901	Koigab Pan 1	Pan	13.332	-20.568	45.3	223.8	2005	7	9	Terra	2005190
5070901	Kuiseb River	River	15.132	-23.624	21.9	216.8	2005	7	9	Terra	2005190
5070901	Kuiseb River Delta	Other - Delta	14.574	-23.130	62.3	219.6	2005	7	9	Terra	2005190
5070901	Omaruru River	River	14.495	-21.903	76.2	224.4	2005	7	9	Terra	2005190
5070901	Rocky Point	Pan	12.495	-18.993	55.1	232.8	2005	7	9	Terra	2005190
5070901	Ugab River	River	13.658	-21.173	66.3	209.5	2005	7	9	Terra	2005190
5111401	Tsauchab River / Sossusvlei	River/Pan	15.316	-24.730	100.7	245.9	2005	11	14	Terra	2005318
6042602	Unknown 18	unknown	15.960	-28.129	68.4	230.3	2006	4	26	Aqua	2006116
6062602	Makgadikgadi Pan	Pan	25.187	-20.673	171.2	238.2	2006	6	26	Aqua	2006177
6062602	Makgadikgadi Pan	Pan	25.390	-20.911	184.8	240.1	2006	6	26	Aqua	2006177
6071302	Makgadikgadi Pan	Pan	25.029	-20.916	126.5	212.5	2006	7	13	Aqua	2006194
6071602	Makgadikgadi Pan	Pan	25.088	-20.915	122.4	222.0	2006	7	16	Aqua	2006197
6082702	Makgadikgadi Pan	Pan	24.973	-20.825	153.7	266.8	2006	8	27	Aqua	2006208
6110602	Oranjemund	Pan / Mine	16.441	-28.594	60.8	223.5	2006	11	6	Aqua	2006310
6052201	Unknown 12	River	14.602	-22.783	47.7	263.8	2006	5	22	Terra	2006142
6052201	Hoarusib	River	12.597	-19.055	77.4	242.9	2006	5	22	Terra	2006142
6052201	Huab Pan 4	Pan	13.435	-20.879	32.9	259.2	2006	5	22	Terra	2006142
6052201	Ugab Pan 4	Pan	13.852	-21.475	35.8	222.7	2006	5	22	Terra	2006142
6052201	Rock Bay	River	14.483	-22.469	23.1	259.3	2006	5	22	Terra	2006142
6052201	Ugab Pan 3	Pan	13.799	-21.392	39.4	218.5	2006	5	22	Terra	2006142
6052201	Etosha	Pan	16.004	-18.794	17.4	238.4	2006	5	22	Terra	2006142
6052201	Gui uin	Other - marsh / vlie	13.035	-19.389	62.7	264.4	2006	5	22	Terra	2006142
6052201	Hunkab Pan	Pan	12.977	-19.862	48.2	243.8	2006	5	22	Terra	2006142
6052201	Uniab River	River	13.197	-20.195	69.1	249.3	2006	5	22	Terra	2006142
6052401	Isirub River	River	15.207	-26.806	47.2	231.5	2006	5	24	Terra	2006144
6062001	Unknown 7	unknown (river)	14.538	-22.744	122.9	260.6	2006	6	20	Terra	2006171
6062001	Unknown 14	River	14.695	-22.168	29.7	224.4	2006	6	20	Terra	2006171
6062001	Onanzi Pan	Pan	15.550	-18.403	73.3	222.3	2006	6	20	Terra	2006171
6063001	Unknown 3	River	14.357	-22.226	34.3	223.8	2006	6	30	Terra	2006181
6063001	Unknown 5	River	14.512	-22.247	69.1	224.5	2006	6	30	Terra	2006181
6063001	Unknown 15	River	14.522	-22.565	17.9	229.3	2006	6	30	Terra	2006181
6063001	Unknown 17	Pan	14.997	-26.293	144.8	231.8	2006	6	30	Terra	2006181

Appendix 4: MODIS Sources (cont)

ID	Source Name	Source Type (PRU)	Longitude	Latitude	Length (km)	Bearing (°)	Year	Month	Day	Platform	Julian Day
6063001	Unknown River	River	14.001	-21.652	56.5	225.9	2006	6	30	Terra	2006181
6063001	Hunkab River	River	13.074	-19.789	106.6	230.2	2006	6	30	Terra	2006181
6063001	Ilhea Point	Pan	14.475	-23.487	53.1	230.4	2006	6	30	Terra	2006181
6063001	Isirub River	River	15.228	-26.961	132.6	219.0	2006	6	30	Terra	2006181
6063001	Swakop River	River	14.534	-22.681	52.9	233.2	2006	6	30	Terra	2006181
6063001	Gui uin	Other - marsh / vlie	12.993	-19.393	98.2	242.4	2006	6	30	Terra	2006181
6063001	Ugab Pan 1	Pan	13.715	-21.271	51.4	223.5	2006	6	30	Terra	2006181
6063001	Ugab River	River	13.648	-21.182	48.7	231.1	2006	6	30	Terra	2006181
6063001	Kuiseb River	River	14.853	-23.203	88.6	226.0	2006	6	30	Terra	2006181
6063001	Uniab River	River	13.200	-20.186	34.2	235.9	2006	6	30	Terra	2006181
6063001	Conception Bay Pan	Pan	14.507	-24.062	82.8	236.8	2006	6	30	Terra	2006181
6063001	Huab River	River	13.526	-20.893	106.5	236.2	2006	6	30	Terra	2006181
6063001	Kuiseb River Delta	Other - Delta	14.483	-23.163	74.6	232.4	2006	6	30	Terra	2006181
6063001	Meob Bay Pan	Pan	14.668	-24.553	105.3	225.9	2006	6	30	Terra	2006181
6063001	Omaruru River	River	14.312	-22.065	82.6	222.0	2006	6	30	Terra	2006181
6070101	Kongapan	Pan	20.703	-27.484	38.5	177.7	2006	7	1	Terra	2006182
6070101	Koppieskraalpan	Pan	20.285	-26.995	48.1	178.6	2006	7	1	Terra	2006182
6070101	Meob Bay Pan	Pan	14.622	-24.560	36.3	208.9	2006	7	1	Terra	2006182
6070101	Omaruru River	River	14.501	-21.900	127.1	224.5	2006	7	1	Terra	2006182
6070101	Kuiseb River Delta	Other - Delta	14.476	-23.200	184.9	226.8	2006	7	1	Terra	2006182
6070101	Cape Cross Pan	Pan	13.977	-21.693	56.8	212.4	2006	7	1	Terra	2006182
6070101	Conception Bay Pan	Pan	14.495	-24.088	103.2	214.7	2006	7	1	Terra	2006182
6070101	Donavan se Pan	Pan	20.277	-27.256	46.7	179.5	2006	7	1	Terra	2006182
6070101	Groot - Witpan	Pan	20.750	-27.749	35.5	176.2	2006	7	1	Terra	2006182
6070101	Hakskeenpan	Pan	20.190	-26.842	49.0	177.7	2006	7	1	Terra	2006182
6070101	Meob Bay Pan	Pan	14.718	-24.662	75.1	208.1	2006	7	1	Terra	2006182
7051902	Fish river	River	17.734	-25.525	87.2	115.7	2007	5	19	Aqua	2007139
7051902	Grasheuwel Pan	Pan	18.826	-26.091	37.1	110.0	2007	5	19	Aqua	2007139
7051902	Grundorner	River	17.940	-25.042	81.8	108.2	2007	5	19	Aqua	2007139
7051902	Haseweb River	River	16.740	-25.152	39.7	118.3	2007	5	19	Aqua	2007139
7051902	Kanibes River	River / Perennial Pan	17.707	-25.765	101.0	118.8	2007	5	19	Aqua	2007139
7051902	Konkiep	River	16.744	-25.533	47.1	107.9	2007	5	19	Aqua	2007139
7051902	Gamanas Pan	Pan	17.722	-26.067	42.4	119.7	2007	5	19	Aqua	2007139
7051902	Gamanas Pan	Pan	17.773	-25.981	179.0	129.4	2007	5	19	Aqua	2007139
7051902	Groot - Witpan	Pan	20.751	-27.736	34.4	128.5	2007	5	19	Aqua	2007139
7051902	Hakskeenpan	Pan	20.241	-26.853	99.9	124.1	2007	5	19	Aqua	2007139
7070402	Etosha	Pan	16.168	-18.885	159.3	252.4	2007	7	4	Aqua	2007185
7070402	Hoanib	River	13.802	-19.232	152.3	237.0	2007	7	4	Aqua	2007185
7071302	Ombonde	River	14.123	-19.374	129.3	232.5	2007	7	13	Aqua	2007194
7071302	Etosha	Pan	16.052	-18.849	144.4	250.6	2007	7	13	Aqua	2007194
7071302	Hoanib	River	13.742	-19.156	145.1	235.5	2007	7	13	Aqua	2007194
7041401	Makgadikgadi Pan	Pan	25.996	-20.497	183.8	229.6	2007	4	14	Terra	2007104
7050601	Unknown 13	River	14.617	-22.530	46.7	233.6	2007	5	6	Terra	2007126
7050601	Etosha	Pan	16.012	-18.820	155.1	251.2	2007	5	6	Terra	2007126
7050601	Hoanib Pan	Pan	12.805	-19.552	114.4	226.8	2007	5	6	Terra	2007126
7050601	Huab River	River	13.515	-20.897	50.4	239.7	2007	5	6	Terra	2007126
7050601	Hunkab Pan	Pan	12.988	-19.869	129.1	222.7	2007	5	6	Terra	2007126
7050601	Omaruru River	River	14.316	-22.063	31.9	232.2	2007	5	6	Terra	2007126
7050701	Huab River	River	13.539	-20.887	81.4	222.6	2007	5	7	Terra	2007127
7050701	Koigab Pan 1	Pan	13.316	-20.382	97.8	222.5	2007	5	7	Terra	2007127
7050701	Kuiseb River Delta	Other - Delta	14.519	-23.112	68.3	217.3	2007	5	7	Terra	2007127
7050701	Swakop River	River	14.566	-22.686	28.0	229.3	2007	5	7	Terra	2007127
7050701	Ugab Pan 1	Pan	13.693	-21.249	17.6	219.7	2007	5	7	Terra	2007127
7050701	Ugab River	River	13.664	-21.168	18.2	228.6	2007	5	7	Terra	2007127
7051101	18 Latitude Pan	Pan	11.824	-17.989	20.2	248.0	2007	5	11	Terra	2007127
7051101	Huab Pan 3	Pan	13.476	-20.860	107.8	244.6	2007	5	11	Terra	2007127
7051101	Cape Fria Pan	Pan	11.963	-18.224	24.9	244.3	2007	5	11	Terra	2007127
7051101	Conception Bay Pan	Pan	14.487	-23.942	30.5	248.4	2007	5	11	Terra	2007127
7051101	False Cape Fria	Pan	12.171	-18.525	76.7	244.7	2007	5	11	Terra	2007127
7051101	Hoanib Pan	Pan	12.795	-19.519	40.4	242.6	2007	5	11	Terra	2007127
7051101	Hunkab Pan	Pan	12.974	-19.854	80.1	235.9	2007	5	11	Terra	2007127
7051101	Ilhea Point	Pan	14.458	-23.462	25.9	255.5	2007	5	11	Terra	2007127
7051101	Koigab Pan 1	Pan	13.327	-20.564	69.8	238.9	2007	5	11	Terra	2007127
7051101	Meob Bay Pan	Pan	14.668	-24.553	23.1	257.6	2007	5	11	Terra	2007127
7051101	Makgadikgadi Pan	Pan	25.861	-20.735	221.5	261.4	2007	5	11	Terra	2007131
7051101	Makgadikgadi Pan	Pan	25.951	-20.355	185.5	265.5	2007	5	11	Terra	2007131
7051201	Unknown 4	unknown (poss river)	14.423	-22.325	44.4	216.5	2007	5	12	Terra	2007132
7051201	Unknown 10	unknown (river)	14.554	-22.801	62.6	215.5	2007	5	12	Terra	2007132
7051201	White Lady Salt Pan	Pan	13.970	-21.773	34.0	226.4	2007	5	12	Terra	2007132
7051201	Cape Cross Pan	Pan	13.949	-21.671	30.5	225.1	2007	5	12	Terra	2007132

Appendix 4: MODIS Sources (cont)

ID	Source Name	Source Type (PRU)	Longitude	Latitude	Length (km)	Bearing (°)	Year	Month	Day	Platform	Julian Day
7051201	Kuiseb River	River	14.821	-23.207	66.0	220.6	2007	5	12	Terra	2007132
7051201	Kuiseb River	River	14.866	-23.358	94.5	220.1	2007	5	12	Terra	2007132
7051201	Omaruru River	River	14.314	-22.066	65.9	218.3	2007	5	12	Terra	2007132
7051201	Rock Bay	River	14.469	-22.463	20.8	212.3	2007	5	12	Terra	2007132
7051201	Terrace Bay 2	Pan	13.109	-20.114	38.0	212.5	2007	5	12	Terra	2007132
7051201	Uniab River	River	13.219	-20.255	32.8	204.4	2007	5	12	Terra	2007132
7052201	Unknown 16	Pan	14.966	-26.156	42.3	269.9	2007	5	22	Terra	2007142
7052201	Tsondab River/Pan	river/pan	15.438	-24.001	135.3	266.1	2007	5	22	Terra	2007142
7052201	Conception Bay Pan	Pan	14.536	-24.165	49.1	268.1	2007	5	22	Terra	2007142
7052201	Tsauchab River / Sossusvlei	River/Pan	15.325	-24.724	115.7	253.5	2007	5	22	Terra	2007142
7052301	Kuiseb River Delta	Other - Delta	14.513	-23.307	57.4	218.0	2007	5	23	Terra	2007143
7060501	Makgadikgadi Pan	Pan	25.275	-20.709	65.2	215.7	2007	6	5	Terra	2007156
7061401	Makgadikgadi Pan	Pan	25.475	-20.587	148.1	184.1	2007	6	14	Terra	2007165
7061401	Makgadikgadi Pan	Pan	25.610	-20.626	134.6	190.6	2007	6	14	Terra	2007165
7061701	Kuiseb River Delta	Other - Delta	14.522	-23.109	101.4	232.9	2007	6	17	Terra	2007168
7070201	Tumas River	River	14.603	-22.894	48.6	260.2	2007	7	2	Terra	2007183
7070201	Conception Bay Pan	Pan	14.493	-23.986	55.6	265.2	2007	7	2	Terra	2007183
7070201	Kuiseb River Delta	Other - Delta	14.405	-23.002	48.3	249.5	2007	7	2	Terra	2007183
7070201	Kuiseb River Delta	Other - Delta	14.495	-23.094	73.4	251.9	2007	7	2	Terra	2007183
7070201	Omaruru River	River	14.319	-22.055	85.4	223.7	2007	7	2	Terra	2007183
7070201	Tsauchab River / Sossusvlei	River/Pan	15.348	-24.714	82.5	256.1	2007	7	2	Terra	2007183
7070201	Makgadikgadi Pan	Pan	26.099	-20.446	249.9	259.0	2007	7	2	Terra	2007183
7070201	Makgadikgadi Pan	Pan	26.170	-21.083	211.1	265.2	2007	7	2	Terra	2007183
7070301	Conception Bay Pan	Pan	14.526	-24.148	58.1	244.0	2007	7	3	Terra	2007184
7070301	Kuiseb River	River	14.623	-23.168	83.8	227.4	2007	7	3	Terra	2007184
7070301	Meob Bay Pan	Pan	14.655	-24.547	38.6	244.4	2007	7	3	Terra	2007184
7071401	18 Latitude Pan	Pan	11.874	-18.127	47.1	240.0	2007	7	14	Terra	2007195
7071401	Cape Fria Pan	Pan	11.966	-18.221	109.0	233.0	2007	7	14	Terra	2007195
7071401	Cape Fria Pan	Pan	12.035	-18.444	72.4	233.0	2007	7	14	Terra	2007195
7071401	Hoanib Pan	Pan	12.803	-19.547	65.7	236.3	2007	7	14	Terra	2007195
7071401	Hunkab Pan	Pan	13.020	-19.944	106.4	224.7	2007	7	14	Terra	2007195
7071401	Khumib	River	12.471	-18.839	62.4	237.8	2007	7	14	Terra	2007195
7071401	Swakop River	River	14.544	-22.682	54.0	239.7	2007	7	14	Terra	2007195
7071401	Terrace Bay 2	Pan	13.057	-20.058	87.7	218.2	2007	7	14	Terra	2007195
7071401	Uniab River	River	13.205	-20.189	112.2	225.2	2007	7	14	Terra	2007195
7071501	Cape Cross Pan	Pan	13.986	-21.720	21.2	226.1	2007	7	15	Terra	2007196
7071501	Conception Bay Pan	Pan	14.489	-24.057	49.2	229.9	2007	7	15	Terra	2007196
7071501	Huab River	River	13.629	-20.868	91.8	234.7	2007	7	15	Terra	2007196
7071501	Hunkab Pan	Pan	12.982	-19.874	75.6	222.1	2007	7	15	Terra	2007196
7071501	Koigab Pan 1	Pan	13.307	-20.538	95.3	227.2	2007	7	15	Terra	2007196
7071501	Kuiseb River Delta	Other - Delta	14.476	-23.078	88.1	230.5	2007	7	15	Terra	2007196
7071501	Omaruru River	River	14.494	-21.901	87.1	223.8	2007	7	15	Terra	2007196
7071501	Ugab River	River	13.640	-21.175	79.9	224.9	2007	7	15	Terra	2007196
7071501	Uniab River	River	13.191	-20.187	116.8	223.5	2007	7	15	Terra	2007196
7073101	Huab Pan	Pan	13.578	-20.938	46.1	234.2	2007	7	31	Terra	2007212
7073101	Huab Pan 3	Pan	13.469	-20.856	16.8	246.9	2007	7	31	Terra	2007212
7073101	Omaruru River	River	14.512	-21.900	93.9	220.2	2007	7	31	Terra	2007212
7073101	Ugab Pan 1	Pan	13.704	-21.257	31.6	220.8	2007	7	31	Terra	2007212
7073101	Ugab River	River	13.635	-21.185	10.2	223.5	2007	7	31	Terra	2007212
7073101	Uniab River	River	13.203	-20.197	30.5	222.4	2007	7	31	Terra	2007212
7080701	Tsondab River/Pan	river/pan	15.451	-23.997	62.7	268.3	2007	8	7	Terra	2007219
7080801	Orange River	River	16.492	-28.641	60.4	215.3	2007	8	8	Terra	2007220
7080801	mine tailing	Anthropogenic	16.313	-28.509	105.3	213.2	2007	8	8	Terra	2007220
7080801	Gui uin	Other - marsh / vlie	13.021	-19.395	132.9	211.9	2007	8	8	Terra	2007220
7080801	Isirub River	River	15.268	-27.021	109.5	213.2	2007	8	8	Terra	2007220
7080801	mine tailing	Anthropogenic	16.149	-28.340	97.9	222.6	2007	8	8	Terra	2007220
7080801	Omaruru River	River	14.312	-22.080	123.6	207.3	2007	8	8	Terra	2007220
7080801	Ugab Pan 3	Pan	13.794	-21.383	107.2	209.7	2007	8	8	Terra	2007220
7080801	Makgadikgadi Pan	Pan	26.112	-21.046	161.7	256.9	2007	8	8	Terra	2007220
7091401	Khan River	near river	15.028	-22.457	125.6	233.7	2007	9	14	Terra	2007257
7091801	Etosha	Pan	16.047	-18.806	98.8	238.2	2007	9	18	Terra	2007261
7091801	Etosha	Pan	16.636	-18.877	161.7	237.0	2007	9	18	Terra	2007261
7102001	Etosha	Pan	16.118	-18.990	140.0	259.6	2007	10	20	Terra	2007293
7102501	Makgadikgadi Pan	Pan	26.015	-20.434	199.2	240.0	2007	10	25	Terra	2007298
7111301	Makgadikgadi Pan	Pan	25.635	-20.534	326.5	243.0	2007	11	13	Terra	2007317
7010101	Etosha	Pan	16.031	-18.683	100.3	250.7	2007	1	1	Terra	2007001
7010101	Etosha	Pan	16.079	-18.912	92.0	250.0	2007	1	1	Terra	2007001
7050601	Unknown 8	unknown (river)	14.544	-22.729	77.5	232.0	2007	5	6	Terra	2007126
8062902	Huab River	River	13.480	-20.897	56.9	250.7	2008	6	29	Aqua	2008181
8081002	Etosha	Pan	15.975	-18.822	150.5	249.9	2008	8	10	Aqua	2008223

Appendix 4: MODIS Sources (cont)

ID	Source Name	Source Type (PRU)	Longitude	Latitude	Length (km)	Bearing (°)	Year	Month	Day	Platform	Julian Day
8040401	False Cape Fria	Pan	12.159	-18.554	38.4	234.0	2008	4	4	Terra	2008095
8040401	Hoanib Pan	Pan	12.845	-19.608	50.4	223.9	2008	4	4	Terra	2008095
8040401	Sechomib	River	12.277	-18.693	46.7	237.0	2008	4	4	Terra	2008095
8040401	Uniab River	River	13.282	-20.173	96.0	226.4	2008	4	4	Terra	2008095
8042101	Kuiseb River Delta	Other - Delta	14.426	-23.070	38.7	244.2	2008	4	21	Terra	2008112
8042101	Kuiseb River Delta	Other - Delta	14.496	-23.111	60.1	241.4	2008	4	21	Terra	2008112
8042101	Omaruru River	River	14.265	-22.098	77.6	227.5	2008	4	21	Terra	2008112
8042101	Tsauchab River / Sossusvlei	River/Pan	15.336	-24.727	90.6	255.8	2008	4	21	Terra	2008112
8042201	Gui uin	Other - marsh / vlie	12.963	-19.392	130.8	217.4	2008	4	22	Terra	2008113
8042201	Huab Pan	Pan	13.579	-20.943	75.8	226.0	2008	4	22	Terra	2008113
8042201	Huab River	River	13.458	-20.912	31.9	246.5	2008	4	22	Terra	2008113
8042201	Hunkab River	River	13.136	-19.754	94.8	219.3	2008	4	22	Terra	2008113
8042201	Khumib	River	12.503	-18.818	74.5	229.2	2008	4	22	Terra	2008113
8042201	Kuiseb River Delta	Other - Delta	14.538	-23.119	174.8	217.2	2008	4	22	Terra	2008113
8042201	Omaruru River	River	14.488	-21.902	162.0	212.7	2008	4	22	Terra	2008113
8042201	Terrace Bay 2	Pan	13.079	-20.078	47.0	219.2	2008	4	22	Terra	2008113
8042201	Torra Bay Pan	Pan	13.261	-20.414	55.5	218.4	2008	4	22	Terra	2008113
8042201	Ugab Pan 1	Pan	13.706	-21.250	184.9	209.7	2008	4	22	Terra	2008113
8042201	Uniab River	River	13.246	-20.220	87.7	225.7	2008	4	22	Terra	2008113
8051901	Makgadikgadi Pan	Pan	25.803	-20.956	260.5	243.5	2008	5	19	Terra	2008139
8051901	Makgadikgadi Pan	Pan	26.176	-21.142	245.4	252.8	2008	5	19	Terra	2008139
8061001	Makgadikgadi Pan	Pan	25.063	-20.878	91.3	235.6	2008	6	10	Terra	2008161
8061001	Makgadikgadi Pan	Pan	24.882	-21.194	109.2	251.3	2008	6	10	Terra	2008161
8061601	Kuiseb River Delta	Other - Delta	14.473	-23.151	89.0	230.8	2008	6	16	Terra	2008168
8061901	Makgadikgadi Pan	Pan	24.938	-21.090	86.8	244.7	2008	6	19	Terra	2008170
8061901	Makgadikgadi Pan	Pan	25.064	-20.924	111.1	251.6	2008	6	19	Terra	2008170
8071801	Makgadikgadi Pan	Pan	24.949	-21.116	85.9	251.3	2008	7	18	Terra	2008199
8071801	Makgadikgadi Pan	Pan	25.070	-20.904	102.9	260.0	2008	7	18	Terra	2008199
8071801	Makgadikgadi Pan	Pan	26.186	-21.109	97.3	267.7	2008	7	18	Terra	2008199
8080501	Etosha	Pan	16.036	-18.964	64.5	249.0	2008	8	5	Terra	2008218
8080501	Makgadikgadi Pan	Pan	25.055	-20.869	68.7	262.1	2008	8	5	Terra	2008217
8080501	Makgadikgadi Pan	Pan	26.169	-21.129	173.9	270.9	2008	8	5	Terra	2008217
8080901	Kuiseb River	River	14.920	-23.253	131.7	267.1	2008	8	9	Terra	2008222
8080901	Kuiseb River	River	14.953	-23.473	133.8	269.9	2008	8	9	Terra	2008222
8081001	Unknown 11	unknown river	14.572	-22.789	98.8	241.2	2008	8	10	Terra	2008223
8081001	Cape Cross Pan	Pan	13.961	-21.683	64.5	250.7	2008	8	10	Terra	2008223
8081001	Torra Bay Pan	Pan	13.316	-20.548	113.6	239.3	2008	8	10	Terra	2008223
8081001	Hunkab Pan	Pan	12.976	-19.871	126.9	236.9	2008	8	10	Terra	2008223
8081001	Huab River	River	13.499	-20.896	155.6	246.0	2008	8	10	Terra	2008223
8081001	Ugab Pan 1	Pan	13.684	-21.235	82.4	225.7	2008	8	10	Terra	2008223
8081001	Uniab River	River	13.195	-20.199	118.2	236.0	2008	8	10	Terra	2008223
8081101	Unknown 6	unknown (river)	14.538	-22.716	23.7	228.1	2008	8	11	Terra	2008224
8081101	Conception Bay Pan	Pan	14.497	-24.084	70.0	232.7	2008	8	11	Terra	2008224
8081101	Kuiseb River	River	14.796	-23.342	71.3	227.8	2008	8	11	Terra	2008224
8081101	Kuiseb River	River	14.866	-23.351	92.0	229.5	2008	8	11	Terra	2008224
8081101	Mcob Bay Pan	Pan	14.661	-24.593	29.7	229.8	2008	8	11	Terra	2008224
8081101	Omaruru River	River	14.270	-22.099	26.0	218.6	2008	8	11	Terra	2008224
8081101	Tumas River	River	14.688	-22.908	91.5	230.5	2008	8	11	Terra	2008224
8081201	Makgadikgadi Pan	Pan	24.835	-21.239	115.8	245.7	2008	8	12	Terra	2008224
8081201	Makgadikgadi Pan	Pan	25.009	-20.939	74.7	251.1	2008	8	12	Terra	2008224
8100701	Makgadikgadi Pan	Pan	25.242	-20.679	224.2	239.0	2008	10	7	Terra	2008280

Appendix 5: Platform specification for MSG

Spectral channel characteristics of SEVIRI in terms of central, minimum and maximum wavelength of the channels and the main application areas of each channel (http://www.eumetsat.int). Spatial resolution is 3 km for channels 1 to 11 and 1.67 km for channel 12.

Channel No.	Spectral Band (μm)	Characteristics of Spectral Band (μm)			Main observational application
		Centre	*Min*	*Max*	
1	VIS0.6	0.635	0.56	0.71	Surface, clouds, wind fields
2	VIS0.8	0.81	0.74	0.88	Surface, clouds, wind fields
3	NIR1.6	1.64	1.50	1.78	Surface, cloud phase
4	IR3.9	3.90	3.48	4.36	Surface, clouds, wind fields
5	WV6.2	6.25	5.35	7.15	Water vapour, high level clouds, atmospheric instability
6	WV7.3	7.35	6.85	7.85	Water vapour, atmospheric instability
7	IR8.7	8.70	8.30	9.1	Surface, clouds, atmospheric instability
8	IR9.7	9.66	9.38	9.94	Ozone
9	IR10.8	10.80	9.80	11.80	Surface, clouds, wind fields, atmospheric instability
10	IR12.0	12.00	11.00	13.00	Surface, clouds, atmospheric instability
11	IR13.4	13.40	12.40	14.40	Cirrus cloud height, atmospheric instability
12	HRV	Broadband (about 0.4 - 1.1 μm)			Surface, clouds

Appendix 6: Platform specification for MODIS

Spectral channel characteristics of MODIS Terra and Aqua in terms of the bands by central wavelength and the main application areas of each channel (http://modis.gsfc.nasa.gov). Spatial resolution is 250 m for bands 1 and 2, 500 m for bands 3 to7 and 1000 m for bands 8 to 36.

Band Number	Spectral Bandwidth	Main observational application
1	620 - 670	Land/Cloud/Aerosols Boundaries
2	841 - 876	
3	459 - 479	Land/Cloud/Aerosols Properties
4	545 - 565	
5	1230 - 1250	
6	1628 - 1652	
7	2105 - 2155	
8	405 - 420	Ocean Color/ Phytoplankton/ Biogeochemistry
9	438 - 448	
10	483 - 493	
11	526 - 536	
12	546 - 556	
13	662 - 672	
14	673 - 683	
15	743 - 753	
16	862 - 877	
17	890 - 920	Atmospheric Water Vapor
18	931 - 941	
19	915 - 965	
20	3.660 - 3.840	Surface/Cloud Temperature
21	3.929 - 3.989	
22	3.929 - 3.989	
23	4.020 - 4.080	
24	4.433 - 4.498	Atmospheric Temperature
25	4.482 - 4.549	
26	1.360 - 1.390	Cirrus Clouds Water Vapor
27	6.535 - 6.895	
28	7.175 - 7.475	
29	8.400 - 8.700	Cloud Properties
30	9.580 - 9.880	Ozone
31	10.780 - 11.280	Surface/Cloud Temperature
32	11.770 - 12.270	
33	13.185 - 13.485	Cloud Top Altitude
34	13.485 - 13.785	
35	13.785 - 14.085	
36	14.085 - 14.385	